NATIONAL TECHNICAL UNIVERSITY OF ATHENS

SCHOOL OF CIVIL ENGINEERING

M.Sc. IN ANALYSIS AND DESIGN OF EARTHQUAKE RESISTANT STRUCTURES

Methods and techniques for the experimental evaluation of concrete's resistance to chlorides attack – A review

M.Sc. Thesis

Atteyehossadat Seyedalhosseini Natanzi

Supervisor:

Efstratios Badogiannis, Lecturer NTUA

Athens 2014

Acknowledgements

A few lines are too short to make a complete account of my deep appreciation of my supervisor Dr. Badogiannis. I wish first to thank him for his unhesitating trust and constant encouragements, which have been essential ingredients for our success during the last year. I would like to extend my thanks to him for his understanding.

I also have to thank Prof. S. Tsivilis and former Assoc. Prof S. Kolias, for their participation on the examination process of my dissertation and for their constructive comments on my work.

I especially thank my family for all their emotional support and encouragement throughout my graduate work in NTUA. I owe my parents much of what I have become. Their love, their support, and their confidence are motivation for me to overcome the obstacles.

Abstract

Chloride ingress is one of the main causes of reinforced concrete deterioration affecting structural serviceability and safety. Corrosion begins when the concentration of chloride at the steel bars reaches a threshold value that destroys a thin passive layer of corrosion products which are preserved by the high alkalinity of concrete.

Chlorides could ingress in concrete by different transport mechanisms:

- Permeability of chlorides water solutions, due to hydraulic gradient.
- Diffusion as a result of a chlorides concentration gradient
- Absorption where the transport of liquids in unsaturated porous concrete occurs due to surface tension acting in capillaries

When chloride ions originated from environmental solutions penetrate into the concrete, some of them remain free ions, dissolved in the pore solution. The rest are captured by the hydration products. This is called chloride binding. Chlorides mainly bound in concrete in the form of Friedel's salt, as the result of their reaction with C_3A and in calcium silicate hydrate (C-S-H) gel, adsorbed onto the C-S-H gel.

Chloride binding in concrete is affected by many factors, such as: type of cement, mineral addition, w/c, curing condition, exposure conditions, chloride source, carbonation and sulphate existence. Literature review showed that:

- CEM I and CEM III have the highest and lowest binding capacity, respectively. Binding capacity increases by the addition of minerals. The addition of Fly Ash or GGBFS, for instance, found to enhance chloride binding capacity at the level of 24% and 68%, respectively
- The amount of bound chlorides increased with increasing W/C, but the ratio of free/ bound chlorides decreased since the total chloride content increased with increasing W/C.
- An increase in curing temperature increases both ionic diffusivity and chloride binding capacity.

Many methods have been proposed for testing chloride ingress in concrete. These methods can be categorized into the categories: diffusion tests, migration tests, indirect test based on

resistivity or conductivity. These methods can determine total or free chloride and binding chloride could be calculated:

- Total chloride can be determined by chemical analysis, using AS 1012.20-1992, ASTM C 1152-97 or BD 1881 part 124-1988.
- Free chloride is more complicated and it can be measured by ion chromatography technique but it will also include at least the diffusing ones and a variable proportion of the physically bound chlorides.

In the last 20 years, some studies have used some non-destructive an in situ methods for developing several non-destructive techniques that have shown good possibilities for measuring, controlling, or modeling chloride ingress in concretes. These methods are: Ion electrode selective, Electrical resistivity, and Optical fiber sensors. Each method measures chloride ions or chloride diffusion coefficient. The use of optical fiber sensors is the most promissory technique. It is not affected by environmental factors, geometrical distribution, ions presences or electromagnetic fields.

The prediction of chloride binding through modeling, concentrates significant research effort. Some of them reproduce the behaviour of chloride binding in hardened cement paste using thermodynamic equilibrium. Other modeled the dissolution and precipitation behaviour of C-S-H, assuming a binary non ideal solid solution.

Finally, there are several challenges favoring the future research on chloride measurement by using non-destructive techniques, with respect to:

- Independence of geometry
- Multi-measurement ability
- Independence of environmental actions
- Chemical stability
- Cost and Accuracy.

Περίληψη

Η διείσδυση χλωριόντων είναι μία από τις κύριες αιτίες υποβάθμισης της λειτουργικότητας και της ασφάλειας των κατασκευών οπλισμένου σκυροδέματος. Η διάβρωση αρχίζει όταν η συγκέντρωση του χλωριόντων στις ράβδους χάλυβα φθάνει μία οριακή τιμή που καταστρέφει το λεπτό παθητικό στρώμα προστασίας που διατηρείται από την υψηλή αλκαλικότητα του σκυροδέματος.

Τα χλωριόντα θα μπορούσαν να εισχωρήσουν στο σκυρόδεμα με διαφορετικούς μηχανισμούς μεταφοράς:

- Διαπερατότητα των χλωριούχων διαλυμάτων νερού, λόγω διαφοράς πίεσης.
- Διάχυση ως αποτέλεσμα διαφοράς συγκέντρωσης των χλωριόντων
- Απορρόφηση όπου η μεταφορά των υγρών στο πορώδες, λαμβάνει χώρα λόγω της επιφανειακής τάσης που ενεργεί σε τριχοειδή

Όταν εισέρχονται στο σκυρόδεμα ιόντα χλωρίου από το περιβάλλον, κάποια παραμένουν ελεύθερα και κάποια διαλυμένα στα υδατικά διαλύματα των πόρων. Τα υπόλοιπα δεσμεύονται από τα προϊόντα ενυδάτωσης. Αυτή η διεργασία ονομάζεται δέσμευση χλωριόντων. Τα χλωριόντα δεσμεύονται στο σκυρόδεμα κυρίως με τη μορφή του άλατος Friedel, ως αποτέλεσμα της αντίδρασής τους με το C_3A, καθώς και προσροφημένα στο ένυδρο πυριτικό ασβέστιο (CSH).

Η δέσμευση χλωριόντων επηρεάζεται από πολλούς παράγοντες, όπως: ο τύπος του τσιμέντου, τα πρόσθετα, ο λόγος N/T, οι συνθήκες συντήρησης και έκθεσης, η προέλευση χλωριόντων, η ενανθράκωση και η ύπαρξη θειϊκών. Η βιβλιογραφική ανασκόπηση έδειξε ότι:

- Τα τσιμέντα τύπου CEM I και CEM III έχουν την υψηλότερη και χαμηλότερη ικανότητα δέσμευσης, αντίστοιχα.
- Η δέσμευση αυξάνεται με την προσθήκη προσθέτων. Η προσθήκη ιπτάμενης τέφρας ή GGBFS, για παράδειγμα, βρέθηκε να ενισχύει την ικανότητα δέσμευσης στο επίπεδο του 24% και 68%, αντίστοιχα,
- Το ποσό των δεσμευμένων χλωριόντων αυξάνεται με την αύξηση του λόγου N/T, αλλά η αναλογία των ελεύθερων/δεσμευμένα χλωριόντα μειώνεται, καθώς η συνολική περιεκτικότητα σε χλωριόντα αυξάνεται με την αύξηση του N/T.

- Η αύξηση της θερμοκρασίας αυξάνει, τόσο τη διάχυση χλωριόντων όσο και τη δέσμευση.

Πολλές μέθοδοι έχουν προταθεί για τον προσδιορισμό των χλωριόντων που εισέρχονται στο σκυρόδεμα. Μπορούν να ταξινομηθούν στις ακόλουθες κατηγορίες: δοκιμές διάχυσης, δοκιμές διείσδυσης, έμμεσες μέθοδοι μέσω ηλεκτρικής αντίστασης ή αγωγιμότητας. Αυτές οι μέθοδοι εκτιμούν είτε τα συνολικά είτε τα ελεύθερα χλωριόντα, μέσω των οποίων μπορούν να υπολογιστούν τα δεσμευμένα:

- Τα συνολικά χλωριόντα μπορούν να προσδιοριστούν μέσω χημικής ανάλυσης, με βάση τα πρότυπα AS 1012.20-1992, ASTM C 1152-1197 ή BD 1881 part 124 - 1988.
- Ο προσδιορισμός των ελεύθερων χλωριόντων είναι πιο δύσκολος και μπορεί να μετρηθεί με την τεχνική ιοντικής χρωματογραφίας. Ωστόσο στην ποσότητα των ελεύθερων χλωριόντων θα περιλαμβάνονται και σε ένα ποσοστό τα φυσικώς δεσμευμένα χλωριόντα.

Κατά τα τελευταία 20 χρόνια, μερικές μελέτες έχουν αξιοποιήσει κάποιες in situ μη-καταστρεπτικές μεθόδους, όπου η εξέλιξη πολλών από αυτές υπόσχεται πολλές δυνατότητες τόσο για τη μέτρηση και τον έλεγχο της διείσδυσης των χλωριόντων στο σκυρόδεμα, όσο και για τη μοντελοποίηση της. Οι μέθοδοι αυτές είναι: αισθητήρες επιλεκτικών ηλεκτροδίων, αισθητήρες ηλεκτρικής αντίστασης και αισθητήρες οπτικών ινών. Κάθε μέθοδος μετρά τη συγκέντρωση των ιόντων χλωρίου ή το συντελεστή διάχυσης χλωριόντων. Η χρήση αισθητήρων οπτικών ινών είναι η πιο πολλά υποσχόμενη τεχνική. Δεν επηρεάζεται από περιβαλλοντικούς παράγοντες, γεωμετρική κατανομή, παρουσία άλλων ιόντων ή ηλεκτρομαγνητικά πεδία.

Η πρόβλεψη της δέσμευσης χλωριόντων μέσω μοντελοποίησης, επικεντρώνει επίσης σημαντική ερευνητική προσπάθεια. Μερικά από αυτά αναπαράγουν τη συμπεριφορά της σκληρυμένης πάστας τσιμέντου του σκυροδέματος στη δέσμευση χλωριόντων, μέσω εξισώσεων θερμοδυναμικής ισορροπίας. Άλλα μοντελοποιούν τη διάλυση και κατακρήμνιση του CSH, υποθέτοντας ένα δυαδικό μη ιδανικό στερεό διάλυμα.

Τέλος, υπάρχουν αρκετές προκλήσεις που ευνοούν τη μελλοντική έρευνα για τη μέτρηση χλωριόντων, χρησιμοποιώντας μη καταστρεπτικές τεχνικές που μπορούν να λαμβάνουν υπόψη:

- τη γεωμετρία
- τη δυνατότητα πολλαπλών μετρήσεων
- τις περιβαλλοντικές δράσεις
- τη χημική σταθερότητα
- - το κόστος και την ακρίβεια της μέτρησης.

Contents

Chapter 1

DURABILITY OF CONCRETE

Concrete is a composite with properties that change with time. During service, the quality of concrete provided by initial curing can be improved by subsequent wetting as in the cases of foundations or water retaining structures. However, concrete can also deteriorate with time due to physical and chemical attacks. Structures are often removed when they become unsafe or uneconomical.

Lack of durability has become a major concern in construction for the past 20 to 30 years. In some developed countries, it is not uncommon to find large amount of resources, such as 30 to 50% of total infrastructure budget, applied to repair and maintenance of existing structures. As a result, many government and private developers are looking into lifecycle costs rather than first cost of construction.

Durability of concrete depends on many factors including its physical and chemical properties, the service environment and design life. As such, durability is not a fundamental property. One concrete that performs satisfactory in a severe environment may deteriorate prematurely in another situation where it is consider as moderate. This is mainly due to the differences in the failure mechanism from various exposure conditions. Physical properties of concrete are often discussed in term of permeation, the movement of aggressive agents into and out of concrete. Chemical properties refer to the quantity and type of hydration products, mainly calcium silicate

hydrate, calcium aluminate hydrate, and calcium hydroxide of the set cement. Reactions of penetrating agents with these hydrates produce products that can be inert, highly soluble, or expansive. It is the nature of these reaction products that control the severity of chemical attack. Physical damage to concrete can occur due to expansion or contraction under

1.1 DURABILITY FACTORS

According to ACI Committee 201, durability of Portland cement concrete is defined as its ability to resist weathering action, chemical attack, abrasion, or any other process of deterioration; that is, durable concrete will retain its original form, quality, and serviceability when exposed to its environment. No material is inherently durable; as a result of environmental interactions the microstructure and, consequently, the properties of materials change with time. A material is assumed to reach the end of service life when its properties under given conditions of use have deteriorated to an extent that the continuing use of the material is ruled either unsafe or uneconomical.

Almost universally, concrete has been specified principally on the basis of its compressive strength at 28 days after casting. Since reinforced concrete structures are usually designed with a sufficiently high safety factor, it is rare for concrete structures to fail due to lack of intrinsic strength. However, gradual deterioration caused by the lack of durability reduces the safety margin of concrete structures to an extent that serious concerns have been raised. Steel corrosion has led to the collapse of canopies, resulting in death and injury of people.

Causes of deterioration and main durability problems

The causes of concrete deterioration is grouped into two categories.

Physical causes:

- Surface wear (abrasion, erosion and cavitation)
- Cracking (Volume changes, loading damage, and extreme temperature damage)

Chemical causes:

- Alkali-aggregate reaction

- Sulphate attack
- Steel corrosion

The most severe durability problems always involve the penetration of water (with corrosive agents) into the concrete. Physical action (e.g., water freezing) or chemical reaction (e.g., alkali-aggregate reaction) will then lead to internal expansion, resulting in significant cracking/spalling of the concrete. Durability of concrete is hence related to the ease of ingress of water and chemicals. Concrete permeability and diffusivity are hence important parameters to be considered.

1.2 CORROSION OF STEEL BARS AND DETERIORATION OF CONCRETE STRUCTURES

1.2.1 Corrosion of steel in concrete

This part discusses the basics of corrosion and how they apply to steel in concrete. Why does steel corrode in concrete? A more sensible question is why steel does not corrode in concrete. We know from experience that mild steel and high strength reinforcing steel bars corrode (rust) when air and water are present. As concrete is porous and contains moisture why does steel in concrete not usually corrode?

The answer is that concrete is alkaline. Alkalinity is the opposite of acidity. Metals corrode in acids, whereas they are often protected from corrosion by alkalis.

When we say that concrete is alkaline we mean that it contains microscopic pores with high concentrations of soluble calcium, sodium and potassium oxides. These oxides form hydroxides, which are very alkaline, when water is added. This creates a very alkaline condition (pH 12-13). The composition of the pore water and the movement of ions and gases through the pores are very important when analysing the susceptibility of reinforced concrete structures to corrosion.

The alkaline condition leads to a ‘passive’ layer forming on the steel surface. A passive layer is a dense, impenetrable film, which, if fully established and maintained,

prevents further corrosion of the steel. The layer formed on steel in concrete is probably part metal oxide/hydroxide and part mineral from the cement. A true passive layer is a very dense, thin layer of oxide that leads to a very slow rate of oxidation (corrosion). There is some discussion whether or not the layer on the steel is a true passive layer as it seems to be thick compared with other passive layers and it consists of more than just metal oxides; but it behaves like a passive layer and it is therefore generally referred to as such.

Corrosion engineers spend much of their time trying to find ways of stopping corrosion of steel by applying protective coatings. Metals such as zinc or polymers such as acrylics or epoxies are used to stop corrosive conditions getting to steel surface. The passive layer us the corrosion engineer's dream coating as it forms itself and will maintain and repair itself as long as the passivating (alkaline) environment is there to regenerate it if it is damaged. If the passivating environment can be maintained, it is far better than any artificial coatings such as galvanizing or fusion bonded epoxy that can be consumed or damaged, allowing corrosion to proceed in damaged areas.

However, the passivating environment is not always maintained. Two processes can break down the passivating environment in concrete. One is carbonation and the other is chloride attack [P.Broomfield, 1997].

1.2.2 The corrosion process

Once the passive layer breaks down then areas of rust will start appearing on the steel surface. The chemical reactions are the same whether corrosion occurs by chloride attack or carbonation. When steel in concrete corrodes it dissolves in the pore water and gives up electrons:

The anodic reaction:

$$Fe \rightarrow Fe^{2+} + 2e^{-} \qquad 1.1$$

The two electrons ($2e^{-}$) created in the anodic reaction must be consumed elsewhere on the steel surface to preserve electrical neutrality. In other words, it is not possible for

large amounts of electrical charge to build up at one place on the steel; another chemical reaction must consume the electrons. This is a reaction that consumes water and oxygen:

The cathodic reaction:

$$2e^- + H_2O + 1/2O_2 \rightarrow 2OH^- \qquad 1.2$$

This is illustrated in Figure 1.1. You will notice that hydroxyl ions ($2OH^-$) are generated in the cathodic reaction. These ions increase the local alkalinity and will therefore strength the passive layer, warding off the effects of carbonation and chloride ions at the cathode. Note that water and oxygen are needed at the cathode for corrosion to occur.

The anodic and cathodic reactions (1.1 and 1.2) are only the first steps in the process of creating rust. However, this pair of reactions is critical to the understanding of corrosion and is widely quoted in any discussion on corrosion prevention for steel in concrete. The reactions will be referred [P.Broomfield, 1997]. .

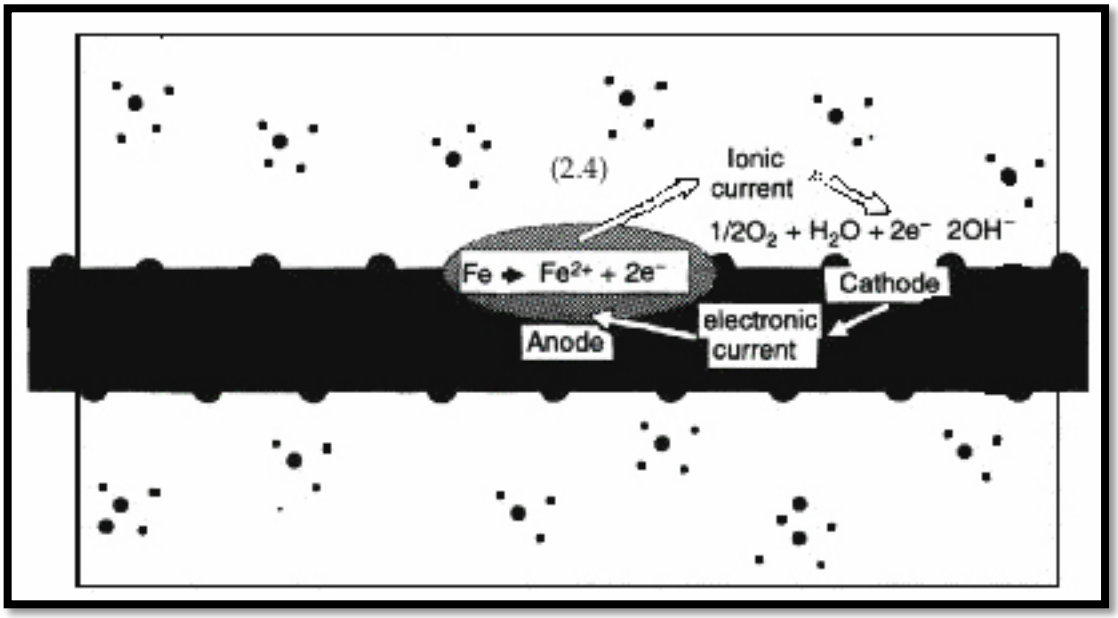

Figure 1.1: The anodic and cathodic reactions [P.Broomfield, 1997].

If the iron were just to dissolve in the pore water (the ferrous ion Fe^{2+} in equation 1.1 is soluble) we would not see cracking and spalling of the concrete. Several more stages must occur for 'rust" to form. This can be expressed in several ways; one is shown below where ferrous hydroxide becomes ferric hydroxide and then hydrated ferric oxide or rust:

$$Fe^{2+} + 2OH^- \rightarrow Fe(OH)_2 \qquad 1.3$$

Ferrous hydroxide

$$4\,Fe(OH)_2 + O_2 + 2H_2O \rightarrow 4Fe(OH)_3 \qquad 1.4$$

Ferric hydroxide

$$2\,Fe(OH)_3 \rightarrow Fe_2O_3.H_2O + 2H_2O \qquad 1.5$$

Hydrated ferric oxide (rust)

The full corrosion process is illustrated in Figure 1.2. Unhydrated ferric oxide Fe_2O_3 has a volume of about twice that of the steel it replaced when fully dense. When it becomes hydrated it swells even more and becomes porous. This means that the volume increase at the steel/concrete interface in two to ten times. This leads to the cracking and spalling that we observe as the usual consequence of corrosion of steel in concrete and the red/brown brittke, flaky rust in the bar and the rust stains seen at cracks in the concrete [P.Broomfield, 1997]..

The electrical current flow, and the generation and consumption of electrons in the anode and cathode reactions are used in halfcell potential measurements and cathodic protection. The formation of protective, alkaline hydroxyl ions is used in cathodic protection, electrochemical chloride removal and realkalization. The fact that the cathodic and anodic reaction must balance each other for corrosion to proceed is used in epoxy coating protection of rebars.

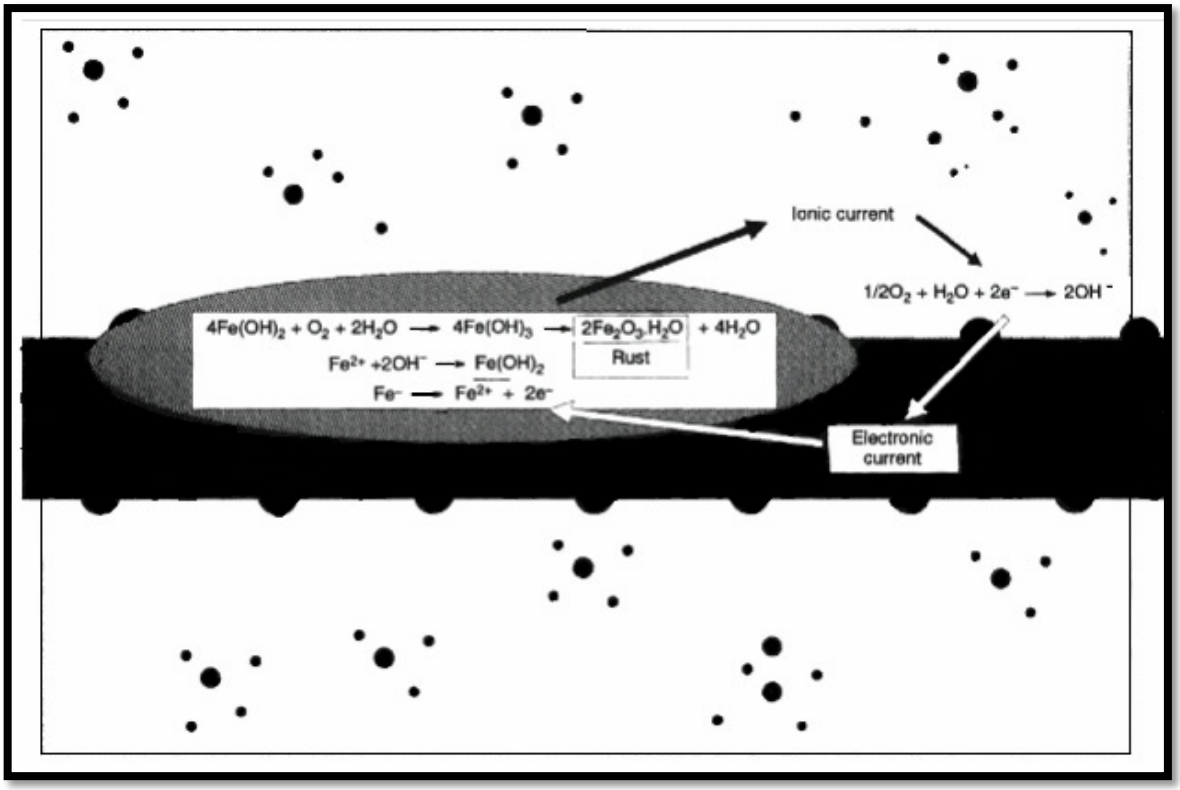

Figure 1.2: The corrosion reactions on steel [P.Broomfield, 1997].

1.3 MECHANISM OF CHLORIDE ATTACK IN CONCRETE

The corrosion of steel in concrete and the effectiveness of the alkalinity in the concrete pores producing a passive layer of protective oxide on the steel surface that stops corrosion are known. We observed that alkalinity in the concrete pores is neutralized by carbonation. The depassivation mechanism for chloride attack is somewhat different. The chloride ion attacks the passive layer but, unlike carbonation, there is no overall drop in pH. Chloride act as catalysts to corrosion when there is sufficient concentration at the rebar surface to break down the passive layer. They are not consumed in the process but help to break down the passive layer of oxide on the steel and allow the corrosion process to proceed quickly. This is illustrated in Figure 1.3. This makes chloride attack difficult to remedy as chloride are hard to eliminate [P.Broomfield, 1997].

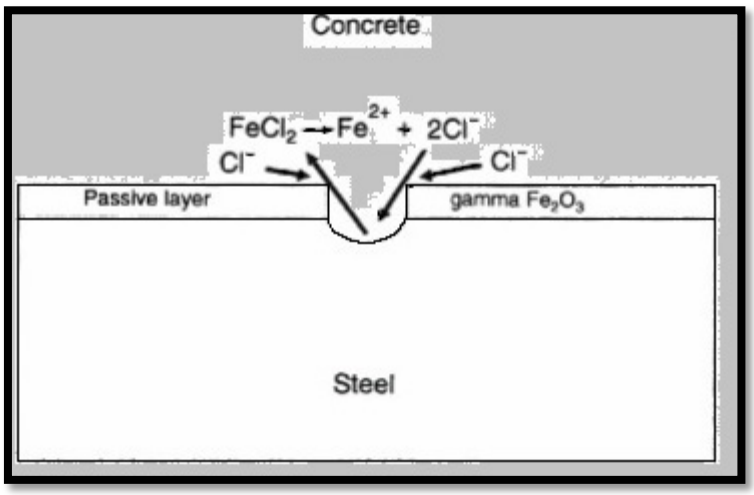

Figure 1.3: The breakdown of the passive layer and 'recycling' chlorides [P.Broomfield, 1997].

Obviously a few chloride ions in the pore water will not break down the passive layer, especially if it is effectively re-establishing itself when damaged.

There is a 'chloride threshold' for corrosion given in terms of the chloride/hydroxyl ration. It has been measured in laboratory tests with calcium hydroxide solutions. When the chloride concentration exceeds 0.6 of the hydroxyl concentration, corrosion is observed (Hausmann 1967). This approximates to a concentration of 0.4% chloride by weight of cement of chlorides are cast into concrete and 0.2% they diffuse in.

In the USA a commonly quoted threshold is 1 lb (5 Kg) chloride per cubic yard (1 cubic meter) of concrete. Although these figures are based on experimental evidence, the actual values are a function of practical observations of real structures.

All these thresholds are approximations because:

1. Concrete pH varies with the type of cement and the concrete mix. A tiny pH change represents a massive change in hydroxyl ion (OH^-) concentration and therefore (theoretically) the threshold moves radically with pH.
2. Chlorides can be bound chemically (by aluminates in the concrete and physically (by absorption on the pore walls). This removes them (temporarily or permanently) from the corrosion reaction. Sulphate resisting cements have

low aluminate (C_3A) content, which leads to more rapid diffusion and lower chloride thresholds.
3. In very dry concrete corrosion may not occur even at very high Cl^- concentration as the water is missing from the corrosion reaction.
4. In sealed or polymer impregnated concrete, corrosion may not occur even at a very high Cl^- concentration if no oxygen or moisture is present to fuel the corrosion reaction.
5. Corrosion can be suppressed when there is total water saturation due to oxygen starvation, but if some oxygen gets in, then the pitting corrosion can occur.

Therefore corrosion can be observed at a threshold level of 0.2% chloride be weight of cement if the concrete quality is poor and there are water and oxygen available. In different circumstances no corrosion may be seen at 1.0% chloride or more if oxygen and water are excluded. If the concrete is very dry or totally saturated (as in (3) or (5) above) then a change in conditions may lead to rapid corrosion [P.Broomfield, 1997].

1.3.1 Chloride transport mechanisms

Chloride ions and other aggressive substances penetrate through concrete via different mechanisms depending on the driving force involved. Diffusion, permeability and absorption (sorptivity) are the most well-known chloride transport mechanisms through concrete. Parallel phenomena such as chloride binding can also influence chloride ingress.

The moisture state of concrete and the service environment determine the driving force and thus the mechanisms by which chloride penetrates into concrete. In saturated concrete that is continuously immersed in an aqueous solution, chloride transport occurs by diffusion through the pore solution. Movement into and through unsaturated concrete, a common state for concrete with surfaces exposed to the atmosphere, is largely controlled by absorption through the capillary pore system and diffusion of chlorides through pore solution.

In highway structures and bridges, concrete is subjected to intermittent wetting events due to rain or condensation and dries out in between these wetting events. Liquid in the pores evaporates progressively from the surface. In this situation, the most likely

scenario is that chloride will enter the concrete initially by absorption and produce a reservoir of chloride ions a relatively short distance from the concrete surface from which diffusion can occur. This reservoir will be topped up by periodic absorption events. If the concrete dries out to a greater depth, subsequent wettings carry the chlorides deeper into the concrete. Thus it would appear that absorption and diffusion are important transport mechanisms associated with chloride ingress in highway structures and bridges [Hong & Hooton, 1999]. However, before discussing these two mechanisms of chloride ingress in detail, the following gives a brief description of permeability that is necessary for an understanding of the theory of absorption. . [P.Broomfield, 1997]

Chapter 2

CHLORIDE PENETRATION IN CONCRETE

Chloride-induced steel corrosion is one of the major worldwide deterioration problems for reinforced concrete structures. The high alkaline environment of concrete forms a passive film on the surface of the embedded steel which normally prevents the steel from corroding further. However, under chloride attack, the passive film is disrupted or destroyed and the steel corrodes spontaneously. The penetration of chloride ions through concrete surfaces to steel reinforcement results in corrosion. This is an issue of concern for reinforced concrete projects, such as parking, bridge, and marine structures.

There are several different transport mechanisms into concrete for chloride ions. These can be divided into the following groups: diffusion, permeation, migration, and convection. The diffusion coefficient is generally assessed to describe chloride penetration into the structure. Chloride penetration rarely happens purely by diffusion; this can only happen in permanently water-saturated concrete. It often happens through difficult-to-model mechanisms such as the exposure of dry concrete containing chloride to water, followed by dry and wet periods. Chloride transport in concrete is a rather complicated process.

In efforts to control this problem, it is necessary to make improvements to the service life prediction models. The calculation of the time for steel corrosion is becoming an

urgent need as a result of the engineering demand of the prediction of the service life of concrete structures [M.Sillanpaa, 2010].

2.1 PERMEABILITY

Permeability is the movement of a liquid under hydrostatic pressure. Permeability can be described by Darcy's law (Equation 2.1), which states that the steady-state rate of flow is directly proportional to hydraulic gradient [Basheer et al, 2001].

$$v = \frac{Q}{A} = \frac{k\rho g}{\eta}\frac{\Delta h}{L} \qquad 2.1$$

where,

v = Apparent velocity of flow or volume of water per unit time per unit area (m/s)

Q = Flow rate (m^3/s)

A = Cross-sectional area of the sample (m^2)

Δh= Drop in hydraulic head through the sample (m)

L = Thickness of the sample (m)

η = Dynamic viscosity of the fluid ($kg/m.s$)

ρ = Density of the fluid (kg/m^3)

g = Acceleration due to gravity (m/s^2)

k= Intrinsic permeability of materials (m^2)

The intrinsic permeability coefficient "k" is independent of the fluid involved.

$$K = \frac{k\rho g}{\eta}\left(\frac{m}{s}\right) \qquad 2.2$$

Thus

$$v = \frac{Q}{A} = K\frac{\Delta h}{L} \quad 2.3$$

where K is the coefficient of permeability or hydraulic conductivity (m/s)

When the flow is of an unsteady state (i.e. the flux changes with time), the hydraulic head may not decrease linearly along the direction of flow and in which case the flow velocity is given by

$$v = -K\nabla h \quad 2.4$$

In a one-dimensional system

$$v = -K\frac{dh}{dx} \quad 2.5$$

The permeability of concrete depends on its porosity as well as on the size, distribution, shape, tortuosity and continuity of pores. Therefore it depends on all factors that influence the pore structure of concrete i.e. water to cement ratio, type of cement, cement replacement materials and the progress of hydration.

Historically, permeability was used as the criteria to characterise the penetrability of concrete regardless of the situation. There are situations when permeability is relevant such as in permanently submerged concrete where water is forced through concrete by hydraulic pressure (head of water). However, in concrete structures which are not in contact with water under pressure, like a bridge exposed to the environment, permeability is generally not one of the most important mechanisms [Emerson, 1990].

2.2 DIFFUSION

2.2.1 Theory

When transport of a substance through concrete is the result of a concentration gradient, diffusion takes place. The diffusion equation can be expressed by Fick's laws and most models for predicting chloride ingress through saturated cement-based materials are based on this law [Khatib et al, 2005]. This methodology is based on papers from the early 1970's [Collepardi et al, 1972] and assumes chloride penetration occurs due to diffusion.

Stationary diffusion (unidirectional and constant mass transfer) is usually described by Fick's first law of diffusion (Equation 2.6). It states that the rate of transfer of mass through unit area of a section, J ($mol/m^2.s$), is proportional to the concentration gradient, $\frac{dc}{dx}$ ($\frac{mol/m^3}{m}$) and the diffusion coefficient, D (m^2/s) [Basheer et al, 2001].

$$J = -D\frac{dc}{dx} \qquad 2.6$$

Non-stationary diffusion i.e. when the concentration c at a location x changes with time it is characterized by Fick's second law (Equation 2.7).

$$\frac{dc}{dt} = \frac{d}{dx}\frac{Ddc}{dx} \qquad 2.7$$

There are many solutions to Fick's second law depending on the boundary and initial conditions as well as the diffusion coefficient. The diffusion coefficient, D, may be assumed constant or a function of different variables such as time/age, porosity, degree of hydration (maturity), aggregate size, temperature, humidity and local chloride concentration and binding [Oh and Jang, 2007].

The fact that the diffusion coefficient changes with age of specimen is difficult to be modelled in practice. Some studies simply assume the diffusion coefficient remains constant with time whereas others have tried to incorporate this feature into their models [Nilsson, 2002].

2.2.1.1 Constant diffusion coefficient

For constant diffusion coefficient, the solution to Equation 2.7 for the boundary condition C_0=C (0,t) (i.e. constant surface chloride concentration) and the initial condition C = 0 for x>0 and t = 0, is given by:

$$C = C_0\left(1 - erf\frac{x}{2\sqrt{Dt}}\right) \quad 2.8$$

Where, *erf* is the standard error function. [Crank, 1956]

Although Equation 2.8 is only valid if both the diffusion coefficient and surface concentration remain constant, it has been extensively used in cases where both parameters vary with time.

2.2.1.2 Time-dependent diffusion coefficient

In 1992, Tang and Nilsson found that the diffusion coefficient of young concrete dramatically decreases with age using their rapid diffusivity test and proposed the following mathematical expression for a time-dependent chloride diffusion coefficient [Tang & Gulikers, 2007]:

$$D(t') = a(t')^{-n} \quad 2.9$$

where $D(t')$ is the time-dependent diffusion coefficient, t' is the concrete age, and a and n are constants, with n normally being referred to as the age factor.

For given values of the diffusion coefficient and age, represented by D_0 and t_0', Equation 2.9 can be rewritten as

$$D(t') = D_0(t_0')^n(t')^{-n} = D_0(\frac{t'}{t_0'})^{-n} \quad 2.10$$

Or more commonly

$$D(t) = D_{ref}(\frac{t_{ref}}{t})^m \quad 2.11$$

where D_{ref} is the diffusion coefficient at some time, t_{ref} (usually 28 days), and m is a variable which describes the rate of change of the diffusion coefficient and is constant for a specific concrete (depending on mix proportion).

Equation 2.11 is the most common form of equation used to predict the change in values of diffusion coefficient with age of concrete [Mangat & Molloy, 1994- Boddy et al, 1999- Stanish & Thomas, 2003- Thomas & Bamforth, 1999- Nokken et al, 2006].

Values of m for different concretes are, as yet, not well established, but some preliminary values have been published. Values in the range of 0.2 to 0.3 are common for normal Portland cement mixtures; while higher values (0.5-0.7) are attributed to fly ash and slag concrete [Thomas & Bamforth, 1999- Boddy et al, 1999- Stanish & Thomas, 2003- Bamforth, 2004].

To determine the value of the m-coefficient, equation 2.11 is fitted to a plot of diffusion coefficient against time (e.g. determined via the bulk diffusion test). The maturity achieved at the end of the exposure period is typically used as the time basis to calculate m-value (total age of concrete). In this case the diffusion coefficients determined are an average diffusion coefficient over the time period of chloride exposure.

The time-dependency of the diffusion coefficient has caused confusion and mathematical mistakes. The time-dependent diffusion coefficient has been substituted directly into the error function equation by many authors including Mangat and Molloy [1994] and Maage et al [1995]. This is mathematically incorrect as the error function is a solution to Fick's equation assuming the diffusion coefficient is constant. In fact, the time-dependent diffusion coefficient cannot be directly put into the error function without time integration. [Tang & Gulikers, 2007]

Tang & Gulikers [2007] showed that substitution of the diffusion coefficient, D(t), directly into the error function equation can underestimate chloride ingress in concrete

in some cases. Therefore, it is important to apply the necessary modification to the error function equation when using a time-dependent diffusion coefficient.

2.2.1.3 Time-dependent surface chloride concentration

The surface chloride concentration is also reported to change with time by some authors. However, the increase in surface concentration is mainly related to concrete exposed to wet/dry cycles rather than those continuously immersed in salt solution. This is because surface concentration of concrete exposed to infinite seawater remains constant due to chemical equilibrium, whereas in the tidal zone the chloride content at the concrete surface may increase due to wet/dry cycles.

The relationship between surface chloride concentration and time of exposure is discussed later. As with the case of a variable diffusion coefficient, in order to use a time-dependent surface chloride concentration it is necessary to first integrate the error function with respect to time.

2.2.1.4 Diffusion test methods

Diffusion tests can be divided into three categories of steady state, non-steady state and electrical tests. The electrical tests can be subdivided into two groups of steady state or nonsteady state electrical tests. Each method has strengths and weaknesses and therefore depending on the situation, suitable tests should be applied.

As far as electrical tests are concerned, they have the advantage that they can be carried out rapidly but the disadvantage is that they measure the conductivity of concrete not its diffusivity. Although, some attempts at correlating the measurements obtained from electrical tests and diffusivity tests have been made, there is still a lack of understanding of fundamental processes involved. That makes interpretation of the results complicated and doubtful. Therefore, it is better to avoid using electrical testing if there is sufficient time to perform diffusivity testing.

All steady-state and non steady-state diffusion tests are time consuming and therefore not suitable for use in quality control. However, they can be used in laboratory

experiments and they also have the advantage of yielding a meaningful value of chloride ion diffusivity.

Of the long-term diffusion tests (i.e. Diffusion Cell, Ponding Test and Bulk Diffusion Test), the Bulk Diffusion Test (NordTest NTBuild 443) is claimed to be the most accurate as it measures pure diffusion. In the Diffusion cell test [Page et al, 1981-Basheer et al, 2001] the condition of specimens is not consistent with the condition of the concrete in practice and in the Ponding test [Stanish et al, 1997] diffusion is not the only mechanism involves in the transport of chloride into concrete. Other mechanisms such as absorption or wicking action are also associated with chloride penetration.

In the Bulk Diffusion test, specimens are saturated with saturated calcium hydroxide solution and all the side surfaces are coated except for one face which is exposed to a 2.8 M NaCl solution for a minimum of 35 days (Figure 2.1). The chloride profile of the concrete is determined by grinding the sample in either a mill or lathe with a diamond tipped bit at 0.5mm depth increments. The chloride content of the powder is then determined according to AASHTO T260 [1994]. The error function solution to Fick's second law discussed earlier (Equation 2.8) is fitted to the curve and the diffusion coefficient is determined. [Stanish et al, 1997]

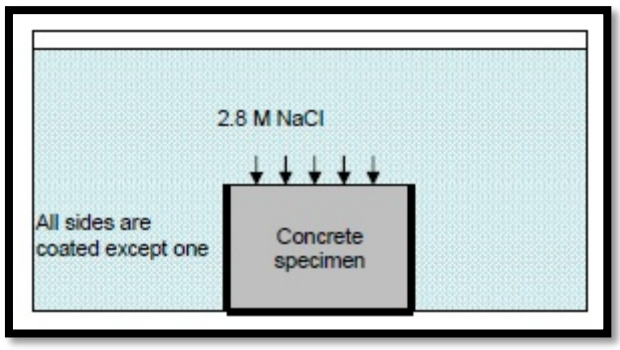

Figure 2.1: Bulk diffusion test set up

2.3 ABSORPTION (Capillary suction)

2.3.1 Theory

The transport of liquids in unsaturated porous concrete due to surface tension acting in capillaries is called absorption. Absorption in concrete is related not only to the pore structure, but also to the moisture content of the concrete. [Basheer et al. 2001]

A linear or a near-linear relationship has been observed between the square root of time and the total volume or mass of liquid absorbed or the depth of penetration (distance of wetting front from surface). The slope of the line is defined as the sorptivity of concrete.

$$A = b + S\sqrt{t} \qquad 2.12$$

Where A is the mass or volume of liquid absorbed per unit of surface or the depth of liquid penetration, S is sorptivity, t is elapsed time and b is initial absorption. In practice it is often observed that there is a rapid initial absorption on the surface and therefore b is the correction factor added to account for this effect.

The relationship between absorption and square root of time can be explained via either theory of capillarity or unsaturated flow.

2.3.1.1 Theory of capillarity

Capillary pressure in a tube is given by

$$P_c = \frac{2\gamma cos\theta}{r} \qquad 2.13$$

P_c = Capillary pressure *(Pa)*

γ = Surface tension *(Pa.m)*

θ =Wetting angle (θ for water= 0)

r = Effective radius of capillary tube *(m)*

According to Poiseuille's equation for the flow of liquid in a tube

$$Q = \frac{dV}{dt} = \frac{\pi p r^4}{8 l \eta} \qquad 2.14$$

Q = Flow rate (m^3/s)

V= Volume of liquid (m^3)

p= pressure gradient (Pa)

l= length of tube (m)

Substituting dV ($dV=\pi r^2 dl$) in Equation 2.14 yields

$$\frac{l dl}{dt} = \frac{p r^4}{8\eta} \qquad 2.15$$

Assuming the capillary pressure to be the only driving force and substituting for p using Equation 2.13 gives

$$\frac{l dl}{dt} = \frac{\gamma r}{4\eta} \; or \; l dl = \frac{\gamma r}{4\eta} dt \qquad 2.16$$

Note cosθ =1.

Thus

$$l = S\sqrt{t} \qquad 2.17$$

Where $S = \sqrt{\frac{\gamma r}{2\eta}}$ is sorptivity

Since sorptivity is proportional to $\sqrt{\frac{\gamma r}{\eta}}$ it would seem that absorption is affected by the surface tension, viscosity of the absorbing liquid and also by the pore radius.

2.3.1.2 Theory of unsaturated flow

One-dimensional capillary absorption can also be modelled using Richard's equation for unsaturated flow. This equation is a combination of Darcy's equation and the law of conservation mass.

As previously noted, Darcy's law for saturated flow, $v = \frac{Q}{A} = K\frac{\Delta h}{L}$, states that the steady state rate of flow is directly proportional to hydraulic gradient and the equation changes to $v = -K\nabla h$ or $v = -K\frac{dh}{dx}$ for unsteady-state flow.

Darcy's law is sufficient to describe only steady-state flow. To model unsteady-state flow, the law of conservation of mass is also required:

$$\frac{\partial\theta}{\partial t} = -\frac{\partial v}{\partial x} \qquad 2.18$$

where θ = Volumetric water content

substituting for *v* in Equation 2.18 yields:

$$\frac{\partial\theta}{\partial t} = \frac{\partial}{\partial x}(K\frac{dh}{dx}) \qquad 2.19$$

In saturated porous medium with an incompressible matrix, $\vartheta\theta/\partial t = 0$; the conductivity is usually assumed to remain constant hence Equation 2.19 becomes

$$K_s\frac{\vartheta^2 h}{\partial x^2} = 0 \qquad 2.20$$

where, K_s is the hydraulic conductivity of the saturated medium.

Darcy's law for saturated flow can be extended using Richard's equation to model flow in an unsaturated porous medium (Equation 2.21). The important differences between saturated and unsaturated flow are the moving force and hydraulic conductivity. In a saturated porous medium the gradient of a positive pressure potential is the moving force and conductivity is constant and maximal. On the other hand, water in an unsaturated porous medium is subjected to suction and conductivity decreases with decreasing water content and flow is a function of suction or wetness.

$$\frac{\partial \theta}{\partial t} = \frac{\partial}{\partial x}[K(\Psi)\nabla h] \qquad 2.21$$

where Ψ is the suction head and ∇h is the hydraulic head gradient which may include both suction and a gravitational component.

In one-dimensional flow with negligible gravitational head:

$$\frac{\partial \theta}{\partial t} = \frac{\partial}{\partial x}\left[K(\Psi)\frac{\partial \Psi}{\partial x}\right] \qquad 2.22$$

The relationship between conductivity and suction is affected by hysteresis. However, the relationship between conductivity and volumetric water content, θ is much less affected by hysteresis. Hence,

$$\frac{\partial \theta}{\partial t} = \frac{\partial}{\partial x}\left[K(\theta)\frac{\partial \Psi}{\partial x}\right] \qquad 2.23$$

In order to simplify the mathematical and experimental treatment of unsaturated flow processes, the flow equation is changed to the form of the diffusion equation

$$\frac{\partial \theta}{\partial t} = \frac{\partial}{\partial x}\left[\frac{K(\theta)}{c(\theta)}\frac{\partial \theta}{\partial x}\right] \qquad 2.24$$

where, $c(\theta) = \frac{d\theta}{d\Psi}$ is called specific water capacity (m^{-1})

Therefore

$$\frac{\partial \theta}{\partial t} = \frac{\partial}{\partial x}\left[D(\theta)\frac{\partial \theta}{\partial x}\right] \qquad 2.25$$

$$D(\theta) = \frac{K(\theta)}{c(\theta)} = K(\theta)\frac{d\Psi}{d\theta} \qquad 2.26$$

where,

x=depth (*m*)

t=time (*s*)

θ = volumetric water content (L^3 / L^3)

D (θ) = Capillary diffusivity (water diffusivity/ unsaturated hydraulic diffusivity) (m^2/s)

K (θ) = unsaturated hydraulic conductivity (m/s)

Ψ = capillary potential (m)

It is important to note that although this equation is similar to the non-linear diffusion equation, it is based on an entirely different concept. The equation describes the flow of water under capillary suction in unsaturated porous solids [Pachepsky, 2003].

Equation 2.25 has a solution of the form [Hall, 2007- Wilson, 2003]

$$x(\theta, t) = \varphi(\theta)\sqrt{t} \qquad 2.27$$

where, φ ($m/\sqrt{s}$) is the Boltzmann variable $xt^{-1/2}$

The total volume or mass of water absorbed can be estimated from [Wilson, 2003]

$$i(t) = t^{1/2} \int_{\theta_0}^{\theta_s} \varphi d\theta \qquad 2.28$$

The integral in this expression is termed sorptivity, S [Philip, 1957]

$$S = \int_{\theta_0}^{\theta_s} \varphi d\theta \qquad 2.29$$

Generally, the mathematical expressions in the literature derive from these two theories; namely, capillarity and unsaturated flow. Some examples of expression which have been used to model sorptivity are provided in Table 2.1.

Table 2.1: Mathematical approaches for concrete absorption/sorptivity

Hall (1977)	$i = S\sqrt{t}$	i=cumulative absorption S=sorptivity t=time
Ho & Lewis (1982)	$i = S\sqrt{t}$	i=volume of water absorbed per unit area S=sorptivity t=time
Bamforth et al (1985)	$x = \frac{r}{2}(\frac{P_0 t}{\eta})^{0.5}$ $x = \sqrt{\frac{2Kt(P_1 - P_2)}{\upsilon\rho g}}$ $K = \frac{r^2 \upsilon\rho g}{8\eta}$	x=distance travelled r=pore radius t=time P_0=driving pressure $P_1 - P_2$ = pressure difference η=viscosity of liquid g=acceleration due to gravity ρ =density of liquid υ = porosity of concrete K= permeability coefficient
Vuorinen (1985)	$x = (2Kht)^{0.5}$	x=depth of penetration K= permeability coefficient h=hydraulic head t=time
Kelham (1988)	$Q = \frac{KA\sigma(dp/dx)}{\eta}$	Q=mass rate of flow of fluid K= intrinsic permeability of medium A= cross sectional area of flow σ =density of fluid dp/dx=pressure gradient η=viscosity of fluid

Note that the constant K which is quoted by Bamforth et al [1985] and Vuorinen [1985] as permeability coefficient is the unsaturated hydraulic conductivity in unsaturated flow theory.

2.3.1.3 Sorptivity test methods

Several approaches have been used to measure sorptivity/absorption of concrete and a number of methods are recommended in codes and standards. These methods can be divided into three groups depending on the test sorption mode where concrete specimens are: 1- immersed in absorbing solution 2- subject to a head of absorbing solution 3- in contact with absorbing solution with suction surface facing down.

In addition to the sorption mode, the sorptivity tests are susceptible in pre-conditioning regime, specimen size, coating and surface finish. The followings discuss different sorptivity test methods.

BS 1881-122 describes a water absorption test for concrete cylinders in which the cylinders are totally immersed in water for 30 minutes. Prior to immersion the cylinders are placed in an oven at 105± 5°C for 72±2 hours at an age of 24 days to 28 days and then cooled for 24 ± ½ hours in an airtight vessel. The absorption of the concrete is defined as the increase in weight resulting from immersion in water as a percentage of the weight of the dry specimen.

In the water the absorption test [BS 1881-122] penetration of water may occur via a combination of transport mechanisms. Initially, water penetrates via absorption until the capillary pores are filled and then diffusion occurs. As a consequence the results obtained from this test method can be complicated to interpret.

In addition, the preconditioning regime of drying at high temperature alters the pore structure and may introduce cracks. The oven-drying regime at the elevated temperatures recommended in BS 1881-122 has been used in many cases to achieve an identical moisture state for samples prior to the absorption test in the laboratory. However, this preconditioning can make it difficult to interpret the results.

BS 1881-208 describes a test for determination of the initial surface absorption of concrete, known as ISAT (Initial Surface Absorption Test). The test involves the measurement of the rate of flow into a prescribed surface area of unsaturated concrete after a stated interval of time from the start of the test (10, 30 and 60min) and under a constant head of water (200±20 mm).

Two pre-conditioning regimes of oven drying and non-oven drying are used. The ISAT is applied for both laboratory and field measurements.

In the case of the laboratory tests, samples of 100 mm cubes are cast and kept under wet hessian for one day before demoulding. In oven drying, specimens are preconditioned in an oven at 105±5ºC until at constant weight (not more than 0.1% weight change over 24 hr), then cooled for at least 48 hours. In non-oven drying, samples remain in the laboratory for a minimum period of 48 hours at a T: 20±2°C.

The results from the ISAT are also difficult to interpret due to the applied head of water and the fact that the samples are pre-conditioned at high temperature as water penetrates by a combination of mechanisms (i.e. permeability and absorption).

A sorptivity test was developed by Fagerlund [1982] in which the water mainly penetrates into the concrete by absorption. The specimens are placed on wet sponges rather than immersing them under water or placing under a head of water which had been used in the previous test methods (Figure 2.2). The samples thicknesses used were 20mm to 30 mm, the suction surface was cut, and the samples were in moisture equilibrium with the surroundings before testing was started.

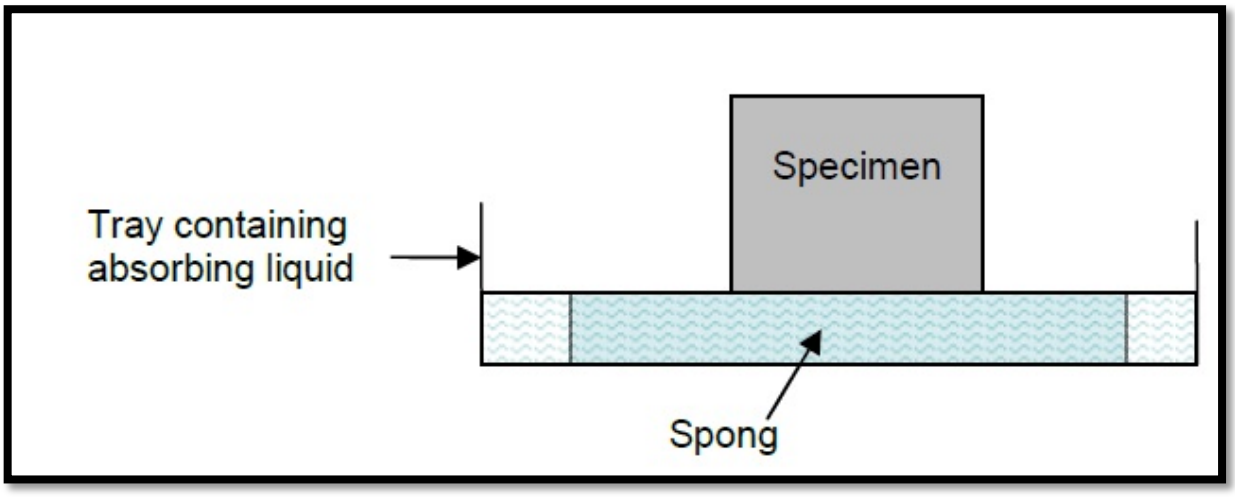

Figure 2.2: Sorptivity test set up

Ho & Lewis [1987] tested sorptivity of concrete specimens (400×170×60 mm) by water spraying at 0.5 KPa air pressure. The depth of penetration was measured by breaking open the samples. Specimens were air-dried for 21 days before testing.

Kelham [1988] applied a 50 mm head of water to the bottom surface of concrete specimens (150 mm diameter and 50 mm thick) and monitored the change in weight of the sample. Prior to the test, concrete samples were cured in water for 24 hours after demoulding, then ovendried at 105°C for 6 days and cooled in a desiccator for 1 day. The applied head of water (50 mm) is small and therefore the effect on water

penetration is negligible. However, the ovendrying preconditioning used may introduce cracks and influence the results.

Accordingly, one of the biggest obstacles to the standardisation of sorptivity testing has been problems associated with the pre-drying regime and the significance of initial moisture content. The effect of drying the specimens has been studied by several researchers and it was found that oven-drying decreased the sensitivity of absorption to the initial moisture content and increased the sorptivity significantly. [Punkki & Sellevold, 1994- Martys and Ferraris, 1997]

Punkki & Sellevold [1994] investigated the effect of the drying procedure and the initial moisture content on the subsequent capillary suction behaviour of concrete. Disc shaped specimens (105 mm dia × 20 mm) were exposed to water on one side and the weight gain was monitored at scheduled times for 4 days. The capillary suction curve of drying at 105°C had a very different shape to the capillary curve at 50°C. Furthermore, in contrast with the specimens dried at 105°C, those dried at 50°C showed different capillary curves for different initial moisture contents. Punkki & Sellevold suggested that more gentle drying procedures are necessary for developing more sensitive capillary tests.

Martys and Ferraris [1997] studied the capillary transport of water in concrete and mortar as a function of water-cement ratio, sand size distribution and curing. Samples were cured in saturated hydroxide solution for a period of 1, 7 and 28 days at 20°C, then either oven-dried (50°C) until constant mass was obtained or air dried (20°C, 30% RH) for four days followed by three days in the desiccator. After that, specimens were exposed to sorptivity tests for more than 400 days. It was shown that the oven-dried samples absorbed nearly as much water than three times as much the air-dried samples.

Dias [2004] recommended using a moderate degree of oven drying (e.g. 3 days at 50°C), so as to increase the sensitivity of the test without significantly reducing its discriminatory power.

Khatib and Mangat [1995] found that concrete samples located at a specific distance from the upper exposed trowelled face have different absorption properties with those located at the same distance from the side face. In all cases concrete close to the top

part (trowelled) of the cube absorbed the largest amount of water compared with the side, which had intermediate values and the bottom, which had the lowest values.

McCarter [1993] studied the influence of surface finish on sorptivity. He found considerably higher sorptivities for top (trowelled) than for bottom (cast) or cut surfaces. However, the depth of water front for the three specimens were similar, indicating that the increased sorptivity of the top surface is mainly due to its increased porosity, perhaps due to a higher paste content near the surface, or to inadequate curing of the surface concrete. Dias [2004] recommended the cast surface for the sorptivity test.

To avoid excessive leaching of calcium hydroxide from the concrete during the sorptivity test, some researchers used saturated calcium hydroxide solution as the absorbing liquid [Sosoro, 1998], while others have noted little or no difference in the absorption rate between this solution and water [Martys and Ferraris, 1997].

The effect of coating the specimen surfaces has been also investigated [Martys and Ferraris, 1997, Dias, 2004]. Martys and Ferraris observed that uncoated specimens which were exposed to the air during the sorptivity tests decreased in weight after the initial increase. The reason was that the reduction in the rate of absorption as the time was increasing combined with the evaporation of moisture from the sample sides led to a decrease in moisture content and thus the weight of the specimen. The uncoated samples placed in a closed container during the sorptivity test had the highest absorption. There was only a small difference between absorption rate of the sample taped on the sides and top surfaces with vinyl tape and those taped only on the sides.

Dias [2004] examined the effect of coating on sorptivity with specimens either coated on side surfaces or coated on side and top surfaces and uncoated specimens. The experimental results indicated that specimen coating have little influence on sorptivity. In standardizing sorptivity test, he recommended coating the side surfaces of the specimen.

The influence of the size of the specimen on the sorptivity of concrete has also been investigated by Dias [2004]. He examined full specimens (100 mm dia. × 100 mm) and sliced specimens (100 mm dia. × 25 mm). He observed that the size of the samples has a little effect on the sorptivity. However, it is important to note that the

thickness of the specimen should be more than the depth of water front to ensure that absorption rate is not affected by the size of the specimen.

While many different methods of sorptivity test have been developed, recently a common procedure has been used for routine and quick sorptivity testing [e.g. Tasdemir, 2003]. In this method, samples are preconditioned by drying at 50°C until constant weight and then allowed to cool in a sealed container for three days. Then one surface of the specimens is exposed to water. Other surfaces are sealed to ensure unidirectional absorption. The increase in specimen weight due to absorption is measured at selected time (typically 1, 2, 3, 4, 5, 9, 12, 16, 20, 25, 36, 49 and 64 minutes). The weight gains are plotted versus square root of the elapsed time. The slope of the line is sorptivity.

This method has also been used in many studies in order to investigate the resistance of concrete to the penetration of chloride where the driving force is absorption. In this case, the absorbing liquid is salt solution instead of water. The chloride penetration is determined by grinding the sample to certain depths and analyzing the chloride content of the concrete powder. For instance, Ramezanianpour & Malhotra [1995] applied this method to investigate the resistance of slag, fly ash and silica fume concretes to chloride penetration under four different curing regimes.

As briefly explained above, sorptivity of concrete has been tested using several different methods. Absorbing solution penetrates into concrete by several transport mechanisms in majority of these methods and pure absorption can be measured only by exposing the suction surface to the absorbing solution.

When sorptivity of concrete is tested by exposing the suction surface to the absorbing solution, the testing period varies from several minutes (25 minutes) to more than a year (400 days) and in some of the test methods specimens are dried artificially at different temperatures. This lack of consistency in the test methods on the one hand and the sensitivity of sorptivity test to initial moisture content on the other hand make it difficult to interpret the reported results, compare them to each other and correlate them to the performance of site structures [Emerson and Butler, 1997].

In addition, none of these methods are representative of site conditions as sorptivity is determined during only one period of wetting. Concrete in the field is intermittently

subjected to wetting events due to rain or condensation and during the drying period internal moisture evaporates progressively from the concrete surface.

In 1997, Emerson & Butler developed a sorptivity test procedure which consisted of a numbers of wetting and drying cycles instead of only one wetting phase to reproduce the site condition. In fact they preconditioned the concrete specimens by exposing them to wet/dry cycles to obtain a sorptivity value which is representative of absorption properties of concrete on site.

The 100mm concrete cubes were subjected to wet/dry cycles using both water and salt solution. Ingress of the liquid was upwards by capillary suction from the exposed surface during the wetting phases. The depths of penetration were calculated from the volume of liquid absorbed which were obtained by a gravimetric technique and the porosity of the specimens. Chloride profiles of samples were also determined by drilling some specimens and analysing the drilled dust. Specimens had higher sorptivities at the first wetting phases and then sorptivities became more stable in subsequent cycles. They suggested consideration of both sorptivities of first wetting phase and sorptivities of subsequent wetting phases.

The procedure for the sorptivity test developed by Emerson & Butler showed the importance of using a pre-conditioning regime of cyclic wetting and drying in order to achieve a repeatable moisture state in samples prior to a test and thus a repeatable sorptivity. Measured sorptivities of pre-conditioned samples were consistent with sorptivities of concretes in the field.

The sorptivity from the first wetting of the cores from one of the concrete pier stems which had been on location for 44 months was approximately the same as the sorptivities from subsequent wettings since the 44 month of exposure had pre-conditioned the concrete. Thus, a pre-conditioning regime is essential in order to achieve a representative sorptivity value for laboratory testing. It is only by this means that a repeatable sorptivity value is obtained. Therefore, the cyclic pre-conditioning regime seems very promising for determination of the absorption characteristic of concrete in the field.

Wetting and drying cycles have been applied in a number of studies. Hong and Hooton [1999] exposed concrete specimens to 25 or 36 wet/dry cycles to study the

effect of wet/dry cycles on chloride ingress in concrete. The wetting phase involved ponding specimens in 1.0 molar NaCl solution for 6 hours and the time of drying was 1 or 3 days. Chloride profiles of samples exposed to various lengths and numbers of cycles were determined for concretes made with different water-binder ratios and different cement replacements. Although they have mentioned that chloride ions penetrate initially by absorption in concrete exposed to wet/dry cycles, they have ponded specimens during wetting phases. As discussed earlier, ponding is not suitable for testing absorption properties of concrete. No measurements were taken on the sorptivity of the concrete. Therefore, the relationship between sorptivity and depth chloride penetration was not discussed.

Polder and Peelen [2002] also used cyclic applications with salt solution and drying regimes to simulate the de-icing salt load of concrete and corrosion of rebar. One face of specimens was exposed to 26 weekly cycles of 24 hours 3% NaCl solution penetration and drying for 6 days in 20°C and 50% RH. They were then exposed to three different climates in a fog room, outdoors and internal with 20°C & 80% RH. Different types of cement and w/c ratios were examined. Chloride penetration, concrete electrical resistivity, steel potential and corrosion rates were measured up to one year of age. However, no measurements were carried out on sorptivity of concrete and thus the relationship between sorptivity and depth chloride penetration was not discussed.

McPolin et al [2005] investigated the rate of chloride penetration during a 48-week cyclic wetting and drying regime. Similar to Hong and Hooton, the concrete specimens were ponded during wetting phases.

To conclude, the sorptivity test method developed by Emerson and Butler seems to be the most suitable approach as it measures the sorptivity by placing the specimens on sponges in contact with water and salt solution and reproduces the site condition by cyclic preconditioning.

2.3.1.4 Factors influencing sorptivity of concrete

Sorptivity is a complex process, a function of both the pore structure of concrete and its moisture state. Pore structure of concrete depends on a variety of factors such as

concrete mix design, curing regime and compaction. The moisture content of concrete depends on the environmental conditions and concrete pore structure. The effect of pre-conditioning, specimen size, coating and surface finish were discussed in the previous section. In this section, the effect of other variables such as concrete mix and curing are investigated.

2.3.2 Effect of chloride binding on absorption

The effect of chloride binding on absorption does not appear to have been investigated to date. However, experimental studies on absorption of chloride contaminated water by concrete [McCarter et al, 1992] have shown that the chloride front moves into the concrete at a slightly slower rate than the pure water in which the chlorides were dissolved, suggesting that chloride binding affects the amount of chloride ions being transported by moisture flow. McCarter et al [1996] using ISAT showed that although the water advanced to a depth of between 40 to 50 mm from the surface, the chloride penetrated only 20 to 25 mm over a period of 24 hours. This shows the significant effect of chloride binding when penetration into concrete occurs by absorption.

Chapter 3

MECHANISM OF CHLORIDE BINDING

Chloride-induced corrosion of steel reinforcement dominates the durability of concrete structures exposed to de-icing salts or seawater. The steel reinforcement in concrete is normally in a passive state against corrosion due to a layer of iron oxide that formed on the steel surface and remains stable in the high alkaline environment of the concrete. However, a localized breakdown of the passive layer occurs when a sufficient amount of chloride ions reaches the steel reinforcement. Then, the corrosion is initiated.

When chloride ions from environmental solutions penetrates into the concrete, some of them are free ions dissolved in the pore solution. The rest are captured by the hydration products. This is called chloride binding. As time proceeding, it is generally recognized that only the free chlorides are responsible for depassivating the reinforcement steel regardless of bound chloride. However, the released bound chloride would be subjected to many harmful factors to the durability problem, such as acidification, carbonation, chemical erosion and stray current, as the bound usually are not firm. The early investigation carried out by Page and Vennesland [1983] showed that Friedel's salt was pH dependent. Glass et al.[2000] found that the bound chloride by different types of cementious material would be released under stable state and the release would be more than 90% when the pH was under 11.5. Ryou and

Ann [2008] and Pruckner and Gjörv [2004] had done similar experiments to validate the result from Suryavanshi and Narayan Swamy [1996], Kayyali and Qasrawi [1992], Valls and Vazquez [2001] and Gerven et al. [2006] have also obtained the phenomenon through tests that bound chloride was released, when subjected to carbonation. Under the action of chemical erosion, the alkali content of the concrete will not drop as acidification and carbonation. However, Friedel's salt is less stable compared with ettringite and aluminum acid calcium carbide. Therefore, Friedel's salt would be substituted and release more chloride ions when SO_4^{2-} and CO_3^{2-}, are abundant. For example, Brown and Badger [2000] have found that Friedel's salt in Na_2SO_4 solution, is totally transformed into ettringite. The research on chloride binding of cement-based materials, showed that under stray current [Geng, 2008] and electrochemical desalination, bound chloride could be got through the charge electricity. In addition, binding chloride would also be released from CSH and Friedel's salt with the temperature raising.

Chloride ions exist in various forms, depending on their origin. In common deicing salt in the form of NaCl, $CaCl_2$, $MgCl_2$ and KCl, while in the seawater exists combined with cations like Na^+, K^+, Mg^{2+}, Ca^{2+} and Sr^{2+}. Research shows that different chloride salt has different effects on inner environment of concrete when emerged: the mixture of $CaCl_2$ restrained the ionization of $Ca(OH)_2$, maintaining a lower pH in the pore solution of concrete, while NaCl offers a higher one. Furthermore, different types of chloride would also result in the changes of microstructure of concrete [Hasson et al 1985]. Concrete with $CaCl_2$, would be looser and contain more pores than concrete with NaCl and KCl, which would result in higher rate of corrosion. Pruckner and Gjorv [2004] showed that the acid neutralization capacity of hydration products (CSH and Friedel's salt) would increase under unstable condition while no obvious changes happened for NaCl. The difference between different chloride cation types could have some effects on the binding capability of chloride in concrete. Consequently, critical theoretical meaning and value has been put into the research of the effect of cation types (Na^+, K^+, Mg^{2+} and Ca^{2+}) on the chloride binding mechanism in concrete. [Zhu et al, 2012]

Zhu et al [2012] claim that chloride binding capability and the pH of pore solution are greatly affected by chloride cation type, with binding capability of Ca^{2+}>Mg^{2+} > Na^{+}~K^{+}.. Na^{+} rises the pH in the pore solution and increases the solubility of Friedel's salt, causing the release of the bound chlorides. K^{+} has similar to that of Na^{+} capability in rising pore solution's pH, leading consequently to a pore solution reach in free chloride ions, too.

Binding of a transported substance will reduce the penetration depth and prolong the time required to penetrate a certain thickness of concrete. The concentration of free substance will also be reduced because of binding effects. Binding of transported substances is also responsible for the slow rate, and small depths, of leaching of calcium hydroxide from concrete and the slow drying of concrete.

The type of interaction behind the binding properties could be very different. Gases, vapours and ions that do not chemically or physically interact with the concrete constituents, will develop a binding capacity, depending on the available pore space and water content of the pore system of concrete. Such a small interaction is relevant for oxygen and alkalis, for example.

A significant example of binding being the decisive part of a transport process is carbonation, where the gas CO_2 is diffusing through concrete but continuously bound, by chemically reacting with CaO, to such an extent that the depth of penetration is very low in a 100-year perspective, even though concrete may be fairly open to the diffusion of a gas. Similar examples are frequent for many transported substances, i.e. moisture, chloride and sulfates.

The binding properties of concrete are given as 'binding isotherms' since most binding properties are temperature dependent. A binding isotherm gives the total or bound amount of the substance versus the state of the substance. [Newman J. et al, 2003]

Chloride binding is of great importance when service life predictions of marine structures are carried out. The common methods of obtaining non-steady state diffusion coefficients are based on fitting profiles of the total chloride content versus

depth. However, since free chlorides in the pore water dominate the driving force (i.e. concentration difference) for diffusion, and the ratio between free and total chlorides is not constant, the resulting diffusion coefficients may be significantly incorrect.

Chlorides may either be chemically bound in compounds like Friedels salt; ($Ca_3Al_2O_6.CaCl_2.10H_2O$), which will be in equilibrium with a constant chloride concentration, or be physically adsorbed on to, for instance, the amorphous calcium silicate hydrate (CSH) gel. Unlike chemically bound chlorides, one could argue that the physical adsorbed chlorides will move towards lower concentrations on the gel surface, but this will certainly be at a much lower rate than the free chlorides in the pore water, which will dominate the diffusion. [Justnes H., 1996]

With regard to the two hydrated phases that can bind chlorides (CSH and AFm), both main chloride binding mechanisms (through physical adsorption and through chemical reactions) will be considered. There are several studies concerning the capacity of the CSH phase to physically bind chlorides. Beaudion, J.J., et al, [1990] identifie three states of chlorides existance: free, adsorbed and interlayer chloride. It is suggested that the adsorbed and interlayer species can be removed by water, while lattice-substituted chlorides cannot be removed by leaching. It is concluded that most of the chloride ions are chemisorbed on the surface of C-S-H and therefore the chloride binding depends on the amount of CSH in the sample. It is also indicated that chloride sorption is dominated by the amount of CSH.

The AFm phase is known to bind chlorides through a chemical reaction, with the formation of Friedel's salt. There are two different mechanisms proposed in literature for this transformation. The first one is the ion exchange mechanism, which implies that chloride ions are bound by replacing hydroxyl ions from the interlayers of the hydroxyl-AFm phase. The second mechanism is based on the fact that the AFm phases have layered structures derived from the structure of portlandite, by the ordered replacement of one Ca^{2+} ion out of three in a $Ca(OH)_2$ layer by an Al^{3+} ion. This substitution causes a charge imbalance in each principal layer, which is corrected by the adsorption of Cl^- ion in the interlayer space. [Qiang Yuan et al, (2009)]

E.P.Nielsen et al [2005] investigate that alkalis have a negative impact on the binding of chlorides because they increase the concentration of chlorides in solution. The absence of iron in white Portland cement is beneficial to chloride binding owing to significant increase in the content of Cl bound by the C-S-H phase compared to conventional Portland cement.

For ordinary Portland concrete with low water/cement ratio, the chloride migration experiments have main conclusions:

- The amount of free and combined chloride is different in non-steady state migration and diffusion experiments. This implies a different rate or mechanism of interaction between chloride and cement phases in the two types of test. For the cement tested, the combined chlorides are similar in diffusion and migration experiments for external chloride concentrations above 1M NaCl (0.25-0.30% free chloride by sample weight).
- The opposite of what happens in diffusion, in a non-steady–state migration experiment, the shape of the chloride isotherm is convex with respect to the x-axis. [Castellote et al,1999]

Blending ground granulated blastfumace slag (GGBS) with some gypsum improve the pore structure and decrease the chloride diffusion coefficient for the expanding reaction between sulfates and C_3A, though sulfates may influence the chloride-binding capability for GGBS.

GGBS can improve the pore structure of OPC concrete and decrease the chloride diffusion coefficient greatly. Sulfates cannot improve the pore structure of GGBS concrete and decrease the chloride diffusion coefficient of GGBS concrete. The internal chloride-binding capability of pastes and mortars increase greatly when 70%OPC is substituted by GGBS. The alkalinity of sulfates also influences the chloride-binding capability greatly. The higher the alkalinity of sulfate, the lower is the chloride-binding capability.

Regardless of internal or external chloride, GGBS can increase the chloride-binding capability greatly, specially the chemical chloride-binding capability, but sulfates and alkalinity decrease the chloride- binding capability greatly. [Luo .R et al, 2003]

The increase of cement replacement by fly ash in concrete resulted in an increase of the percentage of chloride binding capacity (P_{cb}), compared to the total chloride content.

Increasing the exposure time of concrete resulted in a decreasing the percentage of chloride binding capacity (P_{cb}), compared to the total chloride content. [Cheewaket et al, 2010]

3.1 FRIEDELS SALT

The main form of binding of the chloride ions is by reaction with C_3A to form calcium chloroaluminate, $3CaO.Al_2O_3.CaCl_2.10H_2O$, sometimes referred to as Friedel's salt. [Neville, 2002]. Friedal's salt formation provides a sink for chloride and in doing so may decrease the concentration driving force for the migration of chloride towards embedded steel. [Brown and Bothe, 2004]

Trætteberg [1977] was able to identify Friedels salt by XRD and DTA in paste, only when $CaCl_2$ was the chloride source, and not when NaCl was.

Lambert et al [1984] investigated steady state diffusion of 1M NaCl through 3 mm paste discs of pure alite (i.e. C_3S), alite mixed with 12 % C_3A and sufficient gypsum (4 %) to avoid flash set. The water-to-powder ratio was 0.6 and the specimen cured for 7 days prior to chloride exposure. The steady state diffusion coefficients were determined for different temperatures and the activation energy determined for chloride diffusion. The latter was not particularly different (33 kJ/mole) from the activation energy of OPC with the same w/c, which indicates that the mechanism is diffusion through the CSH gel. The addition of C_3A to alite lowered the diffusion rate in spite of coarser pores. Thus, the reason may be formation of Friedels salt that was determined in the latter sample by DTA/TG. However, in theory steady state diffusion is independent of chloride binding unless it will lead to a densification of the pore system.

Midgley and Illston [1986] identified Friedels salt when NaCl intruded well-cured cement paste. They also investigated the pore size distribution and concluded that the chloride ingress lead to a larger fraction of finer pores on the expense of larger.

Theissing et al [1986] investigated chloride binding from both NaCl (≤11%) and $CaCl_2$ (≤10%) in the cured minerals C_3S, C_2S, C_3A and C_4AF (w/b = 0.7). The chloride intruded the paste in the sense that lumps cured for 28 days were placed in chloride solution (solution: solid = 5:1) until equilibrium (10-14 days). Thereafter, the remaining chloride concentration in the solution was determined. The authors found that C_4AF binds just as much chlorides as C_3A, both from NaCl and $CaCl_2$, but that the minerals bind much more chlorides from $CaCl_2$ than from NaCl. C_3A and C_4AF bind much more chlorides than C_3S and C_2S. While the binding in C_3A and C_4AF was attributed to Friedels salt formation, the binding by C_3S and C_2S was explained by sorption.

Several cited studies have found that the pH increases during chloride binding when NaCl is the chloride source. This may be explained by the following reaction:

$$2NaCl_{(aq)} + Ca_3Al_2O_6 \cdot 6H_2O_{(s)} + Ca(OH)_{2(aq)} + 4H_2O \rightarrow$$

$$Ca_3Al_2O_6 \cdot CaCl_2 \cdot 10H_2O_{(s)} + 2NaOH_{(aq)} \qquad 3.1$$

When pH is increased, this will also decrease the already sparingly soluble calcium hydroxide, so the reaction will be slowed down further. This can explain why the chloride binding is higher when calcium chloride ($CaCl_2$) is the chloride source:

$$CaCl_{2(aq)} + Ca_3Al_2O_6 \cdot 6H_2O_{(s)} + 4H_2O \rightarrow Ca_3Al_2O_6 \cdot CaCl_2 \cdot 10H_2O_{(s)} \qquad 3.2$$

The fact that both C_3A and C_4AF binds chlorides [Theissing et al, 1986] shows that a Friedel's salt analogue is formed where aluminium wholly or partly is substituted by iron, or that Friedel's salt itself is formed from the hydration product of the ferrite phase. Formerly the following reaction was put forward for C_4AF hydration;

$$C_4AF + 2CH + 10H \rightarrow C_3AH_6 + C_3FH_6 \qquad 3.3$$

However, it is now commonly accepted that the reaction between the ferrite phase and water is

$$C_4AF + 10H \rightarrow C_3AH_6 + FH_3 + CH \qquad 3.4$$

where FH_3 denotes an amorphous iron hydroxide. Nørlund Christensen et al [1986] identified both C_3AH_6 and CH as reaction products between C_4AF and heavy water by neutron diffraction, while Plowman and Cabrera [1984] identified C_3AH_6 by XRD. Brown [1993] studied the reaction products from the ferrite phase in presence of the calcium sulphates gypsum and hemi-hydrate. He showed that C_4AF like C_3A did form Ettringite in the presence of calcium sulphates, and that little iron was present in the aluminate product. No matter which of reactions 3.3 and 3.4 are correct, both transform the aluminate part of the C_4AF to a product that can take part in the chloride binding process. Thus, if the chloride binding in mature paste or mortar is to be correlated against cement type, the total content of Al should be used rather than C_3A. [Justnes H., 1996]

Luo et al, [2003] claim that Friedel's salt appears at about 8.0 Å for hydrated pastes, its endothermal peak is at about 360 ˚C and its morphology is hexagonal slice whose size is between 2 and 3 μm. The fact that GGBS can form more Friedel's salt is the reason why GGBS can increase the chloride-binding capability, and the reason why sulfate and alkalinity influence chloride binding, is the competition among sulfate ions, hydroxyl ions and chloride ions during the formation on Friedel's salt.

Table 3.1: Properties of mortars [Luo .R et al, 2003]

Code	Mixed ratio (B:W:S)	Binder and content (%)
M1	1:0.6:3	C(100)
M2	1:0.6:3	C(30) + G(70)
M3	1:0.6:3	C(30) + G(65) + CS(5)

Luo et al, [2003] made different samples and they also found that it is difficult to find ettringite in M1 but it is easy to find it in M2. This clarifies that GGBS pastes were formed much more than Friedel's salt. The fact that it is difficult to find ettringite in M2 and it is easy to find it in GGBS pastes, with some sulfates added and with the coexisting phenomenon of Friedel's salt and ettringite in M3 mortars, indicate that competition exists between chloride ions and sulfate ions.

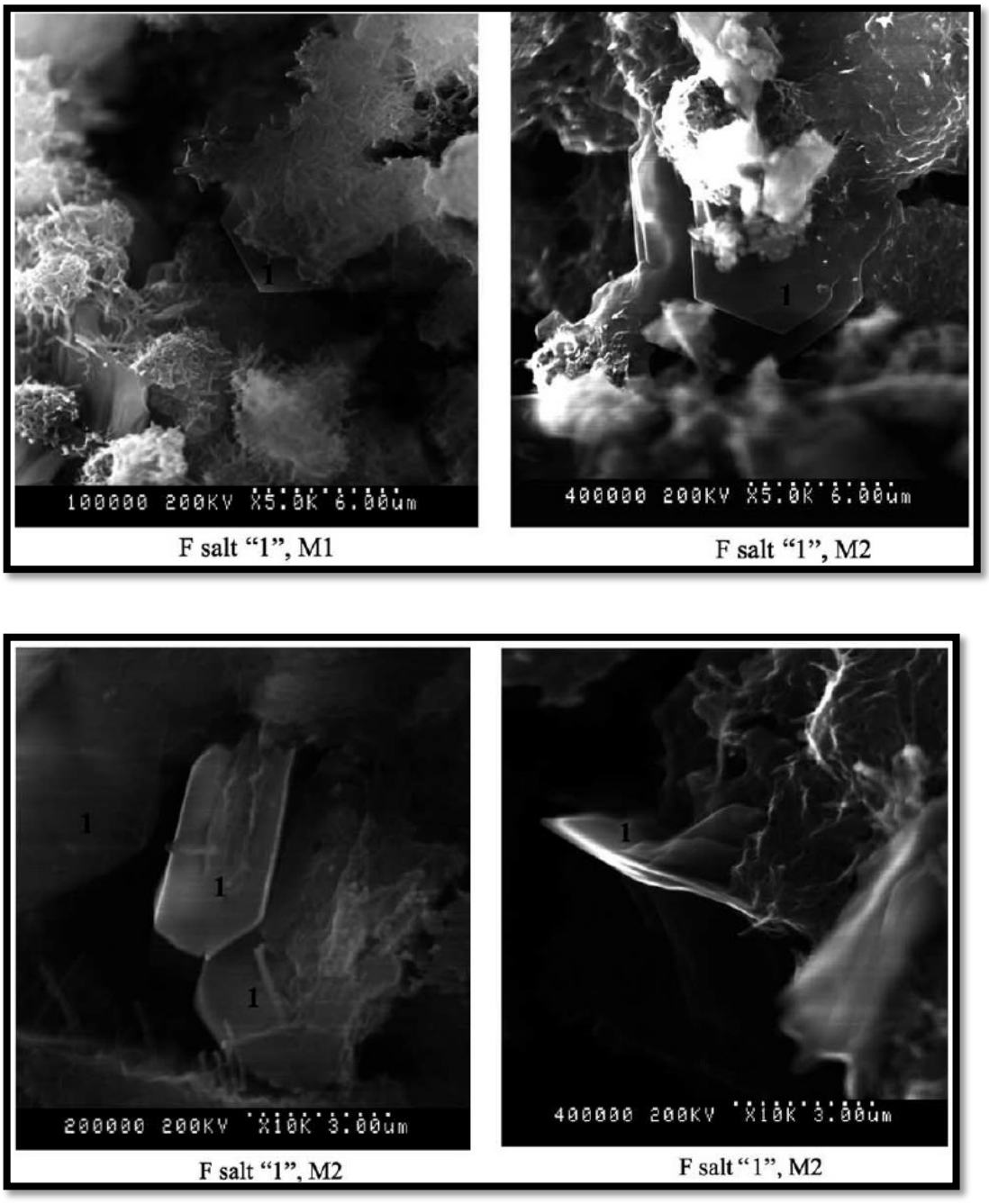

Figure 3.1: photo of morphology of Friedel's salt [Luo .R et al, 2003]

The mechanism of Friedel's salt formation in cement pastes has not been unambiguously identified. Essentially, two mechanisms have been proposed as follows:

Mechanism 1: The conversion of hydroxy-AF_m to Friedel's salt by ion exchange. This mechanism can be tested by following the conversion process as a function of added NaCl. However, NaCl behaves not as a single component but as two components, Na^+ and Cl^-. In this instance, the concentration of Na ($[Na^+]$) becomes greater than $[Cl^-]$ in the aqueous phase of cements because the Cl becomes structurally incorporated into the precipitating Friedel's salt. In order to compensate for the charge imbalance in solution, OH^- is released, thus when $[Cl^-]$ bound, $[OH^-]$ released.

Mechanism 2: The absorption of Cl^- as Friedel's salt forms by precipitation. Friedel's salt consists of two principal $[Ca_2Al(OH)_6 \cdot 2H_2O]^+$ layers that require balancing negative charge for stability. The availability of Cl^- (from dissolved NaCl) would satisfy charge neutrality in the solid but this would disturb the ionic charge balance in the pore solution. To compensate for this however, an equivalent amount of Na^+ ions would be required to leave the pore solution, i.e. be absorbed into solid phases. [Jones et al, 2003]

The stability of Friedel's salt is pH dependent, that is, if the pH falls, for example due to carbonation, the dissolution of Friedel's salt will increase and free-chloride ions are released into the pore solution [Suryavanshi et al, 1996]

Talero et al [2011] investigation shows that the largest Friedel's salt amount has been formed with the PC blends and activated clay blends, at every age. The reason is the greater C_3A and $Al_2O_3^{2-}$ content that blended cements have compared to PC. They claim also in their study that Friedel's salt owns its formation to two different origins: reactive alumina ($Al_2O_3^{-2}$) of pozzolans and tricalcium aluminate (C_3A) of own OPC. The compound formation can be result of the C_4AF reactivity at later ages, as well. They also mentioned a rapid forming present of FS or FS-rf originated from $Al_2O_3^{-2}$, present in pozzolanic cements and a slow forming of FS or FS-lf, from C_3A origin, present in PC. The quantity of Friedel's salt formed in the PC blends (principally, of

pozzolanic origin), has maintained more direct relationship with the respective Al_2O_3 content (%) of the pozzolans, than with their SiO_2(%) content.

3.2 C-S-H GEL SORPTION

The relative ability of C-S-H to bind chloride has important implications for durability assessment. The amount of chloride held by C-S-H in the so-called chemisorbed state is dependent on H/S ratio, C/S ratio and nitrogen surface area. The degree of layering of the C-S-H, decreases with the increase of the surface area [Beaudoin et al, 1990]. They also claim that the C-S-H formed in silica fume pastes, which has a lower C/S ratio than those of C-S-H in ordinary cement paste, binds less chloride, leaving available Cl^- for the pore solution.

Trætteberg [1977] studied the ingress of NaCl and $CaCl_2$ into cement paste and concluded that the chlorides are adsorbed onto the CSH gel and that chloride diffusion takes place on the gel surface. She also thought that neither the C_3A nor the (C_3A+C_4AF) content, were decisive for the chloride intrusion.

Lambert et al [1985)] investigated the chloride binding in pure Alite when 1 and 2 % Cl^- of the Alite weight were added as NaCl dissolved in the mixing water (w/b = 0.6). They concluded that there was no significant chloride binding after 200 days sealed curing at 20°C, which indicates that the adsorption of chlorides play a minor role.

Tang and Nilsson [1993] determined chloride binding isotherms for OPC paste and mortar with w/c = 0.4, 0.6 and 0.8. They concluded that the chloride binding depends on the amount of CSH in the sample and that it is independent of the w/c. The ratio between free and bound chlorides could be described by a Freundlich isotherm for high chloride levels (>0.01 M) and by a Langmuir isotherm for low (< 0.05 M) concentrations. The chloride source was NaCl and hardened, dried (11 % RH) paste was added to the different solutions. They pointed out that a fraction of bound chlorides was irreversible, while others were released when the chloride level again was decreased. [Justnes, 1996]

The experimental results show Chloride binding capacity of OPC concrete is strongly dependent on the content of CSH gel in concrete regardless of the water-cement ratio and the addition of aggregate. [Luping and Nilsson, 1993]

There are several studies concerning the capacity of the CSH phase to physically bind chlorides [Justnes, (1996), Beaudoin et al (1990)]. In Beaudoin et al (1990) work three states of chlorides are identified: free, adsorbed and interlayer chloride. It is suggested that the adsorbed and interlayer species can be removed by water, while lattice-substituted chlorides cannot be removed by leaching. It is concluded that most of the chloride ions are chemisorbed on the surface of CSH and therefore the chloride binding depends on the amount of CSH in the sample. It is also indicated that chloride sorption is dominated by the amount of CSH [Justnes, 1996].

In order to explain the capacity of the CSH phase to physically bind chlorides, the electrical double layer theory has been considered [Hassan, 2001]. According to this model, the chloride binding capacity of the CSH phase depends on a number of parameters, such as: the specific surface of the CSH gel, temperature, concentrations of various ions in the pore solution and their respective electrical charge [Marinescu and Brouwers, 2009].

3.2.1 Structural models of C-S-H:

The calcium silicate hydrates are the principal binding phase in hardened ordinary Portland cement concrete. With more than 100 years of study, the exact compositional and microstructural nature of C-S-H, however, is still unclear. One primary reason for the embarrassing situation is that the formation of C-S-H phase is generally affected by many factors including mainly the composition of the cement, the water-to-cement ratio (w/c), the degree of hydration and the curing temperature. These influential factors cumulatively could result in tremendous variations in the composition, nanostructure and morphology of the C-S-H phase. For this reason, fundamental research on C-S-H chemistry usually starts with pure compounds.

Using X-ray crystallography, Bernal et al. [1952] found that the C-S-H formed in hydrated C_3S pastes was much more amorphous than the C-S-H (I) and C-S-H (II) prepared in dilute suspensions with low and high Ca/Si ratios, respectively. C-S-H (I) has a fibrous structure and is similar to tobermorite, a rare crystalline C-S-H that has a chemically determined constitution of $Ca_5Si_6O_{16}(OH)_2 \cdot 4H_2O$ with a Ca/Si ratio of 0.83. Tobermorite contains linear silicate chains of the 'dreierkette' form in which the silicate tetrahedral coordinate themselves to Ca^{+2} ions in a kinked pattern for every three tetrahedra [Megaw and Kelsey, 1956]. Based on the comparison of C-S-H and clay minerals, Taylor and Howison [1956] suggested that the Ca/Si ratio could be raised above 0.83. Nevertheless, with its structural similarity to C-S-H (I), tobermorite has been used predominantly as the basic structure to model the C-S-H phases of hydrated cement.

Starting with the dreierkette silicate chains as observed in tobermorite, various models have subsequently been proposed for C-S-H. These models fall into two general groups depending on the approaches adopted to increase the Ca/Si ratio to the value as observed experimentally in ordinary cement paste, i.e. 1.7–1.8 [Dent Glasser 1978, Richardson 2000]. The first group of C-S-H models, also known as the T/CH models, consists of the basic tobermorite structure interstratified with layers of calcium hydroxide [Kurczyk and Schwiete, 1960, Kantro et al. 1962]. The second group of models, known as the T/J models, involves the basic jennite structure intermixed with tobermorite [Taylor, 1986]. Also based on dreierkette silicate chains, jennite is a crystalline C-S-H that has the constitutional formula of $Ca_9Si_6O_{18}(OH)_6 \cdot 8H_2O$ and a Ca/Si ratio of 1.5. Compared to tobermorite, jennite has a higher Ca/Si ratio (1.5) and a corrugated central Ca–O part.

Starting from the T/CH and T/J points of view, more comprehensive models have recently been developed to characterise the C-S-H phase of hydrated cement [Richardson and Groves, 1992, Chen et al. 2004]. Richardson and Groves proposed a model starting from a generic form of calcium silicate hydrate consisting of isolated silicate chains of varying lengths and with a variable number of hydroxyl groups attached to the Si atoms. Including a variable amount of $Ca(OH)_2$, this model incorporates both T/CH and T/J viewpoints and shows applicability to interpret a

broader variety of experimental results. Other T/CH and/or T/J-based C-S-H models have been found to be in general agreement with the Richardson and Groves model Cong and Kirkpatrick, 1996, Kirkpatrick et al, 1997, Pan et al, 2010].

Florea and Brouwers [2012] explain that the surface of the C-S-H gel is known to be negatively charged, because the charges of the bridging silica tetrahedra are not always compensated. This observation leads to applying the electrical double layer (EDL) theory, in order to explain the adsorption capacity of different ions of the C-S-H surface. This theory had become more and more complex, allowing for the existence of three electrically charged layers, interfacial regions, and taking into consideration the size of the ions and their distance from the surface of the solid. Henocq [2005] explains the adsorption of chloride ions on the surface of C-S-H by applying the model of the triple layer described by Stern [1924] and Grahame [1947] to the interface C-S-H/pore solution. Based on the interpretation of electrokinetic potential curves, a structure made of a condensed layer of Na^+ ions on the surface, compensated partly by SiO^- groups and partly by an external layer made of hydroxyl ions (and chloride ions, in the presence of chlorides) was proposed. This external layer allows ionic exchanges with the solution. The adsorption of chloride ions can therefore be explained by an exchange mechanism between chloride ions from the pore solution and hydroxyl ions from the C-S-H layers. The OH^- ion is loosely bound, permitting the Cl^- ion to be substituted in the interlayer space and ensure the electroneutrality of the system. This physical adsorption mechanism of chloride ions on the surface of the C-S-H gel explains the fact that C-S-H has a lower chloride binding ability than the AFm phase, which binds chlorides through chemical substitution.

The EDL theory implies the influence of several factors over the chloride binding ability of the C-S-H gel, the most important of which are the C/S ratio of the gel, the composition and pH of the pore solution and associated cation of the chloride ion.

A usual pH is assumed for the pore solution and a C/S ratio of 1.7 for the C-S-H gel. Moreover, the C-S-H gel and the pore solution are considered to be homogenous in composition throughout a hardened paste in equilibrium with its surrounding solution.

Therefore, all C-S-H should have the same chloride binding ability, regardless of its source (C_3S or C_2S) and the pore solution is considered to have a constant pH throughout the sample.

3.3 COMPOUNDS WITH CALCIUM HYDROXIDE

A further mechanism by which chloride can de bound is through the formation of calcium oxychlorides. A number of calcium oxychlorides are known such as $Ca(OH)_2.CaCl_2.H_2O$ (the so-called 1:1:1 compound) and a $Ca(OH)_2CaCl_2$ (a ratio greater than unity) [Brown and Bothe, 2004].

Smolczyk [1969] showed that concrete stored in strong (3M) $CaCl_2$ solution was deteriorated by an expanding product confirmed to be $CaCl_2.Ca(OH)_2.H_2O$. All the calcium hydroxide was disappeared in cement paste stored in this solution.

Trætteberg [1977] did an interesting observation that was not further commented by her: The calcium hydroxide concentration in the outer layer of paste (w/c = 0.5) from 5 different cement types was measured by DTA/TG and XRD after external exposure to NaCl and $CaCl_2$ in 21 days, 10 weeks and 1 year. The paste was relatively unaltered by the storage in NaCl, while the calcium hydroxide content decreased and disappeared after 1 year during exposure to $CaCl_2$ solution with 1.98 % Cl^-. This may be due to compound formation between $CaCl_2$ and $Ca(OH)_2$ as shown in Eq.(3.6). Lambert et al [1985] investigated the chloride binding by pure alite when 1 and 2 % Cl^- by alite weight was added by dissolving NaCl in the mixing water (w/c = 0.6). In contradiction to Ramachandran [1971] who thought that the CSH-gel could bind large amounts of chlorides when the source was calcium chloride, they concluded that there was no significant chloride binding after 200 days sealed curing at 20°C. These observations indicate that calcium chloride form compounds with calcium hydroxide (the other product from alite hydration), while sodium chloride do not.

Markova [1973] identified the compounds $CaCl_2 \cdot 3Ca(OH)_2 \cdot 12H_2O$ and $CaCl_2 \cdot Ca(OH)_2$ in the system $CaCl_2$ - $Ca(OH)_2$ - H_2O at 25°C.

In order to investigate the possible formation of such compounds at lower concentrations than those used by Smolczyk [1969], the present author added an arbitrary amount of calcium hydroxide to a 1 M solution of $CaCl_2$. The mix was shaken daily in one week and thereafter filtered. The precipitate was dried in a dessicator and investigated by XRD. The diffractogramme is shown in Figure 3.2 as a solid line. A number of new reflections were observed that do not arise from calcium hydroxide or any of the calcium chloride hydrates. Furthermore, the chloride concentration in the initial solution was measured to 1.8 M Cl^- and to 1.6 M in the filtrate, which indicates a certain chloride binding. Unfortunately, the ratio between calcium hydroxide and solution was not determined, but the principle was documented. A corresponding experiment was performed for a 2M NaCl solution and the X-ray diffractogramme of the filtered residue is also shown in Figure 3.2 as a dashed line. Only the reflections of calcium hydroxide are apparent with the exception of a few weak ones. The chloride content in the original solution and the filtrate was determined to 1.87 and 1.83 M Cl^-, respectively. The observation indicates that NaCl do not form compounds with calcium hydroxide to any significant extent. The filtrate also had a pH of 12.60, which consist a very weak increase compared to the equilibrium value of 12.55 for pure calcium hydroxide.

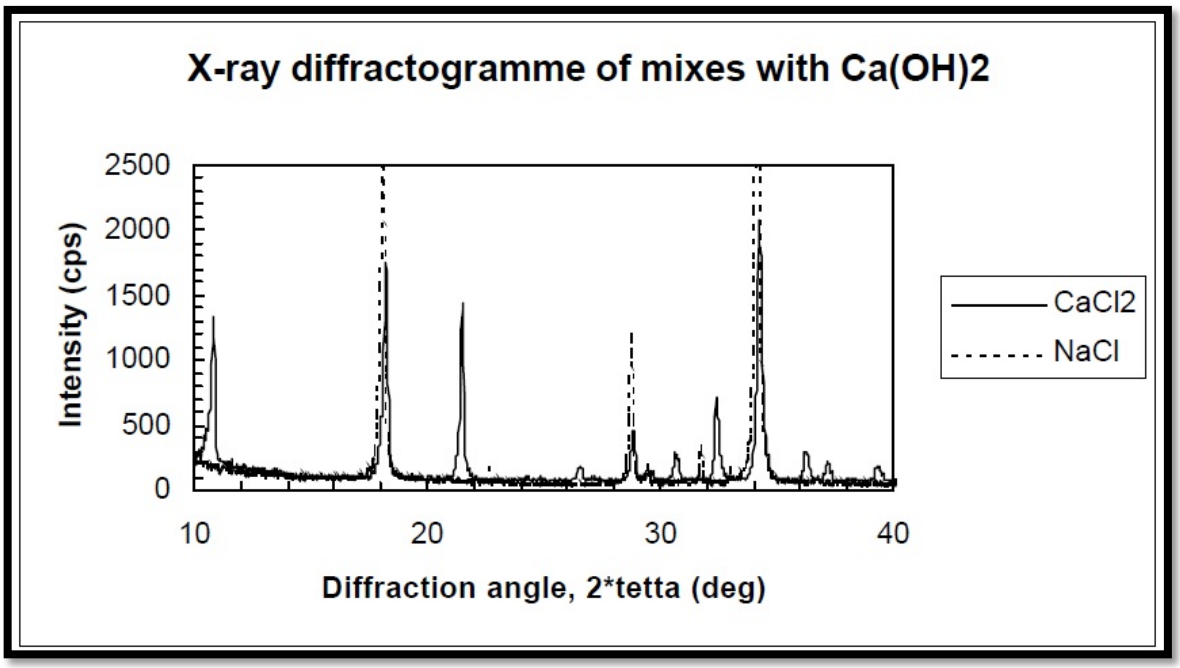

Figure 3.2: X-ray diffractogram of the filtrate from $Ca(OH)_2$ mixed with 1 M $CaCl_2$ (solid line) and 2 M NaCl (dashed line).

The conclusion is that the reaction 3.5 is negligible, and that the reaction 3.6 proceeds well to the right [Justnes, 1996]

$$2NaCl_{(aq)} + 4Ca(OH)_{2(s)} + 12H_2O \rightarrow CaCl_2 \cdot 3Ca(OH)_2 \cdot 12H_2O_{(s)} + 2NaOH_{(aq)} \quad 3.5$$

$$CaCl_{2(aq)} + 3Ca(OH)_{2(s)} + 12H_2O \rightarrow CaCl_2 \cdot 3Ca(OH)_2 \cdot 12H_2O_{(s)} \quad 3.6$$

3.4 OTHERS

3.4.1 Chloride threshold value

Corrosion of the reinforcement will start when the chloride concentration in contact with the steel surface reaches a critical threshold value. Critical chloride threshold is defined as the minimum quantity of total or free chlorides required to initiate rebar

corrosion under optimal moisture, temperature, and oxygen [Cook and McCay, 1997]. This chloride threshold value is, together with other factors, controlled by the availability of oxygen, which is needed for corrosion to take place. Tests show that a precise threshold value is not easy to determine, [Ann and Song, 2007], but it could be seen as the probability for corrosion to start at some range of chloride concentration.

The chloride threshold value has been investigated by numerous researches over the years. Varying techniques for measurements are available to determine chloride threshold values, but there are a lot of uncertainties which make it difficult to rely on the results totally and a wide range of threshold values has been the consequence. [Ann and Song, 2007].

It was suggested in early works that only free chlorides affect the corrosion, but it is most common to express the threshold value in total chlorides, (free + bound). This has the advantages that it is easier to measure the total chloride content and also the fact that when corrosion is initiated, if the pH value drops, a great part of the surrounding bound chlorides will be released and contribute to the corrosion [Ann and Song, 2007].

In Bertolini et al. [2004] research an important factor described is the electrochemical potential of steel, which highly depends on the availability of oxygen at the steel surface. Therefore the state of moisture essentially influences the threshold value. For submerged condition the threshold value is higher than for conditions above sea level and it can be more than one order of magnitude larger. Also the voids close to surface of the reinforcement bar is a factor to account for. When the volume of air voids was decreased from 1.5 % to 0.2 %, the threshold value, which was defined as the chloride content when corrosion initiated, was increased by a factor of 10 from 0.2 % to 2 % of cement weight [Bertolini et al., 2004].

The chloride binding capacity influences the threshold value as well, where especially the amount of C_3A, (related to the AFm phase), in the cement paste affects the binding capacity. It has been shown that the threshold level increased when the C_3A content for plain cement increased [Ann and Song, 2007]. If only the free chlorides contribute to the corrosion it is reasonable to assume that for increased binding capacity, the

corrosion risk will be lower and the threshold value higher. Although this positive effect of binding, the bounded chlorides, as mentioned, may be released when the pH drops and contribute to the corrosion.

A wide range of different threshold values that have been suggested in literature is stated in a table by Ann and Song [2007]. The range reaches from 0.079 up to maximum 2.9 (total chloride % by cement weight), depending on varying detection methods, specimens and conditions.

In the report by Sandberg [1998] experiments on concrete specimens from the Swedish west coast, Träslövsläge, were analysed. For concrete with w/c ratio of 0.4 and 5 % silica fume, threshold values from 0.8 % to 1.4 % by cement weight were found.

In Arya et al. [2014] the authors used a threshold value of 0.05 % of concrete weight when studying chloride profiles of concrete exposed to cyclic wetting and drying.

Fluge [2003] suggests a threshold value of 0.72 % chlorides of cement weight, based on measurement in 110 locations of the Gimsøystraumen Bridge in Norway. From the measurements of corrosion the results are divided into five groups, no corrosion, start of depassivation, corrosion, heavy corrosion and heavy corrosion and pitting. The threshold value was defined as when corrosion has occurred. The level for start of depassivation was found to be 0.44 % of cement weight or 0.08 % of concrete weight.

In Ann and Song [2007] a table is shown giving threshold values (% by cement weight) that are stated in different standards. The standards are BS 8110, ACI 201, ACI 357 and ACI 222 and values are given for prestressed concrete, reinforced concrete exposed to chlorides in service, reinforced concrete that will be dry or protected from moisture during service and for other reinforced concrete. The threshold value is lowest for prestressed concrete, 0.06-0.10 % by cement weight or 0.01-0.02 % by concrete weight, and for reinforced concrete exposed to chlorides the value is 0.10-0.20 % by cement weight or 0.02-0.04 % by concrete weight. The highest value given is 0.40 % by cement weight or 0.07 % by concrete weight and it is for dry, reinforced concrete.

In the report which describes the DuraCrete model, The European Union – Brite EuRam III [2000], critical chloride threshold values are specified for different concrete types and environments. For submerged conditions, these threshold values are very high, 1.6 % to 2.3 % relative to binder. For the tidal and splash environment and for a concrete type with water binder ratio equal to 0.4, the threshold value is stated to 0.8 % relative to binder. These values are characteristic values and have to be divided by partial factors.

Various suggestions of the threshold value were found and one factor is the spread in measurement techniques. Also, the difference between design and characteristic values is not always easy to determine. [Gutierres abd Hallberg, 2014]

3.5 CONCLUSION

They are several factors that influence the chloride binding. Chlorides mainly may either be chemically bound in compounds like Friedels salt; ($Ca_3Al_2O_6.CaCl_2.10H_2O$), or be physically adsorbed on to, for instance, the amorphous calcium silicate hydrate (C-S-H) gel. A further mechanism by which chloride can de bound is through the formation of calcium oxychlorides.

The main form of binding of the chloride ions is by reaction with C_3A to form Friedel's salt (Or calcium chloroaluminate). Two mechanisms have been proposed of Friedel's salt formation in cement pastes. I) The conversion of hydroxy-AF_m to Friedel's salt by ion exchange. II) The absorption of Cl as Friedel's salt forms by precipitation. The stability of Friedel's salt is pH dependent. If the pH falls, for example due to carbonation, the dissolution of Friedel's salt will increase and free-chloride ions are released into the pore solution.

Chlorides could be adsorbed onto the C-S-H gel and that chloride diffusion takes place on the gel surface. The formation of C-S-H phase is generally affected by many factors including mainly the composition of the cement, the water-to-cement ratio (w/c), the degree of hydration and the curing temperature. The chloride binding

capacity of the C-S-H phase depends on a number of parameters, such as: the specific surface of the C-S-H gel, temperature, concentrations of various ions in the pore solution and their respective electrical charge.

Corrosion of the reinforcement will start when the chloride concentration in contact with the steel surface reaches a critical threshold value. Critical chloride threshold is defined as the minimum quantity of total or free chlorides required to initiate rebar corrosion under optimal moisture, temperature, and oxygen. It has been shown that the threshold level increased when the C_3A content for plain cement increased.

Blending ground granulated blastfumace slag (GGBS) can increase the chloride binding capability greatly, specially the chemical chloride binding capability, but sulfates and alkalinity decrease the chloride binding capability greatly. The alkalinity of sulfates also influences the chloride binding capability greatly. The higher the alkalinity of sulfate, the lower is the chloride binding capability. The increase of cement replacement by fly ash in concrete could also resulted in an increase of the percentage of chloride binding capacity, compared to the total chloride content. Also, increasing the exposure time of concrete resulted in a decreasing the percentage of chloride binding capacity.

Chapter 4

EFFECT OF DIFFERENT FACTORS ON CHLORIDE BINDING

Chloride in concrete can be either dissolved in the pore solution (free chlorides) or chemically and physically bound to the cement hydrates and their surfaces (bound chloride).

The aluminate (C_3A) and aluminoferrite (C_4AF) phases in cement have been found to be responsible for the chemical binding of chloride. These two phases form Friedel's salt and calcium chloroferrite. The degree of binding depends on the amount of aluminate and aluminoferrite phases present in the cement [Sumranwanich and Tangtermsirikul, 2004].

In physical binding, chlorides are adsorbed on the amorphous calcium silicate hydrate (CSH) gel [Justnes, 2001]. Physical binding therefore depends upon the volume of hydration products, particularly the amount of C-S-H gel produced [Sumranwanich and Tangtermsirikul, 2004].

Chloride binding in concrete is affected by many factors, such as type of cement, type and proportion of cement replacement material, water to cement ratio, curing time prior to chloride attack, temperature, chloride concentration and so on [Sumranwanich and Tangtermsirikul, 2004]. For example, replacement of cement or addition of fly

ash and ground blast furnace slag increases chloride binding since these mineral additives produce additional calcium aluminates during hydration. [Justnes, 2001]

4.1 CEMENT TYPE

The most important parameter that affects the chloride binding capacity of a hardened paste is the composition of the cement. The C_3A content will determine the amount of AFm phase, while the amount of C_3S and C_2S can be correlated with the amount of CSH formed upon hydration. C_4AF will also play a role. The amount of SO_3 in the cement composition will determine the composition of the AFm phase, as well as the quantity of AFt phase [Marinescu and Brouwers, 2009]

Lambert et al [1985] referred in their introductory review to an investigation [Holden et al, 1983] where the chloride binding of the cement paste increased with increasing C3A (i.e. short hand notation for the clinker mineral $Ca_3Al_2O_6$) content of the cement, and the amount of free chlorides in the pore water increased when sulphate was added as well. They also showed that chloride binding from NaCl lead to a significant increase of the pH (i.e. OH^- concentration).

Arya et al [1990] investigated the chloride binding in two types ordinary Portland cement (OPC) with the same C_3A content and a sulphate resistant Portland cement (SRPC). 1% Cl^- was added as NaCl (w/c = 0.50) and the paste cured for 28 days prior to testing. The chloride binding was considerably less in the SRPC compared with OPC, but there was a significant difference between the two OPCs as well, which was not satisfactorily explained. Unfortunately, the fineness was not given for both. They also investigated paste without added chlorides, which was rather stored in a solution of 20 g Cl^-/l ($\approx$ concentration in sea water) for 28 days after 2 days initial curing before investigation. The difference in chloride binding between the three cements was then much less, but the trend was the same.

Rasheeduzzafar et al [1991] studied the chloride binding in two cements with 2.43 and 14.00 % C_3A, respectively, when different concentrations of NaCl (corresponding

to 0.3, 0.6 and 1.2 % Cl^- Cl^- by weight of cement) was added to the mixing water (w/c = 0.60). The pore water was expressed from the pastes after 180 days sealed curing. They also included data from Page and Vennesland [1983] in their discussion. They concluded that the amount of free chloride decreased with increasing C_3A, and that the amount of bound chloride decreased with increasing OH^- concentration from the cements. An alternative explanation is that the hydroxides originate from the reaction of minor alkali sulphates in the cement (e.g. the clinker mineral Aphthithalite), and that the chloride binding is reduced since sulphates are stronger bound.

The following year Rasheeduzzafar et al [1992] studied the chloride binding in 5 different portland cements with a C_3A content ranging from 2.04 to 14.00 according to Bogue calculations. The chloride source was NaCl dissolved in the mixing water (w/c = 0.60) in dosages of 0.3 to 2.4 % of the cement weight. The chloride binding increased with increasing Cl concentration to a certain level where saturation was obtained. Experiments were also performed where the chlorides diffused into the paste, and the conclusion was then that the binding occurred to a lesser extent.

Ehtesham Hussain et al [1994] measured the chloride binding in three Portland cements with C_3A contents 2.43, 7.59 and 14.00 %. The chloride source was NaCl dissolved in the mixing water (w/c = 0.6) corresponding to 0.6 and 1.2 % $Cl^-$of the cement weight. The samples were cured for 180 days prior to pore water expression. The content of free chlorides decreased with decreasing C_3A, which is consistent with the formation of Friedel's salt. The authors extended the study with the Cl^- concentrations 0.3 and 2.4 % and otherwise similar conditions the following year [Ehtesham Hussain et al, 1995], and concluded that the chloride concentration in the pore water decreased with increasing C_3A content for all Cl^- dosages.

Suryavanshi et al [1995a] compared the chloride binding in SRPC (1.41 % C_3A) with that of OPC (11.2 % C_3A). The chloride source was NaCl dissolved in the mixing water of mortar with 400 kg cement/m_3 and a w/c of 0.7. Even though the chloride binding was considerably greater in the OPC, the SRPC also bound chlorides corresponding to 46, 31 and 12 % of the 1.00, 1.75 and 3.00 % Cl^-additions,

respectively. The authors attributed this to the development of a Friedels salt analogue, where aluminium is replaced with iron, but also to the production of either Friedels salt (see C_4AF hydration under section 9.1) or to mix of the two (i.e. solid solution of aluminium and iron). X-ray diffraction (XRD) and differential scanning calorimetry (DSC) supported this. The authors also [Suryavanshi et al, 1995a] measured the pore size distribution by mercury intrusion porosimetry (MIP) of mortar based on OPC and SRPC and with and without chlorides (1.75 % Cl^- from both NaCl and $CaCl_2$). The total porosity decreased when chlorides were present, but the fraction of coarser pores increased. The authors explained this by the formation of a denser CSH (i.e. change in morphology) due to the free chlorides in the pore water. The difference was greater for SRPC than OPC, which then could be understood by the less binding of chlorides. The lesser total porosity in presence of chlorides, could be attributed to the higher degree of hydration, which chlorides favour, as hardening accelerators.

Dealgrave et al [1997] studied the chloride binding capacity of ASTM type I and V with C_3A contents 7.4 and 1.8, respectively, and w/c = 0.45. The degree of hydration was 67-68 % for both cements upon testing and the bound chloride, C_b (mg Cl^-/g sample), vs. free chloride, C_f (mole Cl^-/l solution), profiles were almost identical for both cement pastes following the Langmuir sorption isotherm $\log C_b = a \cong \log C_f + b$ for $C_f > 0.01$ M. The constants a and b and the correlation factor R^2 of the linear regression analysis were 0.5133, 1.048 and 0.992 for the ASTM type I and 0.4757, 1.037 and 0.997 for the ASTM type V cement, respectively. They concluded like Tang and Nilsson [1993] that the chloride binding was controlled by the total amount of CSH gel in the paste. [Justnes, 1996]

The effect of the cement type on the bound chloride was also investigated by Mohammed and Hamada [2003]. Their research confirmed that a high chloride binding capacity was found in higher calcium aluminate cement than in lower calcium aluminate cement. In addition, the use of pozzolanic materials can increase the binding ability of chloride.

According to Loser et al [2010] research about chloride fraction bound against the total chloride content (Fig. 4.1), concrete produced with CEM III shows the lowest chloride binding. For CEM II, chloride binding is also lower compared to CEM I + V and CEM I, which exhibits the highest fraction of bound chlorides. A lower chloride binding capacity of OPC blended with slag compared to plain OPC was also obtained by some other authors (e.g. Mohammed et al. [2003]), while many other studies found the opposite. Based on the chemical composition, CEM III is expected to have the highest ability to bind chlorides by forming Friedel's salt due to its high Al_2O_3 to SO_3 ratio. A high Al_2O_3/SO_3 ratio will lead to the formation of more AFm phases and less AFt phases and thus increase the potential of the cement to form Friedel's salt. Jones et al. [2003] could show that blending OPC with mineral admixtures such as blast furnace slag or fly ash increases the ratio of AFm to AFt and, thereby, greatly increases the potential sites for chloride binding. In agreement with these observations, Arya et al. [1995] or Luo et al. [2003] found also an increased chloride binding for OPC blended with blast furnace slag. Note that in these studies, chloride was added during mixing.

Therefore the low observed chloride binding of CEM III seems at first glance somewhat surprising, considering the chemical composition and very small ingress of chloride. These findings indicate again, that chloride binding seems not to be the main factor that determines the speed of chloride ingress.

Additionally, the maximum in bound chloride content in Figure 4.1 is for all binders not at the highest total chloride content. [Loser et al 2010]

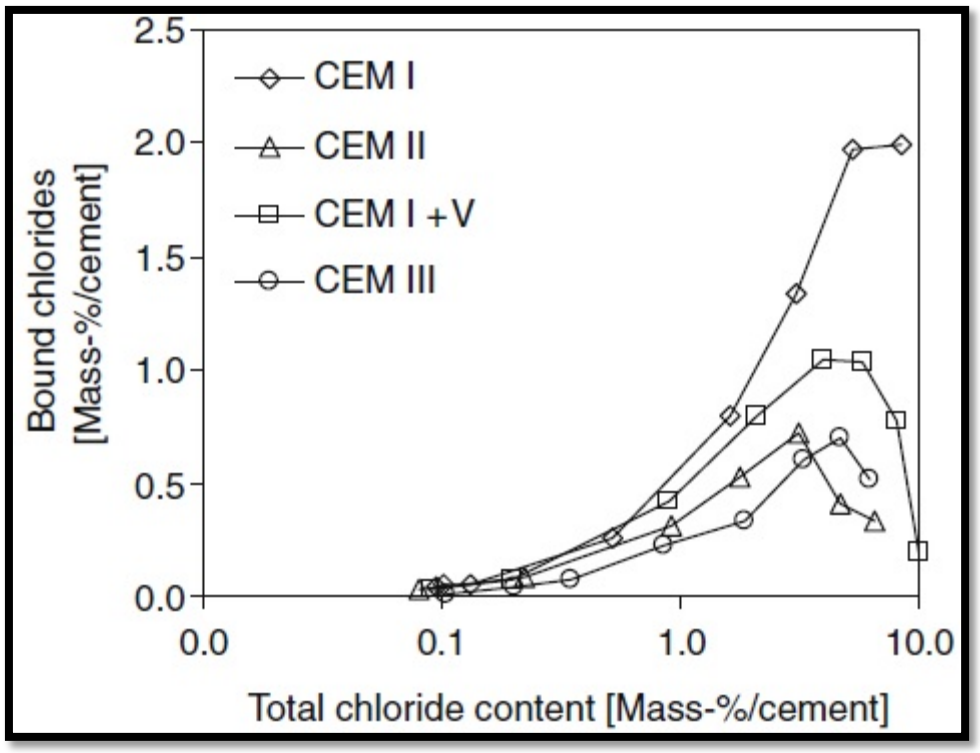

Figure 4.1: Bound chloride content versus total chloride content for different binders with w/b = 0.45. [Loser et al 2010]

Mohammed and Hamada [2003] research shows that the chloride binding ability of calcium aluminate cement (AL) is much higher than OPC, high early strength Portland cement (HES), moderate heat Portland cement (MH), slag cements of Types A (SCA) and B (SCB), and fly ash cement of Type B (FACB). In slag cements, increased replacement of cement by slag cement caused a decrease in the chloride-binding ability.

Rasheeduzzafar et al [1991] carried out field and accelerated laboratory corrosion and chloride penetration studies on ordinary Portland cement (OPC) and sulphate-resisting cement (SRPC) and report better performance of OPC cement over SRPC cement". Page et al [1986] investigated the influence of different cement types on chloride-induced corrosion of reinforcing steel. Their studies showed that OPC performs better then SRPC in terms of chloride binding capacity, chloride diffusivity and reinforcement corrosion.

Al-Khaja [1997] investigate that the chloride diffusion in the sulphate-resisting cement (SRPC) was more than that in the ordinary Portland cement (OPC), in both conventional and high-strength concrete. The superiority of OPC over SRPC, in terms of resistance to chloride ingress, was especially noted for depths of less than 20 mm. He also mentioned the performance of high-strength concrete in decreasing chloride diffusion was better than that of the conventional concrete.

Variation in cement content influences the quantity of cement paste to aggregate and the characteristics of the aggregate/cement paste interface depending on the mix design. Dhir et al [2004] found that sorptivity reduces as the cement content reduces using the initial surface absorption test (ISAT). Specimens were oven-dried at 105ºC prior to the test. Differences in sorptivity with changing cement content were slightly higher with increasing w-c ratio. Similar results were observed by Kolias & Geargio [2005]. They measured sorptivity of concrete by exposing the suction surface to water after preconditioning in an oven at 45ºC for 5 days.

OPC binds considerably more chloride than sulphate resisting Portland cement (SRPC). This is probably attributable to the latter's reduced capacity to form calcium chloroaluminate because of its lower C_3A content. [Arya et al, 1990].

The effect of cement content on chloride diffusion of concrete was investigated by Dhir et al [2004]. Three mixes made with CEM I, CEM II/B-V and CEM III/A cements with w/c ratio of 0.45, 0.55 and 0.65 were examined. Their results showed that cement content had little influence on chloride diffusion of concrete made with similar w/c ratios.

4.2 MINERAL ADDITIVES

The use of mineral admixtures is promising in light of their potential benefits on the durability and sustainability of reinforced concrete. When used to partially replace cement, such materials as fly ash, silica fume, metakaolin and slag have shown to generally improve the resistance of concrete to chloride penetration. The use of fly ash, slag, and other industrial by products may translate to cost savings and reduced energy use, greenhouse gas emissions and landfill waste, without sacrificing quality and long-term performance of the concrete. Additional research, however, is needed to validate the use of such modified mixes for corrosion mitigation in chloride environments [Shi et al, 2012].

The recent thrust for creating sustainable concrete structures has brought particular attention to the many advantages that the concrete industry can gain from including industrial by-products that possess pozzolanic properties in their mixtures [Kayali, 2008]. High strength-high performance concrete has become somewhat synonymous with the inclusion of silica fume at a proportion that has been optimised at around slightly less than 10% of the total binder content on a mass basis [Alexander, 1999]. Quite recently, ternary blends containing combinations of OPC, silica fume, fly ash and GGBFS have started to become more thoroughly investigated [Chindaprasirt et al, 2008, Ganjian and Pouya, 2009]. Clearly, the purpose of such binary or ternary mixture is to harness the most desirable properties suitable for the intended construction. Evidence of better corrosion performance of concretes with binary and ternary blends has recently been supported by various investigators [Fajardo et al, 2009]. Naturally, attention has been directed towards the performance of the pozzolanic industrial by-product materials in environments conducive to the corrosion of embedded steel. Hence the effects of such materials on the microstructural, chemical and physical properties are of paramount importance. The use of materials such as fly ash, silica fume or GGBFS, has been shown to significantly affect the pore solution chemistry and consequently, the electrical conductivity [Shi, 2004]. The beneficial effects of GGBFS, especially in aggressive chloride and/or sulphate rich environments, have been well documented and GGBFS is therefore, regarded as an effective means in producing high performance concrete [Ongerslev, 1989 and

Connell, 1998]. Dhir et al. [1996] investigated the chloride binding capacity of paste containing GGBFS at different replacement levels and concluded that it increased with the increase of GGBFS content. They also found that the binding capacity of the paste at 66.7% GGBFS content was about five times that of plain Portland cement paste. Dhir et al. as well as Luo et al. attributed this capability to increased formation of Friedel's salt [Luo, 2003].

However, the chemical constituents of GGBFS differ considerably from that of Portland cement, fly ash and silica fume, and notably in the amount of magnesia [Ahmed, 2007]. Subsequently, magnesia contributes to form hydrotalcite in significant amounts during hydration [Taylor, 1997]. Hydrotalcite is one of the most representative minerals of the Layered Double Hydroxides (LDHs) group. It occurs both naturally and synthetically and has the chemical formula of $Mg_6Al_2(OH)_{16}CO_3.4H_2O$. However, the chemical formula of hydrotalcite may change depending on the molar ratio $Al^{3+}/(Mg^{2+} + Al^{3+})$ which varies from 0.2 to 0.33 [Miyata, 1980]. Hydrotalcite consists of divalent and trivalent cations dispersed amongst the octahedral layers to form positively charged layers. The negatively charged anions are housed in the interlayer between the positively charged layers [Douglas et al, 2010]. A distinctive and valuable characteristic of hydrotalcite lies in its anion exchange property by which the interlayer anions can be replaced with a wide range of inorganic and organic anions [Patel, 2005]. Hydrotalcite's anion exchange property has been effectively used to neutralise acids in the stomach or to resist corrosion on metal surfaces [Wang, 2010]. Hybrid sol-gel coatings with hydrotalcite are effective in improving mechanical and physical properties of metal surfaces, including resistance against corrosion. When the coated surface is exposed to salt attack, the attacking chloride ion is adsorbed by hydrotalcite and thus the surface gets protection against corrosion. [Buchheit, 2003]

Kayali et al [2012] claim that the ability of GGBFS to protect against chloride induced corrosion is attributed to the effective binding of free chloride ions. The analysis of hydrotalcite effects revealed that hydrotalcite adsorbs a large amount of chloride ions. Furthermore, the XRD analysis has provided evidence that hydrotalcite

is formed in GGBFS pastes and its structure remains unchanged when it adsorbs chloride ions (Figure 4.2)

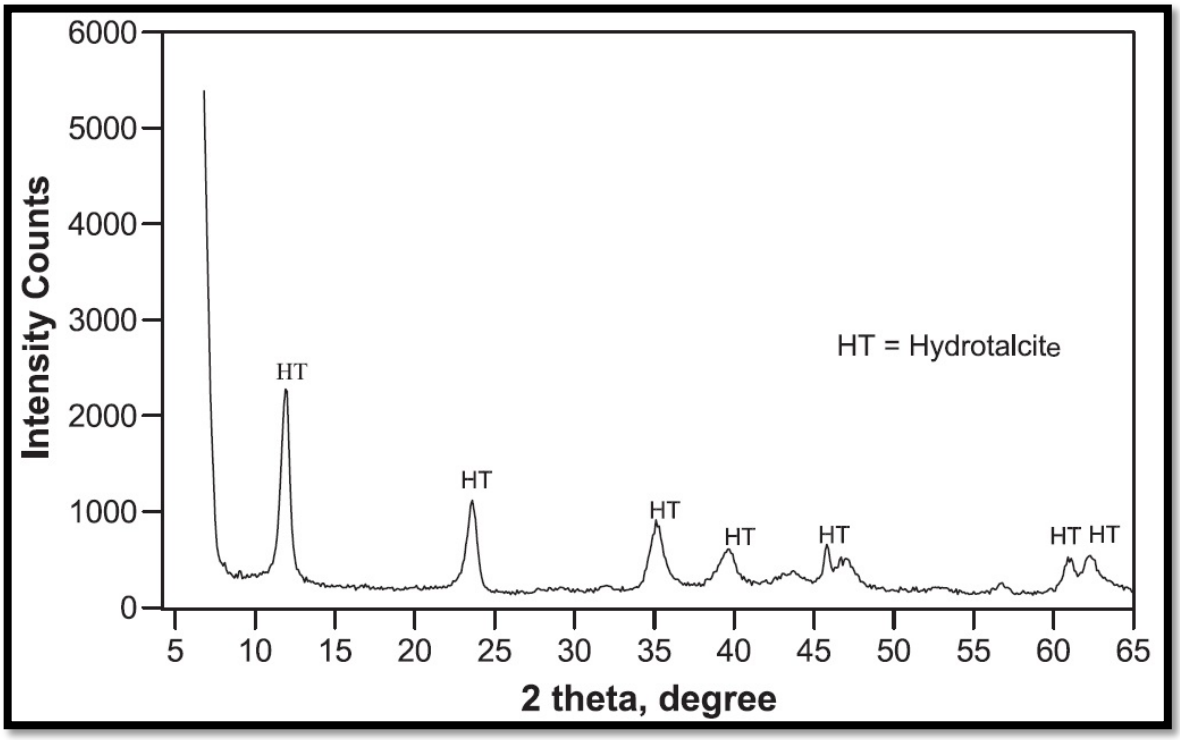

Figure 4.2: XRD patterns of calcined hydrotalcite mixed with chlorides.

Moreover, quantification of the hydrotalcite formation has shown that it comprises about 54% of the crystallised phase in hardened pure GGBFS paste and thus it possesses the largest proportion of its crystalline formations compared to the crystalline C–S–H at 37%. It is therefore concluded that hydrotalcite is responsible for superior chloride binding ability of GGBFS concrete. The ion exchange property that is already utilised in other engineering and pharmaceutical applications is thus shown to offer another important advantage in the ability to bind chloride ions and thus protect against reinforcement corrosion in concrete structures.

The use of fly ash clearly increased the chloride binding capacity in concrete [Dhir, 1999 and Dhir, 1997]. Fly ash contains aluminium oxide (Al_2O_3) at 23.7%, whereas Portland cement type I contains Al_2O_3 at only 5.5%. For this reason, increasing the amount of fly ash in concrete also increases the amount of Al_2O_3, which results in enhancing chloride binding capacity as well [Castellote, 1999].

The addition of limestone, as a mineral admixture to cement, can contribute to the decrease of energy requirements and CO_2 emissions in the manufacture of cement binders. The replacement of 10% of clinker by limestone does not significantly decrease the macroscopic properties of a material (e. g. mechanical strength, drying shrinkage, durability and freeze–thaw resistance). The increase in limestone addition (exceeding 10–15%) causes the gradual decrease of relevant characteristics of a material due to a dilution effect. Recently, however, there was a change in the understanding of the role of limestone during the hydration of cement. In contrast with a traditional view of limestone being just inert filler, it became obvious that limestone behaved, to a certain extent, as a chemically-active mineral addition. On the basis of thermodynamic calculations it was shown that limestone in cement changes the phase composition of aluminate components of the binder [Lothenbach, 2008]. In the presence of calcium carbonate as the main constituent of limestone, the formation of a carbonate type of AFm compound, calcium monocarboaluminate (CO_3-AFm), takes place. Consequently, the sulfate remains bound in ettringite (SO_4-AFt) which results in increased volume of hydrates and in decreased porosity. The formation of carboaluminate-type compounds in Portland-limestone cements was confirmed several times by using powder X-ray diffraction which showed that these compounds formed in a real system by the gradual transformation of calcium hemicarboaluminate into calcium monocarboaluminate [Ipavic et al, 2011]. This phenomenon becomes even more distinctive in the binders with higher contents of aluminum which was recently demonstrated for ternary cement with fly ash and limestone [De Weerdt, 2011].

Although general cement literature designates AFm as one phase, it in reality represents a family of structurally similar compounds. The AFm-type compounds most commonly present in a cement binder include hydroxy-AFm (OH-AFm),

monosulfate (SO_4-AFm) and monocarboaluminate (CO_3-AFm). Studies have shown that these compounds exist in different hydration states and also form solid solutions [Matschei et al, 2007]. Surprisingly, there are very few literature data on the differences of the ability of various AFm compounds to bind chloride. Hirao et al. [2005] determined the ability of monosulfate to bind chloride. They used NaCl as a chloride source and the sorption tests were carried out at a pH value that was controlled by the dissolution of the solid phase. From the binding isotherm, which was corrected for the content of Friedel's salt formed, it could be seen that at 1 M Cl around 50% of theoretically possible chloride was bound. At the concentration of 5 M Cl the quantity of bound chloride was close to a stoichiometric content of chloride in Friedel's salt. These values are relative as they will depend very much on the liquid/solid ratio. The relations between OH-AFm and Cl-AFm were investigated by Birnin-Yauri and Glasser [1998] who synthesized a series of solid solutions between both end-members. They ascertained that OH-AFm bound chloride already at a very low concentration (about 2 mM Cl); at about 14 mM Cl the composition of the solid phase was nearly identical to Cl-AFm. Recently, a comprehensive paper by Balonis et al. [2010] detailed the formation of solid solutions in binary combinations between Cl-AFm and OH-AFm, SO_4-AFm and CO_3-AFm. On the basis of solubility data an equilibrium model was presented that described phase composition during the interaction with chlorides for systems with or without calcium carbonate. The authors demonstrate that chlorides replace sulfate in monosulfate and that low chloride concentration favour the formation of Kuzel's salt, whereas higher chloride concentration cause the formation of Friedel's salt. The released sulfate ions bind into ettringite. In the systems where calcium carbonate is present, chloride ions also, to a certain extent, replace carbonate ions what results in the formation of a solid solution between CO_3-AFm and Cl-AFm. The authors were aware of certain limitations that had to be considered in these theoretical calculations. The most questionable limitation of these calculations was the absence of alkalis. The pH value was in their approach controlled by the solubility of Ca $(OH)_2$, although it is well-known that in real, unleached cement binders the pH keeps the value of well over 13, due to the presence of alkalis in the pore solution [Lothenbach B. and Winnefeld F., 2006]. Besides, calcium chloride was used as the more convenient source of chloride for

their approach although it is sodium chloride that is the most frequent source of chloride in the natural environment [Ipavec et al, 2013].

Ipavec et al [2013] claim that the addition of Pozzolanas significantly affects chloride binding capacity of hydrated cements. They mentioned chloride binding capacity depends primarily on the content of aluminum in individual binder. Silica fume, containing smaller amount of aluminum in comparison to OPC, decreases chloride binding, whereas for slag the opposite is true. Fly ash, containing largest amount of aluminum, strongly increases chloride binding capacity. The results indicate a linear relation between the chloride binding capacity and the amount of aluminum in the binders.

Alkalinity of the medium was found to be an important factor affecting chloride binding. The increase of alkalinity, particularly at lower chloride concentrations (b≈1 M NaCl), inhibits the chemical binding of chloride to a great extent. This effect, however, diminishes at higher chloride concentrations. Under the experimental conditions used, Friedel's salt is the main matrix for chemically bound chloride. Results obtained by NMR method imply that chloride-bearing AFm compounds can also partly form from disordered aluminum combined in silicate phases. This effect is particularly noticeable for binders containing fly ash where larger amount of disordered aluminum is present in a hydrated binder.

Limestone cement concrete, is susceptible to pH change as regard as its chlorides binding capacity. Ipavec et al, [2013], investigate the influence of limestone on chloride binding capacity in real cement systems. It is known to influence mineralogical composition of aluminate phases in a hydrated binder with the CO_3-AFm stabilization. The result of their study indicate that this mineralogical change also affects the amount of chlorides that can be bound into such cement matrix under highly alkaline conditions that are common for the pore solution of a binder. The influence of limestone on chloride binding capacity strongly depends on alkalinity and to a lesser extent on the concentration of chloride ions. At higher alkalinity (pH of about 13.5) chloride binding capacities of limestone blended cements are significantly lower if compared with limestone-free cements. The influence of limestone is,

understandingly, more pronounced for binders containing higher amount of aluminum, which applies to majority of pozzolanic cements. The decrease of chloride binding capacity in the presence of limestone persists also at decreased temperature of about 5 °C. Lowering of the alkalinity mitigates the effect of limestone to such a degree that at pH of about 12.8 almost no discernible effect on chloride binding capacity exists.

Nilsson et al. [1996] suggested that the partial replacement of cement with silica fume will have three main effects which will influence the binding capacity: 1) a reduction in the pH of the pore solution which will increase chloride binding, 2) a dilution of C3A which will reduce binding, and 3) an increase in the amount of the C–S–H which should increase binding. It is also known that this replacement results in the formation of C–S–H with lower C/S than the C–S–H formed without the presence of silica fume [Massazza, 1998]. It is not likely that the dilution of the C3A can solely explain the observed reduction in the binding capacity as a result of the partial replacement of cement with silica fume [Zibara et al, 2008].

Dehghanian and Arjmandi [1997] investigation shows that slag blended cement concrete containing up to 30% slag with water-cement ratio of 0.45 did not influence on chloride diffusion rate compared to concrete with no slag. This conclusion was obtained for concretes with 108 days of age. However, it is believed that with concrete age, the chloride diffusion rate for slag blended cement concrete will be reduced.

In order to enhance the durability of concrete, the use of supplementary cementitious materials such as silica fume, fly ash and ground granulated blast furnace slag have been proposed by many researchers. More recently, metakaolin has also been used as a concrete constituent, replacing part of the cement content. Zeolite has been also used as a cement blending material particularly by the cement industry in China.

Silica fume is a highly effective pozzolanic material because of its extreme fineness and high silica content. Silica fume increases the early strength while reducing the penetrability. Fly ash tends to have a low reaction rate and requires long period of time to enhance the pore structure. The use of fly ash improves the interfacial

transition zones (ITZ) between the cement matrix and the aggregate and this can lead to a reduction in porosity. Slag has a slow hydration reaction and replacing cement with a high content of slag can have a negative effect on strength and porosity at early age. Metakaolin is an effective pozzolan with high reaction rate which results in enhanced early and ultimate strength of concrete. Zeolite has the characteristics of typical pozzolans, causes high long-term strengths and low heat of hydration but with the disadvantage of low early strength. Zeolite increases the number of micro pores (d <625 A°) and decreases the amount of harmful large pores (d >938 A°) in the cement paste [Toutanji et al, 2004, Huat, 2006, Janotka et al, 2003].

Many studies have been carried out to investigate the effect of cement replacement materials on absorption properties of concrete and the beneficial of the use of supplementary cementitious materials is observed in many cases. Some examples are presented in the following paragraphs.

Chan and Ji [1999] carried out ISAT and chloride diffusion tests on concretes containing zeolite, silica fume and PFA. Specimens were oven-dried at 105°C to constant weight after they were cured for 28 days, then tested by ISAT (BS1881:Part 5). The cubes for chloride diffusion testing were coated on five faces and immersed in a 5M sodium chloride solution for 30 or 60 days. It was shown that even at low water to binder ratio (i.e. 0.28), the replacement of cement by zeolite, PFA and silica fume at levels from 5% to 30% improves the permeation characteristics of concrete.

The effect of metakaolin and silica fume was investigated by Abdul Razak et al [2004]. ISAT, water absorption and sorptivity tests were carried out on the specimens cured in different conditions at 7, 28, 56 and 90-day age. Prior to testing, samples were cured in water or wet burlap or plastic sheet and air for 28 days and oven dried to constant mass. They found that 10% replacement of cement with metakaolin or silica fume enhanced the overall near surface absorption properties of concrete.

Although the advantages of the use of mineral admixtures have been observed in many cases, contradictory results have been reported in a number of studies. This is due to the fact that the properties of concretes made with cement replacement

materials depend on the fineness of cement replacement/particle size, water to binder ratio of the mix and the percentages of cement which have been replaced.

Furthermore, the performance of cement replacement concretes is very sensitive to the curing regime. In order to obtain good strength and durability, it is essential to cure concretes especially those containing fly ash or slag properly for an extended period of time [Toutanji et al, 2004]. Variation in the results due to the different curing regimes has been reported by several authors including McCarter & Watson [1997], Mackechine [1996], Gopalan [1996] and Dias et al [2003]. The results are discussed below.

McCarter and Watson [1997] showed the dependency of the sorptivity to the water-binder ratio and curing conditions. They measured the sorptivity and de-sorptivity of ordinary Portland cement concretes with and without partial replacement with pulverised fly ash (30%), ground granulated blast furnace slag (50%), micro silica (10%) and metakaolin (10%) by subjecting them to a cycle of drying followed by water infiltration. The sorptivity of pulverised fly ash and ground granulated blast furnace slag concretes varied with changes in water-binder ratio and curing condition. They showed both smaller and greater sorptivities than sorptivity of OPC concrete dependent on water/ binder ratio of the mix and curing regime. Micro silica and metakaolin concretes produced the lowest sorptivity and desorptivity coefficients, even under poor curing conditions.

Mackechnie [1996] found that OPC concretes had higher sorptivity values than fly ash and ground granulated blast furnace slag (GGBS) concretes when moist or wet cured, whereas dry cured concretes showed the opposite trend.

Gopalan [1996] tested sorptivity of pure OPC concrete and concretes containing 20% and 40% fly ash with three w/b ratios of 0.53, 0.62 and 0.88. Samples subjected to standard fog curing for 7 days, after which they were either kept in the fog room or transferred to a controlled environment room with the same temperature as the fog room and lower relative humidity. All the specimens tested at the age of 28, 91 and 180 days. It was found that curing condition had a significant effect on the durability

of fly ash concrete, as a proper curing of 40% fly ash concrete reduced the sorptivity by 37% and inadequate curing increased it by 60%.

Dias et al [2003] examined the sorptivity of concrete containing 0%, 15% and 25% pulverised fly ash with two different curing regimes. They found that increasing the percentages of pulverised fly ash caused an increase in sorptivity for the air-cured specimens, but the differences between OPC concrete and pulverised fly ash mixes are very much less and virtually negligible for the water-cured specimens.

Preez and Alexander [2004] examined water sorptivity of concretes containing 50% GGBS, 30% pulverised fly ash and 7% condensed silica fume cured either in a standard temperature bath (wet-cured) or by different site curing methods such as air curing, hessian and damp sand. In the case of wet-cured specimens, the fly ash concrete had smaller water sorptivity than GGBS and condensed silica fume at 28 days. However, the fly ash and GGBS concretes yielded similar 120 day results, with the condensed silica fume concrete showing marginally poorer performance. In the case of the air-dried specimens, they all had similar sorptivity at the age of 28-day. After 120 days, sorptivities of fly ash and condensed silica fume concrete were similar and slightly lower than slag concrete.

Tasdemir [2003] examined effect of different mineral admixtures on the sorptivity of concrete under three curing conditions. The results showed that regardless to the curing regime the fly ash and silica fume concretes had higher and lower sorptivity than the OPC concrete, respectively.

In addition to enhancing the pore structure of concrete and thus reducing the sorptivity, concrete containing mineral admixtures have generally shown excellent performance regarding the resistance to chloride penetration. This resistance has been associated with the low mobility of chloride ions as a result of either the reduction in the number of interconnected pores due to their pozzolanic and filler effect or the chemical binding with cement hydrate [Basheer et al, 2002].

The increase in chloride binding as the GGBS content increases has been reported by several authors [Dhir et al, 1996, Luo et al, 2003]. Arya and Xu [1995] found that for

chloride derived from NaCl and introduced at the time of mixing, chloride binding occurred in order of: GGBS>PFA>OPC>SF.

In addition to the typical sorptivity tests with one period of wetting, wetting and drying cycles has been also used to investigate absorption characteristic and chloride penetrability of cement replacement materials. Polder and Peelen [2002] found that concrete with blast furnace slag, fly ash or both had less chloride penetration than OPC concrete exposed to wet/dry cycles. It is worth noting that the fly ash cement increased electrical resistivity (which reflects its properties with regards to chloride penetration) compared to Portland cement from eight weeks and cement with a high percentage of slag developed a significantly higher resistivity after one week. This result was obtained after storing specimens in a fog room for six days then exposing them in a climate room at 20°C and 80%RH for three weeks prior to the cycles. [Polder & Peelen, 2002]

Page and Vennesland [1982] reported on the effect of silica fume (SF) replacements (10, 20 and 30%) on the chloride binding in OPC with w/(c+s) = 0.50. The chloride source was NaCl dissolved in the mixing water to 0.0, 0.4 and 1.0 % Cl^- of dry material. Pore solution analyses revealed that the pH decreased with increasing SF replacement. The amount of free chlorides in the pore water after 35 and 70 days curing increased markedly when OPC was replaced with 10 % SF, but did not increase further for higher replacements. They showed also by differential thermal analysis and thermogravimetry (DTA/TG) that the amount of Friedels salt decreased with increasing SF replacement in addition to the calcium hydroxide (CH) content. The reduction in Friedels salt was explained by reduced pH. An alternative explanation could be the formation of more stable calcium-aluminium-silicate-hydrates (e.g. hydroglossular or *Strätlingite).* The results were later published [Page and Vennesland, 1983].

Byfors et al [1986] investigated the chloride binding from added NaCl (1% Cl^-) in OPC and OPC with slag and fly ash. For the latter two, pH increased when NaCl was added, due to the ion exchange during binding. The pastes were cured for 3 months prior to testing. They also studied OPC with 10% SF and found in contradiction with

all other publications that the chloride binding increased compared to OPC. This could be understood if SF was added rather than replacing OPC, but this is not clear from the paper.

Jensen and Pratt [1989] measured the chloride binding in OPC mixed with 30% fly ash (ASTM Class F). The chloride source was artificial seawater, both intermixed and intruded. They showed by microstructure studies that the reaction product from the pozzolanic reaction of fly ash (FA) was CSH (calcium silicate hydrates) and CAH (calcium aluminate hydrates), where the latter can give rise to increased chloride binding capacity. When sea water was used as mixing water, the sulphates first formed Ettringite (AFt) and later Friedels salt was formed on the expense of monosulphate (AFm). When ordinary paste was exposed to sea water, a layer of precipitated Brucite, $Mg(OH)_2$, and Aragonite, $CaCO_3$, was formed while the areas within showed chloride and sulphate penetration. The chloride penetration was the fastest and formed Friedels salt (more in the samples with FA due to CAH), while the following sulphate front decomposed this and formed Ettringite.

Arya et al [1990] investigated the chloride binding in OPC replaced with 0, 15 and 35 % FA, 70 % ground blast furnace slag (GBFS) and 15 % SF. 1 % Cl^- as NaCl was intermixed in the samples with water-to-binder ratio (w/b) 0.5 and cured for 28 days before testing. Both FA and GBFS replacement increased the chloride binding, while SF decreased it. They also studied similar paste samples (only 30 % FA) without chlorides intermixed, but which after 2 days curing were stored in a solution of 20 g Cl^- /l for 28 days. The difference in chloride binding was less, but the trend the same, when the chlorides diffused in.

Arya and Xu [1995] made OPC samples with different mineral replacements; 65 % GBFS, 35 % FA and 10 % SF, keeping w/b = 0.5. NaCl was added to the mixing water in a dosage corresponding to 1.0 % Cl^- of the dry material. The chloride binding was measured and found to increase in the order 10 % SF < pure OPC < 35 % FA < 65 % GBFS. They did also measure the rate of chloride initiated corrosion. For 1 % Cl^- the rate increased with the order OPC < GBFS < SF < FA, while the ranking was SF < GBFS < OPC < FA for 3 % Cl^- intermixed. The difference in ranking

between chloride binding and corrosion rate was explained by that while $Cl^{-}OH^{-}$ are decisive for chloride initiation, other factors (e.g. porosity) governs the corrosion rate after initiation.

Haque and Kayyali [1995] investigated the chloride binding in concrete with 0 and 15 % FA addition when the chloride source was NaCl dissolved in the mixing water within the a range of dosages from 0.2 to 1.0 Cl^- of the cement weight. The w/b was 0.37 without FA and 0.32 with FA. The addition of FA increased the chloride binding, but the authors also pointed out that the use of super-plasticiser (SP) seemed to decrease it.

Mangat and Molloy [1995] studied among other things the chloride binding in concrete based on OPC replaced with 15, 20 and 25 % low calcium FA, OPC replaced with 20, 40 and 60 % GBFS and OPC replaced with 5, 10 and 15 % SF (with 92 % SiO_2). The chloride penetrated from the outside by cyclic 6 h wetting and 6 h drying of sea water with varying exposure time, by storage in the tidal zone of the North sea for 7.4 years and by submersing in a sea water tank for 270 days. The most interesting conclusions were that 1) the amount of bound chlorides close to the surface is not influenced by the replacement of FA or GBFS, 2) at larger penetration depths the chloride binding is reduced when the cement is replaced by FA or GBFS and 3) the replacement of cement by SF reduced the chloride binding considerably.

Delagrave et al [1997] also studied the effect of 0 and 6 % SF on the chloride binding capacity of ASTM type I cement (7.4 % C3A) with w/c = 0.45 and ASTM type III cement (7.7 % C_3A) with w/c = 0.25. Assuming completely reacted SF and determining a degree of hydration of 62, 68, 52 and 47 % for ASTM type I without and with 6 % SF and ASTM type V without and with 6 % SF, respectively, they calculated the amount of CSH gel and found that bound chloride, C_b (mg Cl^-/g cement gel), vs. free chloride concentration, C_f (mole Cl^-/l solution), profiles were about equal. The exception was the ASTM type III cement with 6 % SF and w/(c+s) = 0.25, with a significant lower chloride-binding capacity. The authors points out that the composition of the gel may be changed with for instance a lower C/S ratio since

the degree of hydration is lowered by the SF due to self-desiccation, which also may effect the morphology or specific surface [Justnes, 1996]

The mineral admixtures, like fly ash, ground blast furnace slag, and silica fume, cannot only decrease the permeability of concrete, but also decrease the free chloride and increase the bound chloride content in concrete. This effect is more obvious with the increase of the cement content and the water-to-binder ratio [Lu et al, 2002].

Papadakis [2000] investigated the effect of silica fume, and low- and high-calcium fly ash on the diffusion of chloride in concrete using the NordTest (NT Build 443). He found that the mixes incorporating a supplementary cementitious material, exhibited significantly lower total chloride contents at all depths, apart from a thin layer near the exposure surface. This feature results in a lower diffusion coefficient.

The results of 90-day salt ponding and accelerated chloride migration tests carried out on concrete mixes containing fly ash or slag by Yang and Wang [2004] also showed that in both cases the diffusion coefficient significantly decreased due to an improvement in the pore structure. They also reported a reduction in the diffusion coefficient as the w-b ratio decreased.

Preez and Alexander [2004] observed that GGBS concretes give a superior performance on chloride conductivity at 28 days, whereas fly ash concretes initially yield poorer (i.e. larger) conductivity values at 28 days but improve with time so as to be indistinguishable from the GGBS results at 120 days. This can be explained by the slower rate of reaction of fly ash.

4.3 CEMENT CONTENT AND WATER TO BINDER RATIO (W/C OR W/B)

Water-cement ratio has a very important effect on the pore structure and quality of concrete. It has been observed that the sorptivity of concrete decreases with a decrease in water cement ratio due to refinement of the pore structure [Parrott, 1992- Dhir et al, 2004- Kolias & Geargio, 2005].

The investigation on the effect of w/c ratio on the chloride penetration under cyclic wetting and drying also showed that the chloride penetration decreases as the w-c ratio decreases [Polder and Peelen, 2002].

No results were found on the effect of w/c ratio on sorptivity when concretes are preconditioned by a wet/dry cyclic regime and the significance of its effect on sorptivity and chloride penetration as compared to other variables.

Midgley and Illston [1986] tested the ingress of NaCl in cement paste water cured for 1 month as a function of w/c. The chloride intrusion increased with increasing w/c as expected.

Tritthart [1989b] showed that the chloride content in the pore water of 3 month old cement paste decreased with decreasing w/c within the range 0.4-1.0 both for added NaCl and $CaCl_2$ when the Cl^- concentration was fixed to 1 % of the cement weight. This was explained by that at higher w/c there was more water to dilute the chlorides, and when this was taken into account the chloride binding was approximately independent of w/c.

Arya et al [1990] measured the chloride binding in OPC with w/c = 0.4, 0.5 and 0.6. 1 % Cl^- of the cement weight was intermixed as NaCl and the pastes cured for 28 days prior to testing. The chloride binding increased with increasing w/c. *This may* be due to increased degree of hydration with increasing w/c. The authors also investigated pastes without intermixed chlorides, where the pastes were placed in NaCl solutions of 20 g Cl^-l after 2 days initial curing for 26 days. The amount of bound chlorides increased with increasing w/c, but the ratio free/bound chlorides decreased since the total chloride content increased with increasing w/c.

Mangat and Molloy [1995] studied the effect of w/c and cement content on chloride binding in OPC concrete among other things. The chloride penetrated from the outside by cyclic 6 h wetting and 6 h drying of seawater with varying exposure time, by storage in the tidal zone of the North Sea for 7.4 years and by submersing in a seawater tank for 270 days. They concluded that the amount of bound chloride increases with increasing cement content and w/c [Justnes, 1996]

Cheewaket et al [2010] investigate for specimens with Water to binder ratios (W/B) 0.45, 0.55, and 0.65, the W/B ratio of concrete has small effect on the chloride binding capacity of concrete exposed to a marine environment.

Previous research had reported that the physical bound of chloride content in cement paste increases with the increasing of total chloride and W/B ratio [Sumranwanich and Tangtermsirikul, 2004]. Besides, the total chloride content in concrete increases when the W/B ratio increases. This is due to a higher W/B ratio results in higher porosity in concrete and thus greater chloride ingresses into the concrete [Cheewaket et al, 2010].

The water cement ratio (w/c) has some influence on the isotherms of pastes, but has little influence on the isotherms of the mortars, and the binding capacity of the pastes is apparently higher than that of the mortars [Luping and Nilsson, 1993].

Marinescu and Brouwers [2009] claim that an increased water-to-cement ratio leads to increased chloride binding of OPC, partly because it promotes a higher hydration degree and partly because it leads to a higher porosity of the hardened cement paste, thus facilitating the transport of free chlorides through the structure.

As the w/c ratio increases, there is a proportional decrease in the chloride concentration in the mix water. This might have been expected to cause a reduction in chloride binding. However, Arya et al [1990] research shows that for OPC mixes, chloride binding increases as w/c increases, (although this effect is only slight at higher w/c ratios). This is probably due to the greater porosity and permeability of the higher w/c ratio paste allowing greater access of chloride ions to the cement particles.

Dhir et al [1996] research shows the binder type has the most significant effect on chloride durability, given equality in strength. Water reductions to improve chloride resistance can be usefully employed in situations where binder choice is restricted and increasing binder content could lead to other problems. They also mentioned the reducing the water content of a concrete mix and thereby the binder content for equal design strength affects chloride resistance. Within the range of parameters tested, this

was found to have no significant effect for both the Portland cement (PC) and pulverized-fuel ash (PFA) concrete.

Dehghanian and Arjmandi [1997] claim that an increase in water-cement ratios more than 0.55 increased the chloride diffusivity of concrete. This effect was more pronounced for a higher slag contents. Water-cement ratio of 0.45 provided the lowest chloride permeability for the concretes with higher slag contents.

Bamforth et al [1997] sited work by Frey et al [1994] who investigated the effect of cement composition, cement grade and w/c ratio on chloride diffusion coefficient of PC concrete (Table 4.1). It can be seen that the diffusion coefficient increases with increasing w/c ratio and reducing cement grade and alumina content.

Table 4.1: Diffusion coefficients for Portland cement of different compositions [Bamforth et al, 1997]

Cement grade	C3A	Al2O3	C4AF	$D_c \times 10^{-12}$ at w-c ratio of:			
				0.4	0.5	0.6	0.7
PC35	<1%	<3%	-	6.0	7.0	10.0	19.0
PC45	<1%	<3%	-	2.9	3.0	5.0	11.0
PC55	<1%	<3%	-	1.7	2.1	3.2	6.5
PC35	≈10%	-	≈7%	0.2	0.5	1.1	3.0
PC45	≈10%	-	≈7%	0.09	0.25	0.50	1.5
PC55	≈10%	-	≈7%	0.05	0.07	0.11	0.21

Page et al. [1981] found that the diffusion coefficient became 4 to 6 times greater when the w/c ratio increased from 0.4 to 0.6. They also found that diffusivity increased with increasing temperature.

Midgley & Illston [1984] also investigated the effect of chloride concentration using two solutions containing 30 and 150 g/l NaCl. Their results showed that the depth of chloride penetration increases with w/c ratio and chloride ion concentration. The study also concluded that the presence of chloride ions alters the pore-size distribution of the hardened cement paste and smaller pores are associated with higher chloride

concentrations as Friedel's salt (calcium chloroaluminate) and calcium chloride precipitate in the coarser pores, and thereby decrease the number of coarser pores. [Suryavanshi and Swamy, 1998]

In summary, the cement content has little influence on chloride diffusion of concrete made with similar w/c ratios. The diffusion coefficient increases with increasing w/c ratio and reducing cement grade. Temperature has a complicated effect on chloride diffusion. An increase in the exposure temperature increases both ionic diffusivity and chloride binding capacity. Moreover, elevated temperatures accelerate cement hydration and pozzolanic reaction but also causes micro-cracking at the aggregate/matrix interface. The net effect of higher exposure temperature on OPC concrete is an increase in chloride transmission whereas the opposite is true for PFA concretes.

4.4 CURING CONDITIONS

It has been confirmed by experiment that water immersion curing reduces absorption properties of concrete. Increasing the duration of curing also reduces the porosity of concrete and its absorption properties.

Tasmir [2003] and Abdul Razak et al [2004] investigated the effect of different curing conditions (e.g. air curing, polyethene and wet burlap curing and water curing) on sorptivity of concrete containing different mineral admixtures. The results showed that air-cured and water-cured concretes had the highest and the lowest sorptivity, respectively.

Although there has been little dispute amongst the majority of researchers about the effectiveness of immersion curing and the benefits of longer periods of curing, real concretes in structures are rarely cured to such a high standard. Furthermore, in the case of concrete structures on site, the effect of curing after long-term site exposure is of greatest significance. Therefore, it is critical to clarify the effectiveness of site curing methods on the concrete properties [Cather, 1996].

Nolan et al [1997] investigated the effectiveness of commonly-used site curing regimes. Curing was by formwork retention, wrapping in wet hessian or wrapping in polyethene for periods of between one and seven days. Specimens were also subjected to both air and water storage. As might be expected, the air-stored and the water-cured specimens were shown to have, respectively, the greatest and smallest water absorption determined using total immersion and water sorptivity. However, in between these two extremes, there were no well defined trends observed in the properties of concrete.

Preeze and Alexander [2004] also investigated the effectiveness of site curing methods on sorptivity of concretes containing ground granulated blast furnace slag, fly ash and condensed silica fume. Specimens were cured using practical site methods currently employed in the industry including air curing, curing compound (resin based compound), wet hessian and damp sand. Then they were exposed to a warm and humid coastal environment. Curing of companion control cube samples in a water tank was the benchmark curing method. The results showed that full wet curing was the most effective method, as expected. While variation in sorptivity existed at early ages (28 days) between site and wet cured samples, at later age (120 days) the variation reduced such that the different site curing methods were indistinguishable.

Similar to Preeze and Alexander [2004], Buenfeld & Yang [2001] in CIRIA C530 Report stated that, at early ages, the curing regime could have a significant effect on the pore structure of concrete very near to the cured surface. Poor curing resulted in higher porosity paste near the surface in relation to the bulk concrete. However, the benefits gained from curing were found to diminish with long-term exposure, with the influence of nine months U.K. exposure (outdoor, unsheltered or sheltered) having a greater influence on microstructure and durability performance than the initial curing. However, their research was limited to two durability tests of abrasion and carbonation.

No experimental data was identified relating to the effect of curing regime on sorptivity of concrete exposed to wet/dry cycles.

Trætteberg [1977] showed that cement paste increased its resistance towards chloride with increasing maturity as expected.

Tritthart [1989b] investigated bound chlorides in cement paste (w/c = 0.60) with both NaCl and $CaCl_2$ added to 0.6 % Cl^- of the cement weight as a function of curing time. He proved that most of the binding of chloride takes place the first days and that more chlorides are bound from calcium chloride than sodium chloride. pH increased in the same period and was always higher in the samples with added NaCl.

Arya et al [1990] studied the chloride binding in OPC with w/c = 0.5. 1 % Cl^- from NaCl was intermixed and the samples cured for 28, 56 and 84 days prior to testing. The amount of bound chlorides increased with increasing curing time, although most of the binding happened before 28 days. They also investigated the same mixes cured for 28 days at 8, 20 and 38°C, and found that the chloride binding increased with increasing curing time. Since the temperature interval was in a relatively low range, the increase in chloride binding is most likely due to increased maturity rather than changes in microstructure. OPC (w/c = 0.5) without chloride was also cured at ambient temperature for 2, 7, 28, 56 or 84 days prior to exposure to 20 g Cl^-/l for 28, 56 or 84 days. The chloride binding in these samples increased with increasing exposure time, while there was a weak tendency of decreasing binding with increasing age prior to chloride exposure.

Ehtesham Hussain et al [1995] cured 3 cements with a C_3A content of 2.43, 7.59 and 14.00 % at 20 and 70°C to measure the temperature effect on chloride binding when 0.3, 0.6 and 1.2 % Cl was added to the mixing water (w/c = 0.6) in the form of NaCl. The chloride content of the pore water increased drastically when the curing temperature was increased from 20 to 70°C, and the effect increased with increasing C_3A since the highest C_3A gave the most binding at 20°C. The OH^-concentration decreased when the curing temperature increased, but not to the same extent as the increase in chloride concentration. [Justnes .H, 1996]

Chloride binding increases as the curing temperature increases. This effect is almost certainly attributable to faster reaction rates at the higher temperatures. This result contradicts Roberts' finding [1962] that cements hydrated at elevated temperatures

bind less chloride than when setting occurs at normal temperatures. This discrepancy may be attributable to the much shorter hydration times used, generally less than 7 days, and/or the use of a leaching method to estimate the percentage of binding achieved. [Arya et al,1990] They also mentioned that chloride binding continues to increase well after the free chloride content has stabilised. This may be due to chloride ions gradually reacting with the ettringite present to produce calcium chloroaluminate. Their results also show that, for OPC pastes cured in sealed conditions, curing time after two days has no significant effect on chloride binding.

Al-Khaja [1997] showed that significant increase in the chloride ingress into concrete was observed when the exposure temperature was increased from 20 to 45˚C, particularly at small depths. However, at depths of more than 45 mm, the increase in temperature had an insignificant effect. The effect of temperature on chloride ingress is more pronounced in the conventional concrete than in the high-strength concrete. The increase in chloride diffusion due to elevated temperature can be considered as a significant factor affecting concrete durability, vis-a-vis reinforcement corrosion.

Larsen [1998] investigated the effect of temperature (5, 21 and 40˚C) on chloride binding. For samples immersed in NaCl solutions, the highest binding capacity was observed at 5˚C and the lowest at 21˚C, with 40˚C a bit higher than at 21˚C. For mixed- in chlorides, the binding capacity gradually decreased from 5 to 21 to 40˚C. This trend was most likely caused by the difference in chloride concentration of the two exposures. The effect of temperature also became weaker for decreasing pH and C3A content [Larsen, 1998]. One problem arise in warm weather as a rise in temperature will lead to dissolution of some of the bound chloride. Hence, the chloride content in the pore solution will increase, the chloride diffusion will accelerate and the chloride will penetrate deeper into the concrete surface [Larsen, 1998]. At the end, the chloride threshold value may be reached and corrosion is initiated. The increased temperature also reduce the concrete resistivity, potentially leading to increased corrosion rate.

Zibara [2001] found that the effect of temperature was influenced by chloride concentration of the exposure solution. The capacity was slightly reduced as the

temperature rose from 0˚C to 23˚C to 28˚C at 0.1 M and 1.0 M chloride concentrations. At higher chloride concentrations (3M) an increase of temperature resulted in slightly more bound chlorides. Zibara suggest the trend can be explained by the transformation of the ettringite phase into Friedel's salt at a much faster rate for 3 M.

Yuan et al. [2009] pointed out the fact that thermal vibrations increase due to higher temperature, resulting in less bound chloride. It is well known that the reaction rate of a chemical reaction increases as the temperature rise. Thus, elevated temperatures accelerate hydration. The degree of hydration will affect binding by altering the pore structure and pore solution composition [Glass et al., 1997]. However, high temperatures may also increase the solubility of Friedel's salt.

Dehghanian and Arjmandi [1997] claimed that curing method had a marked effect on chloride permeability in concrete. Submersion in water for 9 and 18 days provided the best curing condition for reducing the chloride diffusion rate in concrete.

From research results a high rate of chloride diffusion in the cementitious repair materials containing polymer latex additives relative to plain concrete. The effect of inadequate initial curing on chloride penetration (e.g., exposure to chlorides after 24 h of casting or 28-day air curing) is more pronounced in concrete mixes than in generic repair materials. [Mangat P.S., Limbachiya M.C, 199]

Preez and Alexander [2004] examined the effect of site curing on the chloride conductivity of concrete. Generally, air-cured and wet-cured concretes had the greatest and smallest chloride conductivities respectively. Although the effect of different site-curing methods, including air, hessian, sand and curing compound, on chloride conductivity of GGBS and PFA concrete was visible after 28 days, the variation between site-cured samples disappeared after 120 days. Nevertheless, there was a difference between wet-cured and site-cured concrete even after 120 days.

The advantage of moist curing on the enhancement of concrete pore structure and thus its permeation properties has been reported in many studies. Ramezanianpour [1995] examined the effect of different curing regimes on resistance to chloride penetration

using ASTM C 1202 (Standard Test Method for Electrical Indication of Concretes Ability to Resist Chloride Ion Penetration). The curing regimes investigated were moist curing, room temperature curing, two days moist curing followed by curing at room temperature, and curing at 38°C and 65%RH which were applied until the day of testing at 7, 28 and 180-day.

The results showed that moist curing is essential to achieving the lowest chloride penetration in concrete. Concretes which received no curing after demoulding showed the poorest performance. Concretes which were moist cured for only two days performed significantly better than uncured concretes.

The effect of poor curing on concrete diffusivity is more severe for concretes made with cement replacement materials. Although the benefits of using cement replacement materials in enhancing the resistance of concrete to chloride penetration has been noted in many cases, it has also been widely reported that concrete contains slag and fly ash are very sensitive to curing and poor curing practices can adversely affect the properties of such mixes. [Ramezanianpour, 1995- Barnett et al, 2006]

Moist curing is essential to achieve the lowest chloride penetration in concrete. The effect of poor curing on concrete diffusivity is more severe for concretes made with cement replacement materials. Slag and fly ash concretes are very sensitive to the curing regime and poor curing practices can adversely affect their properties.

4.5 EXPOSURE CONDITIONS

Trætteberg [1977] showed that carbonated cement paste had much larger intrusion of chlorides than non-carbonated, which indicates that carbonation reduces the binding capacity since the porosity should be reduced.

Tritthart [1989b] stored cement paste with w/c = 0.5 and 0.7 in chloride solutions with pH = 12.5, 13.0 and 13.7, and found that the absorbed chloride content decreased with increasing pH.

Ehtesham Hussain et al [1994] investigated the chloride binding in three Portland cements with C_3A content 2.43, 7.59 and 14.00 %. The chloride source was NaCl dissolved in the mixing water (w/c = 0.6) to 0.6 and 1.2 % Cl^- Cl^- of the cement weight. They also studied the effect of simultaneously added sulphate as Na_2SO_4 so that the total sulphate content increased to 4 and 8 % of the cement weight. The samples were cured for 180 days before pore water pressing. The amount of free chlorides in the pore water increased with increasing sulphate addition, which indicate that sulphates are stronger bound than chlorides by C_3A. pH also increased with increasing additions of sodium sulphate according to the following reaction;

$$Na_2SO_{4\,(aq)} + Ca(OH)_{2\,(s)} \rightarrow CaSO_{4\,(s)} + 2\,NaOH_{\,(aq)} \qquad 4.1$$

The present author confirmed reaction (4.1) by making a mix of 0.2 mole CaO and 200 ml water (forms calcium hydroxide momentarily) and the same mix with the addition of 0.2 mole $Na_2SO_4.10H_2O$. The mixes was resting for 1 day before the water was filtered off and the pH measured by a pH-meter. Lime and water gave pH = 12.55 in accordance with the OH^- concentration in equilibrium with solid $Ca(OH)_2$, while the mix including sodium sulphate gave pH = 13.20. Thus, reaction (4.1) is shifted significantly to the right.

Ehtesham Hussain et al [1995] studied the effect of pH of pore water on chloride binding in a cement with 14.00 % C_3A and the addition of 0.3, 0.6 and 1.2 % Cl^- Cl^- by weight of cement. When the pH was increased from 13.72 (524 mM OH^-) $OH^-$to 13.88 (755 mM OH^-) the concentration of chloride was approximately doubled for the two lowest chloride additions.

Delagrave et al [1997] determined the chloride binding isotherm for ASTM type I cement with w/c = 0.45 for NaCl in the presence of saturated lime (pH = 12.55) and an alkaline solution of 1g NaOH$NaOH^+$ 4.65 g KOH/l (pH = 13.0), respectively. The chloride binding was least for the highest pH.

Neville [1995] pointed out in a review that both sulphate ingress and carbonation would release already bound chlorides in cement paste [Justnes, 1996].

The effect of temperature on chloride diffusion can be modelled using the Arrhenius' equation:

$$D_T = D_{ref} \exp\left[\frac{E}{R}\left(\frac{1}{T_{ref}} - \frac{1}{T}\right)\right] \qquad 4.2$$

where E is the activation energy of chloride diffusion coefficient in concrete (Table 4.2) and R is the gas constant (1.98 cal/K.mol)

Table 4.2: Activation energies of chloride diffusion in concrete [Lin et al, 1993]

w/c ratio	0.4	0.5	0.6
E cal/mol	9932	10611	7585

Dhir et al [1993] investigated the effect of exposure temperature on concrete diffusivity using a diffusion cell. They tested concretes made with 0% to 50% PFA content and strengths between 20 and 60 N/mm² and cured in water or air. They found that exposure temperature has a major effect on the rate of chloride diffusion, concrete structure and chloride binding capacity. An increase in the exposure temperature increased the ionic diffusivity. However, it also increased the chloride binding capacity. Furthermore, the hydration and pozzolanic reactions were accelerated at higher temperatures and thus the pore structure was more dense. Another effect of using high exposure temperatures is that they can cause micro-cracking at the aggregate/matrix transition zone.

For the pure OPC mix, the net result was a 3 to 5 fold increase in chloride transmission as the exposure temperature increased from 20ºC to 45ºC. However, all

the PFA mixes (with greater than 10% PFA) showed an opposite trend. This is probably due to the acceleration of the pozzolanic reactions with the higher temperature in PFA concrete.

They also found that the diffusion coefficient decreased with increasing PFA content. This effect was found to increase with exposure temperature. Poor curing resulted in an increase in the diffusion coefficient but this effect decreased with increasing exposure temperature, particularly for PFA concrete.

4.6 CHLORIDE SOURCE

The problem of chloride attack arises usually when chloride ions ingress from outside. This can be caused by de-icing salts. Another, particularly important, source of chloride ions is seawater in contact with concrete. Chlorides can also be deposited on the surface of concrete in the form of air-borne very fine droplets of sea water (raised from the sea by turbulence and carried by wind) or of air-borne dust which subsequently becomes wetted by de-icing salts. It is useful to point out that air-borne chlorides can travel substantial distances: 2 km has been reported, but travel over even greater distances is possible, depending on wind and topography. The configuration of structures also affects the movement of air- borne salts: when eddies occur in the air, salts can reach the landward faces of structures.

Brackish groundwater in contact with concrete is also a source of chlorides. Ingress into concrete could also occur from conflagration of organic materials containing chlorides. Hydrochloric acid is formed and deposited on the surface of concrete where it reacts with calcium ions in the pore water. Ingress of chloride ions can follow.

Chlorides can be present in concrete because they have been incorporated in the mix through the use of contaminated aggregate or of seawater or brackish water, or by admixtures containing chlorides.

As a possible source of chlorides in the mix, Portland cement itself contains only a very small amount: normally, no more than 0.01 per cent by mass. However, ground

granulated blastfurnace slag may have a significant chloride content if its processing involved quenching with seawater. Drinking water may well contain 250 ppm of chloride ions; at a water/cement ratio of 0.4 the water would contribute the same amount of chloride ions as Portland cement. For concrete, the chloride content of the aggregate should not exceed 0.5 per cent by mass of the total aggregate; this is reduced to 0.03 per cent when sulfate-resisting cement is used. For prestressed concrete, the corresponding figure is 0.01 percent [Neville, 2002].

Tritthart [1989b] studied the effect of the chlorides NaCl, $CaCl_2$, $MgCl_2$ and HCl on chloride binding in cement paste (w/c = 0.6) after 3 months curing when the total chloride addition was 1 % Cl^- Cl^- of the cement weight. He found that calcium chloride lead to more bound chlorides than sodium chloride, and that magnesium and hydrogen chloride gave similar result as calcium chloride. The pH increased when NaCl was added and decreased when $CaCl_2$ was added. The latter was explained by sparingly soluble calcium hydroxide and the common ion effect. Magnesium chloride gives the same effect as calcium chloride due to the following ion exchange;

$$MgCl_{2\,(aq)} + Ca(OH)_{2\,(s)} \rightarrow CaCl_{2\,(aq)} + Mg(OH)_{2\,(s)} \qquad 4.3$$

which means that the pore water essential will consist of an equivalent molar concentration of calcium chloride and thereby identical exposure. The reason why hydrochloric acid gives the same result as calcium chloride is caused by the immediate neutralisation reaction;

$$2HCl_{\,(aq)} + Ca(OH)_{2\,(s)} \rightarrow 2H_2O + CaCl_{2\,(aq)} \qquad 4.4$$

Al-Hussaini et al [1990] added NaCl and $CaCl_2$ (≤ 2 % Cl^- by weight of cement) to the mixing water of mortar (w/c = 0.5) based on OPC with 12.7 % C_3A. After 28 days curing the mortars were crushed and free chlorides analysed as water soluble while total chloride were analysed as acid soluble. The authors found that it was more free chlorides when the source was NaCl than $CaCl_2$ and that the amount of free chlorides increased with increasing chloride dosage.

Arya et al [1990] investigated chloride binding in OPC paste with w/c = 0.5 when 0.5, 1.0 and 2.0 Cl^- Cl^- from NaCl and $CaCl_2$ was intermixed and the paste cured 28 days

prior to testing. Calcium chloride gave much more chloride binding than sodium chloride at the same chloride dosage. The authors also investigated cement paste without intermixed chlorides that was placed in solutions of 20, 45 and 90 g Cl^-/l as NaCl after 2 days pre-curing and stored for 28 days prior to testing. The ratio of free/bound chlorides decreased with increasing chloride concentration even though the total amount of bound chloride increased somewhat. They also investigated similar paste without chlorides stored in 20 g Cl^-/l from NaCl, sea water (18.5 g Cl^-/l), $CaCl_2$ and $MgCl_2$ after 2 days pre-curing and exposure for 28 days prior to testing. Sea water lead to somewhat less chloride binding than NaCl, which most likely is due to the inherent sulphates blocking some of the chloride binding sites. The exposure to calcium chloride lead to much more chloride binding than sodium chloride, which is explained by the easier formation of Friedel's salt. The exposure to magnesium chloride lead to almost the same chloride binding as calcium chloride, which again is in accordance with the ion exchange shown in reaction 4.2.

Chatterji [1994] studied the steady state diffusion of different chlorides through 3 mm paste (w/c = 0.40 and cured for 7 days prior to exposure) based on Aalborg white Portland cement with a low C_3A content. The chloride source was 0.5, 1.0 and 3.0 M NaCl, 1.0 and 2.0 M KCl, and 0.25 and 0.50 M $CaCl_2$ solutions. The chloride diffusion coefficient decreased with increasing chloride concentration for a given salt, but was substantially larger for calcium chloride than for the alkali chlorides. In theory the steady state diffusion coefficient is independent of chloride binding since the chloride binding capacity of the paste is saturated when the steady state flow of chlorides is reached. However, the increased coefficient for $CaCl_2$ could be due to micro cracking caused by the formation of expansive product shown in reaction 3.6.

Neville [1995] pointed out in his review that calcium chloride leads to more chloride binding than sodium chloride in cement paste.

Delagrave et al [1997] compared the chloride binding isotherms for ASTM type I cement with w/c = 0.45 when the chloride source was calcium chloride and sodium chloride. The result showed that the chloride binding was much higher when calcium was the cation rather than sodium [Justnes, 1996].

4.7 OTHERS

4.7.1 Aggregate type and gradation

Aggregate particles influence the microstructure of cement paste at the interfacial transition zone (ITZ). Generally, the ITZ has higher porosity and lower content of unhydrated cement as compared to the bulk paste. Aggregate size and type can affect the volume and the porosity of the ITZ and thus they can influence the permeation properties of concrete such as sorptivity [Elsharief et al, 2004].

In addition, different aggregate types have different absorption properties and this can affect the sorptivity of concrete. Dhir et al [2006] studied the effect of aggregate type on the absorption properties of concrete by ISAT. The results indicated that for five normal weight aggregates used in the experiment, concrete absorption generally reduced with reducing aggregate absorption.

The influence of aggregate type and aggregate size on sorptivity of mortar was studied by Elsharief et al [2004, 2005]. They found that mortars with greater aggregate gradation have higher sorptivity than that with smaller aggregate gradation. They attributed that to the low pore tortuosity in the former compared to the latter. They also found that lightweight aggregate mortar had lower sorptivity than normal aggregate mortar due to dense paste surrounding lightweight aggregate.

McCarter et al [1996] examined the absorption properties of concretes containing different types of aggregate including natural gravel, crushed granite and crushed quarts-dolerite. Results indicated that the aggregate type of similar grading had little or no effect on the depth of water penetration using ISAT.

4.7.2 Compaction

Compaction influences the microstructure and pore size distribution of concrete and thus affects the permeation characteristics of concrete. Gonen and Yazicioglu [2007]

investigated the effect of compaction on the sorptivity of concrete. They used three levels of compaction porosity: poor (vibration or 25 times by spading), medium (15 times by spading) and high (non-compacted). The result showed that the compaction pores had a very important effect on sorptivity. The maximum sorptivity was observed on the non-compacted specimens and the minimum sorptivity on the specimens compacted by vibration.

4.7.3 Concrete grade

Dias [2004] investigated the effect of concrete grade on sorptivity by using two concrete grades of 20 and 30. He found that concrete grade had a significant effect on sorptivity. The grade 20 specimens showed higher sorptivity than the grade 30 specimens.

The influence of concrete grade on its absorption properties has been reported by several authors [Tasdemir, 2003- Gopalan, 1996]. They correlated sorptivity of concretes to their compressive strength and found that the sorptivity of concrete decreases as the compressive strength increases, depending on the curing regime and concrete mix.

4.7.4 Influence of sulphate

The presence of sulphate, present either in the cement composition or as part of the chloride host solution (external), has a negative effect on the binding capacity. External sulphates are known to influence both the chemical and physical binding capacities, while sulphates from the cement mainly influence chemical binding capacity. The sulphate contents in cement influences the type and the quantity of calcium aluminate hydrates that are produced, which in turn influences the binding capacity of cement especially at low chloride concentrations [Zibara, 2001]. Zibara [2001] found that the binding capacity of C_3S and C_2S are reduced in the presence of sulphates in the exposure solution. XRD results showed less Friedel's salt indicating

the negative effect of sulphates on chemical binding. Zibara suggests that the presence of sulphates in the pore solution leads to a competition between $SO_4^2$and chloride ions for adsorption sites on the C-S-H surface, thus reducing the physical binding capacity [Ytterdal, 2014]. The same trend was reported by Xu [1997] and De Weerdt et al. [2014a].

4.7.5 Carbonation

There are not many studies of the influence of carbonation of chloride binding. Generally, literature shows that carbonation reduces the binding capacity. Carbonation is the process in which CO_2 from the air penetrates into the concrete and reacts with calcium hydroxyl as follows;

$$Ca(OH)_2 + CO_2 \rightarrow CaCO_3 + H_2O \qquad 4.5$$

Zibara [2001] exposed carbonated cementitious pastes to chloride solutions. In most of the cases, the carbonated samples experienced a reduced binding capacity of more than 90% compared to non- carbonated samples. Zibara explains the severe negative effect of carbonation as a result of the transformation of C-S-H and C-A-H into $CaCO_3$ in the presence of CO_2.

According to Larsen [1998], both samples carbonated before and after chloride exposure will contain less bound chlorides. The results showed that samples carbonated before exposure had no bound chlorides, while samples carbonated after exposure had more bound chlorides.

4.8 CONCLUSION

Chloride in concrete can be either dissolved in the pore solution as a free chloride or chemically and physically bound to the cement hydrates and their surfaces as a bound chloride. Chloride binding in concrete is affected by many factors, such as: type of

cement, mineral addition, w/c, curing condition, exposure conditions, chloride source, carbonation and influence of sulphate play an important role as well.

Chloride binding of the cement paste increase with increasing C_3A and decreased with increasing OH^- concentration from the cements. High chloride binding capacity was found in higher calcium culminate cement.

Chloride binding was controlled by the total amount of CSH gel in the paste. From the research it is shown CEM I has the highest bound chloride and CEM III the lowest bound chloride between four different type of cement. CEM III is expected to have the highest ability to bind chlorides by forming Friedel's salt due to its high Al_2O_3 to SO_3 ratio. A high Al_2O_3/SO_3 ratio will lead to the formation of more AFm phases and less AFt phases and thus increase the potential of the cement to form Friedel's salt.

Adding minerals such as fly ash, silica fume, metakaolin and slag improve the resistance of concrete to chloride penetration by affecting significantly the pore solution chemistry and the electrical conductivity. It has been show that fly ash contains aluminium oxide at 23.7% results in enhancing chloride binding capacity. Binding capacity of the paste at 66.7% GGBFS was about five times more than plain Portland cement, due to increase in formation of Friedel's salt.

The amount of bound chlorides increased with increasing W/C, but the ration of free/ bound chlorides decreased since the total chloride content increased with increasing W/C.

Larger temperature and optimal relative humidity accelerate chloride ingress and corrosion propagation processes. An increase in curing temperature increases both ionic diffusivity and chloride binding capacity. Because, the hydration and pozzolanic reaction are accelerated are higher temperatures and the pore structure is more dense.

Another important environmental factor is the presence of acidic gaseous pollutants such as: carbon dioxide, sulfur dioxide, and nitrogen oxides. These acidic compounds are produced by industrial processes or by urban activity, and can be transferred to the concrete matrix by either dry or wet deposition. Their ingress from the surface of concrete depends mainly on the porosity of the concrete matrix. It has been observed

that the presence of sulfate can improve the resistance of concrete matrix to chloride ingress at an early exposure age but can increase chloride penetration at a later exposure. In addition, once the sulfates pollutants have reached the reinforcement, and in water presence, there is a pH reduction that accelerate corrosion processes [Torres-Luque et al., 2014].

The presence of sulphate has a negative effect on the binding capacity. It influences the type and the quantity of produced calcium hydrates.

Carbonation reduces the binding capacity, due to transformation of C-S-H and C-A-H into $CaCO_3$ in the presence of CO_2.

Chapter 5

EXPERIMENTAL METHODOLOGY FOR THE STUDY OF THE CHLORIDE BINDING

5.1 INTRODUCTION

Concrete exposed to chloride environment such as seawater or roads where de-icing salt are used in very cold weathers may have durability problems because of the chloride-induced reinforcement corrosion. The premature deterioration of concrete structures is increasingly demanding methods for better prediction of the distresses and for evaluation of the suitability of concrete mixes to the desired service life. Owing to its important role with regard to durability of concrete structures, many methods have been proposed for testing chloride ingress in concrete. A collection of more than ten different test methods is available through an international committee. These methods can be categorised into three categories: diffusion tests, migration tests, and indirect test based on resistivity or conductivity.

The chloride in concrete or in the aggregate material can be considered present in either a bound form covalently linked with the alumina phase or in a free, mobile, ionic form. It is thought that only the free chloride is significant in the rebar corrosion process and limits have been suggested for acceptable chloride content prior to service exposure of a concrete. The values are usually expressed in terms of water soluble chloride.

When these methods are applied to a sample, the total chloride value is invariably higher than the value for free chloride determined by the water extraction. The difference in the two values is then a measure of the bound chloride in the sample. The acid decomposition/digestion procedure appears to give a reliable measure of the total chloride in a sample, measuring all of the free and combined chloride in the concrete and aggregate material. However, the rate of corrosion of a rebar embedded in concrete appears to be highly dependent upon the concentration of free chloride in the material and bound chloride appears not to be involved in the corrosion process. Indeed, experimentation on corrosion rates for steel embedded in concrete containing the chloride contaminated aggregate studied in this report showed that the steel was passivated and that corrosion was not occurring . Thus it is important to have a test for free chloride which is reproducible and clearly distinguishes between total chloride and the chloride involved in the corrosion process. [Hope et al, 1985]

5.2 METHODS USED FOR

Torres-Luque [2014] classified the most common chloride content measurement techniques (Figure 5.1), which can be broadly classified as field and laboratory techniques. The most common are field destructive tests. These techniques take samples from in-service structures and determine chloride profiles by using chemical or physical lab techniques. Destructive techniques are mostly used for short term decision making (e.g., repair and maintenance).

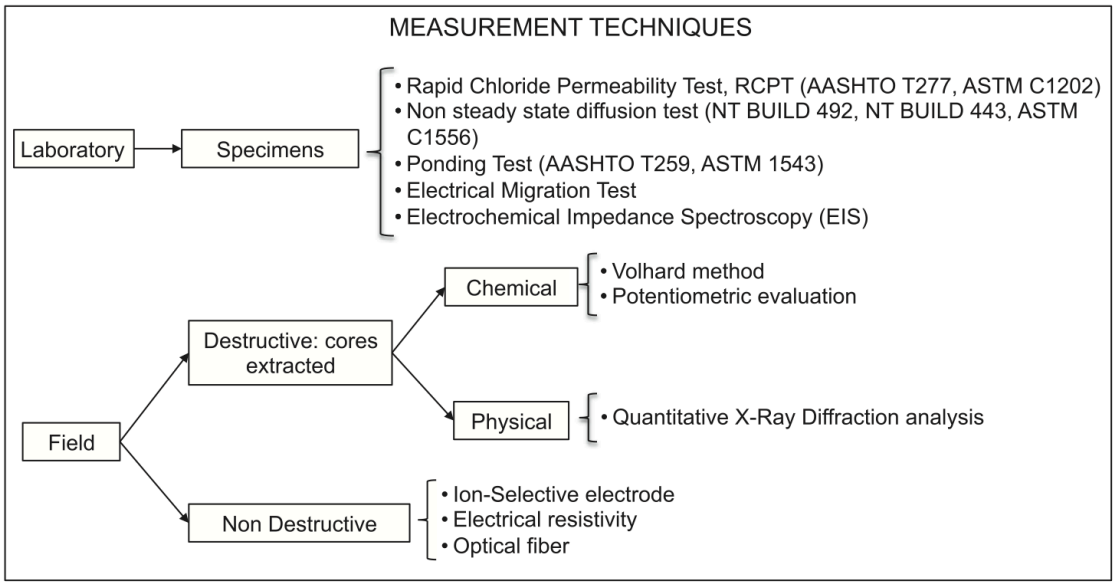

Figure 5.1: Common techniques for measuring chloride content and estimating diffusion coefficient in concrete structures [Torres- Luque et al., 2014].

5.2.1 Total chloride determination

The chloride content of hardened concrete can be determined by chemical analysis, using AS 1012.20-1992, ASTM C 1152-97 or BS 1881 Part 124-1988. The latter involves a more simple extraction procedure. All three of these standards are for the determination of total or "acid soluble" chlorides. Essentially the powder sample is digested in nitric acid to dissolve the cement matrix and liberate all the chlorides present. The extract is then analysed for chloride ion content using a Volhard titration, a chloride ion selective electrode or similar technique.

In addition to the free chlorides present in the pore water or capillaries of the concrete, any chlorides added to the mix and "bound" in the cement phase will also be detected by these methods.

For water-soluble or "free" chloride determination, the concrete sample is extracted by refluxing with boiling water. This is not however a common procedure except in the US.

All of the above analytical methods first require the concrete to be sampled. Powder samples extracted by hammer drill are suitable, as are crushed samples from core sections.

The sampling procedure should avoid wet methods which might wash out chlorides from the concrete and lead to an ambiguous or lower result. If cores are taken for chloride analysis using wet coring, the diameter should be at least 40 mm. [CTI technical note, 2004]

The total chloride concentration can be assessed after grinding by chemical analysis (nitric acid extraction), for example according to the AFPC-AFREM procedure [Chaussadent and Arliguie, 1999], or by means of X-ray fluorescence. [Baroghel-Bouy, 2008]

Lu et al [2002] find the relationship between the free and total chloride diffusivity in concrete by using an electrochemical method.

Torres- Luque et al. [2014] classified common techniques for measuring chloride content in concrete structures (Table 5.1).

Table 5.1: Common techniques for measuring chloride content in concrete structures [Torres- Luque et al. 2014].

Technique	General conditions	Measured parameters	Complementary techniques
	Techniques for long time decision-making		
Rapid Chloride Permeability Test, RCPT	Time = 6 h 3%NaCl + 0.3N NaOH Power supply (DC) = 60 V	Charged passed. Chloride penetrability	
Nonsteady state diffusion test	Specimen cured for 28 days. 2.8 M NaCl for 35 days. 0.5 mm slice	Fick's second law. Diffusion coefficient	Volhard method
Electrical migration test	Power supply (DC) = 10–15 V	Diffusion coefficient. Ernst–Planck equation	Volhard method
Impedance	Specimens cured for 24 h at 95%RH. Electrode KAg $(CN)_2$. NaOH + NaCl. 0.1–11.31 Hz. Power supply (AC) = 10 mV	Diffusion coefficient	
Ponding test	Cured for 14 days. 50%RH 28 days. 3%NaCl for 90 days. 12.7 mm slice	One-dimensional chloride ingress profile	Potentiometric evaluation
	Techniques for short time decision-making		
Quantitative X-ray diffraction analysis	Diffractometer system. Standard: TiO_2	Free chloride	Volhard method
Volhard method	Dried and powdered sample. Titration NH_4SCN	Total chloride content	
Potentiometric evaluation	Wet and powdered sample. Titration $NaNO_3$	Free chloride	

Table 5.1 shows the objectives of each technique in summary:

- Three of them aim to directly determine chloride concentration (Quantitative X-ray diffraction analysis and Potentiometric evaluation for free chlorides and Volhard method for total chloride content).
- RCPT relates charge passed through a concrete slab to chloride penetrability in order to define the permeability of the material.
- Non-steady state diffusion test and electrical migration test use diffusion models and complementary chemical techniques for characterizing the material.
- Impedance and ponding test accelerate diffusion processes for determining diffusion coefficient and chloride ingress profile.

Summarizing, the chloride threshold determination method is still an open subject with a significant impact on defining maintenance policies (Torres- Luque et al., 2014).

The free and total chloride in concrete are determined using an electrode couple of Ag/AgCl–SCE. Two calibrated curves are determined first. One is the electrode potential difference to chloride concentration in standard NaCl-$Ca(OH)_2$ solutions in which the $Ca(OH)_2$ is saturated. Another is the electrode potential difference to chloride concentration in standard NaCl–0.1 N HNO_3 solutions. The two plots are

shown in Figures. 5.2 and 5.3. The accuracy using these two curves to determine the chloride concentration in the same type solutions is within 0.2%.

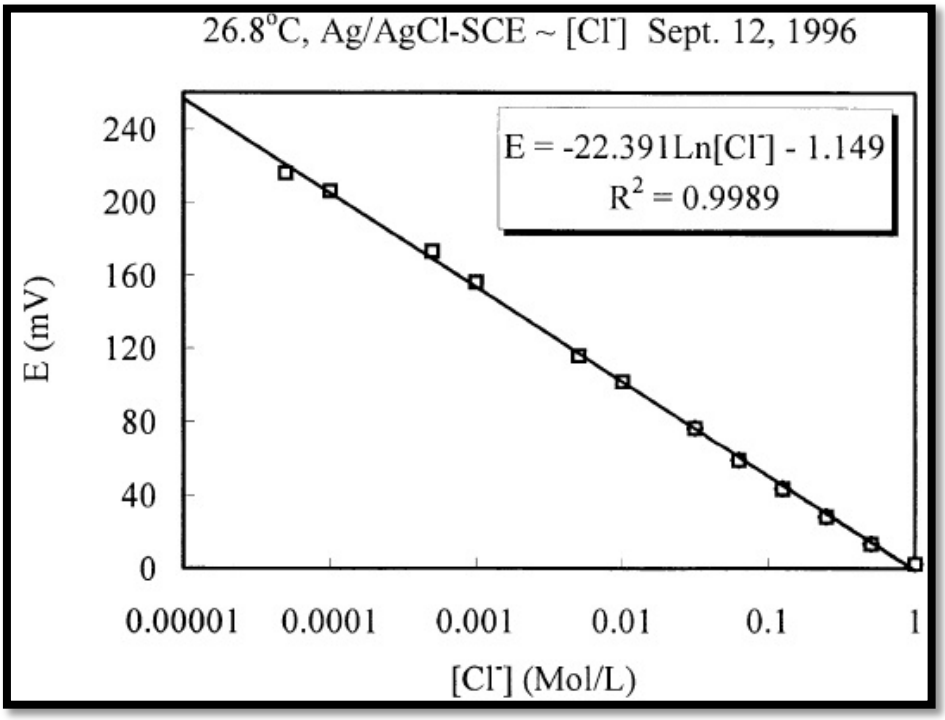

Figure 5.2: The calibrated relationship between the potential difference of Ag/AgCl –SCE couple and the chloride concentration in NaCl – $Ca(OH)_2$ solutions.

The free and total chloride profiles in concrete are determined as follows. After the concrete specimens (100×100×300 mm) are cured at 20 ± 2 ˚C (RH 90%) for 4 weeks, the top 20-mm was cut off and coated with wax, while leaving the newly cut surface uncoated, and then immersed in 3.5% NaCl solution. After 3 months of immersion, the specimen was drilled along the vertical direction from the uncoated surface using a driller with a powder collector. The collected powder was then placed in 50 ml of saturated $Ca(OH)_2$ or 0.1 N HNO_3 solution. The solution was stirred continually and kept for at least 48 h. The potential difference of the Ag/AgCl–SCE electrode couple was measured. The chloride concentration of the solution was

calculated according to the calibrated equations and changed to that in concrete. The chloride concentration profile may be plotted after the variations of the chloride concentration with the concrete depths obtained. The free and total chloride diffusivities in concrete can be calculated using Fick's second law.

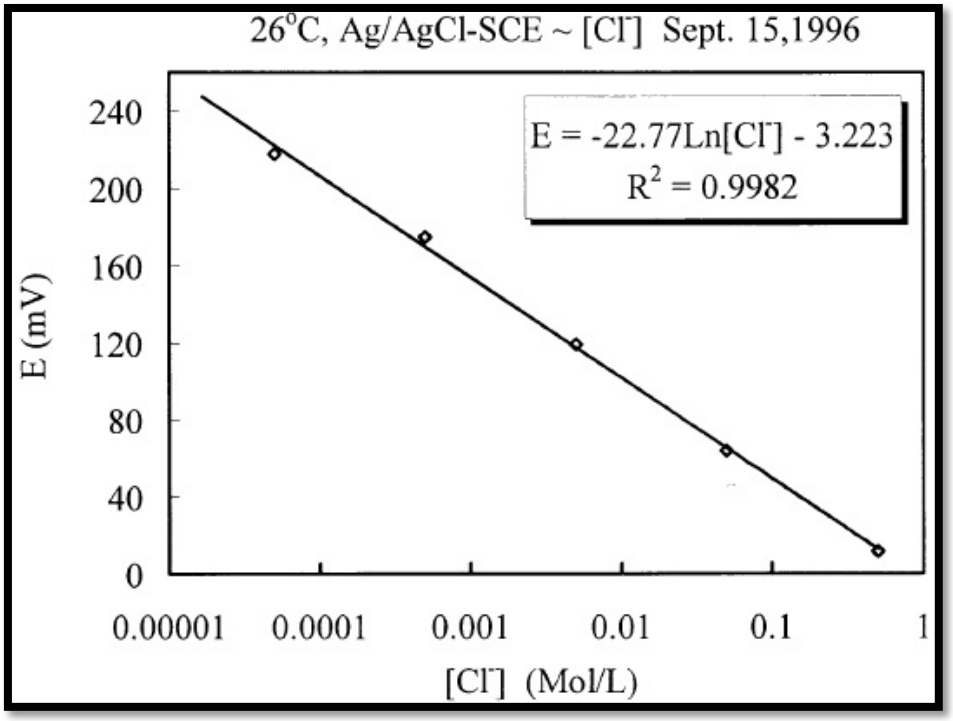

Figure 5.3: The calibrated relationship between the potential difference of Ag/AgCl–SCE couple and the chloride concentration in NaCl– 0.1 N HNO_3 solutions.

The relationship between the free and total chloride diffusivities in concrete is shown in Figure 5.4. It is found that the total chloride diffusivity is times 2.2 to 3.4 to the free chloride diffusivity. The mathematical average is about 2.8. Considering the probability and error of measurements, it is assumed that the total chloride diffusivity is near 3.0 times the free chloride diffusivity. That is to say, the bound chloride content is about two times the free one. This rough relationship may be useful when predicting the service life of concrete and comparing the permeability of concrete.

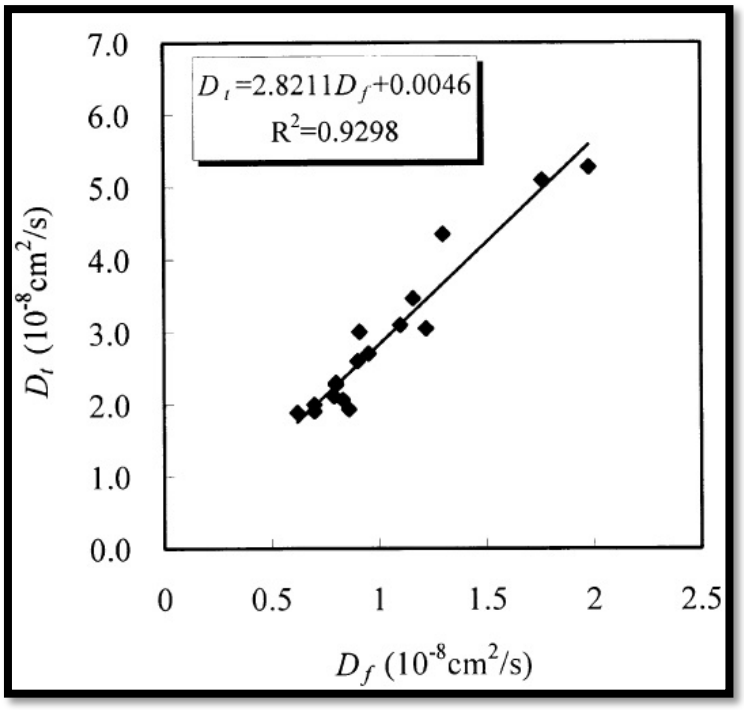

Figure 5.4: The relationship between free and total chloride diffusivity in concrete.

5.2.2 Free chloride determination

The free chloride in concrete is a factor in the corrosion of embedded steel while bound chloride is not. Various procedures for the recovery and determination of free chloride in concrete have been examined.

The chloride content of concrete has become of increasing importance with recognition of a relationship between it and the corrosion of reinforcing steel embedded in the concrete. Severe corrosion of the steel or rebar can occur when the concrete becomes carbonated or chloride is present at the interface between the rebar and the concrete. Carbonation adjacent to the rebar is normally prevented by an adequate concrete cover. Chloride may be present either from the original mix ingredients or it may accumulate in the concrete over a period of time from factors such as the application of deicing salts to a roadway surface.

The free chloride is generally considered to be the water soluble part of the total but the measurement is not well defined and the values obtained are dependent upon the subdivision of the sample and the nature, temperature and duration of the extraction step. Indeed the current thinking of ACI Committee 222 "Corrosion of Metals in Concrete" is that limits on chloride content should be stated in terms of total chloride since measurement is better defined and more reliable than that for soluble chloride.

The recommended procedures for chloride analyses start from ground samples of the concrete or component raw materials. For total chloride, the current American Association of State Highway and Transportation Officials (AASHTO) Specification requires that the representative sample pass a #50 (300 μm) sieve. The total chloride is then determined after a nitric acid decomposition/digestion of the ground sample. For the determination of free, water soluble chloride the current Ontario Ministry of Transportation and Communications (OMTC) Specification requires that the representative sample be first ground to pass a #50 (300 μm) sieve. A weighed portion is then transferred to a mortar and further ground as a slurry before analysis. It is stated that the final sample should completely pass a #I00 (150 μm) sieve and 75% should pass a #200 (75 μm) sieve. The chloride is extracted from the final grind by boiling with water for 5 minutes and then allowing the mixture to stand for 24 hours at room temperature prior to analysis of the aqueous phase.

Once the chloride is in solution, the recommended determination of the chloride content is by a conventional precipitation titration using a standard silver nitrate reagent. The titration is normally followed by a potentiometric monitoring of the chloride ion concentration with an ion selective electrode. The final end point is determined from the inflection point on a graph of E (CelI) vs added titrant. The ion selective electrode can be used to directly analyse the solution for chloride ion concentration after suitable calibration but this is not recommended due to a higher degree of uncertainty.

The relationship between the bound chloride and the free chloride can be described by Freundlich isotherm at high free chloride concentrations and Langmuir isotherm at low free chloride concentrations [Tang and Nilsson, 1993].

As regards the free chlorides, the approach is more complicated, since the free chloride amount appears to greatly depend on the method of determination. This means that the definition of the free chlorides has to be linked to the method used. Typically, the free chlorides will include at least the "diffusing" ones (present in the pore solution) and a variable proportion of the physically bound chlorides (those weakly physically adsorbed onto the solid matrix), depending on the method. It is worth noting that a good correlation has been pointed out between the water-soluble chloride content provided by the AFPC-AFREM procedure and by means of pore solution extraction (squeezing of samples) [Casellote and Andrade, 2001], which is often considered as a reference method. Higher values are systematically found in the case of the AFPC-AFREM procedure. For example, a factor 1.83 is considered in [Nagataki et al, 1993], which can be used to correct the raw data provided when applying the AFPC-AFREM procedure. The free chloride concentration can also be measured by the ion chromatography technique as mention in Meck and Sirivivatnanon, [2003] research [Baroghel-Bouy, 2008].

Determination of free and bound chloride is very important. The binding capacity is the capacity of a material (c) to bind chlorides (c_b) when the ion concentration changes.

$$Binding\ capacity = \frac{\partial c_b}{\partial c} \qquad 5.1$$

The dimension of the binding capacity depends on the units chosen for c_b and c, respectively. Obviously the binding capacity depends on the concentration, but is sometimes assumed to be a constant. As seen the chloride binding capacity is very high at low chloride concentrations.

One important, but not obvious, question is whether the concentration of chloride in the pore water is equal to the concentration in the surrounding sea water or exposure solution. Some recent ideas on determining free chloride by leaching in water cause confusion about free and water soluble chloride that really question such a statement.

Glass and Buenfeld [1995] claim that equilibration of the pore solution in cement or concrete specimen with a chloride containing storage solution provides an accurate

method of determining chloride binding relationships. However this method has the disadvantage of being time consuming. They made a cylindrical cement paste specimens of w/c=0.5 in 49 mm diameter moulds which were then sealed and rotated to prevent segregation. The cement composition is given in Table 5.2. After 28 days curing at 22˚C the specimens were removed from the moulds, and stored in saturated lime water for 1 week.

Table 5.2: Oxide and Bogue Composition of the Cement.

Oxide Composition									Bogue Composition			
CaO	SiO_2	Al_2O_3	Fe_2O_3	MgO	Na_2O	K_2O	SO_3	Ig. Loss	C_3S	C_2S	C_3A	C_4AF
64.7	20.7	4.6	3.0	1.0	0.13	0.65	3.0	1.3	62.2	12.4	7.12	9.12

Then they sliced some specimens into 5 mm thick discs and they were stored in sealed containers holding 0.1321 of storage solution. The storage solution initially contained 0.135M NaCl and 0.3M NaOH. Five of these containers were treated in an ultrasonic bath for 2 periods of 30 minutes each day on five days of the week. At intervals containers holding both the ultrasonically treated and untreated specimens were removed for analysis. One disc was ground and treated with boiling nitric acid to extract the acid soluble chloride, while the pore solution in the remaining discs was expressed under pressure using a pore press.

Sets of crushed and disc specimens were stored in separate containers holding a 0.132 M chloride solution. The volume of the solution added was adjusted such that the total chloride content in each container expressed as a percentage by weight of cement was the same. The change in the storage solution concentration with time was determined.

One specimen was electrochemically treated using an experimental arrangement. A DC voltage (7V) was applied to drive chloride ions through the specimen from the cathodic chamber to the anodic chamber. The applied current was approximately 30 mA. The chloride concentration in both the anodic and cathodic chambers was

monitored as a function of time. After 14 days the specimen was removed and the pore solution expressed.

The acid soluble chloride together with the chloride contents of the expressed pore solutions and the storage solutions were analysed by potentiometric titration against silver nitrate.

The time dependence over a sixty day period of normal storage (no ultrasonic treatment) of the chloride content in the expressed pore solution and storage solution as well as the acid soluble chloride content is given in Table 5.3. As the result of variations in the sample weights, the initial chloride content available for contamination varied when expressed per unit weight of cement although the variation between samples subjected to the same treatment is small.

Table 5.3: Results Obtained on Samples Subjected to Normal Storage.

Storage Duration days	Sample Weight (wet) (g)	External Solution			Pore Solution		Acid Soluble Cl^- (% cement)	Calculated Total Cl^- (% cement)
		Initial Cl^- (% cement)	Final Cl^- (mole/l)	(% cement)	(mole/l)	(% cement)		
7	159.13	0.63%	0.059	0.27%	0.040	0.057%	0.32%	0.35%
14	157.62	0.63%	0.053	0.25%	0.051	0.072%	0.37%	0.38%
28	156.95	0.64%	0.050	0.23%	0.064	0.091%	0.39%	0.40%
60	157.24	0.63%	0.048	0.23%	0.062	0.087%	0.41%	0.41%

Table 5.4 gives the results obtained when the samples were ultrasonically treated. After 14 days the chloride concentration of the external storage solution and the expressed pore solution as well as the acid soluble chloride content stabilised. The chloride concentration of the expressed pore solution was marginally higher than the storage solution concentration, although this may be insignificant. The acid soluble chloride levels were significantly lower than the maximum achieved in the absence of treatment. This would partly result from the differences in the available chloride per unit weight of cement.

Table 5.4: Results Obtained on Samples Subjected to Ultrasonic Treatment.

Storage Duration days	Sample Weight (wet) (g)	External Solution			Pore Solution		Acid Soluble Cl^- (% cement)	Calculated Total Cl^- (% cement)
		Initial Cl^- (% cement)	Final Cl^- (mole/l)	(% cement)	(mole/l)	(% cement)		
7	173.16	0.58%	0.056	0.24%	0.050	0.071%	0.30%	0.34%
14	169.57	0.59%	0.052	0.22%	0.051	0.072%	0.35%	0.36%
28	172.33	0.58%	0.051	0.22%	0.052	0.074%	0.34%	0.36%
45	170.48	0.59%	0.051	0.22%	0.051	0.073%	0.34%	0.37%
60	170.98	0.58%	0.050	0.22%	0.052	0.074%	0.34%	0.37%

The acid soluble, storage solution and expressed pore solution chloride content of ultrasonic treated samples is compared with untreated samples in Figure 5.5. To minimise the effect of the variation in initial sample weights, the plotted values are presented as a percentage of the total chloride in the system (the initial chloride content of the storage solution) expressed relative to the cement weight.

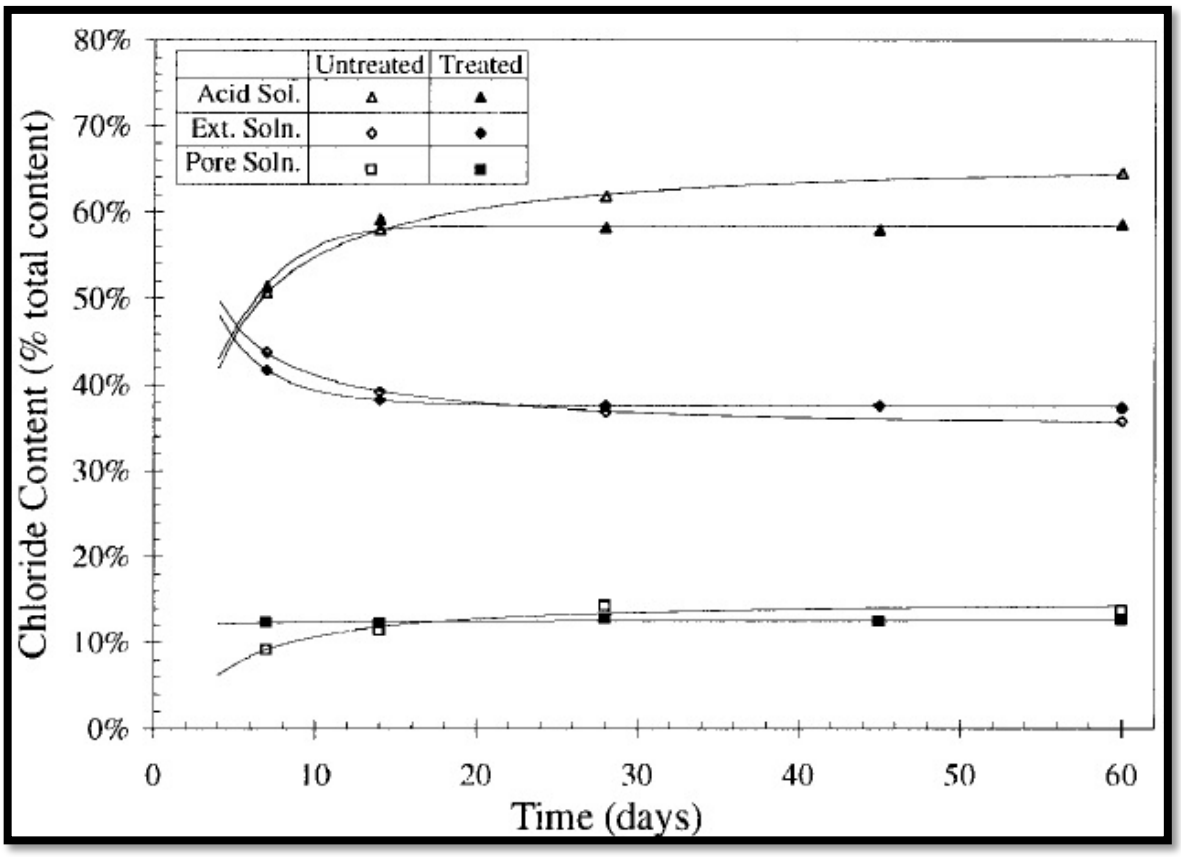

Figure 5.5: The acid soluble, storage solution and expressed pore solution chloride content of ultrasonically treated and untreated samples presented as a percentage of the total chloride in the system expressed relative to the cement weight.

The total chloride content of the samples can be calculated by assuming that it is equal to that, removed from the storage solution. The results, given in Tables 5.3 and 5.4, show that the calculated total chloride content was generally higher than the acid soluble chloride content. In the case of ultrasonically treated samples this difference was typically 7.9% while a smaller difference of typically 4% was observed on untreated samples.

The results of preliminary work into the electrochemical acceleration of chloride ingress are given in Table 5.5. During the treatment chloride migrated through the specimen increasing the concentration in the anode chamber of the cell from 0.026 M

to 0.094 M while that in the cathode chamber decreased to 0.099 M. However the concentration of chloride in the pore solution expressed from the sample at the end of the experiment was only 0.048 M.

Table 5.5: Chloride concentrations determined during and after electrochemical treatment

Duration days	Chloride Concentration (mole/l)		Pore Solution (mole/l)
	Cathode Chamber	Anode Chamber	
0	0.225	0.026	
6	0.154	0.041	
10	0.125	0.068	
14	0.099	0.094	0.048

Table 5.6 gives the initial results comparing the use of discs with crushed specimens. This shows that chloride removal from the storage solution occurs much more rapidly when the specimens are crushed. Investigations into the side effects of using crushed specimens are continuing.

Table 5.6: Storage solution chloride concentration for discs and crushed specimens

Duration (days)	Chloride Concentration (mole/l)	
	Discs	Crushed Specimens
0	0.1325	0.1325
3		0.0706
7	0.0874	0.0614
14	0.0696	0.0561

Ultrasonic treatment significantly reduces the time required to achieve equilibrium or steady state conditions (Fig.5.5). However, while it initially results in the more rapid removal of chloride from the storage solution, after 28 days higher acid soluble and expressed pore solution chloride contents as well as lower storage solution chloride contents were observed in the absence of treatment. This indicates that such treatment prevents some chloride from being bound.

Preliminary studies on electrochernically accelerating chloride ingress indicates that problems may also be encountered when using this method. In this case the chloride concentration in the specimen pore solution remained significantly below that in the anode and cathode chambers despite the passage of chloride ions through the specimen to equalise these concentrations. Possible reasons for this include a less tortuous route taken by chloride in the presence of an electric field and a dominating specimen-solution interfacial resistance controlling the rate of chloride transport through the specimen.

Ultrasonic treatment appears to prevent the formation of loosely bound chloride which would otherwise be released when the pore solution is expressed. Thus the chloride concentration in the expressed pore solution is much closer to that in the storage solution of ultrasonically treated specimens (Table 5.4) and the expressed pore solution concentrations after 60 days of treatment are significantly lower than those determined in untreated specimens.

The calculated total chloride contents (Tables 5.3 and 5.4) suggest that total chloride is underestimated when determined by acid extraction. Indeed if the bound water content of the samples (assumed to be constant) increased during storage, the differences between the calculated and measured values would be greater. This may partly be due to errors associated with the method, such as the loss of vapour borne chloride on exposing the sample to boiling nitric acid. Other possible explanations include the retention of some strongly bound chloride in the insoluble residue.

On the basis of their work chloride may be classified as being free if its concentration in the pore solution cannot exceed that of the storage solution, loosely bound if it is

released into the pore solution expressed under pressure and bound when it is not released by pore solution expression. [Glass and Buenfeld, 1995]

Tang and Nilsson [1993] claim the common method of determining the chloride binding capacity involves dissociating the free chloride fraction from the total chloride content by analyzing the pore solution squeezed out from the concrete under high pressure. However, it would be very difficult by this method to obtain the binding characteristics of chloride ions which penetrate into concrete. Therefore, they establish a new method based on the adsorption from solution.

They used OPC and the dolomite sand without any chloride, passing through 1 mm sieve, was chosen as fine aggregate. For both OPC pastes and mortars (cement:sand = 1:2), deionized water was used and the water-cement ratios were 0.4, 0.6 and 0.8. After moulded in a plastic pipe mould of size φ70x140 mm, the specimen was subjected to continuous rotation at about 10 rpm for 24 hours about a horizontal axis to prevent significant segregation, then demoulded and cured with plastic pipe under saturated lime water at room temperature (about 22 °C). After curing for about 6 weeks, the central region of the specimen was wet-crashed and water-sieved into 0.25-2 mm particles. The particulate samples were vacuum dried in a desiccators filled with silica gel at room temperature for about 3 days to remove most of the water, then stored in a desiccator with decarbonized air at 11% RH kept by saturated LiCl solution for at least 7 days so that only a monolayer of water was adsorbed on the gel.

In order to establish chloride adsorption isotherm, About 25 g particulate sample dried at 11% RH was put into a given weight cup, then the cup was vacuumed within a desiccator for 2 hours before filled with a given concentration NaCI solution saturated with $Ca(OH)_2$. The volume of solution filled inside the cup was calculated from the increment of the weight of the cup and the density of the solution. The cup was covered and stored at 20 °C for equilibrium. According to their preliminary experiment, the adsorption equilibrium could be reached in the first seven days, as shown in Figure 5.5. Theissing et al. [1978)] also found the equilibrium could be reached within 10-14 days. Therefore, two week time is enough for various samples to

reach the adsorption equilibrium. After equilibrium, the inside solution was pippetted to determine the chloride concentration by potentiometric titration using 0.01 N $AgNO_3$ and chloride selective electrode. The content of bound chlorides was calculated by the following equation.

$$C_b = \frac{35.45V(c_0 - c_1)}{W} \qquad 5.2$$

Where C_b: bound chloride content, mg/g-sample, V: volume of solution ml, c_0 and c_1: initial concentration and equilibrious concentration of chloride solution, mol/l, W: weight of dry sample, g.

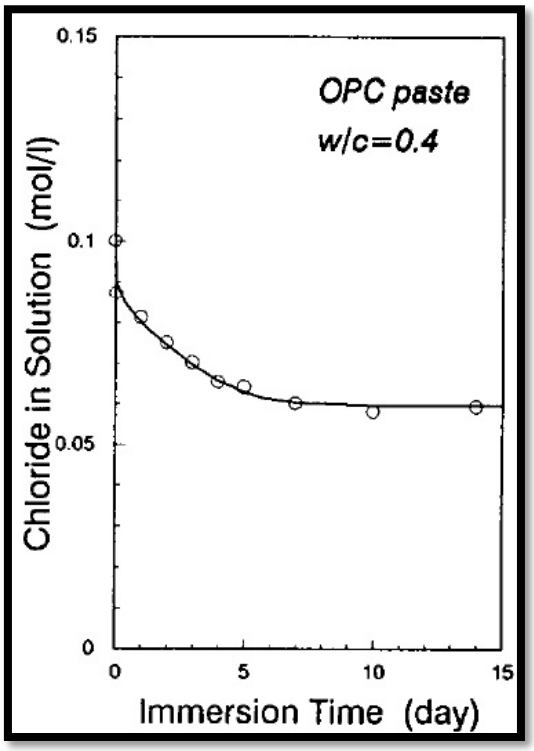

Figure 5.6: Relation between adsorption equilibrium and time

The weight of dry sample can be calculated from the difference in weight of the sample dried in a desiccator at 11%RH and in an oven at 105 °C. Since for most cases the C-S-H gel in concrete predominates the adsorption, at least physical adsorption, it

is useful to express the bound chloride content by unit weight of the gel. In this case, the sample weight W in Eq.(5.2) should be substituted by the weight of the gel W_{gel}.

$$W_{gel} = \frac{(1 + W_n^0) f_c \alpha}{1 + W_n^0 f_c \alpha} W \qquad 5.3$$

where W_n^0: non-evaporable water, assuming W_n^0= 0.25, α: degree of hydration, f_c: cement content in concrete by weight,

$$f_c = \frac{W_{cement}}{W_{cement} + W_{aggregates}} \qquad 5.4$$

The hydration degree of the paste was determined by ignition method. The ignition loss of cement was also taken into account for necessary correction. The hydration degree of the mortar was assumed as the same as that of the paste with the corresponding water/cement ratio.

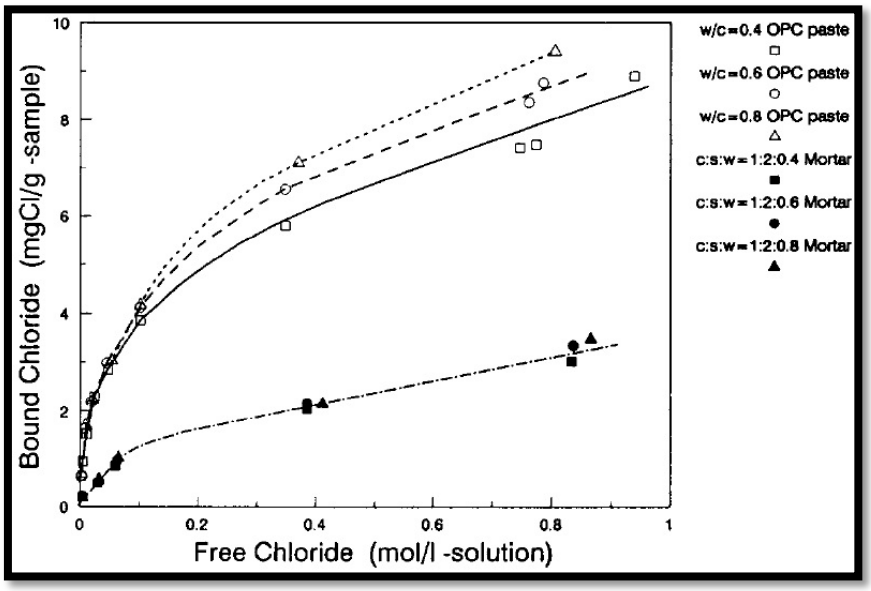

Figure 5.7: Chloride adsorption isotherms of OPC pastes and mortars (in unit weight of sample)

The adsorption isotherm can be drawn from the data C_b and C_1, through a series of test with different initial concentration.

For the chloride desorption isotherm, the surplus solution in the cup was removed as much as possible, and about 200 ml deionized water saturated by $Ca(OH)_2$ was added to the cup. Then the cup was stored at 20 °C for new equilibrium before the inside solution was peppetted and analyzed in the same way described above. The bound chloride content in this case can be calculated by the following equation.

$$C_b = \frac{35.45[c_0V - c_1V' - c_2(V + V'' - V')]}{W} \qquad 5.5$$

where V': volume of solution removed out, including first pippetted, ml, V'': volume of deionized water added, ml.

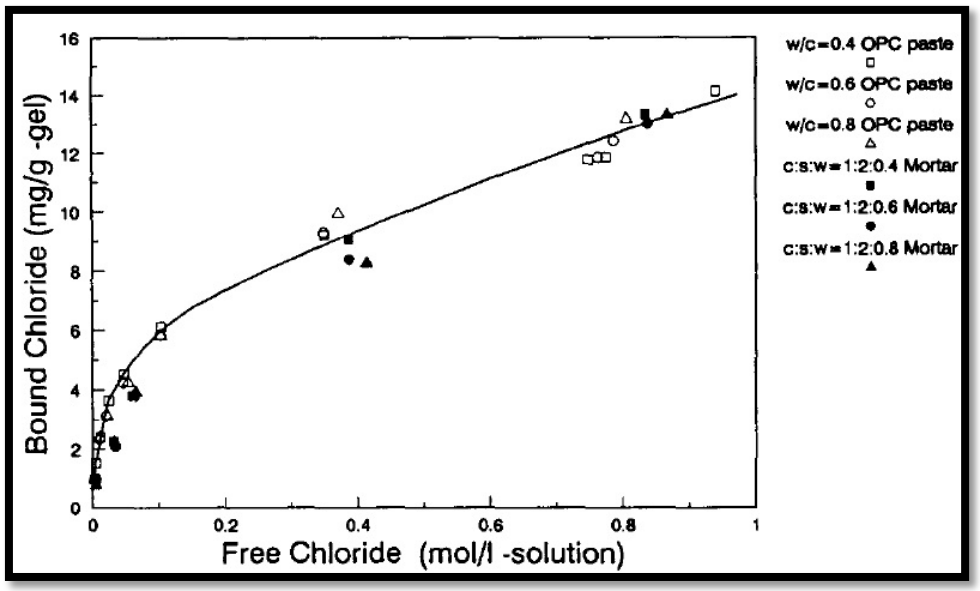

Figure 5.8: Chloride adsorption isotherms of OPC pastes and mortars (in unit weight of CSH gel)

For water desorption isotherm, the pore structures of the samples were determined by water desorption isotherms. About 120 g of particulate sample dried at 11%RH was put into a cup. Then the cup was vacuumed for 24 hours before filled with distilled water. The water-saturated sample was distributed among seven weighing cups. These weighing cups were put into seven different RH chambers with relative humidity from 11% to 95% individually and stored at 20 °C for about two months to obtain the

constant weight. The detailed structures of RH chambers and other procedures of water desorption experiment was described by Xu [1990]. D.H. method [1994] was used to calculate pore size distribution and surface area. The shape of pores was assumed as parallel plate. The thickness of adsorption layers was determined by the following semiempirieal relationship [1979].

$$t = \frac{3.48}{[\log\left(\frac{p_s}{p}\right)]^{1/3}} \qquad 5.6$$

Where t: average thickness of adsorption layers, Å, p/p_s,: relative pressure.

They assumed that the free chloride concentration in pore solution is equal to that in equilibrious solution.

From Figure 5.6 we can obtain that the water cement ratio has some influence on the isotherms of pastes, but it has a little influence on the isotherms of the mortars, and the binding capacity of the pastes is apparently higher than that of the mortars. When the content of bound chlorides is expressed by unit weight of C-S-H gel, however, it is found that no matter the pastes or the mortars with different water cement ratios, they have almost the same chloride binding isotherm, as shown in Figure 5.7. Although the pore size distributions of various samples are much different, the surface areas of the C-S-H gel in different samples are almost the same, because a large size pore does not make an apparent contribution to the total area. These findings show that the chloride binding mainly occurs through the interface between pore solution and hydrated products in concrete and the binding capacity strongly depends on the content of C-S-H gel regardless of the water/cement ratio and even the addition of aggregate. [Tang and Nilsson,1993]

Cheewaket et al [2010] explain that the chloride binding capacity in concrete can be calculated by subtracting the free chloride content from total chloride content. In their study, the chloride binding capacity was analysed in term of percentage chloride binding capacity compared to the total chloride content. Regression analyses were then performed to obtain their relations. For example, $C_f = (0.8556)C_t$, where C_f is the free chloride content and C_t is the total chloride content of concrete after 7 years

exposure. According to the relation, the percentage chloride binding capacity (P_{cb}) as compared to the total chloride content can be easily determined from Eq. (5.7):

$$P_{cb} = \frac{[(C_t - C_f)\times 100]}{C_t} \quad 5.7$$

By substituting C_f in terms of Ct [C_f = (0.8556)C_t] in Eq. (5.7), the percentage chloride binding capacity (P_{cb}) of concrete after 7 years exposure is 14.4%.The results showed that P_{cb} decreased with the exposure time. Previous research proposed a model for predicting the time dependent chloride binding based on experimental data in the laboratory [Sumranwanich and Tangtermsirikul, 2004]. Their model states that a larger chloride binding capacity is expected for longer exposure periods for paste. However, it did not present the bound chloride content as compared to the total chloride content in cement paste. With increasing exposure time, more total chloride ingress was found, and the bound chloride content was greater, even though the percentage chloride binding capacity (P_{cb}) as compared to the total chloride content was smaller.

They research proposes an equation for determining the free chloride content from the total chloride content ingress in concrete by using the data gathered from the marine site over 7 years. Figure 5.8 shows the relationship between free and total chloride contents of concretes with W/B ratios of 0.45, 0.55, and 0.65 at 3, 4, 5, and 7 years exposures.

Using the experimental data, the following linear relationships are proposed for cement and fly ash concrete as shown in Eqs. (5.8)–(5.13):

for Portland cement type I concrete, C_f =0.8541(C_t); (R^2=0.9963) 5.8

for Portland cement type V concrete, C_f =0.8773 (C_t); (R^2=0.9977) 5.9

for 15%-fly ash concrete, C_f =0.8350(C_t); (R^2=0.9985) 5.10

for 25%-fly ash concrete, C_f =0.8011(C_t); (R^2=0.9979); 5.11

for 35%-fly ash concrete, C_f =0.7734(C_t); (R^2=0.9986) 5.12

for 50%-fly ash concrete, $C_f = 0.7661(C_t)$; ($R^2 = 0.9949$) 5.13

Here, C_f and C_t are the free and total chloride contents in concrete, respectively. According to the equations, the free chloride contents of Portland cement types I and V, 15%-fly ash, 25%-fly ash, 35%-fly ash, and 50%-fly ash concretes are 85.41%, 87.73%, 83.5%, 80.11%, 77.34%, and 76.61% of the total chloride content, respectively. The relations show that as the percentage replacement of fly ash increases, the free chloride content in terms of the total chloride content decreases, which corresponds to the increase in the chloride binding as previously presented. These equations are very useful in determining the free chloride content, which affects steel corrosion. In addition, they could also be used to determine the threshold chloride with regard to the design of concrete durability.

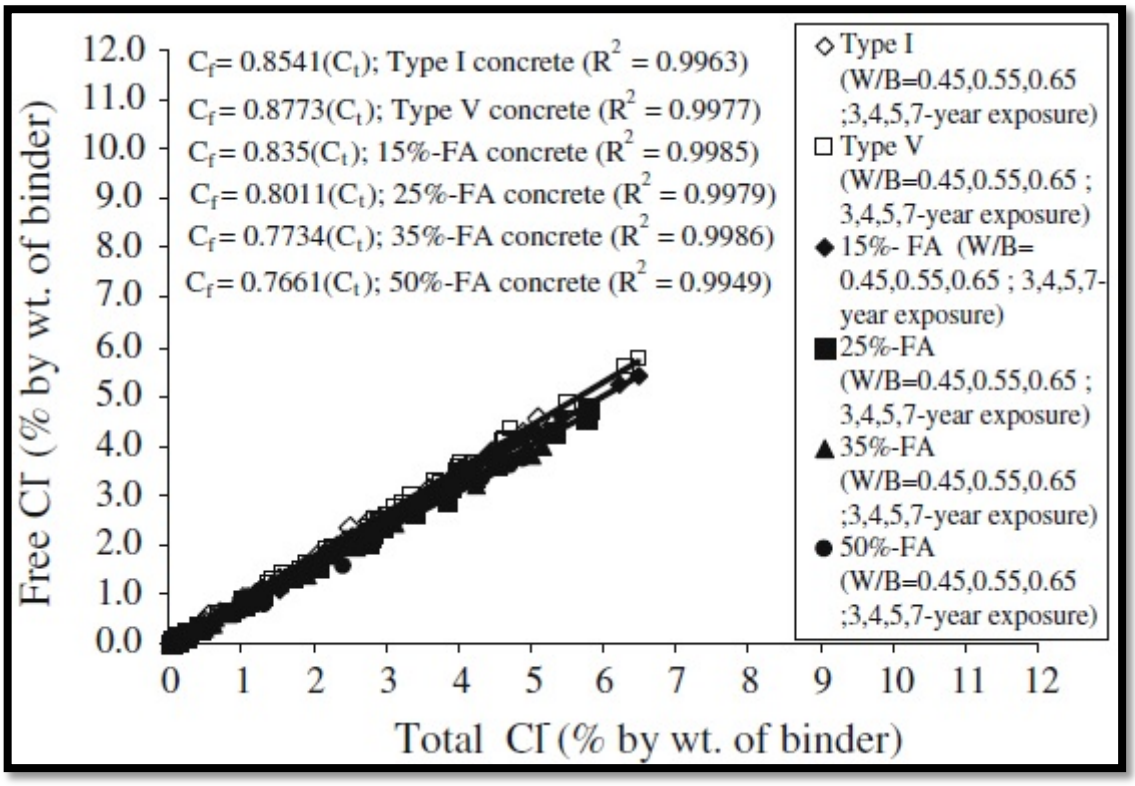

Figure 5.9: Relationship between free and total chloride contents of concrete with W/B ratios of 0.45, 0.55, and 0.65 at 3, 4, 5, and 7 years exposures [Cheewaket et al [2010]]

Yun et al [2004] used pulse nuclear magnetic resonance (NMR) in order to detect chloride in a cement matrix

5.3 CHARACTERIZATION OF CEMENT HYDRATION PRODUCTS THAT BOUND CHLORIDES

Florea and Brouwers [2012] try to correlate the total amount of chloride bound in concrete with the amounts bound by different hydration products. They used pure hydration products, through this method important information about the mechanisms through which single hydration products bind chlorides were gathered.

They chose Ordinary Portland Cement (OPC) as binder throughout their study, since it is the most abundantly used cement type and the most basic system in terms of hydration modeling that still contains all phases involved in chloride binding.

First they model paste. For the hydration of OPC pastes, a global degree of hydration can be assumed for all clinker minerals, when hydration has progressed over 50%. Typical hydration kinetics at ambient temperature for pure clinker minerals (C_3S, C_2S, C_3A with and without added gypsum, C_4AF), as well as for an OPC, are given in [Hewlett, 2004]. Another important point to consider is that the hydration degree will increase with the increase of the water to binder (w_0/b_0) ratio used for the hydration of an OPC paste.

The reactions that describe the saturated hydration of OPC are presented in Table 5.7. These reactions assume that no carbonation of the paste has taken place. The relations in Table 5.8, which are deduced from the chemical equations in Table 5.7, can be used to calculate the molar amounts of hydration products. These are the maximum amounts that can be formed after a complete hydration of cement. Since this is usually not the case, each amount has to be multiplied by the degree of hydration, α.

Table 5.7: The chemical equations describing the saturated hydration of OPC

$C_3S + 4.5H \rightarrow C_{1.7}SH_{3.2} + 1.3CH$
$C_2S + 3.5H \rightarrow C_{1.7}SH_{3.2} + 0.3CH$
$C_3A + C\bar{S} + 14H \rightarrow C_4A\bar{S}H_{14}$
$C_3A + CH + 21H \rightarrow C_4AH_{22}$
$C_3A + 3C\bar{S} + 36H \rightarrow C_6A\bar{S}_3H_{36}$
$C_4AF + 2C_3S + 22H \rightarrow C_6AFS_2H_{18} + 4CH$
$C_4AF + 2C_2S + 20H \rightarrow C_6AFS_2H_{18} + 2CH$

The mass of reacted cement, b, can be calculated using the following relation:

$$b = \alpha(b_0 - m_{U0}) \qquad 5.14$$

where b_0 is the initial mass of cement before the start of hydration. The initial mass of cement is made out of the masses of clinker minerals (m_{C3S}, m_{C2S} etc.) and that of the unreacted oxides, m_{UO}:

$$b_0 = m_{C_3S} + m_{C_2S} + m_{C_3A} + m_{C_4AF} + m_{C\bar{S}} + m_{U_0} \qquad 5.15$$

Table 5.8: Molar relations between the amounts of hydration products and the mineral composition of OPC

$n_{C_4A\bar{S}H_{14}} = \alpha \cdot 0.5 n_{C\bar{S}}$
$n_{C_{1.7}SH_{3.2}} = \alpha(n_{C_3S} + n_{C_2S} - 2n_{C_4AF})$
$n_{C_6AFS_2H_{18}} = \alpha n_{C_4AF}$
$n_{C_6A\bar{S}_3H_{36}} = \alpha \cdot 0.25 n_{C\bar{S}}$
$n_{C_4AH_{22}} = \alpha(n_{C_3A} - 0.5 n_{C\bar{S}})$
$n_{CH} = \alpha(1.3n_{C_3S} + 0.3n_{C_2S} - n_{C_3A} + 1.4n_{C_4AF} + 0.5n_{C\bar{S}})$

These equations are used when the hydration of individual phases is considered. The mass of the hydration products can also be expressed as a function of the mass fractions of clinker minerals in the binder. These mass fractions by weight of binder of the clinker minerals have the following expressions:

$$x_{C_3S} = m_{C_3S}/b_0\,; \qquad x_{C_2S} = m_{C_2S}/b_0 \quad ; etc. \tag{5.16}$$

where Eq. (5.14) has been inserted.

Knowing how many moles of each hydration product were formed (see Table 5.8), their masses can also be computed using their molecular masses:

$$m_{C_4A\bar{S}H_{14}} = n_{C_4A\bar{S}H_{14}} M_{C_4A\bar{S}H_{14}}\ ; \quad m_{CH} = n_{CH} M_{CH} \quad etc. \tag{5.17}$$

The molecular masses of hydration products formed under saturated conditions are listed in Table 5.9. Using these molecular masses, the mass relations can be computed from the molar relations as shown in Table 5.8.

Table 5.9: The formula and molecular mass for each hydration product formed in saturated state and after drying at 11% rh.

Saturated state (100% rh)		Dried state (11% rh)	
Formula	[g/mol]	Formula	[g/mol]
$C_6A\bar{S}_3H_{36}$	1327.34	$C_6A\bar{S}_3H_{12}$	894.98
C_4AH_{22}	722.72	C_4AH_{13}	560.58
$C_{1.7}SH_{3.2}$	213.09	$C_{1.7}SH_{2.1}$	193.27
CH	74.00	CH	74.00
$C_6AFS_2H_{18}$	1042.67	$C_6AFS_2H_8$	862.47
$C_4A\bar{S}H_{14}$	658.62	$C_4A\bar{S}H_{10}$	586.56

A number of experimental studies found in literature determine the chloride binding capacity of hardened cement paste on samples dried at 11% rh. When a saturated

hardened cement paste sample is dried to 11% rh, some of the hydration products modify their water content. The corresponding formulas and molecular masses can also be found in the second column of Table 5.9. Upon 11% rh drying, the mass of the hydration products changes due to the water loss, but the molar quantities remain the same. Therefore, the mass of the hydration products after 11% rh drying can be calculated using the equations listed in Table 5.8 and the molecular masses from Table 5.9, Eq. (5.17) thus becoming:

$$m_{CSH} = m_{C_{1.7}SH_{2.1}} = n_{C_{1.7}SH_{3.2}} M_{C_{1.7}SH_{2.1}} \; ; \qquad 5.18$$

$$m_{C_6A\overline{S_3}H_{12}} = n_{C_6A\overline{S_3}H_{36}} M_{C_6A\overline{S_3}H_{12}}$$

Knowing the hydration degree and the mass of the formed hydration products, the mass of the whole sample dried to 11% rh can be calculated. The sample dried to 11% rh consists of dried hydration products (see Table 5.9), unreacted cement minerals and uncombined oxides. The formula for the mass of the whole sample after drying to 11% rh is given as:

$$m_{spl} = m_{C_{1.7}SH_{2.1}} + m_{C_4A\bar{S}H_{10}} + m_{C_6AFS_2H_8} + m_{C_6A\bar{S}_3H_{12}} + m_{C_4AH_{13}} + m_{CH} + (1-\alpha)(b_0 - m_{U0}) + m_{U0} \qquad 5.19$$

where m_{UO} can be determined from Eq.(5.15)

They used equilibrium method in their study for chloride binding isotherms.and for chloride binding isotherms related to binder composition and hydration products they termed either $C^0_{b,hp}$ for chloride binding capacities expressed in mg Cl/g hydration product conditioned to 11% rh, or $C_{b;hp}$ for the chloride binding capacities expressed in mg Cl/ g sample at 11% rh. The molar mass of each hydration product can be found in Table 5.9 and has already been incorporated in the following isotherm expressions where so needed. The term m_{hp} refers to the mass of the specified hydration product, in grams, calculated using Table 5.9. The mass of sample in grams at 11% rh, m_{spl}, is always computed according to Eq. (5.19). Eq. (5.20) gives the general relation between $C^0_{b,hp}$ and $C_{b;hp}$:

$$C_{b,hp} = C^0_{b,hp} \times \frac{m_{hp}}{m_{spl}} \quad 5.20$$

The chloride concentration of the external solution, c, is always expressed in mol Cl/l solution.

For the chloride binding capacity of the AFm phase they also refer: Hirao et al [2005] studied the chloride binding of the pure AFm phase. They have found the following Freundlich-type isotherm which describes chloride binding by the monosulfate phase, in mg Cl/ g monosulfate:

$$C^0_{b,SO_4-AFm} = 51.89c^{0.58} \quad 5.21$$

Birnin-Yauri and Glasser [1998] consider that 100% of the quantity of HO-AFm is completely transformed into Friedel's salt at a free chlorides concentration greater than 0.015 mol/L. Considering the fact that one mole of hydroxy-AFm binds two moles of chloride ions in order to form Friedel's salt, and using the molecular masses from Table 5.9, the amount of chloride which can be bound by C_4AH_{13}, in mg Cl/ g HO-AFm becomes:

$$C^0_{b,HO-AFm} = 126.5 \quad 5.22$$

Constant for external chloride concentrations over 0.015 M.

The sum of Eqs. (5.21) and (5.22) used henceforth to compute the total binding capacity of the AFm phase.

For the chloride binding capacity of the C-S-H phase, Zibara [2001] also determined the chloride binding ability of the hydration products of pure C_3S and C_2S in mg Cl/ g C-S-H gel formed, compensating for the amount of CH formed, because it is considered not to bind chlorides:

$$C^0_{b,C_3S} = 6.65c^{0.334} \quad 5.23$$

$$C^0_{b,C_4S} = 7.89c^{0.136} \quad 5.24$$

Even though their coefficients are quite different, the isotherms defined by Eqs. (5.23) and (5.24) show almost the same behaviour for the C_3S and C_2S phases when the amount of C-S-H generated is taken into account. A combination of these isotherms that takes into account the C_3S:C_2S ratio of the cement will be used throughout this study. In order to combine these isotherms into one equation, the mass fraction of C_3S (δ_{C3S}) and C_2S (δ_{C2S}) in their sum will be used:

$$\delta_{C_3S} = \frac{m_{C_3S}}{m_{C_3S} + m_{C_2S}} \quad 5.25$$

$$\delta_{C_2S} = \frac{m_{C_2S}}{m_{C_3S} + m_{C_2S}} = 1 - \delta_{C_3S} \quad 5.26$$

Eq. (5.27) describes the chloride binding capacity of the C-S-H phase in mg Cl/g C-S-H, as it will be computed in all following results and termed $C_{b;C\_S\_H;\,Z}$.

$$C^0_{b,C-S-H,Z} = \left(6.65\, c^{0.334}.\delta_{C_3S} + 7.89 c^{0.136}.\delta_{C_2S}\right) \quad 5.27$$

Hirao et al. [2005] experimentally determined a Langmuir-type isotherm for the chloride binding of the C-S-H phase, in mg Cl/g C-S-H gel conditioned at 11% rh:

$$C^0_{b,C-S-H,H} = 21.84.\frac{2.65c}{1 + 2.65c} \quad 5.28$$

Elakneswaran et al. [2009] also propose a chloride binding isotherm for the C-S-H phase in mg Cl/g C1.7SH2.1, which has been fitted to the following Freundlich isotherm, termed $C_{b;C\_S\_H;\,E}$:

$$C^0_{b,C-S-H,E} = 12\, c^{0.63} \quad 5.29$$

Figure 5.9 shows isotherms C^0_{b,SO_4-AFm} (Eq. (5.21)), $C^0_{b,HO-AFm}$ (Eq. (5.22)), $C^0_{b,C-S-H,Z}$ (Eq. 5.27)), $C^0_{b,C-S-H,H}$ (Eq. 5.28)) and $C^0_{b,C-S-H,E}$ (Eq. 5.29)), describing the chloride binding ability of monosulfate, hydroxy-AFm and respectively C-S-H, in mg Cl/g hydrated phase. Figure 5.10 shows the isotherms C^0_{b,SO_4-AFm}, $C^0_{b,HO-AFm}$, $C^0_{b,C-S-H,Z}$, $C^0_{b,C-S-H,H}$, $C^0_{b,C-S-H,E}$ applied to HCP2 using Eq. (5.20), and so taking into consideration the relative amount of each hydrate in the cement paste.

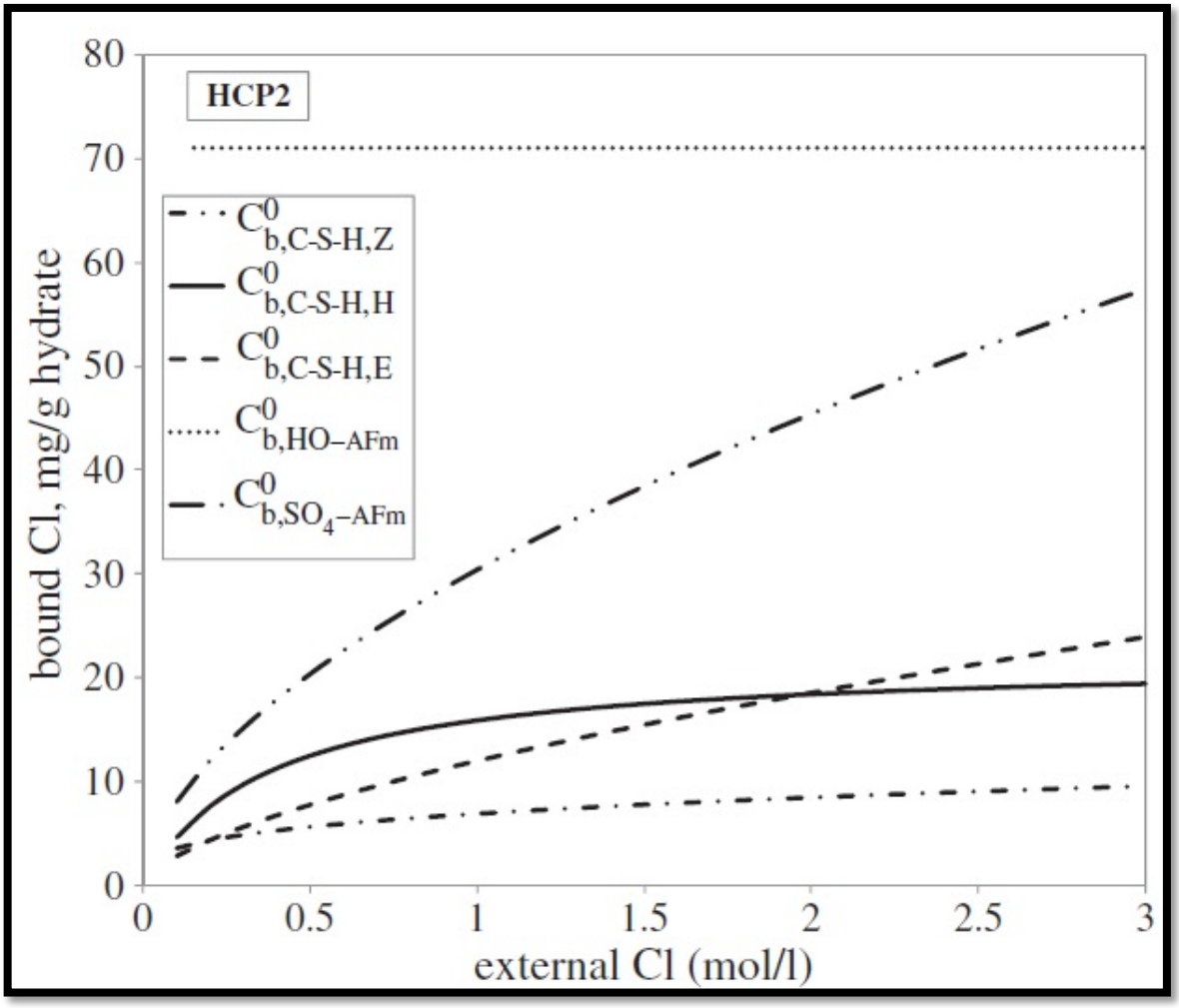

Figure 5.10: Isotherms (10), (11), (16), (17) and (18) describing the chloride binding ability of hydroxy-AFm, monosulfate and respectively C-S-H at 11% rh.

The difference between the $C^0_{b,C-S-H,Z}$, $C^0_{b,C-S-H,H}$, $C^0_{b,C-S-H,E}$ isotherms can have multiple explanations. The quantitative effects of a number of influencing factors cannot be precisely asserted. The first factor that needs to be considered is the very large w_0/b_0 (10:1) ratio employed in Hirao et al [2005], which will not be found in any real concrete structure, as opposed to the w_0/b_0 of 0.5 employed in Zibara [2001]. Also, the fact that in Hirao et al [2005] the solid and liquid fractions of the sample were separated by suction filtering and not by drying using acetone leads to the conclusion that the chloride amounts that can be bound by the gel water of the C-S-H, when fully rehydrated in chloride solution, were also included in the measurement.

Furthermore, a small fraction (evaluated as ≤5%) of the free chlorides that entered the capillary space upon rehydration could still be present at the time of the chloride content measurement. In the case of the binding isotherm $C^0_{b,C-S-H,E}$ determined in Elakneswaran et al [2009] research, the results were deduced from the isotherms of HCP and portlandite. The phase assemblage was predicted using a speciation software, and corrected for the chemically bound chlorides determined through XRD measurements. The maximum external chloride concentration used in these experiments was 1 M. However, at such low concentrations, the results given by XRD are not conclusive. Conversely, Zibara [2001] measured the chloride binding of hydrating C_3S and C_2S pastes with a w_0/b_0 of 0.5 with NaOH and KOH additions to mimic the control solution. The obtained values were corrected for the amount of CH formed.

Table 5.10: Composition of all hardened cement pastes.

	Type of cement	w_0/b_0	Age at time of immersion (weeks)	m_{spl} (g)	α	α_F	β_F
HCP1	OPC 1	0.5	8	113.26	0.8	11.11	0.37
HCP2	OPC 2	0.5	8	110.87	0.8	9.37	0.39
HCP3	OPC 3	0.3	8	113.79	0.75	7.60	0.31
HCP4	OPC 3	0.5	8	114.70	0.8	8.20	0.26
HCP5	OPC 3	0.7	8	115.62	0.85	8.43	0.29
HCP6	OPC 4	0.4	6	109.55	0.58	8.03	0.28
HCP7	OPC 4	0.6	6	110.87	0.66	9.50	0.37
HCP8	OPC 4	0.8	6	111.03	0.67	10.32	0.40

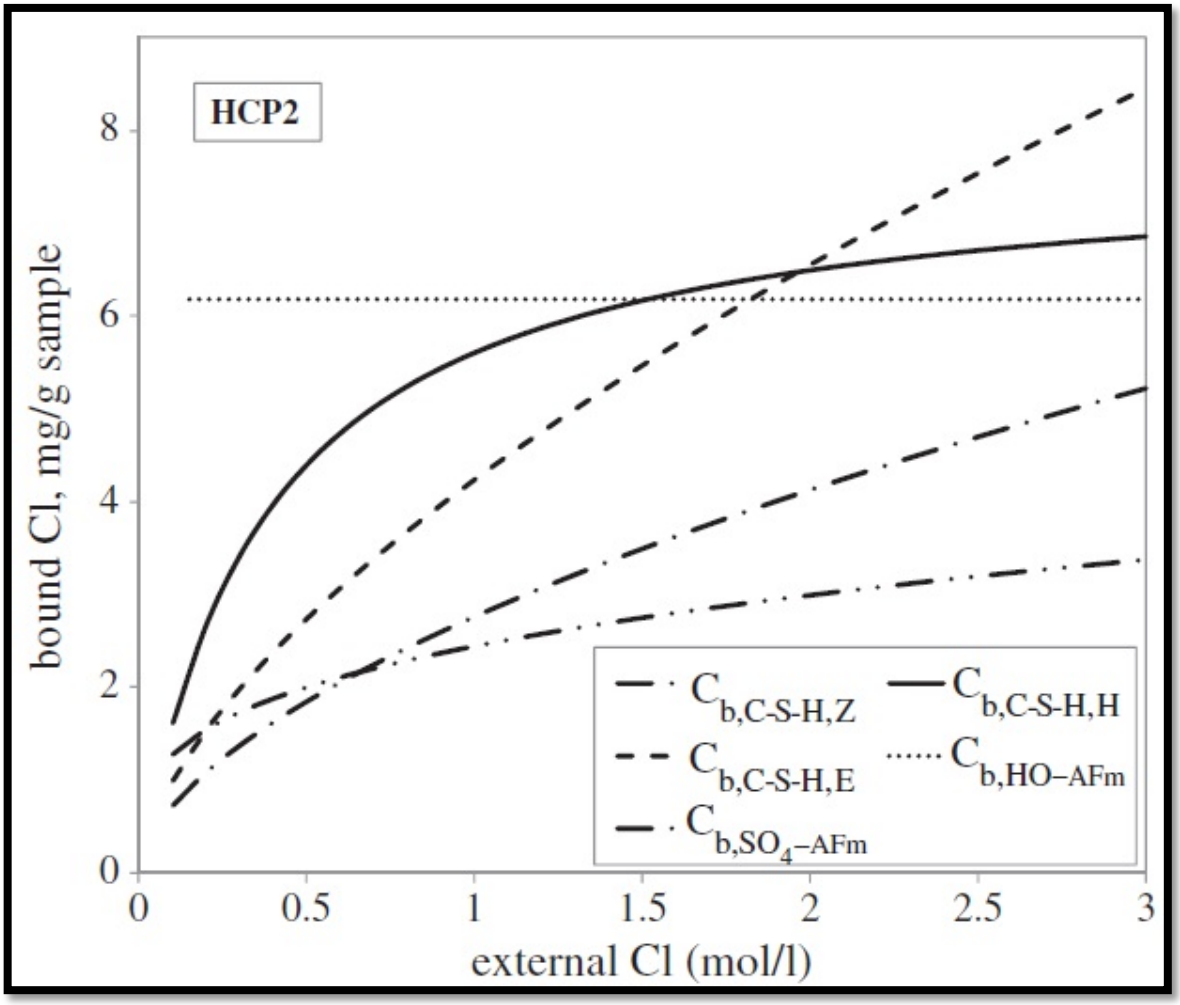

Figure 5.11: Isotherms (5.23), (5.24), (5.29), (5.30) and (5.31) applied to HCP2 (Table 5.10) using Eq. (5.22), and so taking into consideration the relative amount of each hydrate in the cement paste.

In order to distinguish between the three mentioned isotherms for the chloride binding of C-S-H, the total bound chlorides will be calculated for all eight considered hardened cement pastes. The obtained values will be compared to the experimental data and the best C-S-H isotherm will be chosen based on relative error and standard deviation values.

Using the C-S-H chloride binding isotherm (Eq.5.28) proposed by Hirao et al. [2005], $C_{b,H}$ is computed as its sum with Eqs. (5.21) and (5.22). In the same way, $C_{b,Z}$, the

sum of Eq. (5.27) with Eqs. (5.21) and (5.22) can be calculated. Last, using Eq. (5.29), Eqs. (5.21) and (5.22), the sum of the C-S-H isotherm proposed by Elakneswaran et al. [2009] and the isotherm of AFm, termed $C_{b,E}$, is computed. Figure 5.12 compares these three composed isotherms with the experimentally determined values for the composition of HCP6 as an example. The $C_{b,E}$ isotherm is the poorest fit in terms of its shape when compared to the experimental data. Moreover, its relative error starts at 50% and increases with the increase of the external chlorides concentration. Therefore, this isotherm does not satisfactorily describe the chloride binding capacity of C-S-H. In terms of the shape of the curve, the $C_{b,H}$ isotherm is closest to the experimental data. However, it can be seen that, again, its predicted values are 50% higher than the experimentally obtained data. The $C_{b,Z}$ isotherm has the lowest relative errors and standard deviations from experimental results, when compared to the $C_{b,H}$ and $C_{b,E}$ isotherms, even if the shape of the curve is not the best fit. The higher predicted values for the lower range of external chlorides can be attributed to the assumption that all HO-AFm is already transformed into Friedel's salt, which might not be completely accurate for all cement pastes. Given these data, the $C^0_{b,C-S-H,Z}$ isotherm (Eq. (5.27)) is chosen as the best to describe the chloride binding capacity of the C-S-H phase. The isotherm $C_{b,Z}$ will be referred to as "the basic model" henceforth. An "extended model" will now be presented, in order to include the chloride binding abilities of other hydrated phases in an OPC paste. The contributions of these phases are not as significant as the ones of AFm and C-S-H, but their addition shows a positive effect on the results of the new chloride binding model.

Table 5.11: The oxide and mineral compositions of all OPCs considered in Florea and Brouwers [2012].

Oxide	OPC 1	OPC 2	OPC 3	OPC 4
	[%mass]	[%mass]	[%mass]	[%mass]
CaO	62.38	61.33	63.58	62.10
SiO_2	18.89	18.43	21.26	19.90
Al_2O_3	5.51	5.36	4.09	5.30
Fe_2O_3	2.55	2.64	2.89	2.80
SO_3	4.12	4.43	2.79	3.50
RO	5.53	5.37	4.40	4.09
LOI	1.02	2.44	0.99	2.31
C_3S	58.00	57.23	57.63	51.95
C_2S	10.50	9.76	17.60	18.01
C_3A	10.26	9.71	5.93	9.27
C_4AF	7.72	8.00	8.74	8.47
$C\bar{S}$	6.99	7.52	4.73	5.93

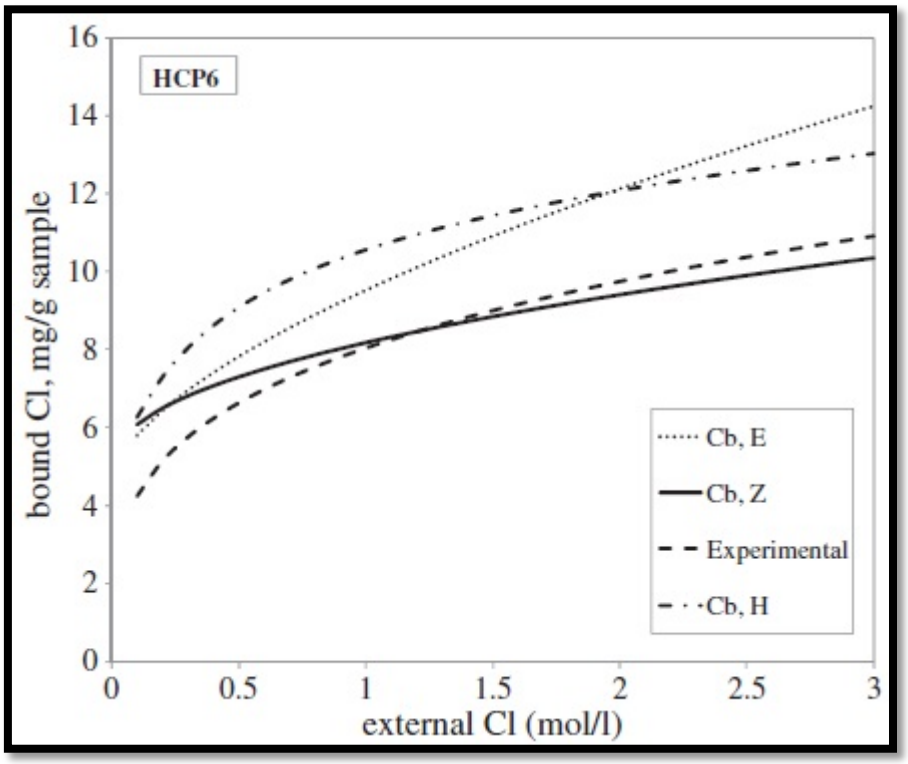

Figure 5.12: Comparison between $C_{b,Z}$, $C_{b,H}$ and $C_{b,E}$ and the experimental data from Zibara [2001], for composition HCP6 (Table 5.10).

The other hydrated phases that are considered in literature to be able to bind chlorides are portlandite, Friedel's salt and ettringite. Elakneswaran et al. [2009] have obtained

chloride sorption isotherms of portlandite and Friedel's salt. Eqs. (5.30) and (5.31) describe the sorption capacity of portlandite and Friedel's salt, in mg Cl/g portlandite and mg Cl/g FS respectively, for free chloride concentrations under one mol/L:

$$C_{b,CH}^{0} = 0.087c^{0.62} \quad 5.30$$

$$C_{b,PS}^{0} = 0.31c^{0.46} \quad 5.31$$

The mass m_{FS} is computed for Friedel's salt at 11% rh, $C_3A{\cdot}CaCl_2{\cdot}6H_2O$, with the molar mass of 489.27 g/mol:

$$m_{FS} = 6.9.\left(C_{b,c_4A\bar{S}H_{10}} + C_{b,C_4AH_{13}}\right) \quad 5.32$$

Ettringite is also mentioned in Elakneswaran et al. [2009], and believed to give a chloride sorption capacity lower than portlandite and Friedel's salt, but higher than tobermorite. The amount of AFt increases with the intrusion of chloride ions and the formation of Friedel's salt, so this contribution needs to be taken into account. In order to do this, the first assumption is that ettringite has the same chloride binding ability as tobermorite, so that its minimum influence can be assessed. Then, the amount of newly formed ettringite, m_{ettr}, needs to be estimated from the amount of Friedel's salt (Eq. (5.31)), using the molecular mass of AFt and the initial ettringite amount formed before the intrusion of chlorides, from Table 5.12:

$$C_{b,AFt} = C_{b,C_2S}^{0}\frac{m_{ettr}}{m_{spl}} = 6.65c^{0.334}\frac{m_{C_6A\bar{S}_3H_{12}} + 0.3m_{FS}}{m_{spl}} \quad 5.33$$

Isotherms incorporating the contribution of Portlandite, ettringite, Friedel's salt and all the possible combinations between them were constructed by adding the contribution of the respective phases to the $C_{b,Z}$ isotherm.

Table 5.12: Relations between the mass of hydration products and the mass fractions of OPC minerals

$m_{C_6AFS_2H_{18}}/b = 2.146x_{C_4AF}$
$m_{C_6A\bar{S}_3H_{36}}/b = 2.437x_{C\bar{S}}$
$m_{C_4A\bar{S}H_{14}}/b = 1.209\,x_{C\bar{S}}$
$m_{C_4AH_{22}}/b = 2.675x_{C_3A} - 2.654x_{C\bar{S}}$
$m_{C_{1.7}SH_{3.2}}/b = 0.933x_{C_3S} + 1.237x_{C_2S} - 0.877x_{C_4AF}$
$m_{CH}/b = 0.422x_{C_3S} + 0.129x_{C_2S} - 0.274x_{C_3A} + 0.213x_{C_4AF} + 0.271x_{C\bar{S}}$
$m_{UO}/b = 1 - x_{C_3S} - x_{C_2S} - x_{C_3A} - x_{C_4AF} - x_{C\bar{S}}$

The influence of adding the binding capacity of portlandite or Friedel's salt alone is beneficial, even though very low, for all cases considered (compositions from Tables 5.11 and 5.10). Adding the contribution of the AFt phase does not improve the precision of the model, its influence being also very low, but either positive or negative for the considered hardened cement pastes. The combined effect of two of these phases, or all three together, is beneficial in most, but not all cases. However, since these effects are extremely low (with contributions usually well under 1% of the total bound chlorides), they should only be taken into account for theoretical models with precise phase assemblages. For practical cases in which a high precision is not needed, the use of the basic model is recommended.

5.4 METHODS AND TECHNIQUES

5.4.1 Total chloride determination

Over the past years some None-destructive techniques (NDT): external techniques and embedded sensors have been developed for measuring chloride content in reinforced concrete structures. Ion selective electrode (ISE), Electrical resistivity (ER)

and Optical fiber sensors (OFS), Electrochemical impedance spectroscopy (EIS) are three main methods that were used.

There are specific NDT devices developed by different research groups for each method. For ISE and OFS all developed devices work in the same way while for ER techniques, the geometry, and experimental parameters are different. In the next parts the main characteristics, advantages and drawbacks of each methods will be discussed [Torres-Lugue et al., 2014].

5.4.1.1 Ion selective electrode (ISE)

Ion selective electrode (ISE), also called potentiometric sensor, has been a useful technique in laboratory tests because it can determine free chloride, avoiding destructive and chemical tests (pulverization and titration) [Muralidharan, 2005]. In field, this device is based on embedded sensors that could be used to determine free chloride concentration near the rebar without changing the environment surrounding [Angst and Polder, 2014]. ISE assesses the changes in potential difference that are related to the chemical activity and concentration of chloride ions, using Nernst equation:

$$E = E^0 + \frac{RT}{nF}\ln(\alpha_{Cl^-}) - E_{ref} \qquad 5.34$$

where E is the measured voltage [V], E^0 is the standard electrode potential (generally Ag/AgCl), R is the gas constant [J mol^{-1} K^{-1}], T is the absolute temperature [K], n the number of electrons, F is the Faraday constant [C mol^{-1}], α_{Cl^-} is the chemical activity of chloride ions [mol dm^{-3}], and E_{ref} is the standard potential of the reference electrode [V].

To measure the electrical potential difference, it is necessary to complement the ISE with a reference electrode (RE) that is normally a calomel electrode [Elsener, 2003. Atkins et al, 1996] (Figure 5.13). There are two geometrical arrays of RE, the first one (Figure 5.13a) is an electrode situated several centimeters from the ISE, and the second one is a Luggin capillary (e.g., geometric shape of RE in Figure 5.13b). The

first geometric array can produce errors since the resistivity changes within the concrete matrix and may produce changes in the measurement [Atkins et al , 1996] .On the other hand, Luggin capillary avoids this phenomenon due to its proximity to the ISE.

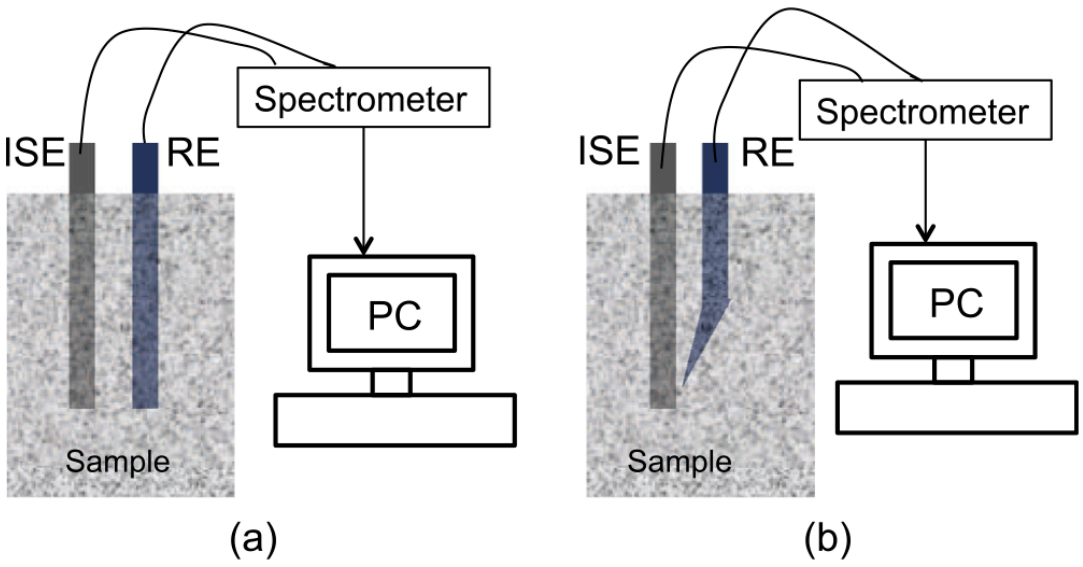

Figure 5.13: Techniques scheme based on ISE method (a) Normal RE and (b) RE with Luggin capillary.

ISE has some advantages taking into account chemical and practical factors. For instance, it shows chemical stability in aggressive environments, its fabrication is easy through electrochemical processes, it can be adapted to other sensors for measuring other parameters (e.g. temperature, ions presence), and it has a known behavior due to its wide use in electrochemistry [Atkins et al., 2001]. Nevertheless, there are factors that induce measurement errors and must be considered: temperature, alkalinity, electrical field presence and RE durability and prior calibration. Atkins et al. (2001) stated that temperature can lead to measurement shifts. Vera et al. (2010) demonstrated that high alkalinity of the pore solution can produce an interference in potentiometric response of an IES, especially at low chloride concentrations. Electrical field presence caused by corrosion processes, cathodic protection, chloride

extraction, and other sensors produces shifts in potential difference measurements. Finally, as RE is necessary, it must show long term stability, but according to Elsener et al. [2003] is not possible under their experimental conditions. Besides, sometimes a prior calibration of reference electrodes is necessary. This calibration can change once the electrode is in the concrete because its alkalinity may affect the potential values [(McCarter and Vennesland, 2004), (Duffo and Farina, 2009)].

Currently, Duffó et al. [2009] made embedded electrodes that assess rebars' corrosion processes, temperature inside concrete, oxygen availability, and chloride content; this last one is measured with an Ag/AgCl electrode. As they reported, these kinds of sensors could be an inexpensive, accurate and promising technique for concrete durability assessment [Torres-Lugue et al., 2014].

5.4.1.2 Electrochemical impedance spectroscopy (EIS)

EIS is one of the most used electrochemical techniques. It similarly works to ISE; however, EIS need three electrodes (Figure 5.14), while ISE just uses two of them (Figure 5.13). This technique works with a reference electrode (RE), a work electrode (WE), and an auxiliary electrode (AE). And it is based on measuring of impedance (real and imaginary) and phase angle while a constant voltage, and alternating current are applied; the analysis is done by equivalent circuits' modeling that resemble the response of the experiment, and give some parameters that can be related to physical phenomena that are occurring on the sample.

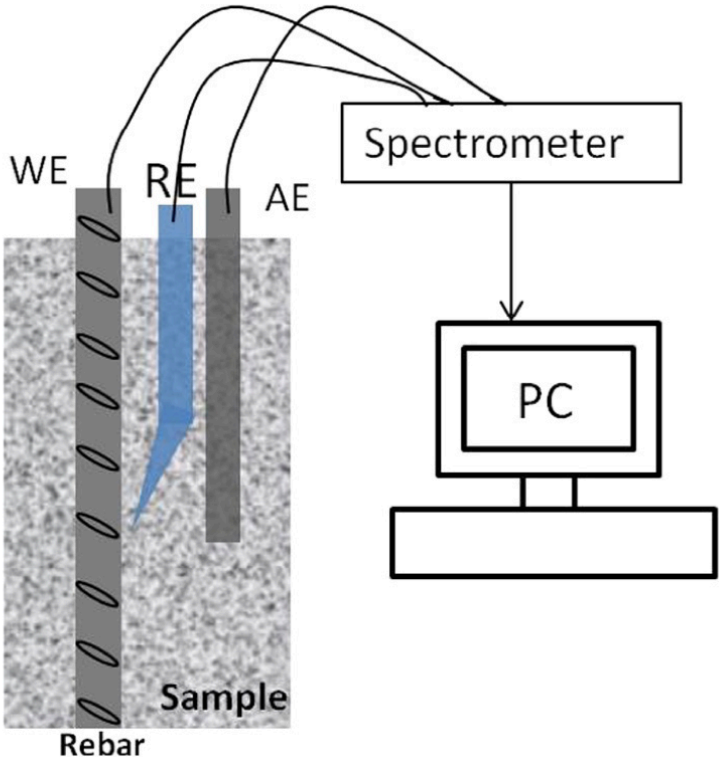

Figure 5.14: Electrochemical impedance spectroscopy scheme.

This technique is non-destructive and, in civil engineering field, it has been used for determining corrosion type of rebar in situ [Duffo et al., 2009], electrical impedance of the material (i.e. electrical resistance and capacitance) [(Duffo et al., 2009), (Koleva et al. 2008), (Keddam et al. 1997)], behavior of the interfaces (e.g. concrete-reinforcement) [(Koleva et al. 2008), (Kolena et al. 2008)], microstructure changes due to degradation processes [(Koleva et al. 2008), (Kolena et al. 2008), (Sanchez et al, 2008)], and in chloride diffusion coefficient estimation in mortars samples in laboratory [(Shi et al., 1999), (Deus et al., 2014)].

At late 90s several studies start to use EIS as sensor and biosensor for determining in a non-destructive way corrosion, degradation processes, and inorganic ions in polymeric materials [Fernandez-Sanchez, 2005]. In concrete structures, in 2008 and 2009 Vedalakshmi et al. estimated the diffusion coefficient of free chloride using EIS by analyzing capacitive behavior of the system. Though they proposed it as a non-destructive and in situ method for measuring chloride into concrete, other works in this field have not been found [Torres-Lugue et al., 2014].

5.4.1.3 Electrical resistivity

Electrical resistivity (ER) has been related to RC corrosion, to the moisture and heat transfer in concrete and, lately, to the presence of chloride ions. This technique is related to chloride ingress because chloride presence can increase electrical current and reduce the resistivity of concrete. Consequently, ER could be used to estimate chloride profiles by determining chloride diffusion coefficients. This method applies a voltage, measures the current flow and then computes electrical resistance that is proportional to electrical resistivity through Ohm's law:

V=IR

$$R = \frac{A}{l}\rho \qquad 5.35$$

where V is the potential difference [V], I the electrical current [A], R the electrical resistance [Ω], A the surface through the current passes [m^2], l the length [m], and ρ the electrical resistivity [Ωm]. The electrical resistivity is a unique characteristic and inherent for each material, and it depends on experimental conditions.

In 1999 Gowers and Millard made several recommendations about resistivity measurement technique for corrosion assessment using a Wenner array (Figure 5.15a); they were not intended for chloride measurement. Some of them were related to geometrical position, number of contact electrodes, space between them and distance from the rebar, to avoid measurement errors caused by surface contact area and electrical conductivity of the reinforcement. Other recommendations were made according to weather (temperature, relative humidity, and rainfall) and concrete composition (aggregates' size) that evidenced measurement disturbances. Also, they pointed out the importance of carbonation and chloride presences that increases or decreases resistivity, respectively. Consequently, carbonated surface or concrete with chlorides can produce wrong measurements. Finally, they did not recommend direct current (DC) because it produces errors in electrical potential measurements by electrode polarization.

Two years later, in 2001 Polder studied another geometric array called disc technique (Figure 5.15b). According to Polder, even when the resistance can be converted to resistivity using a cell constant measured (depending on the cover depth and the rebar diameter), a precise calculation of the cell constant is not possible because the current flow cannot be predicted. In addition, the necessity to connect the rebar to the measurement system implies an invasive method of assessment. To calibrate the technique, Polder [2001] and, some years later, McCarter and Vennesland [2004] high- lighted the necessity of a prior calibration and standardization of a reference material that must be the same studied material.

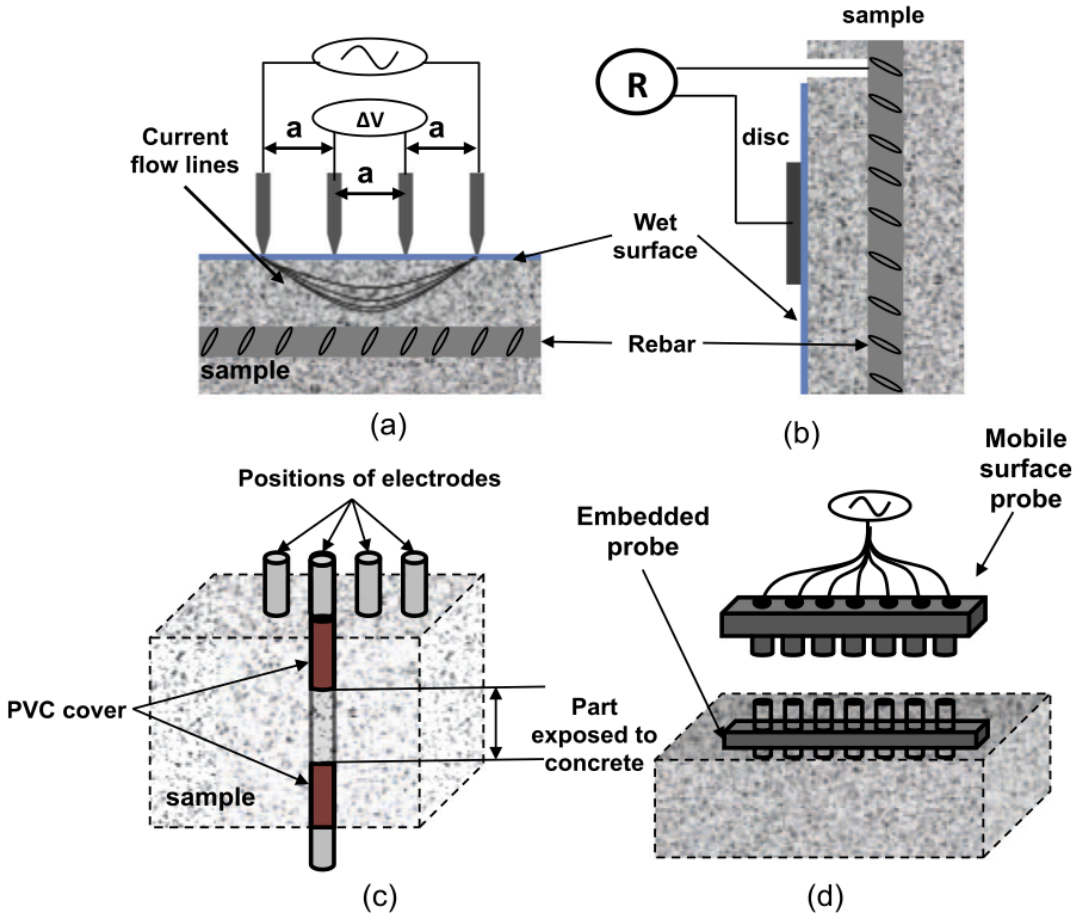

Figure 5.15: Techniques scheme based on ER method (a) Wenner array. (b) Disc. (c) Embedded electrodes. (d) Multi-electrode resistivity probes.

According to McCarter and Vennesland [2004], resistivity not only depends on the geometry but also on the capillary connectivity, level of pore saturation, and concentration and mobility of ions in the pore solution. For those reasons, the assessment of the moisture content of concrete is very important to improve the effectiveness of the technique. Polder [2001] suggested that the surface should be wetted by using wet sponges or wooden plugs to improve the electrical contact. Currently, Basheer et al. [2002] and McPolin et al. [2005] use another kind of device that has electrodes embedded into the concrete (Figure 5.15c), and each one has a part that is exposed to the concrete's environment. The measurement involves the same physical principle of Wenner or disc arrays (Eq.5.35) but in this case, the resistance is measured between pairs of electrodes. According to Basheer et al. [2002], the measurements can be affected by alternative cementitious materials (ACM) presence that can change resistivity because of continued hydration. However, their results (apparent diffusion coefficient) are in agreement with those obtained by ponding test.

ER methods are mainly used to determine the diffusion coefficient of concrete. For instance, McCarter et al. [2009] showed that Nernst-Einstein's equation relates the diffusion coefficient of a porous material (D_{eff}), diffusion coefficient of chloride ions in the free electrolyte (D_0), porosity (Φ), tortuosity (τ), bulk electrical resistivity (ρ), and resistivity of the interstitial pore fluid (ρ_0):

$$\frac{D_{eff}}{D_0} = \frac{\Phi}{\tau} = \frac{\rho_0}{\rho} \qquad 5.36$$

Lately, Loubser Du Plooy [2013] has proposed the multi-electrode resistivity (Figure 5.15d). This device is composed by two probes, one embedded and the other one mobile. The multi-electrode resistivity works as the Wener array technique does, and also needs moisture for improving the measurements. According to her results, this technique can be used for exploring the dependency of resistivity and chloride diffusivity on cement type and degree of hydration.

On the whole, after a comprehensive calibration, ER methods could be used to determine chloride diffusion coefficients. Nevertheless, they are very sensitive to the moisture content. For most of ER techniques the surface must be wet because the

conductivity is zero for dry concrete. In addition, to ensure repeatability and accuracy, calibration relationships should be determined for different moisture levels. Measurements also depend on the geometry and the reinforcing configuration. Indeed, rebar presence and corners can modify measurements because these conditions modify the electrical field. There is not enough information about the durability of these devices in field. Consequently, more studies about durability of the devices based on ER are necessary. [Torres-Lugue et al., 2014].

5.4.1.4 Optical fiber sensors

In the past ten years some researchers have developed optical fiber sensors (OFS) for free chloride content assessment. This method involves detecting the refractive index shift due to the chloride presence that changes the light behavior that increases for larger chloride content [Tang et al. 2007]. To make the measurement, the incident light can be ultraviolet [Lam et al, 2009] laser [Tang et al. 2007]. The output light is studied by an optical spectrum analyzer (Figure 5.16) that gives the transmission spectra used to estimate the refractive index by [Tang et al. 2007]:

$$\lambda_m = [n_{core}^{01}(n_1, n_2, \lambda_m) - n_{clad}^{0m}(n_2, n_s, \lambda_m)]\Lambda \quad 5.37$$

where λ_m is the central wavelength that depends on the effective refractive index of the fundamental core mode n_{core}^{01} (n_1 ; n_2 ; λ_m) and the effective refractive index of the mth cladding mode n_{clad}^{0m} (n_2 ; n_s ; λ_m), where n_1 ; n_2 ; n_s are the refractive indices of core, the cladding, an the surrounding medium respectively, and Λ is the grating period. When a change in the chloride concentration exists, refractive index changes in the surrounding medium, the cladding effective refractive index changes and, therefore a definite shift in the central wavelength, λ_m (Figure 5.16).

According to Lam et al. [2009] and Tang et al. [2007] the sensitivity of OFS can be improved using gold nanoparticles (gold colloids) that are deposited on the active grating surface of the OFS.

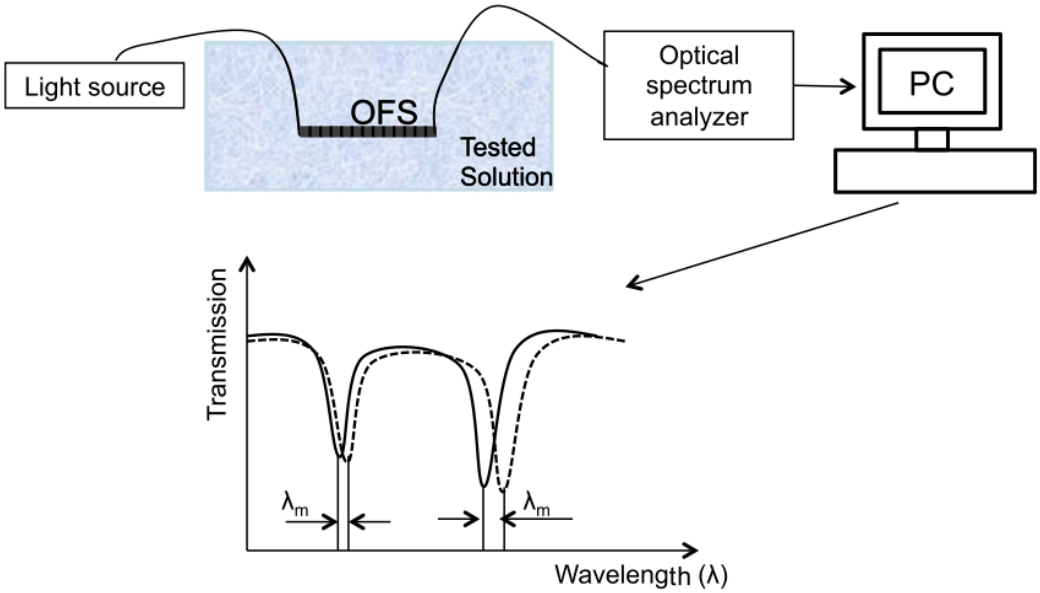

Figure 5.16: Optical fiber sensors scheme.

For example, Tang et al. [2007] found that lower limit of detection with and without gold colloids are 0.02 wt% (wt – weight solute×100/weight solution) and 0.04 wt%, respectively. Similarly, Lam et al. [2009] stated that the mean diameter of the gold particles affects the sensitivity. Particles of 16 nm provide a more sensitive device than 3 nm and 8 nm sizes.

OFS presents several advantages over other methods: it is energy saving, very sensitive to small chloride concentrations, and measures are not affected by electromagnetic fields [(Lam et al, 2009), (Falciai et al., 2001)]. In addition, because of its geometry (long and thin) and its interaction capacity with the surrounding, the distribution of sensors is more convenient for large structural applications. This means, that since each segment of the fiber can act as a sensor, little perturbations anywhere in the structure can be detected [Li et al., 2004].

However, OFS have some drawbacks that are important for a reliable and accurate measurement. For instance, optical fiber needs adequate protection to prevent its break during casting or service life. This protection must allow light transmission

without obstructing or bending the optical fiber because the data can be missed [Li et al., 2004]. Furthermore, OFS needs additional protection to isolate the fiber from corrosive environment and high temperatures [Li et al., 2004] taking into account that temperature changes can affect the measurement, as Shu et al. [2001] and Tang and Wang have evidenced [Tang and Wang, 2007]. In their results, temperature variation (0–120 °C) can vary the shift in peak wavelength from 1 to 7 nm. Finally, until now, tests in concrete samples have not been reported [Torres-Lugue et al., 2014].

5.4.1.5 Grounding penetrating radar (GPR)

GPR is a widely used geophysical technique. In civil engineering GPR has been used for determining element thickness and locating metallic rebars, ducts, voids, honeycombs, delamination, cracking, and interfaces (e.g. asphalt-concrete). This technique compares an incident electromagnetic wave to the reflected wave after its interaction with concrete and reinforcement (Figure 5.17). Incident wave is measured by detecting the direct wave, this wave interacts just with the concrete not with rebar, and reaches the receiving antenna, traveling smaller distance than reflected waves.

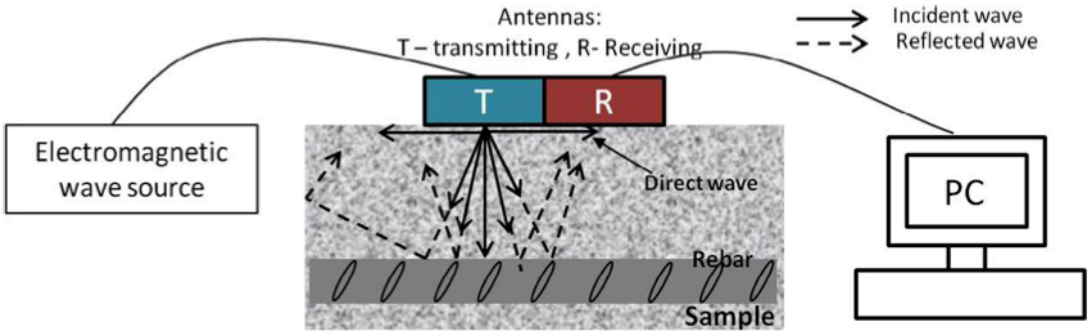

Figure 5.17: Grounding penetrating radar scheme

GPR shows highly dependence on geometric position, water presence, and chloride content. Geometric position influences the reflective wave since when corners or geometrical changes are present they behave as an interface between two different media, this phenomenon is known as border effects [Hugenschmidt and loser, 2008]. Water presence and chloride content affect wave signal in opposite ways, taking into

account that reflection phenomena depends on wave velocity, and this depends on conductivity and capacitance. According to Soutsos et al. [2001] humidity causes the reduction of relative permittivity and conductivity while chloride presence does not affect permittivity but increases conductivity of the material. However, Robert [1998] determined that chloride ions do affect relative permittivity at low frequencies (less than 1 GHz). In addition, GPR repeatability depends on rebar depth (that cannot be controlled on site), and Sbartaï et al. [Sbartaï at al, 2008] recommended to make the measure as far as possible from rebar.

Several works on GPR technique for measuring chloride content [(Soutsos et al., 2001), (Sbartaï at al, 2008), (Hugenschmidt and loser, 2008)] agree on qualitative nature of the technique and the necessity of a mathematical model to numerically relate chloride concentration to GPR measurements. In 2009, Sbartaï et al. proposed an artificial neural network (ANN) getting a good prediction accuracy (absolute error less than 1% approx.) but limited by specific material used for concrete mixture, geometry, and radar device used [Torres-Lugue et al., 2014].

5.4.2 Methods for the quantification of the chloride binding

The complex physicochemical interactions between chloride ions and the cement matrix depend on the chemical composition of the solution in contact with the material and of that of the matrix. The overall interactions can be quantified at the macroscale and at equilibrium by the so-called *chloride binding isotherm*, which links the bound chlorides amount to the free chloride concentration of the pore solution, at a given temperature, for a given material and at a given age. The chloride binding isotherm is the most influent parameter on the prediction results in terms of average chloride penetration depth or concentration profiles.

Different mathematical expressions have been given to chloride isotherms. A lineal relationship was used by Tuutti [1982] and Arya and Newman [1990]. However,

experimental data of most researchers do not fit this kind of relationship. In most cases, relationships between free and combined chlorides are not linear.

With the aim of fitting this nonlinear relationship, other researchers used the Langmuir isotherm to describe chloride binding. Tang and Nilsson [1993] found that a Langmuir isotherm does not fit experimental data when free chloride concentration is higher than 0.05 M, while a Freund-lich isotherm can be applied in the range of free chloride concentration from $0.01 < C_l < 1$ M [Castellote etal,1999].

Several experimental techniques are available to directly assess binding isotherms.

A binding isotherm can experimentally be assessed by immersion of crushed specimens in solutions of various known chloride concentrations (equilibrium method). This can be performed by measuring for each solution, where the concentration is kept constant, the amount of bound (or total) chloride ions in the material at the equilibrium state. If the concentration of each solution is not kept constant, the binding isotherm can be assessed by measuring the drop in chloride concentration of the solution at the equilibrium state.

Until now such a method has rather been applied to hardened cement pastes (hcp) or mortars.

Moreover, in migration tests, once the steady-state (ss) regime is achieved, the free chloride concentration is almost constant throughout the specimen and may be assumed as equal to the concentration of the contact solution. Therefore, the binding isotherm can be assessed from a series of ss migration tests with various upstream chloride concentrations and by measuring for each of them the amount of total chlorides inside the specimen at the end of the test.

Furthermore, when both total and free chloride concentration profiles have been experimentally determined after a diffusion or a migration test in non-steady-state (nss) conditions, the binding isotherm can be plotted (profile method) [Baroghel-Bouy, 2008]

The interaction between chloride and the matrix of cement-based materials is still not very well understood. Instead, for most applications a 'binding isotherm' is used to give the relation between the free and bound chloride. Here a number of questions are still disputed, besides the approach by a binding isotherm at all. Since the binding isotherm is a pure empirical 'property', it must be measured and the effect of a number of parameters must be quantified.

The shape of the binding isotherm is one such question, (Figure 5.18). Does most of the binding really occur at concentrations close to zero, or is the chloride binding significantly concentration-dependent?

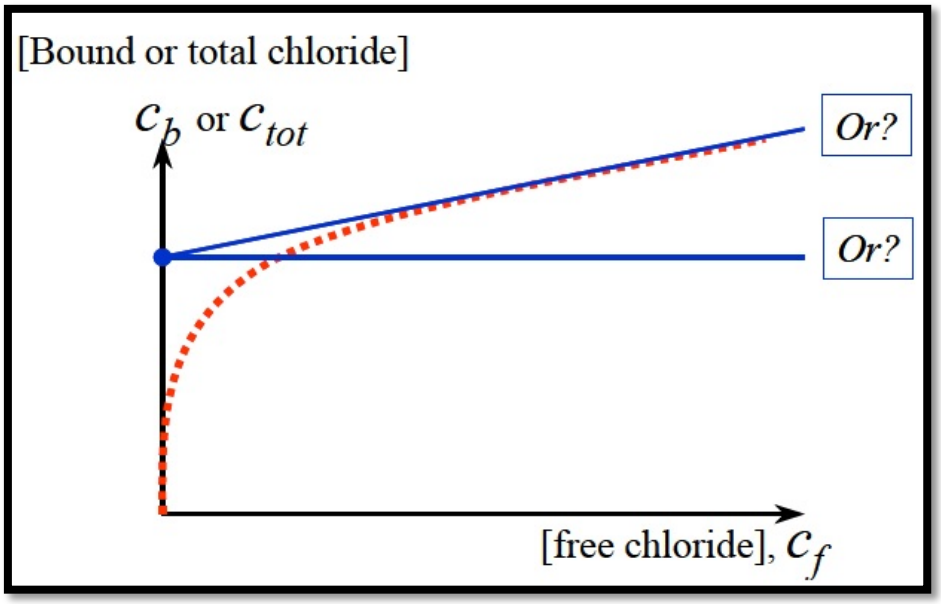

Figure 5.18: Alternative shapes of a possible 'binding isotherm'.

Bigas et al [1995] proposed a new approach of modelling the binding process as a Freundlich isotherm, by the calculation of its equation from several traditional diffusion tests in steady state conditions.

The Fick's second law gives the chloride concentration C as a function of the distance X from the exposed surface and as a function of the time t, assuming a constant D, intrinsic chloride diffusion coefficient in a semi infinite porous medium:

$$\frac{\vartheta C}{\vartheta t} = D\frac{\vartheta^2 C}{\vartheta x^2} \qquad 5.38$$

Equation (5.38) is valid only if there is no interaction between chloride and solid phases. In fact, when binding process (chemical and physical) occurs, the chloride penetration is slower. Then, the determination of D should be reduced to:

1. the measurement of the effective diffusion coefficient De,

2. the quantification of the binding process.

The differential equation describing the migration of chloride into concrete should be written as :

$$\frac{\vartheta C}{\vartheta t} = D_a\frac{\vartheta^2 C}{\vartheta x^2} \qquad 5.39$$

with $D_a = \frac{D_\tau}{a} = \frac{D_e}{a}$ defined as the apparent diffusion coefficient, taking into account the binding phenomenon between the liquid phase and the solid phase. The capacity factor a is expressed as $\alpha = z + (1 - 7)\ \rho_s\ K_d$. Assuming an instantaneous exchange driven by a linear binding isotherm, K_d is the binding capacity as $C_s = K_d\ C$ with C_s as bound chloride, τ as concrete porosity and ρ_s its density.

In fact, the apparent diffusion coefficient D_s which takes into account chloride binding, is not a constant because the binding isotherm is non linear. Classical determinations of binding isotherm are done on crushed materials, neglecting the real microstructure of the concrete, particularly the microcracks: Our original approach, which takes into account the bulk microstructure of the material, is based on the data obtained with classical diffusion tests.

Bigas et al [1995] made mortar samples (Table 5.13) with 28 day characteristics for cured in water at 20°C are: compressive strength = 40 MPa, density ρ_s= 2400 Kg/m^3, water porosity τ_{water} = 0.16 and mercury porosity τ= 0.14.

Table 5.13: Mix proportions [Bigas et al., 1995].

Materials	
CPA CEMI	519 Kg/m^3
Siliceous sand (0.6/1.2 mm)	1067 kg/m^3
Siliceous sand (1.2/2.5 mm)	457 kg/m^3
Water	255l/m^3

After curing, slices were removed from 11*22 cm cylinders and placed in diffusion cells. The diffusion area is 7.088.10-^{3} m^2, and the volume of both compartment of these cells is 3.73 10^{-4} m^3. Each cell was filled with an alcaline solution of KOH (4.65 kg/m^3) + NaOH (l kg/m^3) at pH 13.

Different concentration gradients (Table 5.14) are obtained using different initial concentrations C_O of chloride and using different thicknesses of slices.

Table 5.14: Experimental program. The X sign indicates the tested variables [Bigas et al., 1995].

	C_0=169.6 g/l	C_0=20.2 g/l	C_0=10.0 g/l	C_0=5.0 g/l	C_0=1.0 g/l
L=1 cm	X	X	X	X	X
L=1.5cm		X	X		

The downstream solution was removed at regular term (twice a month) to maintain the C = 0 condition at X = L. At each term the chloride content was determined by potentiometric method.

For modelling of linear binding, the resolution of Fick's second law, shows an asymptotic increase of the quantities of diffused chloride with time when steady state occurs (Figure 5.19). The time lag t_i, is defined as the abscissa of the intercept of the asymptot:

$$t_i = \frac{\alpha L^2}{6D_e} \qquad 5.40$$

D_e, is assumed to be independent of C_O, and calculated from the slope of the asymptot.

Without binding, the capacity factor a is represented by the porosity and the time lag is:

$$t_i = \frac{\tau L^2}{6D_e} = \frac{L^2}{6D} \qquad 5.41$$

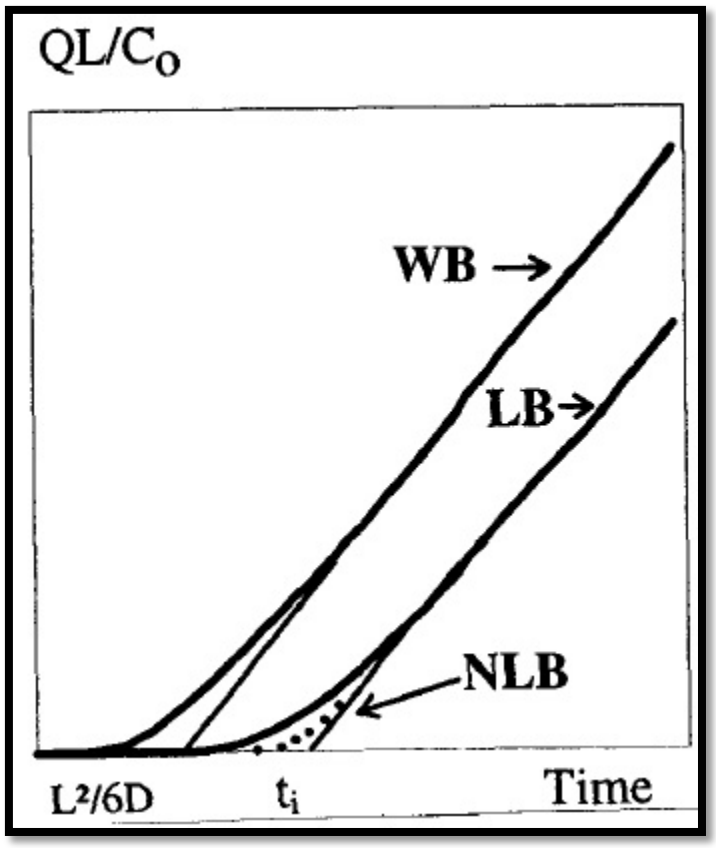

Figure 5.19: diffusion curves: WB diffusion without binding, LB diffusion with linear binding, NLB diffusion with non-linear binding [Bigas et al., 1995].

The steady state regime, characterized by a linear concentration profile in the liquid phase between the upstream and the downstream cells, is independent of the non linearity or linearity of the isotherm. In case of non-linear binding, we can write:

$$\frac{QL}{C_0} = D_e t - \alpha_{eq}\frac{L^2}{6} \qquad 5.42$$

where a_{eq} is the equivalent capacity factor of the diffusion with linear binding which has the same asymptotic flow as the diffusion with non linear binding. The abscissa of the intercept of the asymptot is:

$$t_i = \frac{\alpha_{eq}L^2}{6D_e} = \frac{L^2}{6D} + \frac{L^2}{6D_e}(1-\tau)\rho_s K_{deq} \qquad 5.43$$

where K_{deq} is the equivalent binding capacity of the equivalent linear isotherm.

For definition of an equivalent linear isotherm and an equivalent capacity factor they assume that the non-linear binding is described by a Freundlich isotherm C_S = a CY with $0 \leq y \leq 1$. The basis of our modelling is to make the non-linear Freundlich binding isotherm similar to an equivalent linear isotherm.

The equivalent linear isotherm, associated to a_{eq}, is defined as the one, which gives at $C_0/2$, the same bound chloride concentration as the non-linear isotherm (Figure 5.20).

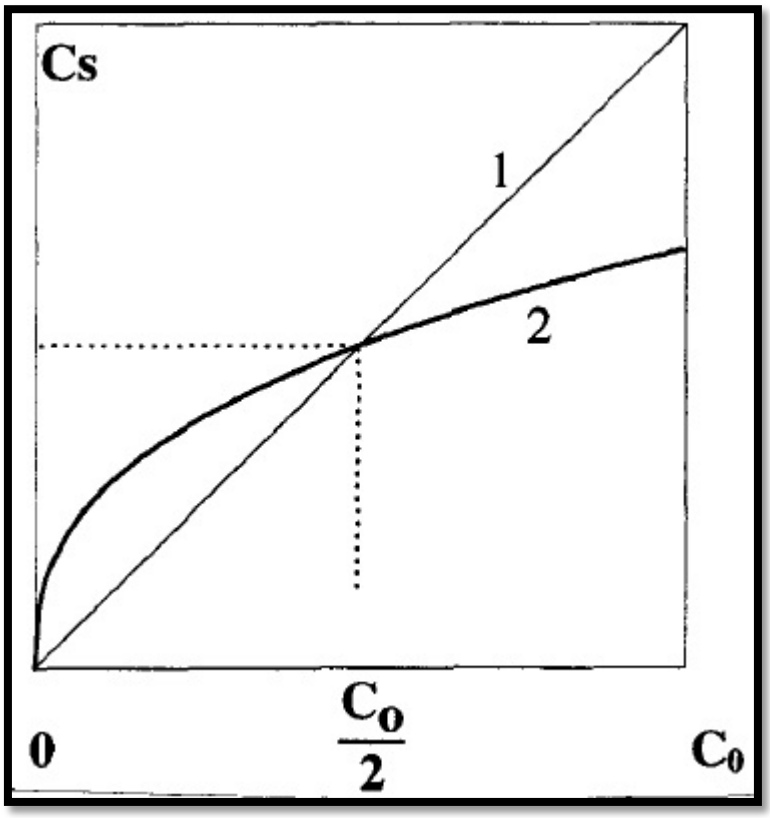

Figure 5.20: Chloride binding isotherms, Curve 1 is the equivalent linear isotherm and curve 2 is the Freunlich isotherm [Bigas et al., 1995].

For each diffusion test drived for a given concentration or a given thickness, they obtain the data for ti, D_e and a_{eq} (Table 5.15) by a graphic determination from the diffusion curves.

Table 5.15: Experimental data for ti, D_e and a_{eq} [Bigas et al., 1995].

C_o (kg/m3)	L (10^{-2} m²)	t_i (d)	D_e experimental (10^{-12} m²/s)	α_{eq} experimental
169.6	1	35	1.15	0.210
20.2	1	64	1.93	0.639
20.2	1.4	131	2.04	0.706
10.0	1	86	2.43	1.081
10.0	1.44	175	2.45	1.075
5.0	0.95	112	2.63	1.69
1.0	0.96	200	2.93	3.29

On the basis of these experimental results, we make a numerical simulation resolving the Fick's second law in the case of binding drived by an equivalent linear isotherm (in this case y = l). Then they obtain the corrected values of D_e and a_{eq}. Also the decrease in the concentration in the upstream cells can be calculated for a given term (Table 5.16).

Table 5.16: Adjusted data obtained by numerical simulation with the equivalent linear isotherm [Bigas et al., 1995].

C_o (kg/m3)	L (10^{-2} m)	D_e : corected values (10^{-12} m²/s)	α equivalent: corrected values	K_{deq} (10^{-3} m3/kg)	$\frac{C_0 - \Delta C_0}{C_0}$
169.6	1	1.18	0.215	0.037	0.949
20.2	1	2.04	0.676	0.26	0.897
20.2	1.4	2.19	0.763	0.30	0.859
10.0	1	2.75	1.226	0.53	0.799
10.0	1.44	2.77	1.212	0.51	0.792
5.0	0.95	3.07	1.985	0.89	0.753
1.0	0.96	3.62	4.072	1.95	0.633

Two main observations should be made: Firstly, the effective diffusion coefficient is a function of the chloride concentration and secondly the equivalent capacity factor is a function of the chloride concentration.

For determination of the Freundlich isotherm parameters, the definition of the equivalent linear isotherm specifies that the retention rates are the same for $C_0/2$ considering linear or Freundlich isotherm.

So it can be written:

$$K_{deq}\left(\frac{C_0}{2}\right) = a(\frac{C_0}{2})^y \qquad then \qquad K_{deq} = a(\frac{C_0}{2})^{y-1}$$

and:

$$\alpha_{eq} = \tau + (1-\tau)\rho_s\alpha(\frac{C_0}{2})^{y-1} \qquad 5.44$$

Based on experiments, each diffusion test give us several couples of data (C_o; a_{eq}) and from the equation (5.44) the equivalent capacity factor % can be considered as a linear function of $(\frac{C_0}{2})^{y-1}$. A linear regression procedure is then carried out to determine the Freundlich parameters y and a. In this procedure y is considered as a parameter varying from 0 to 1.

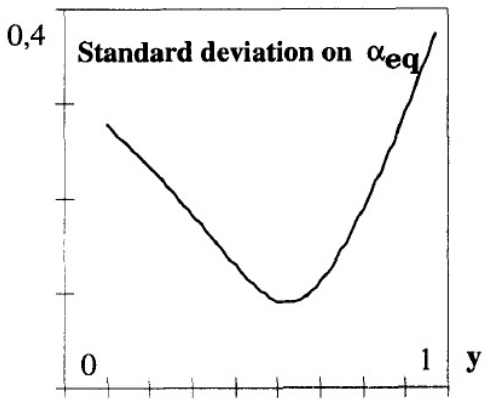

Figure 5.21: Standard deviation on a_{eq} vs. y.

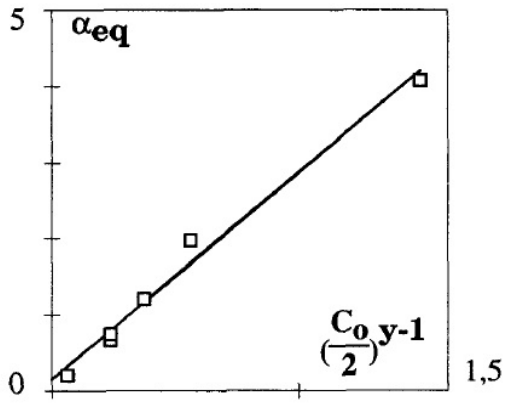

Figure 5.22: a_{eq} vs. $(\frac{C_0}{2})^{y-1}$ for y=0.38

Experimental data of a_{eq} are plotted (Figure 5.22) as a function of $(\frac{C_0}{2})^{y-1}$ and for each value of y, they determine the regression straight line and the standard deviation. The value of y chosen is the one which gives us the minimum standard deviation (Figure 5.21) associated to a realistic value of the porosity.

Next it is then possible to determine the porosity τ and the coefficient << a >> of the Freundlich equation calculated from the slope [(1 - τ) ρ_s a] of the regression straight line.

From our experimental studies, we obtain a minimum standard deviation and a porosity value of 0.14 for y = 0.52. The straight line equation is:

$$\alpha_{eq} = 0.149 + 2.73(\frac{C_0}{2})^{-0.52} \qquad 5.45$$

So, we get a = $1.34.10^{-3}$

For our mortar, the non-linear isotherm equation expressed as a Freunlich isotherm is:

$C_s=1.34.10^{-3}\ C^{0.38}$

In this paper seven classical chloride diffusion tests on mortar made with CPA-CEM I 42.5 have shown the dependence between the chloride concentration C_0 in the upstream cell and the quantity of chloride bound by the solid phase. The non-linearity of chloride binding for the bulk material could be expressed by a Freundlich isotherm.

The advantage of their method, contrary to classical experimental techniques in which the binding isotherms are obtained from crushed specimens, is the access to the non-linear binding isotherm equation for the real microstructure of concrete in service. Then, it could be possible to study the influence of the microstructure on the binding of chloride ions [Bigas et al, 1995].

Tang and Nilsson [1995] apply the modified BET equation to the chloride binding isotherms. The results show that there is a good correspondence between the theory and the experiment data.

The BET multilayer adsorption theory has widely been used in many fields for the determination of surface specific area. The most usual form of the BET equations is:

$$\frac{S}{S_m} = \frac{\alpha x}{(1-x)[1+(\alpha-1)x]} \qquad 5.46$$

$$x = \frac{p}{p_s} \qquad 5.47$$

where S: the amount of the adsorbed adsorbate, S,: the monolayer adsorption capacity, p: the vapour pressure of the adsorbate, p_s*:* the saturation vapour pressure of the adsorbate, *a:* adsorption constant;

The adsorption constant a is related to the difference between the adsorption energy at the first layer and those at the second or higher layers. The original derivation of the BET equation assumed that the adsorption energy at the second is the same as at the higher layers and is equal to the heat of liquification, that is,

$$\alpha \propto \exp\left(\frac{E_1 - E_2}{RT}\right) \quad and \quad E_2 = E_3 = \cdots = E_n = H_1$$

where E: the adsorption energy at the layer as designated by the sub number; Hi: the heat of liquification; R: gas constant; T*:* temperature.

The problem of the original BET theory is that when **x**→1, the adsorption becomes infinite. To avoid this infinite adsorption, Brunaer et a1 [1969] introduced a parameter K <l, so that $x = K\frac{p}{p_s}$ in Eq. (5.46). This treatment was based on the fact that even at the saturation vapour pressure the number of adsorption layers is still limited. Since in the original derivation x is defined as the ratio of the adsorbed fraction at the first layer to that at the second layer, a very small value of K implies a very small number of adsorption layers. Therefore, this treatment seems contrary to the original assumption of multilayer adsorption, where the number of adsorption layers tends to the infinite.

Xu [1990] tried another approach by assuming that the adsorption energy at the second layer is not equal to those at the third or higher layers, that is, *E2 # E3* and *E3 = E4 = = E, = HI,* and derived the following modified equation,

$$\frac{S}{S_m} = \frac{\alpha x[1-(1-\beta)(1-\beta x)^2]}{\beta(1-\beta x)[1-\beta x+\alpha x(1-\beta x+x)]} \qquad 5.48$$

where

$$\beta \propto \exp\left(\frac{H_1 - E_2}{RT}\right)$$

Although the expression of Xu's modification seems more complicated than the original expression Eq. (5.46) the parameter β gives a strong physical meaning since it is related to the difference between the adsorption energy at the second layer and the one at the third or higher layers.

It is well known that the hydrated products of cement provide a huge surface area for physicorption. On the other hand, the formation of Friedel's salt implies a chemisorptions of chloride ions. Therefore, chloride binding in concrete involves both chemisorption and physisorption. It is possible to apply Eq. (5.48) to the chloride binding isotherms by assuming $= \frac{c}{c_s}$, where c is the free chloride concentration and c_s the concentration in a saturated solution, for a NaCl solution, c_s = 216 gCl/l = 6.09 mol/l. Tang and Nilsson [1993] found that when the bound chlorides were expressed based on the weight of hydration gel, the influences of water-cement ratios and aggregate content could be eliminated. In the literature the unit based on the weight of cement are often used. This expression is, in fact, proportional to that based on the weight of hydration gel if the hydration degree is constant. A comparison between Freundlich's equation and the modified BET equation is shown in Figure 5.23.

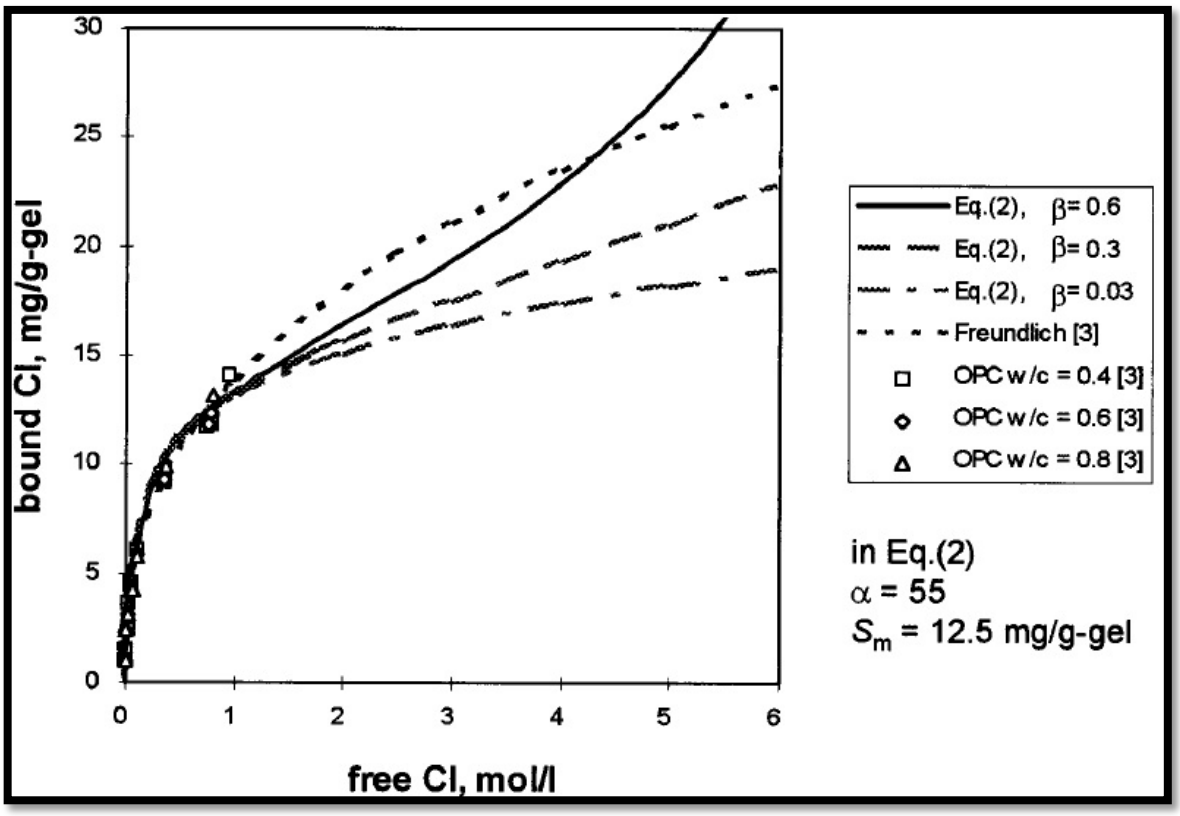

Figure 5.23: A comparison between Freundlich's equation and the modified BET equation.

It can be seen from Figure 5.23 that both Freundlich's equation and the modified BET equation correspond very well when the free chloride concentration is lower than 1 mol/l, in spite of different β values. Owing to the lack of experimental data, we do not know the tendency of chloride binding at higher concentrations. According to the reported data, the rate of chloride binding becomes less and less with the increment of the free chloride concentration. It is reasonable to assume that the value of β should be about 0.3 or less. This β value may have significant importance for the chloride penetration in the splashing zone or in an environment where the de-icing salt is used [Tang and Nilsson, 1995].

Baroghel-Bouny et al [2008] proposed two methods of assessment of chloride binding isotherms of cementitious materials in saturated and isothermal conditions.

One of the methods is based on numerical inverse analysis performed by means of a multispecies transport model. This model involves the species Cl^-, OH^-, Na^+ and K^+, and is based on the Nernst-Planck equation. In this case, Freundlich's equation is used to describe globally the chloride binding isotherm.

In the second method, physical adsorption onto C-S-H and formation of Friedel's salt by chemical reactions are addressed separately. The chemical reactions are assumed as instantaneous and independent of the chloride concentration. The chloride binding isotherm can thus be described by an analytical formula, which includes two components. The physical and the chemical components involve respectively the C-S-H content and the residual content of equivalent aluminates of the material, at the considered age. These contents are derived here from an analytical hydration model.

ASSESSMENT OF CHLORIDE BINDING ISOTHERM BY NUMERICAL INVERSE ANALYSIS (METHOD 1)

An indirect method, by means of numerical inverse analysis, is proposed in order to assess chloride binding isotherms. The method consists in measuring a total chloride concentration profile at a given exposure time on a sample submitted to a non-steady-state (nss) diffusion test in laboratory or on a core extracted from a submerged structure. This is very convenient, since such profiles are the experimental data which are the most often available on real structures. The experimental data are then analysed by using a numerical multi-species transport model. A global description of the isotherm by Freundlich's formula is adopted here. A simple numerical algorithm is used to identify the binding isotherm, which best reproduces the experimental total chloride concentration profile.

A model has been developed in saturated and isothermal conditions, according to a multi-species approach, on the basis of the works reported. This model includes the species Cl^-, OH^-, Na^+, and K^+, along with the electrical interactions between ions.

In water-saturated concrete, the contribution of advection can be neglected. The transport of each ion *i* is then described by the Nernst-Planck equation (Eq. (5.49))

which includes three components, diffusion under concentration gradient, movement under chemical activity effect, and migration under electrical field:

$$J_i = -D_i \left[grad c_i + c_i grad(ln\gamma_i) + \frac{z_i F}{RT} c_i grad\psi \right] \quad 5.49$$

where J_i, D_i, c_i, γ_i and z_i are respectively the flux (in mol.m^2.s^{-1}), the effective diffusion coefficient (in m^2.s^{-1}), the concentration (in mol/m^3 of pore solution), the chemical activity coefficient (-) and the valence number (-) of each ionic species *i*. F is the Faraday constant (9.64846×10^4 C.mol^{-1}), R the ideal gas constant (8.3143 J.mol^{-1}.K^{-1}), T the absolute temperature (in K) and ψ the local electrical potential which arises in the medium as a result of the ions movements (in V).

The set of mass balance equations for each species either present as an ion or included in a solid compound reads:

$$\frac{\partial n_i}{\partial t} + div J_i = 0 \quad 5.50$$

where *Ji* is the flux given by Eq. (5.49) and *ni* (i = O, H, Cl, Na and K) denotes the total molar content of *i* in the ionic species or solid compound. For example, n_{Cl} = $\varphi c_{Cl} + s_{Cl}$, where φ is the porosity (-) of the water-saturated material.

To complement the system of equations, another relation is needed to account for the electrical potential. Poisson's equation is the most general equation. This equation has been used by Marchand et al. [2002]. Other authors have used the nil current assumption. In this paper, the electrical interactions between ions are computed by assuming local electroneutrality within the medium (see Eq. (5.51)):

$$c_i z_i = 0 \quad 5.51$$

Electroneutrality condition is a consequence of Poisson's equation under some conditions. Therefore, using the electroneutrality condition instead of Poisson's equation should give rise to a very small error under usual conditions, while this is more convenient from a numerical point of view. As a matter of fact, a good agreement has been reported between the chloride concentration profiles (and the

electrical potential distributions) obtained with the three approaches (nil current, Poisson's equation and electroneutrality condition), thus validating the use of simpler approaches (electroneutrality condition or nil current).

In the model, the adsorption of ions present in the pore solution is neglected, except for Cl^- (and OH^-, assuming that $s_{Cl} + s_{OH}$ = constant, if binding consists in ionic exchange between Cl^- and OH^-, as often assumed). In addition to the boundary conditions, the input data required for the model are therefore the effective diffusion coefficients of the ionic species, the chloride binding isotherm, the porosity, and the initial composition of the pore solution (initial conditions). The material properties are assumed in this model to be independent of age and depth. Several studies have indicated that the pore walls affect in a greater extent the diffusion of cations than that of anions, in particular as a result of their surface charge. Nevertheless, here the effective diffusion coefficients of the various ionic species Di (with $i \neq Cl^-$) will be drawn from that of chlorides D_{Cl} and from Eq. (5.52), as in:

$$\frac{D_i}{D_i^o} = \frac{D_{Cl}}{D_{Cl}^o} (= \tau . \varphi) \qquad 5.52$$

where D^o_{Cl} and D^o_i are the ionic diffusion coefficients in an infinitely diluted solution (which values can be found in Physics handbooks), and τ is the tortuosity of the material.

The system of non-linear equations (Eq. (5.49) to Eq. (5.52)) is solved by means of a standard Newton algorithm [2000], the spatial discretization is performed by the finite volume method, and an implicit approximation of the normal derivative ensuring the best stability of the scheme is used.

From the porosity, the effective chloride diffusion coefficient and the initial pore solution composition, the equations of the multi-species transport model are solved with different values of the Freundlich's isotherm parameters μ and γ, which are adjusted in an iterative manner in order to minimise the (error) function χ (where μ and γ are regarded as the variables). This function gives the deviation between model and measurement.

The values of μ and γ, which yield the smallest error value, provide the best estimate of the binding isotherm for the material and age considered. This minimization procedure is performed automatically by using the downhill simplex method proposed by Nelder and Mead [1965]. It is important to apply the minimization procedure several (5-10) times by using different initial values for the fitting parameters, in order to ensure that the global minimum of the χ function has been correctly located.

ASSESSMENT OF CHLORIDE BINDING ISOTHERM BY AN ANALYTICAL FORMULA (METHOD 2)

Another method is proposed to assess chloride binding isotherms. In this method, physical adsorption onto C-S-H and formation of Friedel's salt by chemical reactions are addressed separately. On the basis of the general shape of the experimental chloride binding isotherms published in the literature, chloride binding can be described in a simplified manner by an analytical formula (Eq. (5.51)) which includes the two following components (Figure 5.24a):

- The chemical component, which results from Friedel's salt formation at very low chloride concentrations. These chemical reactions are assumed here to occur instantaneously when the material is put in contact with chlorides. The chemically bound chloride amount (= Friedel's salt amount) is therefore independent of the chloride concentration and is considered as a function of the residual content of *equivalent* aluminates of the material at the considered age $N_{(C3A)eq.} = NC_3A + 0.5 \cdot NC_4AF$ (exchanges with hydrated sulfoaluminates are not taken into account here). This equivalent content concept allows accounting for the contribution of both C_3A and C_4AF to Friedel's salt formation, despite the lack of a detailed description of the mechanisms. The 0.5 factor has been selected in order to take into account the lower reactivity and accessibility of C_4AF,
- The physical component, which results from adsorption onto C-S-H. It can be described by Freundlich's formula or by Langmuir's formula. Here Freundlich's description has been chosen, as it provided a better fit on experimental data. The physically bound chloride amount depends on the chloride concentration and involves the C-S-H content of the material at the considered age $N_{C\text{-}S\text{-}H}$,

$$s_{Cl}=N_{C\text{-}S\text{-}H}.\mu'c_{Cl}{}^{\gamma'}+\delta.(N_{C3A}+0.5N_{C4AF}) \quad 5.51$$

where $N_{(C3A)eq.} = N_{C3A} + 0.5 \cdot N_{C4AF}$ and $N_{C\text{-}S\text{-}H}$ are expressed in mol per m^3 of material, and the parameters μ', γ' and δ are assumed to be independent of the (concrete) mix composition for a given binder type (e.g. CEM I).

Binding isotherm description according to Eq. (5.51) means that in Figure 5.24 the Friedel's salt amount is the ordinate at x=0, while the remainder of the isotherm depends only on the C-S-H amount. This description is thus consistent with Tang and Nilsson's approach [1993].

The set of parameters μ', γ' and δ has been calibrated by using a broad range of experimental data from the literature, obtained at various ages on pastes and mortars. Unlike method 1, the method proposed in this section provides fixed values for parameters μ', γ' and δ, which remain valid whatever the (concrete) mix-composition (but for the same binder type) and age. Only the C-S-H content ($N_{C\text{-}S\text{-}H}$) and the residual content of equivalent aluminates ($N_{(C3A)eq.}$) remain to be estimated for each material and age, in order to assess the analytical binding isotherm. These values can be deduced from the mix composition by an analytical hydration model. Examples of analytical binding isotherms obtained with the same set of parameters μ', γ' and δ are displayed in Figure 5. 24 illustrating a good agreement with experiments. According to stoechiometric considerations, the theoretical maximum δ value, which corresponds to full accessibility to reaction sites, should be 2. The fitting results are consistent with these considerations, since the calibration provides $\delta < 2$ ($\delta = 1.3$ with Freundlich's formula and $\delta = 1.9$ with Langmuir's formula).

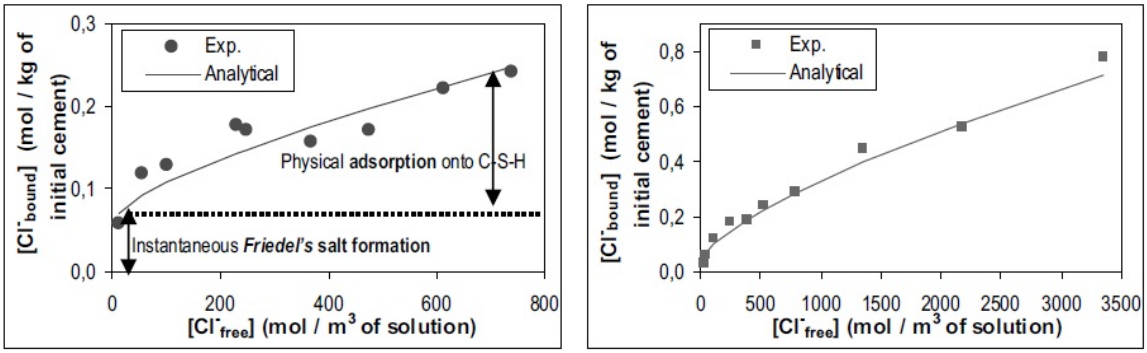

a) hcp C30 (W/C = 0.30 ; age = 28 days) b) mortar M1N (W/C = 0.50 ; age = 90 days)

Figure 5.24: Experimental chloride binding isotherms for hcp C30 and mortar M1N from the literature and analytical isotherms obtained for both materials with the same set of parameters μ', γ' and δ, and illustration of the simplified analytical description of chloride binding isotherms.

The numerical inverse analysis can modify the binding isotherm by means of a multispecies transport model and from a total chloride concentration profile measured at a given exposure time. This method is particularly appropriate to the monitoring of existing structures, since such profiles are the experimental data which are the most often available in this case and since prediction of the future evolution of the structure can easily be deduced. This method has been validated by comparison with binding isotherms obtained experimentally by the equilibrium and the profile methods, and by testing it in predictions.

The binding isotherm can also be easily calculated by an analytical formula based on the chemical composition of the material. Even if the profile prediction performed by using this method of assessment of the binding isotherm does not seem as good as in the case of method 1, the analytical formula has several advantages:

- Physical and chemical bindings are addressed separately. This aspect is important for mix optimization, in order to meet durability requirements: the binding capacity of a cementitious material can thus be enhanced by acting on both components (e.g. increasing both the C-S-H content and the equivalent aluminate content of the binder),
- No experiment is required to assess the binding isotherm,

- It is easy to use. In particular, such a simplified description can easily be implemented in sophisticated physicochemical models of coupled moisture-chloride transport. It is very convenient from a numerical point of view, since it avoids the incorporation of the equations and the additional ionic and solid species associated with the dissolution precipitation reactions (Ca^{2+}, $Al(OH)_4^-$, *Friedel's* salt, $Ca(OH)_2$, aluminates or sulfoaluminates, ...). The discontinuous feature of the chemical equilibrium equations can indeed induce numerical difficulties. Note that a more theoretical-based version of the proposed analytical equation, which involves the hydroxyl ion concentration of the pore solution in the physical component. The effect of the pH on binding can in this case be investigated,
- By using such a method of assessment of the binding isotherm, the profile prediction can be performed by a model at any time, without requiring a profile at a previous exposure time. [Baroghel-Bouny et al, 2008]

Castellote et al [1999] proposed another chloride-binding isotherm calculated from non-stationary migration experiments. They made specimens on concrete (w/c=0.4), cylinders 75mm in diameter and 150mm in height. They were demoulded at 24 h and cured for 28 days underwater. They were then stored until testing time in a $Ca(OH)_2$-saturated solution. Table 5.17 contains the mix proportion of the concrete fabricated.

Table 5.17: Concrete dosage used

Cement (kg/m^3)	Sand (kg/m^3)	Coarse aggregate (kg/m^3)	Water (kg/m^3)	Water/cement ratio
380	771	1177	152	0.4

They made two series of non-steady-state migration tests (see Figure 5.25) at constant voltage. One of them used different chloride concentrations in the external solution, and in the other, the migration time was changed. The conditions were:

- Series with different chloride concentrations: The catholyte containers (300 mL in volume) were filled with 0.05, 0.1, 0.5, and 1 M NaCl solutions. The test lasted 21 days. The applied voltage was 12 V.

- Series where, containers were filled with 0.5 M solution of NaCl. A voltage difference of 12 V was applied during 7, 14, 21, and 28 days.

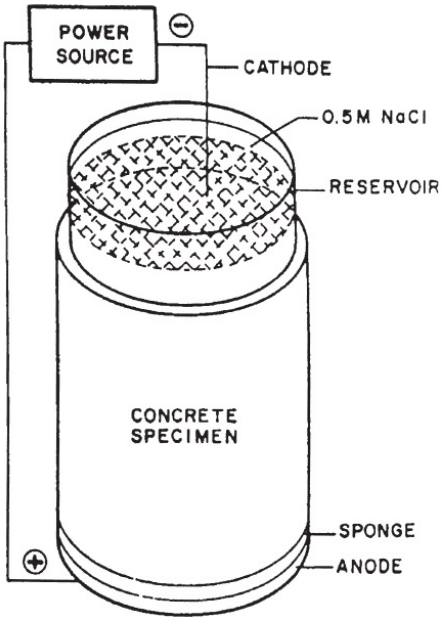

Figure 5.25: Sketch of the experimental arrangement.

At the end of each experiment, the specimen was cut in slices (about 5–10 mm thick) that were analysed by X-ray fluorescence to obtain the total amount of chlorides. Free chlorides were also determined by a leaching method in an alkaline solution.

To quantify the ability of the cement matrix to bind chlorides, the results of total and free chlorides obtained from the different experiments have been fitted to the general BET adsorption isotherm. Adaptation for adsorption from a liquid was made following Tang and Nilsson [1995], replacing the ratio of pressures by the concentration ratio.

To fit the experimental data into the BET equation, the ratio V/V_m has been substituted by %/%*m*. Thus, instead of obtaining V_m (the volume of adsorbate needed to cover the surface of the cement matrix with a monolayer), what is calculated is the percentage of combined chlorides equivalent to cover this surface with a monolayer. The other

parameters obtained are the BET characteristic constant *C* and the number of monolayers *n*.

Therefore, resulting chloride isotherm equation is shown in Eq. (5.54):

$$\frac{V}{V_m} = \frac{Cx}{(1-x)} \frac{1-(n+1)x^n + nx^{n+2}}{1+(C-1)x + Cx^{n-1}} \qquad 5.54$$

In this equation all the parameters have the original meaning (BET) except for *x*, which now is the ratio between *Cf* =free chlorides in the pore solution (g/L) and C_{sat}=chloride concentration of a saturated NaCl solution at the temperature T (g/l) [see Eq. (5.55)]:

$$x = \frac{C_f}{C_{sat}} \qquad 5.55$$

To convert data of percentage of free chlorides (%) into concentrations (g/l), it is necessary to measure the volume of pore solution per weight of the sample. This has been done by mercury porosimetry analysis of the concrete being the averaged value of 2.9*E*-5 m^3 (solution)/Kg (sample). Complete saturation of the concrete has been assumed.

The fitting of the experimental data to the Eq. (5.54) is given in Figure 5.26. Although the fitting has a correlation factor of only 0.818, it should be appreciated that all data lie between the margin of 95% confidence and the residues are in the range of ±0.03 units, which is good, considering the intrinsic heterogeneity of the concrete.

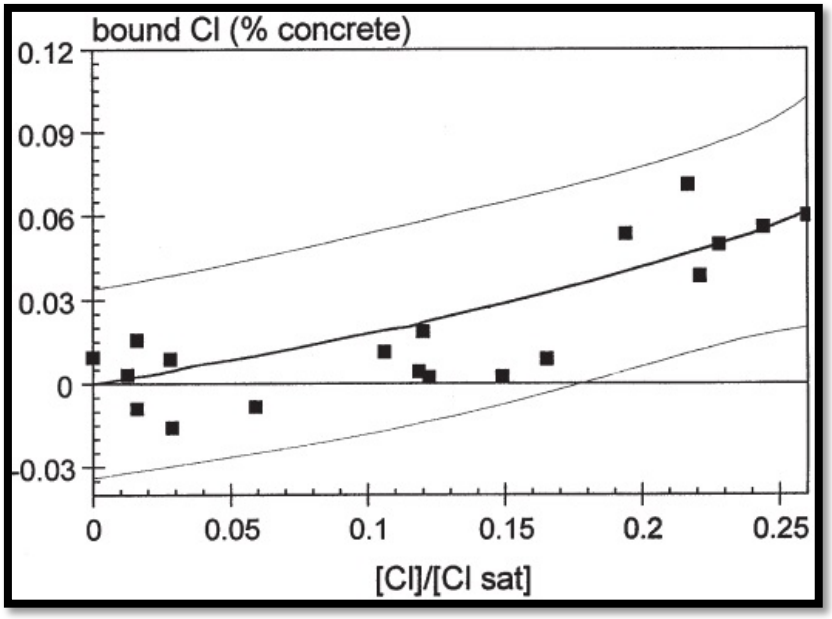

Figure 5.26: Fitting of the experimental data to a BET isotherm. (Dotted lines show the 95% confidence interval.)

The parameters obtained from the fitting were:

%m = 0.257 (percentage of chlorides needed to cover with a monolayer the internal surface of the cement matrix), C=0.597 (BET characteristic constant), and n= 1078 (number of monolayers).

It is important to point out that the most important data obtained from the fitting is the BET characteristic constant, *C.* Concerning the other parameters, they do not have a practical significance except that the very high value for n confirms the non-Langmuirian behaviour of the isotherm; that is the particular case for n= 1.

It is also important to remark that the shape of this isotherm can be ascribed to an isotherm of type III or V. In the type III, the convex character persists all along the x-axis, while in the type V an inflexion point appears for high enough x values. The range of values C_f/C_{sat} obtained does not enable discrimination of whether the isotherm is type III or type V.

The value of the BET constant C lower than 2 also confirms that the isotherm is of type III or V, both characteristics of weak and nonfavourable interaction between the

adsorbate and the substrate. The values of *C* previously obtained by Tang and Nilsson [1995] from natural diffusion experiments were above 50, which indicates a strong interaction between adsorbate and substrate.

To clarify further the differences in chloride-binding ability between diffusion and migration experiments, Figure 5.27 presents the curve of combined chlorides (percentage by cement weight) in function of the chloride concentration in the pore solution calculated in the present experiment together with the Langmuir isotherm proposed by Sergi et al. [1992] for diffusion experiments in ordinary Portland cement paste. Even though extrapolation of both isotherms can be mechanistically misinterpreted, it is necessary to proceed in this manner, because comparison of both curves enables some interesting observations. Extrapolating both isotherms, a chloride concentration is found in which combined chlorides are similar. This meeting point of both curves corresponds to a 0.48% of total chloride with respect to the weight of sample, a value that can only be reached at high chloride concentrations in migration experiments.

From Figure 5.27 it seems reasonable to think that a limit in the percentage of combined chlorides should exist, which enables the statement that the chloride isotherm in migration experiments should be of type V.

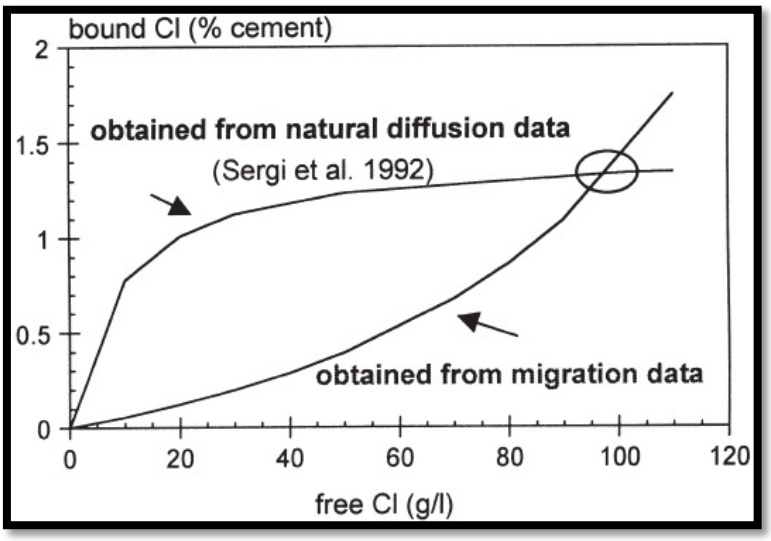

Figure 5.27: Chloride-binding isotherms from migration and diffusion experiments.

The amount of free and combined chlorides is different in non-steady-state migration and diffusion experiments. This implies a different rate or mechanism of interaction between chlorides and cement phases in the two types of test. For the cement tested, the combined chlorides are similar in diffusion and migration experiments for external chloride concentrations above 1M NaCl (0.25–0.30% free chlorides by sample weight).

The opposite of what happens in diffusion, in a nonsteady- state migration experiment the shape of the chloride isotherm is convex with respect to the x-axis. The value of the BET characteristic constant was calculated to be <2, which indicates an unfavourable interaction between the adsorbate and the substrate. This type V of BET isotherm appears to be due to the limited binding ability of chlorides in a migration experiment, attributed to a change in the controlling step of the global process. It seems that the instantaneous equilibrium assumed in an isotherm is not fulfilled during migration experiments with low external chloride concentration. [Castellote et al, 1999]

Marinescu and Brouwers [2009] used equilibrium method for quantifying the chloride binding capacities of OPC hydration products. This technique implies the immersion of small pieces obtained by crushing the concrete sample in a chloride solution of known concentration, in a sealed environment, until equilibrium is reached. They claim a equilibrium between the concentration of free chlorides in the pore solution and the chloride concentration of the external solution is reached within two weeks. Due to the small dimension of the sample pieces, the concentration of chloride ions in the pore solution is considered to be equal to the concentration of the external solution at the time of equilibrium.

Figure 5.28 compares the chloride binding isotherms of C_3S and C_2S as found in Hassan [2001] research. The C-S-H isotherm is computed using the C_3S/C_2S ratio on an arbitrary OPC composition, in order to calculate the average chloride binding capacity of the C-S-H phase. Due to the fact that usually C_3S will be found in a

greater proportion in OPC than C_2S, the C-S-H line is closer to the chloride binding isotherm of the C_3S paste.

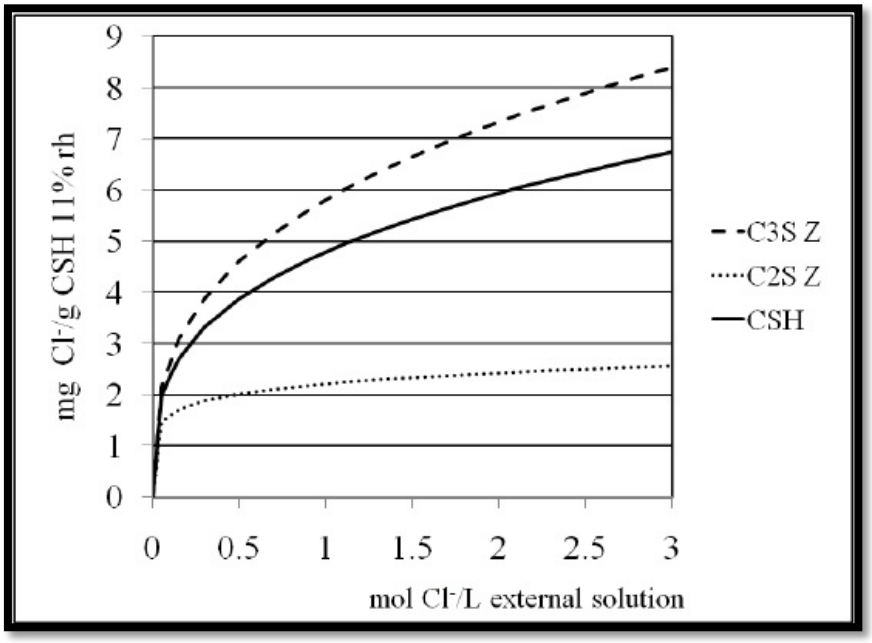

Figure 5.28: Chloride binding isotherms of the CSH phase in the hardened cement paste, from Hassan [2001]. All results represent mg of bound Cl^- /g of CSH dried at 11% rh.

Quantifying the amount of chlorides bound by the AFm phase has to take into account the different types of AFm that can co-exist in hardened cement paste (monosulfoaluminate, hydroxy-AFm, monocarboaluminate or hemicarboaluminate etc.) and also the extent of their solid solutions between themselves and with Friedel's salt.

In Hirao et al [2005], the chloride binding capacity of a C_3A-gypsum hydrated paste was fitted on a Freundlich isotherm, with a maximum at around 3 mol NaCl/L solution. In Birnin–Yauri and Glasser 1998 research, the hydroxy-AFm phase is considered to be completely converted to Friedel's salt at a very low concentration of free chlorides, around 0.015 mol NaCl/L solution.

Figure 5.29 compares the Freundlich isotherm from Hirao et al [2005], which is attributed here to monosulfoaluminate-AFm, to an isotherm based on the results in

Birnin–Yauri and Glasser 1998 research, about hydroxy- AFm chloride binding. No mention on the possibility of carbonation was found in Birnin–Yauri and Glasser 1998 research, or Hirao et al [2005], so the formation of hemicarboaluminate or a solid solution could not be assumed.

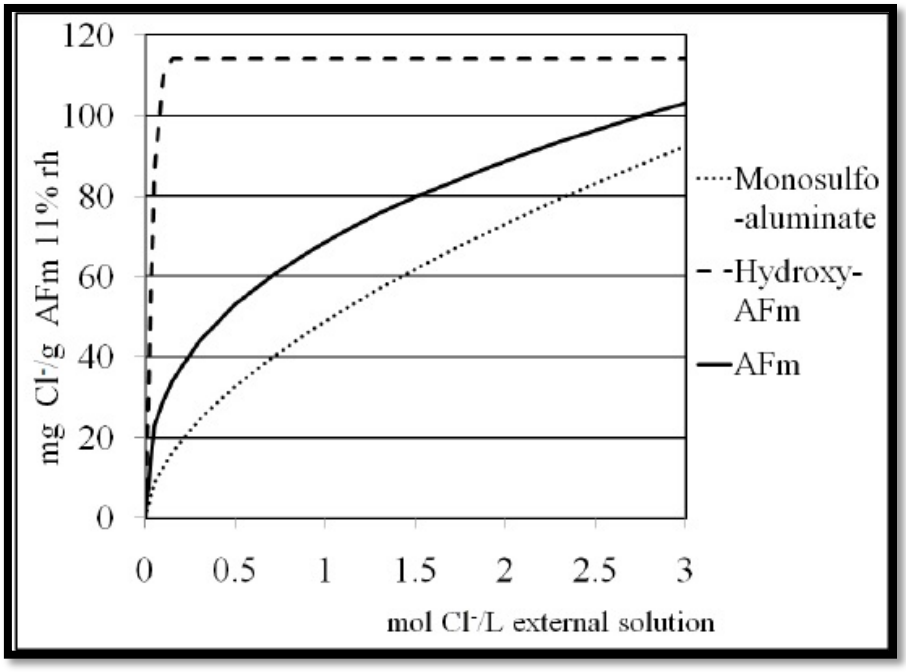

Figure 5.29: Chloride binding isotherms of the AFm component in the hardened cement paste, from Birnin–Yauri and Glasser 1998 research and Hirao et al [2005].

The "AFm" isotherm represents a probable chloride binding isotherm of the AFm phase in OPC, fitted on a whole range of OPC compositions and hardened OPC phase parameters found in literature. In order to relate this isotherm to the hardened cement paste composition, the reactions between other AFm phases and chloride ions have to be taken into account, as well as the extent of the solid solutions that Friedel's salt can form. Another factor that could influence the experimental results can be the hydration of unreacted cement particles in the chloride-containing pore solution, in

the case of cement pastes cured for a short time before immersion into chloride solutions.

Figure 5.30 shows the breakdown of bound chlorides in an OPC paste, between the AFm and the CSH phases.

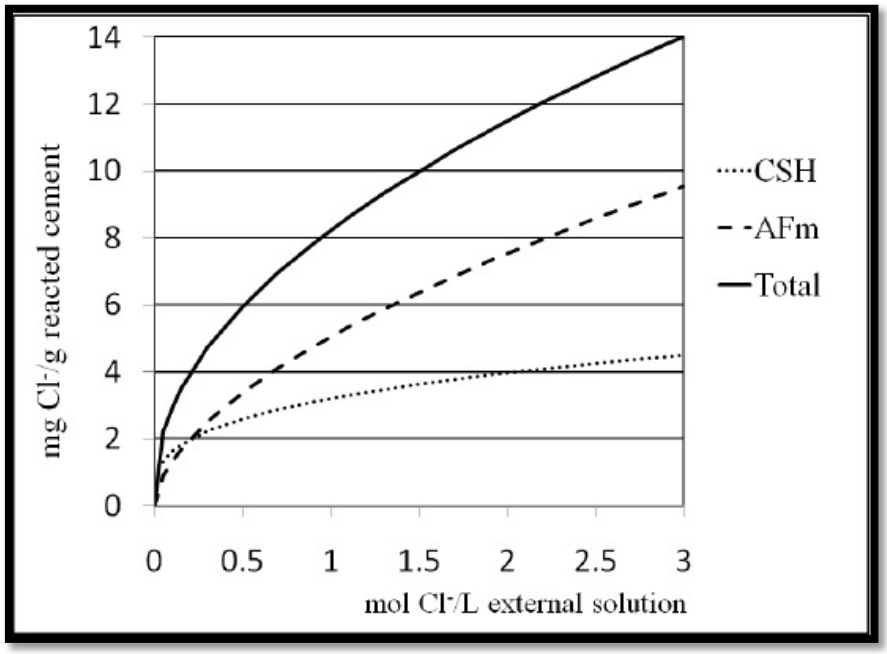

Figure 5.30: Bound chloride isotherm as the sum of the binding isotherm of the AFm and the binding isotherm of the CSH phase.

The "Total" line represents the sum of the "AFm" and "CSH" isotherms (computed the same way as in Figure 5.28 and Figure 5.29), and is lower than an experimental OPC chloride bonding isotherm of the same OPC hardened paste.

The fact that both the C-S-H binding capacity and the total binding capacity of hardened OPC pastes can be described using Freundlich adsorption curves suggests that the AFm chloride binding capacity should follow the same trend. This trend, also observed experimentally, leads to the conclusion that the chloride ions adsorption mechanism is the dominant one for AFm chloride binding.

It can be seen in Figure 5.30 that the C-S-H phase accounts for approximately one third of the total bound chloride. However, with the development of the model to include other AFm phases and further approach experimental values, its contribution is expected to be found slightly lower.

Loser at al [2010] calculate the chloride binding capacity of the different binders with evaluating the difference between the acid-soluble and the water-soluble chloride content following European standard EN 14629, with the only difference in dilution solution being water or diluted nitric acid. The water-soluble chloride content was determined at selected samples which were taken from the same powders used for the acid-soluble chloride content profiles in the test ASTM C 1556 after 50 days immersion. The samples selected for analysis were all mixtures with CEM I as binder and the CVC-mixtures of the other binders with a w/b of 0.45. Note that for their following discussion the chloride content determined with diluted nitric acid is defined as the total chloride content whereas the water-soluble chloride content is defined as the free chloride content. The results are expressed as mass% chlorides per mass of unit cement in each mixture proportion.

One has to be aware that, contrary to the reference method for determining free chloride content (mass%/cement) by analysing expressed pore solution from uncrushed samples, bound chlorides can also be extracted by dissolving the chlorides with water. But, as shown in a Round-Robin test [2001], the free chloride content can be determined reasonably rigorously if the contact time between water and crushed concrete sample lasts a short time. Moreover, the results presented in this paper are used for a relative comparison between different binders only and not as absolute values. Therefore, this procedure of obtaining free chloride content should be accurate enough for using the results as a basis to asses the influence of chloride binding on the test results and for comparison to thermodynamic modelling.

Mu et al [2011] claim that Freundlich and Langmuir binding isotherms are better than the linear binding isotherms to match results in cracked self-compacting concrete.

Wang et al [2009] used an inverse analysis and an optimization method to fit the effective chloride diffusion coefficient and the chloride binding isotherm parameters

from experimental total chloride concentration profiles. They also used two types of binding isotherm: a Freundlich isotherm and an adsorption isotherm related to ion exchange and completed by Friedel's salt formation (double-layer based isotherm). Recently, a double-layer based isotherm, which is related to the ion exchange theory, was used to describe the binding of chloride ions onto the C-S-H.

A double-layer based binding isotherm associated with adsorption of Cl^- ions according to the theory of ion exchange. This isotherm is completed by the chemical reaction between Cl^- ions and aluminates leading to the formation of Friedel's salt.

In order to fit Freundlich isotherm and double-layer based isotherm parameters by inverse analysis they claim that the Freundlich isotherm (see Eq.(5.56)) seems to be an excellent fitting equation of the experimental binding data in a large range of free chloride concentrations (from 0.01 mol.L^{-1} to 1 mol.L^{-1}).

$$s_{Cl}=\mu c_{Cl}^{\gamma} \qquad 5.56$$

where μ and γ are the Freundlich's parameters. s_{Cl} and c_{Cl} are respectively the content of chloride ions which are bound to the solid (mol/m^3 concrete) and the concentration of free chloride ions in the pore solution (mol/m^3 solution). μ and γ depend on the mix design parameters of the material (content of cement), and on the composition of the binder.

Recently the double-layer theory (ion exchange) has been used to describe the adsorption of chloride ions onto C-S-H. According to this theory, the adsorption capacity of the C-S-H depends both on the content of C-S-H, and on the concentrations of OH^- and Cl^- ions in the pore solution (see Eq. (5.57)).

$$s_{Cl} = N_{CSH}\frac{\alpha c_{Cl^-}}{c_{OH^-}+\beta c_{Cl^-}} + 2N_{C_3Aeql}\Gamma(c_{Cl^-})\begin{cases}\Gamma(c_{Cl^-})=0 & c_{Cl^-}=0\\ \Gamma(c_{Cl^-})=1 & c_{Cl^-}>0\end{cases} \qquad 5.57$$

where α and β are the double-layer based isotherm parameters. C_{OH} is the concentration of free OH^- ions in the pore solution (mol/m^3 solution). N_{CSH} and N_{C3Aequ} are the content of C-S-H (mol/m^3 solid) and residual content of equivalent

aluminates (mol/m^3 concrete) respectively, (the chemical reaction between Cl^- and C_4AF is taken into account through N_{C3Aequ}, since $N_{C3Aequ} = N_{C3A} + 0.5N_{C4AF}$).

Profiles of total chloride content were used to determine the parameters of the binding isotherm by inverse analysis. These profiles were obtained by diffusion tests in nonsteady state conditions, as shown in Figure 5.31. The surface of the specimens is coated by epoxy resin except the bottom surface which is immersed into a NaCl (0.513 mol/L) and NaOH (0.1 mol/L) solution. The duration of the test is 90 days. Free and total chloride concentration profiles are obtained by grinding followed by a chemical analysis of the powder which is extracted at different depths of the specimen.

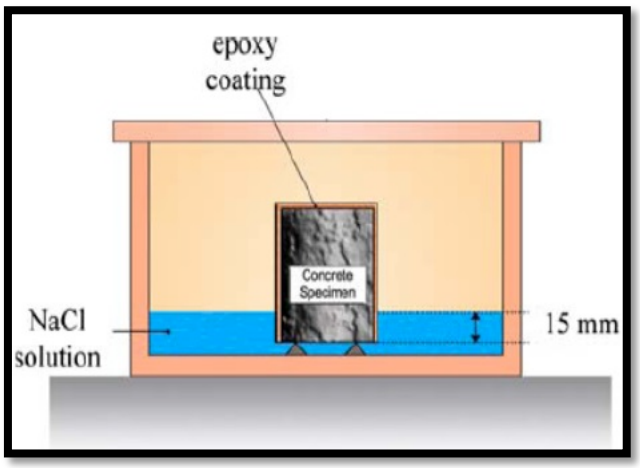

Figure 5.31: Diffusion test in non-steady-state conditions

Two concretes were tested: BO and M25. The contents of the solid phases (C-S-H and C_3A) and the initial concentration of the ions (Na^+, K^+) of the pore solution are calculated thanks to a hydration model. The porosity values correspond to an accessible-to-water porosity. By inverse analysis of experimental profiles, the optimal diffusion coefficients will be searched as well as the isotherm parameters.

According to their results both the effective chloride diffusion coefficients (D_{Cl}) and the Freundlich parameters μ and γ have been fitted by inverse analysis.

Some initial values of D_{Cl}, μ and γ were given for several primary simulations from which an optimal value of γ was observed (0.9). This value of γ was kept constant to search for the optimal value of D_{Cl} and μ. When the optimal value of D_{Cl} is found, the iterative procedure is applied again to seek the optimal values of μ and γ. Thus, γ = 0.9 was proved to be the optimal value.

The experimental profiles of total Cl concentration are illustrated in Figure 5.32. The simulated profiles which lead to the best fitting are also shown in the same figures. Figure 5.33 shows the binding isotherms which are either deduced by the fitting of the total chloride concentration profile or determined by using the experimental values of total and free chloride concentrations. Freundlich parameters μ and γ are dependent on the material composition, as illustrated in Table 5.18. As mentioned, γ weakly depends on the material composition. It is a relatively intrinsic parameter. The free chloride concentration has been predicted and compared with experimental profiles with a very good agreement, as has been shown in Figure 5.33.

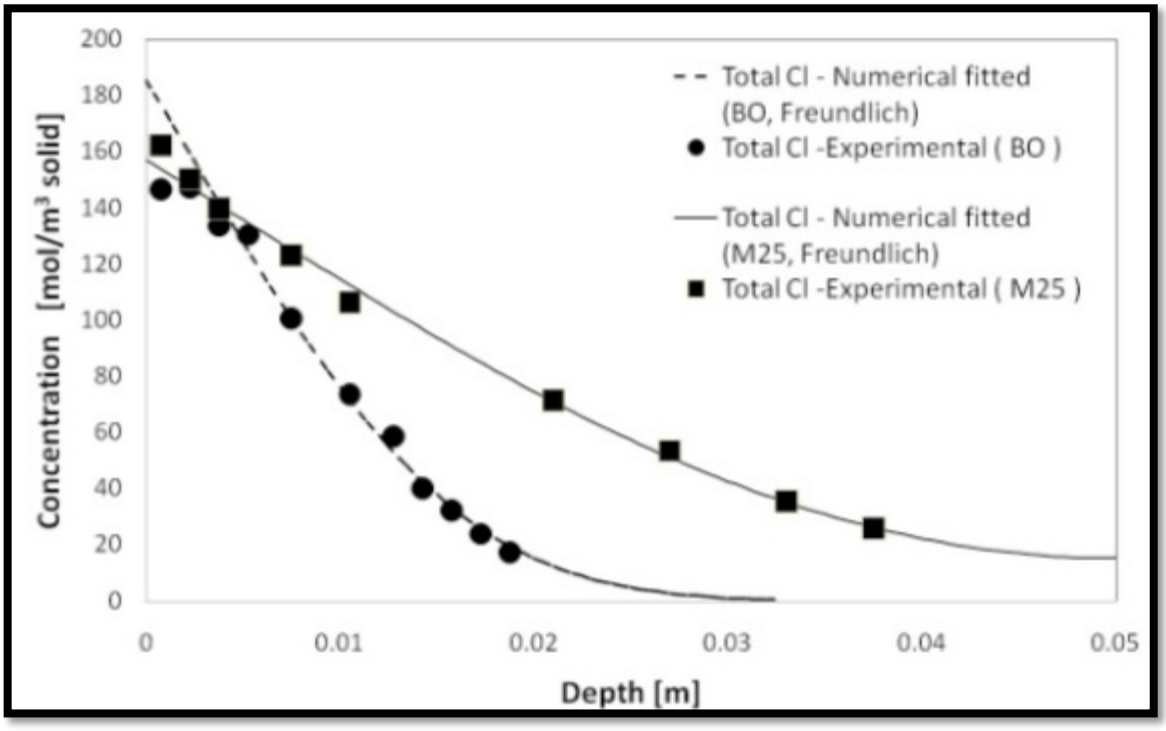

Figure 5.32: Profiles of total Cl content: experimental profiles compared with fitted numerical profiles (Freundlich -isotherm) after a 90-day non-steady state diffusion test.

Table 5.18: Optimal effective chloride diffusion coefficients and Freundlich parameters

Concrete	D_{Cl}	μ	γ
BO	2.89E-12	0.31	0.90
M25	1.31E-11	0.44	0.90

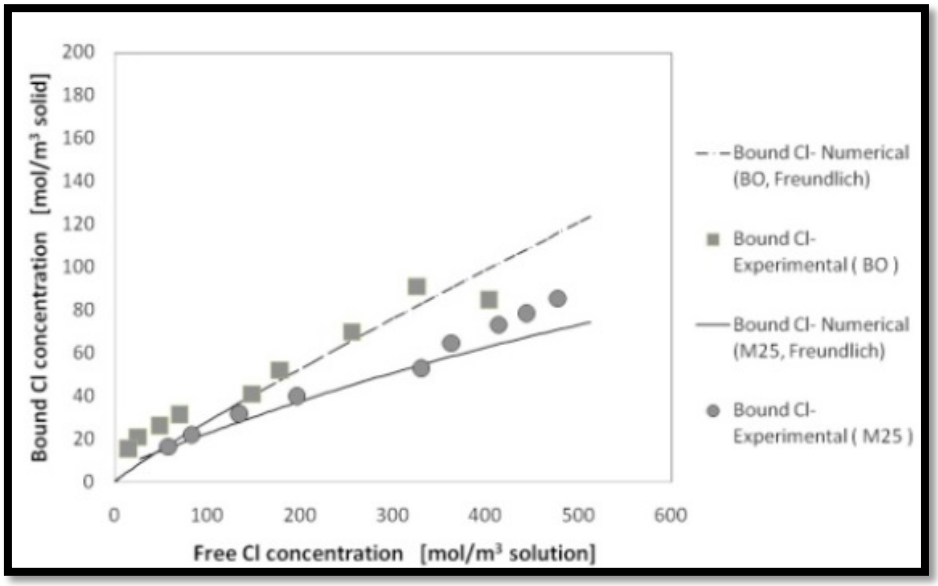

Figure 5.33: Chloride binding: experimental profiles compared with numerical predicted profiles (Freundlich-isotherm) after a 90-day non-steady state diffusion test.

The optimal values of D_{Cl} have been used to determine the double-layer based isotherm parameters.

The double-layer based isotherm parameters α and β are assumed to be intrinsic and independent on the mix design of the concrete. The parameters which minimize the difference between experimental profiles of total Cl content and simulated ones are given in Table 5.19 (Note that concrete BO and M25 use the same cement of CEM I).

Table 5.19: Parameters of DL-isotherm

Concrete	α	β
BO,M25	0.11	0.4

They claim that OH^- plays a role in the binding isotherm. According to the double-layer theory, the fixation of chloride ions is actually governed by the exchange between OH^- ions from C-S-H and Cl^- ions from the pore solution to insure the local electroneutrality, as illustrated in Figure 1. Hence, this procedure may be affected by the concentration of OH^- in the pore solution: the higher the OH^- concentration in the pore solution is, the less Cl^- ions are assumed to be bound. On the other hand, the concentration of OH^- influences the electric potential which governs the mobility of ions through the pore solution.

Nguyen et al proposed a method of assessment of the chloride binding isotherm by numerical inverse analysis. It consists in measuring a total chloride concentration profile after a non-steady-state diffusion test or from cores extracted from a real structure, which are the data most often available. The experimental results are then analysed by using the proposed numerical model. A simple numerical algorithm is used to determine the binding isotherm, which results in the best reproduction of the experimental total chloride concentration profiles.

In this case, the complicated chloride binding phenomenon is described globally by means of Freundlich's non linear isotherm. With the initial conditions (pore solution composition) and the effective diffusion coefficients determined by the methods

proposed by Nguyen et al. [2006], the equations are solved with different μ and γ values, which are adjusted in an iterative manner in order to minimise the χ error function, as described in the following.

For each combination of μ and γ values, the error between the model and the measurements is calculated by:

$$\chi = \sqrt{\sum_{k-1}^{M} [c_k^{mes}(x_k) - c_k^{num}(x_k)]^2} \qquad 5.58$$

where c_k^{mes} and c_k^{num} are the measured and predicted chloride concentrations at depth x_k, respectively, and M is the total number of measurements.

The values of the isotherm parameters μ and γ, which lead to the smallest error, provide the best estimate of the binding isotherm for the material considered. This analysis procedure is performed automatically by using the downhill simplex method of Nelder and Mead [1965]. The method only requires evaluations of the χ function, not of derivatives. It is not very efficient in terms of number of function evaluations but it is easier. It is important to apply the minimization procedure several (5-10) times by using different initial values for the fitting parameters, in order to ensure that the global minimum of the χ function has finally been located. Note that the relevance of the proposed method can be evaluated a posteriori through its ability to accurately fit a lot of experimental plots, thanks to the identification of two material binding parameters.

Estimation results of chloride binding isotherm by inverse analysis are shown in Figure 5.34. The binding isotherm parameters μ and γ are identified by "numerical inverse method" from an experimental total chloride concentration profile (see Figure 5.34a) obtained after 44-day nonsteady- state diffusion test in laboratory with two hardened cement pastes CO and CN (CEM I 52.5; W/C = 0.35 and 0.45 respectively). Experimental binding isotherms were determined by using the equilibrium method proposed by Tang and Nilsson [1993] on crushed pastes. Fig. 1b shows the

comparison between the results obtained from the numerical method and the experiments. A rather good agreement is displayed. In particular, the numerical model predicts correctly the binding capacity at high chloride concentrations for the paste CN.

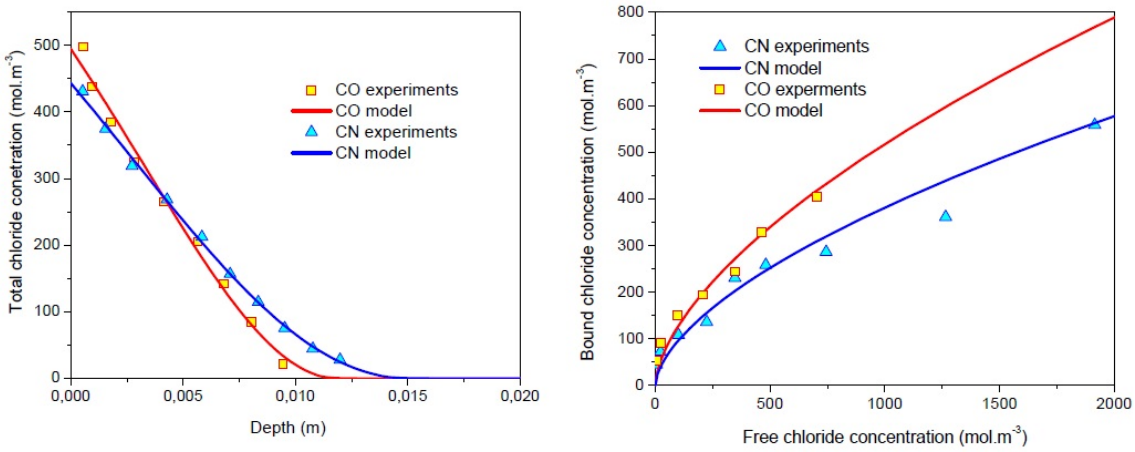

a) Total chloride concentration profiles (experimental data and fit with LCPC model)

b) Chloride binding isotherms (experimental and numerical results)

Figure 5.34: Chloride concentration profiles and binding isotherm in the case of non-steady-state diffusion tests. Measurements and numerical results with the LCPC model

The numerical inverse method has been applied to various concretes submitted to nonsteady- state diffusion tests to evaluate its reliability in predicting the chloride binding isotherm (Figure 5.35). As shown in Figure 5.35a, good fitting results were obtained with the profiles in every case with a correlation coefficient higher than 0.97. As depicted in Figure 5.335b, the good correlation between isotherms obtained numerically and experimentally from the profiles is a good argument to validate the proposed method. In particular, the method can easily be applied to concretes with different water-to-binder ratios and which incorporate supplementary cementing materials (e.g. concrete B80-SN contains SF and concrete CFA contains fly ash).

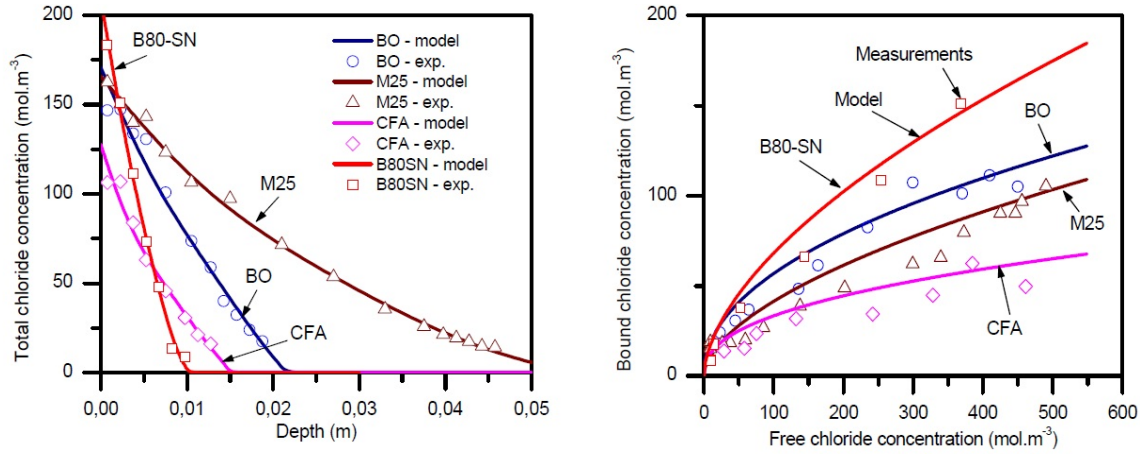

a) Total chloride concentration profiles b) Binding isotherms

Figure 5.35: Some examples of fitting results for concentration profiles by using the reverse analysis method

However, the dependence of the actual binding isotherm on the ionic concentrations of the pore solution and on the solid phases present in the material is very important and cannot be directly included in the non-linear binding analytical model adopted (Freundlich or Langmuir description). When additional data are available on chloride binding mechanisms, such a semi-empirical relationship can be replaced by a more chemically-based description.

5.5 MODELS FOR THE PREDICTION OF CHLORIDE BINDING

Hosokawa et al [2006] developed a model reproduce the behaviour of chloride binding in hardened cement paste using PHREEQC based upon thermodynamic equilibrium. They used the surface complexation model [Dzombak and Morel, 1990] for the modelling of the binding behaviour of C-S-H because the binding interaction is considered to be a sorption reaction on the surface of C-S-H, where the silanol (SiOH) on the surface is the sorption site. Using surface-complexation model, the sorption to the silanol site is modelled based on the electrostatic interaction at the solid fluid interface.

They also used the model proposed by Sugiyama [2006] to model the dissolution and precipitation behaviour of C-S-H, assuming a binary nonideal solid solution of $Ca(OH)_2$ and SiO_2. The model can predict both dissolution and precipitation of the C-S-H with a continuous change in the Ca/Si ratio of the solid phase. PHREEQC is not designed to perform the calculation of the proposed modelling of C-S-H, so the source codes of PHREEQC were customized and calculation procedures were installed into this program.

For modelling of ionic binding to C-S-H surface first they explain the basic characteristic of surface binding-site of C-S-H. The reaction of silanol site and their intrinsic equilibrium constant $logK^s$ are

$SiOH \rightarrow SiO^- + H^+$ $\quad logK^s=-12.3$ 5.59

$SiOH+CA^{2+} \rightarrow SiOCa^+ + H^+$ $\quad logK^s=-9.4$ 5.60

For the surface complexation model, K^s is given below:

$$K^s = \frac{\alpha_{SiO^-}\alpha_{H^+}}{\alpha_{SiOH}} exp\left(-\frac{F\Psi}{RT}\right) \quad 5.61$$

where a_i is the activity of species i, Ψ is the potential at the surface [V], R is the gas constant (8.3147 [J mol^{-1} K^{-1}]), F is the Faraday constant (96485 [C mol^{-1}]), T is absolute temperature [Kelvin] (fixed as 298 K in their study). Incorporating the surface complexation model and using the density of silanol sites per one mole of SiO_2 (surface site density: ρ_s), equal to be 0.045, the values of Ψ are obtained by calculating equilibrium of the solution with C-S-H.

Figure 5.29 shows the calculation results of Ψ and C/S as a function of the calcium activity in the solution and compares them with results previously obtained by Villias-Terrisse et al [2001]. The calculation results correspond closely with the results obtained by Villias-Terrisse et al [2001]. The point of zero charge is situated at about –p(Ca) = –2.9 in both cases. It has been established that the value of surface potential of C-S-H becomes positive when C/S is higher and becomes negative when C/S is lower. This validates the variation of surface potential shown in Figure 5.36.

For the surface complexation model in PHREEQC, equations (5.59) and (5.60), and the corresponding $logK^s$ values are considered accurate in describing the basic characteristics of surface binding-sites of C-S-H.

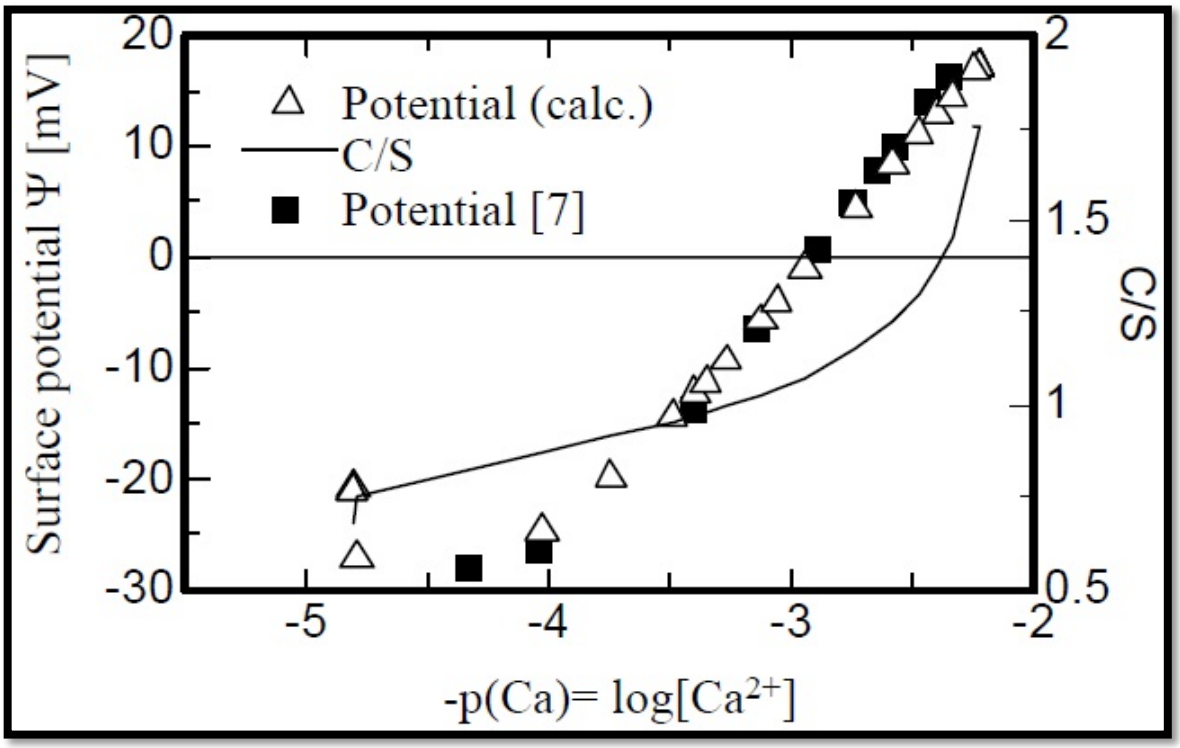

Figure 5.36: Calculation results of surface potential and C/S of C-S-H with solution under equilibrium

For derivation of Ks for each reaction of binding by C-S-H, Na^+, K^+, Cl^-, $SO4^{2-}$ are considered as the ions able to bind with the surface of C-S-H. The reaction of each ion on the surface is shown below.

$$SiOH + Na^+ \rightarrow SiONa + H^+ \quad 5.62$$

$$SiOH + K^+ \rightarrow SiOK + H^+ \quad 5.63$$

$$SiOH + Ca^{2+} + Cl^- \rightarrow SiOCaCl + H^+ \quad 5.64$$

$$SiOH + Ca^{2+} + SO_4^{2-} \rightarrow SiOCaSO_4^- + H^+ \quad 5.65$$

As the values of $logK^s$ are unknown, they were derived with PHREEQC by calibration with the sorption experimental data (Na^+ and K^+: C/S = 4, water solid ratio = 15), and (Cl^- and SO_4^{2-}: C/S = 1, water solid ratio = 10). Surface site density ρ_s was also derived using calibration.

Table 5.20: $logK^s$ and ρ_s of each sorption reaction derived by calibration

Sorption reactions	C/S of C-S-H									
	0.85	1.2	1.5	1.75	1.45	0.85	1.2	1.5	1.75	1.45
	$logK^s$					ρ_s				
$SiOH + Na^+ \longrightarrow SiONa + H^+$	-11.1	-11.4	-11.7	-11.7	–	0.1	0.12	0.07	0.05	–
$SiOH + K^+ \longrightarrow SiOK + H^+$	-11.3	-11.6	-11.6	-11.6		0.12	0.08	0.06	0.05	
$SiOH + Ca^{2+} + Cl^- \longrightarrow SiOCaCl + H^+$	–				-8.9	–				0.22
$SiOH + Ca^{2+} + SO_4^{2-} \longrightarrow SiOCaSO_4^- + H^+$	–				-6.0	–				0.22

Heath et. al. [1996] showed that the value of $logK^s$ of Ca^{2+} increases with increase of C/S and the values of $logK^s$ of Na^+ and K^+ decrease with the increase of C/S of C-S-H as shown in table 5.20 because the sorption reaction of alkali ions is competitive to that of Ca^{2+}. Therefore, variations of $logK^s$ of Na^+ and K^+ with C/S are considered correct. The derived values of $logK^s$ of Cl^- and SO_4^{2-} are –8.9 and –6.0 respectively. The $logK^s$ were calibrated to a sigmoidal function (equation (5.66)) as a function of C/S in order to obtain the values for $logK^s$, Na^+, and K^+.

$$logK^s = \frac{\alpha}{1 + \exp\left(b.\left(\left(\frac{C}{S}\right) - c\right)\right)} + d \qquad 5.66$$

where a, b, c, d are constants.

The values of surface site density ρ_s of Na^+ and K^+ depend on the C/S of C-S-H and $logK^s$. The difference between ρ_s of Cl^- and those of alkali ions are more dramatic than the variation of ρ_s of alkali ion with C/S. This is due to the difference of the process of the synthesized C-S-H used for calibration of $logK^s$ and ρ_s. Since the C-S-

H used in the experiment for Cl^- and SO_4^{2-} binding were synthesized by the hydration of alite, the C/S in the experiment for Cl^- and SO_4^{2-} binding is considered to be an accurate representation of C-S-H in the actual hardened cement paste. Thus, 0.22 derived from the experiment for Cl^- and SO_4^{2-} will be used as the ρ_s of C-S-H hereafter.

They also model the ion exchange reaction with AFm phases. The reaction between monosulfate and Freidel's salt is the ion exchange reaction of AFm phases. The reaction equation of the ion exchange is shown below.

$$XSO_4 + 2Cl^- \rightarrow XCl_2 + SO_4^{2-} + 2H_2O \qquad 5.67$$

where X represents ion exchange sites of AFm phase.

Ion exchange ratio, *x,* is defined as the number of sites of SO_4^{2-} replaced by Cl^- in monosulfate. Therefore, the composition of AFm phase under the equilibrium can be derived.

$$C_3A{\cdot}Ca \cdot xCl_2 \cdot (1-x)SO_4 \cdot H_{12-2x} \qquad 5.68$$

Since the equilibrium constant K^{ex} of this ion exchange reaction is unknown, K^{ex} was determined using PHREEQC by calibrating K^{ex} to the results of sorption experiment, in which the amount of bound Cl^- by monosulfate was measured by immersing a known amount of monosulfate into NaCl solution for a given concentration range.

Figure 5.37 shows the values of the amount bound Cl^- and the ion exchange ratio *x* obtained from PHREEQC are illustrated with the experimental results. K^{ex} was determined to be 1.934.

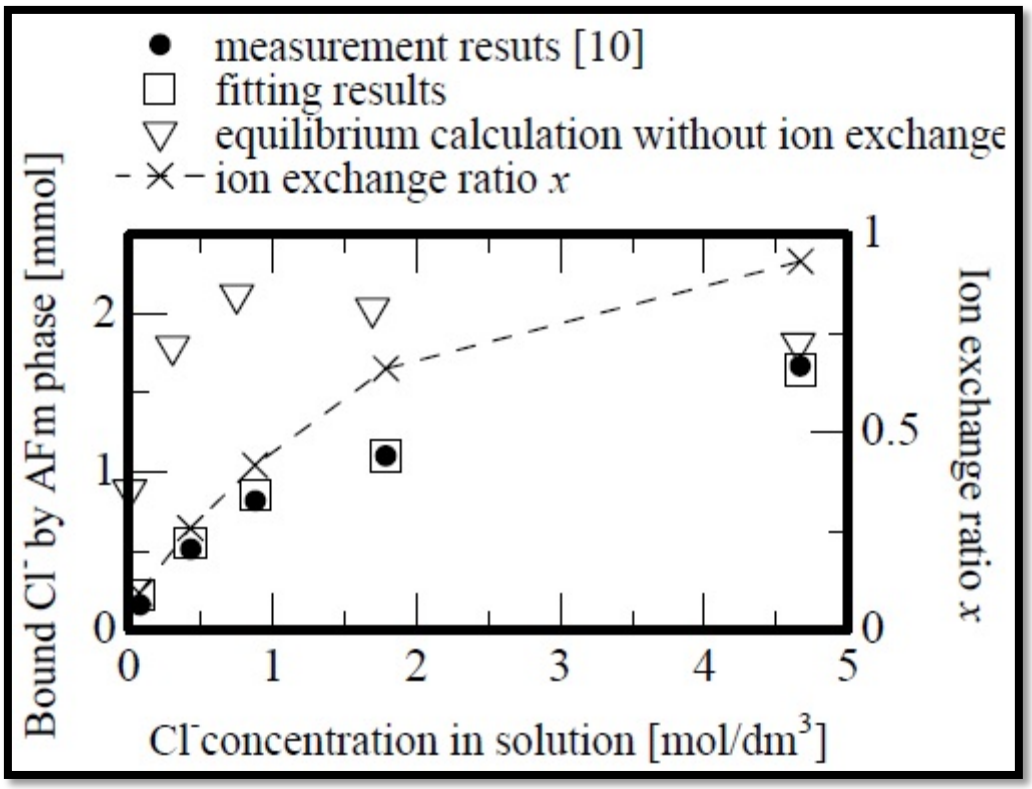

Figure 5.37: Results of fitting for determination of K^{ex}

The equilibrium calculation results of bound Cl^- in the case without the ion exchange reaction of AFm are also plotted in Figure 5.37. In the range of lower Cl^- concentration, the ion exchange ratio x is lower, while at about 5 mol/dm^3 of Cl^- concentration the ion exchange ratio x becomes closer to 1. Calculations without considering the ion exchange reaction of AFm vary greatly from experimental data due to the fact that monosulfate can react and change to Friedel's salt even in the low Cl^- concentrations.

For validity of the models of ion bindings onto C-S-H surface and ion exchange reaction with AFm verified by the reproduction of experimental results of Cl^- binding in hardened cement paste, in which the hardened cement paste was immersed into NaCl solution, they defined the procedure of determining the solid phase composition of hardened cement paste. The solid phase composition of hardened cement paste was determined using the reaction equations and hydration ratios of each mineral of cement based on the model proposed by Sakai *et. al.* [2004] and then used as the initial input data. The hydration reaction of each mineral is assumed as follows:

$C_3S + 5H \rightarrow C_{1.755}SH_{3.755} + 1.245CH$ 5.69

$C_2S + 4H \rightarrow C_{1.755}SH_{3.755} + 0.245CH$ 5.70

$C_3A + C\overline{S} + 12H \rightarrow C_3A \cdot C\overline{S} \cdot H_{12}$ 5.71

$C_3A + CH + 12H \rightarrow C_4AH_{13}$ 5.72

$$C_4AF + \frac{1}{3}(m+1)H \rightarrow C_3A + \frac{1}{3}C_2F_3H_m + \frac{1}{3}CH$$ 5.73

m in equation 5.73 assumed negligible. The hydration ratio of each phase is shown below in Table 5.22. The initial mineral composition of cement before hydration was determined from chemical composition of cement with the following assumptions:

(i) all Na_2O and K_2O of cement are contained in sulfate mineral,

(ii) (ii) the composition of all minerals are pure. The chemical composition of cement used in the experimental is shown in Table 5.21, and the mass content based on the assumptions listed and hydration ratio set for each mineral are shown in Table 5.22.

Table 5.21: Chemical composition of cement used in the experimental (mass %)

Ig. loss	SiO_2	Al_2O_3	Fe_2O_3	CaO	SO_3	Na_2O	K_2O
0.32	21.8	5.54	3.07	65.7	1.90	0.18	0.42

Table 5.22: Mass content and hydration ratio of each mineral in the cement

Mineral	Content (mass%)	Hydration ratio
C_3S	55.58	0.85
C_2S	20.32	0.47
C_3A	9.44	0.90
C_4AF	9.28	0.62
$CaSO_4$	2.21	1.0
Na_2SO_4	0.41	1.0
K_2SO_4	0.78	1.0

Calculations based on the thermodynamic model are dependent on the solubility constant K_{sp} and the corresponding dissolution/precipitation reaction for each hydrate. In Table 5.23 principal reactions and K_{sp} are listed.

Because each equation is expressed as a protonation equation, it should be noted that existent forms of several species are different from the actual ones. For example, the aluminum ion Al^{+3} actually exist as $Al(OH)_4^-$ in pore solution. K_{sp} is determined according to the reaction equation so that K_{sp} is affected by the manner of expression of the equation.

The K_{sp} value of $C_2F_3H_m$ has not been investigated up to now. Therefore, $C_2F_3H_m$ is excluded from the calculation.

Table 5.23: Reaction equation and thermodynamic solubility constant K_{sp} for each phase (25˚C)

Phase	Reaction equation	$\log K_{sp}$
C-S-H	Solid solution between $Ca(OH)_2$ and SiO_2	Function of CaO/SiO_2
Portlandite	$Ca(OH)_2 + 2H^+ \longrightarrow Ca^{2+} + 2H_2O$	22.80
Monosulfate	$C_3ACaSO_4{:}12H_2O + 12H^+ \longrightarrow 4Ca^{2+} + 2Al^{3+} + SO_4^{2-} + 18H_2O$	73.83
Ettringite	$Ca_6Al_2(SO_4)_3(OH)_{12}{:}26H_2O + 12H^+ \longrightarrow 2Al^{3+} + 6\ Ca^{2+} + 38H_2O + 3SO_4^{2-}$	58.24
Friedel's salt	$C_3ACaCl_2{:}10H_2O + 12H^+ \longrightarrow 4Ca^{2+} + 2Al^{3+} + 2Cl^- + 16H_2O$	73.2
C_4AH_{13}	$C_4A{:}13H_2O + 14H^+ \longrightarrow 4Ca^{2+} + 2Al^{3+} + 20H_2O$	103.5

For calculation of chloride binding in hardened cement paste (Figure 5.38) they used the model for ion exchange reaction of AFm and base on the developed model using PHREEQC correspond closely with experimental results. Figure 5.38 also shows the calculations results obtained using a model that neglects the ion exchange reaction of AFm. In the case without the ion exchange reaction, a significant error between calculation and experimental occurs especially in the range of lower concentration of chloride. This error is due to the behaviour of production of AFm phases. If the ion exchange reaction of AFm is not considered, the calculated amount of Friedel's salt becomes higher with low concentrations of chloride (Figure 5.39b). Whereas, when the ion exchange reaction is taken into consideration, the calculated amount of both Friedel's salt and monosulfate are more representative of the actual amounts in the C-S-H (Figure 5.39 a).

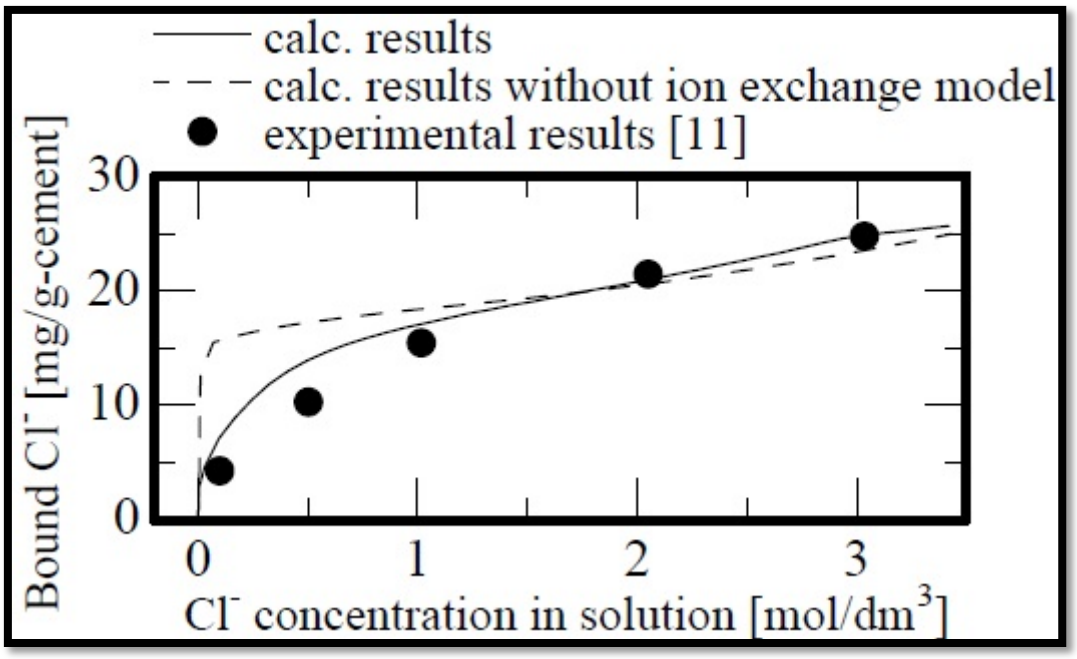

Figure 5.38: Calculation and experimental results of Cl^- binding by hardened cement paste.

The model of ion bindings onto C-S-H surface also takes into consideration the behaviour of Cl^- binding in hardened cement paste. Figure 5.40 shows the variation of distribution of Cl^- in hydrate. According to the model of ion exchange reaction of AFm, the amount of bound Cl^- by AFm decreased and the amount of bound Cl^- by C-S-H increased. This is one of the reasons that PHREEQC with the model of ion exchange reaction can accurately predict the experimental results of bound Cl^- in hardened cement paste.

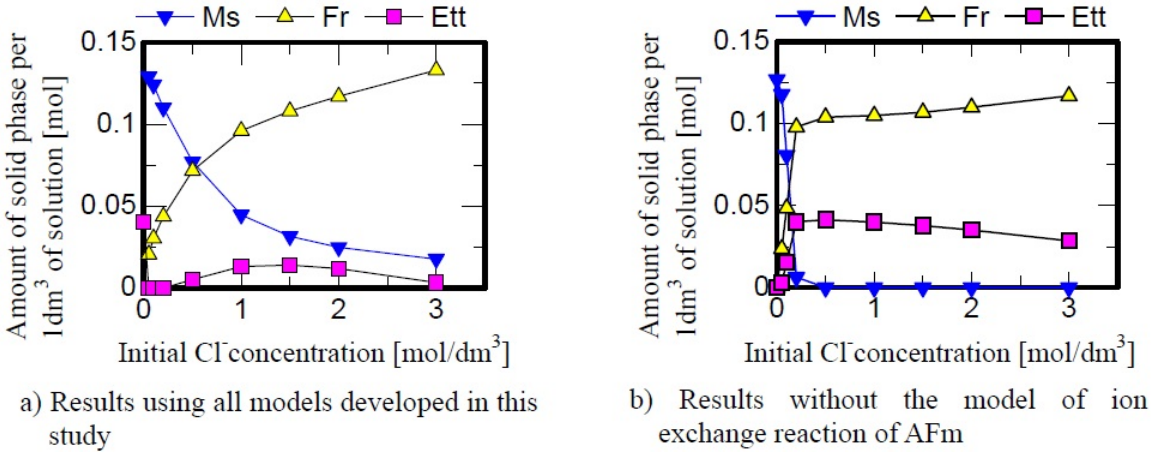

a) Results using all models developed in this study

b) Results without the model of ion exchange reaction of AFm

Figure 5.39: Calculation results for the amount of AFm and Ett versus initial Cl^- concentration

Yoshida et.al.[2002] investigated the ion exchange reaction of AFm and Cl^- using XRD, and reported the reaction stops when the amount of bound Cl^- by hardened cement paste reaches approximately 1 mass% of cement. This corresponds closely with the calculated results using this model where at the approximately the same amount of bound Cl^-, ion exchange ratio x equal to 0.92, the exchange stops. Taking into consideration the accuracy limits of XRD measurements, the model accurately predicts the amount of bound Cl^- in hardened cement paste.

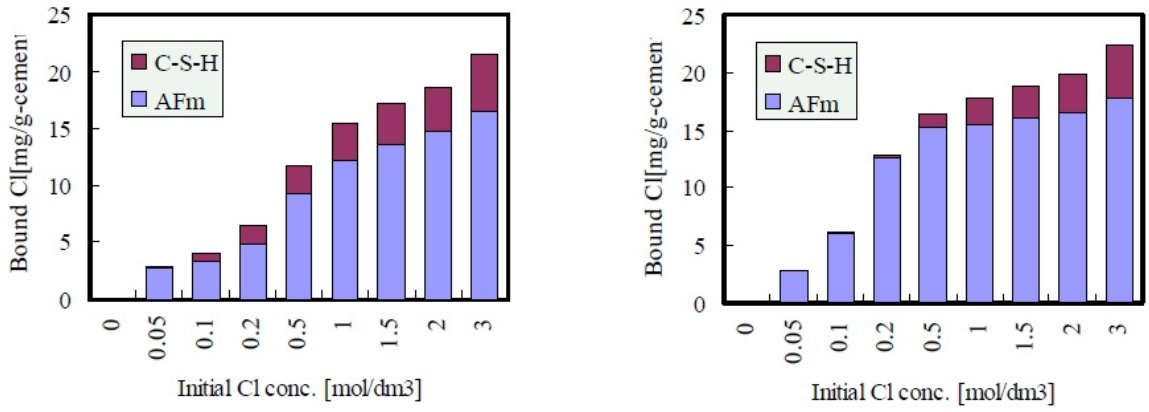

Figure 5.40: Distribution of bound chloride ion in hydrate.

The amounts of AFm and ettringite with versus initial Cl^- concentration are shown in Figure 5.41. In the case with the all models developed in this study, the amount of formed Friedel's salt increases and the amount of formed ettringite decreases in comparison with the results neglecting SO_4^{2-} binding by C-S-H. When the concentration of NaCl solution is 3.0 mol/dm^3, the amount of formed ettringite approaches zero. This is because the amount of bound SO_4^{2-} on the surface of C-S-H exceeds the consumption SO_4^{2-} by ettringite in equilibrium calculations based on the model developed for SO_4^{2-} binding with C-S-H. According to the XRD measurements as shown in Figure 5.42, the peak intensities of ettringite and monosulfate become weaker with increasing NaCl concentration. The peak of ettringite also disappears at the 3mol/dm^3. The models developed for PHREEQC effectively reproduce the varying formation of hydrates caused by the reactions of chloride binding in hardened cement paste.

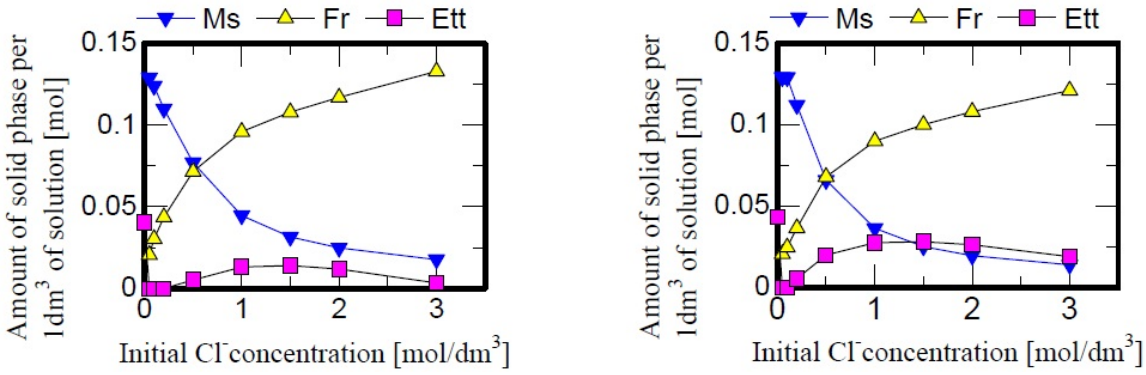

Figure 5.41: Calculation results for the amount of AFm and Ett versus initial Cl^- concentration

Based on the models developed, the rate at which Cl^- occupies the silanol site decreased in comparison when SO_4^{2-} binding by C-S-H was neglected. However, the calculated amount of bound Cl^- did not change regardless of the model for SO_4^{2-} binding as shown in Figure 5.43. This is due to the increases of bound Cl^- by AFm shown in Figure 5.41 cancelled out by the decrease of bound Cl^- by C-S-H.

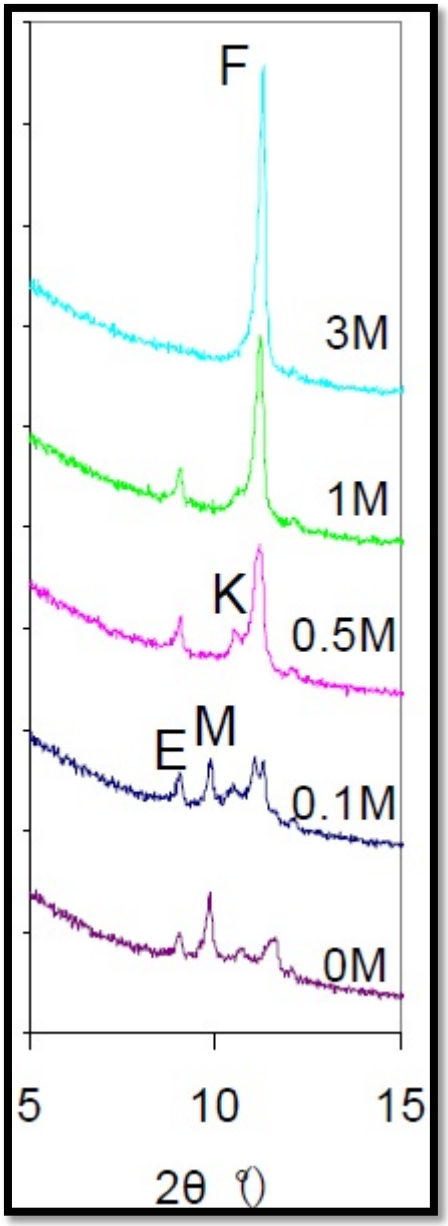

Figure 5.42: The XRD measurement results in the experiment F: Friedel's salt, M: monosulfate, E: Ettringite, K: Kuzel's salt

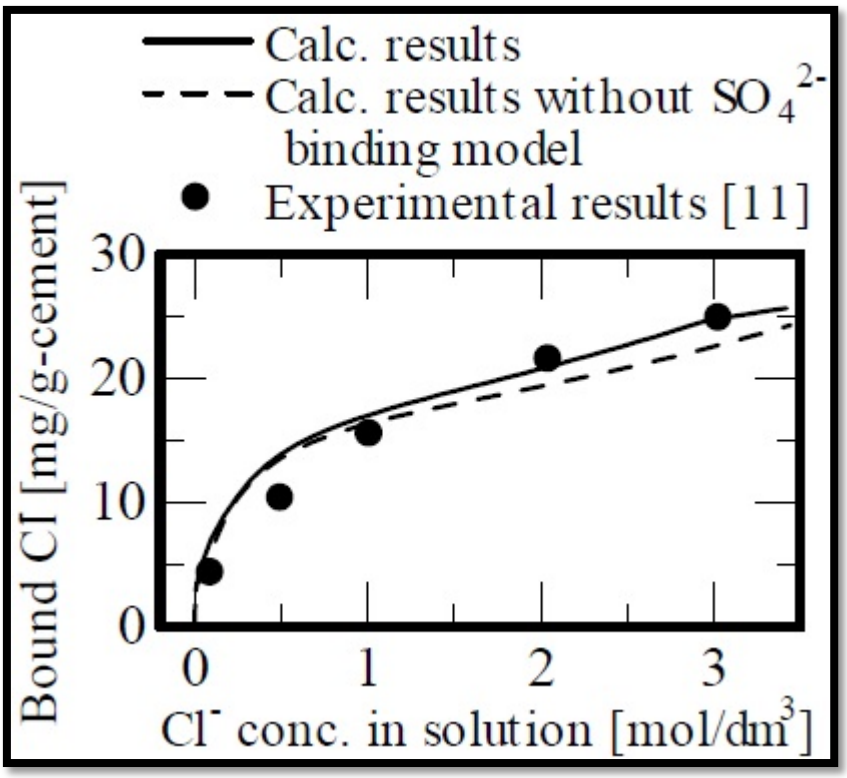

Figure 5.43: Calculations and experimental results of Cl^- binding by hardened cement paste.

Models developed in this study accurately predict the binding phenomena in hardened cement paste. [Hosokawa et al, 2006]

5.6 CONCLUSION

Many methods have been proposed for testing chloride ingress in concrete. These methods can be categorised into three categories: diffusion tests, migration tests, and indirect test based on resistivity or conductivity. Taking samples from in-service structures and determining chloride profiles by using chemical or physical lab

techniques are mostly common. Destructive techniques are mainly used for short term decision making. These methods can determine total or free chloride.

Total chloride determination can be determined by chemical analysis, using AS 1012.20-1992, ASTM C 1152-97 or BS 1881 Part 124-1988.

Common techniques for measuring chloride content in concrete structures shows the objectives of each technique in summary:

- Three of them aim to directly determine chloride concentration (Quantitative X-ray diffraction analysis and Potentiometric evaluation for free chlorides and Volhard method for total chloride content).
- RCPT relates charge passed through a concrete slab to chloride penetrability in order to define the permeability of the material.
- Non-steady state diffusion test and electrical migration test use diffusion models and complementary chemical techniques for characterizing the material.
- Impedance and ponding test accelerate diffusion processes for determining diffusion coefficient and chloride ingress profile.

The free chloride in concrete is a factor in the corrosion of embedded steel while bound chloride is not. The free chloride is generally considered to be the water soluble part of the total but the measurement is not well defined and the values obtained are dependent upon the subdivision of the sample and the nature, temperature and duration of the extraction step. Approach free chloride is more complicated, this means that the definition of the free chlorides has to be linked to the method used. Typically, the free chlorides will include at least the "diffusing" ones (present in the pore solution) and a variable proportion of the physically bound chlorides (those weakly physically adsorbed onto the solid matrix), depending on the method. The free chloride concentration can also be measured by the ion chromatography technique.

Ultrasonic treatment appears to prevent the formation of loosely bound chloride which would otherwise be released when the pore solution is expressed.

The relationship between the bound chloride and the free chloride can be described by Freundlich isotherm at high free chloride concentrations and Langmuir isotherm at low free chloride concentrations.

With increasing exposure time, more total chloride ingress was found, and the bound chloride content was greater, even though the percentage chloride binding capacity as compared to the total chloride content was smaller.

Cement hydration products can also influence chloride binding.A number of experimental studies found in literature determine the chloride binding capacity of hardened cement paste on samples dried at 11% rh. When a saturated hardened cement paste sample is dried to 11% rh.

Finding Freundlich-type isotherm describes chloride binding by the monosulfate phase, in mg Cl/ g monosulfate

An equation was provided to compute chloride binding capacity of the C-S-H phase in mg Cl/g C-S-H.

Ettringite is also mentioned and believed to give a chloride sorption capacity lower than portlandite and Friedel's salt, but higher than tobermorite. The amount of AFt increases with the intrusion of chloride ions and the formation of Friedel's salt, so this contribution needs to be taken into account. In order to do this, the first assumption is that ettringite has the same chloride binding ability as tobermorite, so that its minimum influence can be assessed. Then, the amount of newly formed ettringite needs to be estimated from the amount of Friedel's salt.

Several None-destructive techniques were developed for measuring chloride content in reinforced concrete structures during past years. Ion selective electrode (ISE), Electrical resistivity (ER) and Optical fiber sensors (OFS), Electrochemical impedance spectroscopy (EIS) are three main methods that were used. Each method measures chloride ions or chloride diffusion coefficient, and depending on the chloride threshold used by technician/owner, he/she must choose between free chloride and chloride diffusion coefficient. Also, depending on that chloride threshold it could be necessary to measure other kind of parameters. Fabrication process is very

specific for each method. ISE are easily produced using electrochemical processes that are well known, predictable and cheaper than OFS. The key aspect that influences all measurements methods (ISE, ER or OFS) is temperature. ER is also highly dependent on moisture content, temperature and ions presence.

ISE devices can generally resist aggressive environments, but important parameters, such as limit of detection, depend on environmental pH. In addition, the reference electrode, that is essential for their optimal performance, is less resistant than the other parts of the device. On the other hand, ER do not need special care because the embedded parts are generally built in stainless steel and other parts are not permanently placed in the concrete nor exposed to environment. The OFS method requires extra protection for isolating optical fibers from water, temperature, and concrete alkalinity. Since optical fibers are placed in the concrete mix during casting they should be protected against breaking and bending. ISE is less robust concerning chemical reactions and mechanical actions.

For quantification of chloride binding, the physicochemical interactions between chloride ions and the cement matrix can be quantified at the macroscale and at equilibrium by the so-called *chloride binding isotherm*, which links the bound chlorides amount to the free chloride concentration of the pore solution, at a given temperature, for a given material and at a given age. The chloride binding isotherm is the most influent parameter on the prediction results in terms of average chloride penetration depth or concentration profiles. Researchers used the Langmuir isotherm to describe chloride binding. Several experimental techniques are available to directly assess binding isotherms. Two other type of binding isotherm are Freundlich isotherm and an adsorption isotherm. Recently, a double-layer based isotherm, which is related to the ion exchange theory, was used to describe the binding of chloride ions onto the C-S-H. It is claimed that OH^- plays a role in the binding isotherm. According to the double-layer theory, the fixation of chloride ions is actually governed by the exchange between OH^- ions from C-S-H and Cl^- ions from the pore solution to insure the local electroneutrality. Hence, this procedure may be affected by the concentration of OH^-

in the pore solution: the higher the OH^- concentration in the pore solution is, the less Cl^- ions are assumed to be bound. On the other hand, the concentration of OH^- influences the electric potential which governs the mobility of ions through the pore solution.

Chloride binding isotherm could assess by numerical inverse analysis, analytical formula and non stationary migration experiments.

Models to predict chloride binding were also developed. Hosokawa et al [2006] developed a model reproduce the behaviour of chloride binding in hardened cement paste using PHREEQC based upon thermodynamic equilibrium. Sugiyama [2006] modelled the dissolution and precipitation behaviour of C-S-H, assuming a binary nonideal solid solution

of $Ca(OH)_2$ and SiO_2. The model can predict both dissolution and precipitation of the C-S-H with a continuous change in the Ca/Si ratio of the solid phase. PHREEQC is not designed to perform the calculation of the proposed modelling of C-S-H, so the source codes of PHREEQC were customized and calculation procedures were installed into this program. The ion exchange reaction with AFm phases was also modelled. The reaction between monosulfate and Freidel's salt is the ion exchange reaction of AFm phases.

For validity of the models of ion bindings onto C-S-H surface and ion exchange reaction with AFm verified by the reproduction of experimental results of Cl^- binding in hardened cement paste, they defined the procedure of determining the solid phase composition of hardened cement paste.

Calculations based on the thermodynamic model are dependent on the solubility constant and the corresponding dissolution/precipitation reaction for each hydrate.

Yoshida et.al.[2002] investigated the ion exchange reaction of AFm and Cl^- using XRD, and reported the reaction stops when the amount of bound Cl^- by hardened cement paste reaches approximately 1 mass% of cement. Taking into consideration the accuracy limits of XRD measurements, the model accurately predicts the amount of bound Cl^- in hardened cement paste.

Chapter 6

RESEARCH TRENDS

6.1 METHODS

As it is described in chapter 5 they are several methods to measure and predict total chloride and chloride binding.

It is possible to identify the following challenges for future research on chloride measurement by using Non-destructive techniques (NDTs):

- Independence of geometry: the presence of rebars, corners, or electrical fields in RC structures can distort electrical or electro- chemical signals, causing underestimation/overestimation of the measurements. New measurement techniques should be capable to take data from concrete structures regardless of the geometrical configuration of the structural component nor the layout of the reinforcement.
- Multi-measurement ability: NDTs should be developed or combined with other NDTs to assess more parameters that induce errors in the measurement of chloride concentrations, this can help to better understand the interactions and therefore to obtain measures independent of specific conditions. For example, the assessment of carbonation reaction is important taking into consideration that it can produce pH fall, porosity changes, and corrosion acceleration. At the end, it is probable that this reaction interferes on NDT's

chloride concentration measurements, as well as other important parameters: sulfate presence, pH, temperature and moisture content.

- Independence of environmental actions: the measurements under specific conditions for temperature, moisture content, pH, and/ or the presence of sulfates or CO_2 may produce errors that should be carefully controlled. The challenge of NDTs is then to develop sensors that avoid or compensate environmental conditions effects.
- Chemical stability, durability and maintainability: most structures are planned for lifetimes between 50 and 100 years. Thus, NDTs should be able of withstanding chemical changes inside the concrete matrix and to be operational or easily replaceable during the structural lifetime.
- Costs: it is necessary to develop measuring methods that are not expensive in terms of costs of construction, installation and maintenance during the structural lifetime.

Although other NDTs have been proposed such as electrochemical impedances spectroscopy, grounding penetrating radar and capacitive methods, until now, there is not enough results about their performance, accuracy, robustness, and chemical stability. (Torres-Lugue et al., 2014).

REFERENCES

'Guideline for practical use of methods for testing the resistance of concrete to chloride ingress', 2002

AFREM test procedures concerning chlorides in concrete: extraction and titration methods', prepared by T.Chaussadent & G.Arliguie, *Mat. Struct.* **32** (217) (1999) 230-234

Ahmed MS. Effects of systematic increase of pozzolanic materials on the mechanical, durability, and microstructural characteristics of concrete. Canberra: The University of New South Wales; 2007.

Alexander MG, Magee BJ. Durability performance of concrete containing condensed silica fume. Cem Concr Res 1999;29:917–22.

Al-Hussaini, M.J., Sangha, C.M., Plunkett, B.A. and Walden, P.J. (1990): "The Effect of Chloride Ion Source on the Free Chloride Ion Percentages in OPC Mortars", Cem. Concr. Res., Vol. 20 (1990) pp. 739-745.

Al-Khaja Waheeb A., 'Influence of temperature, cement type and level of concrete consolidation on chloride ingress in conventional and high-strength concretes', Construction and Building Materials, Volume 11, Issue 1, February 1997, Pages 9–13

Andrade C. Calculation of chloride diffusion coefficients in concrete from ionic migration measurements. Cem Concr Res 1993; 23: 724–42.

Angst UM, Polder R. Spatial variability of chloride in concrete within homogeneously exposed areas. Cem Concr Res 2014; 56(0): 40–51.

Ann, K.Y., Song, H-W. (2007): chloride threshold level for corrosion of steel in concrete. Corrosion Science, Vol. 49, No. 2007, June 2007, pp. 4113-4133.

Arya .C, Buenfeld N.R, Newman J.B, 'FACTORS INFLUENCING CHLORIDE-BINDING IN CONCRETE', CEMENT and CONCRETE RESEARCH. Vol. 20, pp. 291-300, 1990

Arya C, Newman J. An assessment of four methods of determining the free chloride content of concrete. Mater Struct 1990; 23: 319–30

Arya, C. and Xu, Y. "Effect of Cement Type on Chloride Binding and Corrosion of Steel in Concrete", Cem. Concr. Res., Vol. 25 (1995) No. 4, pp. 893-902.

Arya, C. et al. (2014): Modelling chloride penetration in concrete subjected to cyclic wetting and drying. Magazine of Concrete Research, Vol. 66, No. 7, February 2014, pp. 364-376.

Atkins C, Carter M, Scantlebury J. Sources of error in using silver/silver chloride electrodes to monitor chloride activity in concrete. Cem Concr Res 2001; 31(8):1207–11.

Atkins C, Scantlebury J, Nedwell P, Blatch S. Monitoring chloride concentrations in hardened cement pastes using ion selective electrodes. Cem Concr Res 1996; 26(2): 319–24.

B. Lothenbach, G. Le Saout, E. Galluci, K. Scrivener, 'Influence of limestone on the hydration of Portland cements', Cement and Concrete Research. 38 (2008) 848–860.

Balonis M., Lothenbach B., Le Saout G., Glasser F.P., 'Impact of chloride on the mineralogy of hydrated Portland cement systems', Cem. Concr. Res. 40 (2010) 1009–1022.

Baroghel Bouny .V, Chaussadent .T, Raharinaivo A., 'Experimental investigations on binding of chloride and combined effects of moisture and chloride in cementitious materials', 1st RILEM workshop on Chloride Penetration into Concrete 15-18 October 1995, St Rémy lès Chevreuse, France

Baroghel-Bouny .V, Nguyen T.Q, Dangle .P, Belin.P, 'Assessment of chloride binding isotherms', international RILEM symposium on concrete modelling-CONMOD'08 26-28 May 2008, Delft, The Netherlands

Basheer P, Gilleece P, Long A, Carter WJM. Monitoring electrical resistance of concretes containing alternative cementitious materials to assess their resistance to chloride penetration. Cem Concr Compos 2002; 24: 437–49.

Bastidas-Arteaga E, Chateauneuf A, Sánchez-Silva M, Bressolette P, Schoefs F. Influence of weather and global warming in chloride ingress into concrete: a stochastic approach. Struct Safety 2010; 32: 238–49.

Beaudoin J.J., Ramachandran V.S. and Feldman R.F., 'INTERACTION OF CHLORIDE AND C-S-H', CEMENT and CONCRETE RESEARCH, Vol. 20, pp. 875-883, 1990.

Bernal, J.D., Jeffery, J.W., and Taylor, H.F.W., 1952. Crystallographic research on the hydration of Portland cement. A First Report on Investigations in Progress. Magazine of Concrete Research, 4 (11), 49–54.

Bertolini, L. et al. (2004): Corrosion of Steel in Concrete. WILEY-VCH Verlag GmbH & Co., Weinheim, Germany, 2004, 392 pp.

Bigas J.P, Lambert .F, Ollivier J.P, 'An original method to determine the non linear chloride binding isotherm from bulk specimens of mortat', 1st RILEM workshop on Chloride Penetration into Concrete 15-18 october 1995, St Rémy lès Chevreuse, France.

Birnin-Yauri, U.A. and Glasser, F.P. (1998), "Friedel's salt, $Ca_2Al(OH)_6(Cl,OH).2H_2O$: its solid solutions and their role in chloride binding", Cem. And Concr. Res., Vol.28, No.12, pp.1713-1723

Broomfield Jone P., 'Corrosion of Steel in Concrete', E&FN Spon, London, 1997

Brown .P, Bothe Jr .J, 'The system $CaO-Al_2O_3-CaCl_2-H_2O$ at 23±2 ˚C and the mechanisms of chloride binding in concrete', Cement and Concrete Research, Vol .34, 2004

Brown PW, Badger Steven. 'The distributions of bound sulfates and chlorides in concrete subjected to mixed NaCl, $MgSO_4$, Na_2SO_4 attack'. Cement and Concrete Research 30, 2000

Brown, P.C. (1993): "Kinetics of Tricalcium Aluminate and Tetracalcium Aluminoferrite Hydration in the Presence of Calcium Sulphate", J. American Ceramic Society, Vol 76 (1993), No. 12, pp. 2971-2976.

Brunauer, S., Skalny, J. and Bodor, E.E., 'Adsorption on nonporous solids', *J.* Colloid and Interface Science, 30(1969) 546-5 52.

Buchheit RG, Guan H, Mahajanam S, Wong F. Active corrosion protection and corrosion sensing in chromate-free organic coatings. Prog Org Coat 2003;47:174–82.

Byfors, K. (1986): 'Chloride Binding in Cement Paste", Nordic Concrete Research, Publication No. 5, pp. 27-38.

Byfors, K., Hansson, C.M. and Tritthart, J. (1986): "Pore Solution Expression as a Method to Determine the Influence of Mineral Additives on Chloride Binding", Cem. Concr. Res., Vol. 16 (1986) pp. 760-770.

C. Arya, J.B. Newman, An assessment of four methods of determining the free chloride content of concrete, Materials and Structures 23 (1990) 319–330.

Castellote M, Andrade C, Alonso C. Chloride-binding isotherms in concrete submitted to non-steady-state migration experiments. Cem Concr Res 1999;29:1799–806.

Castellote, M., Andrade, C., 'Round-Robin Test on chloride analysis in concrete. Part II: Analysis of water soluble chloride content', *Mat. Struct* **34** (2001) 589-598.

Chatterji, S. (1994): "Transportation of Ions Through Cement Based Materials. Part 3; Experimental Evidence for the Basic Equations and Some Important Deductions", Cem. Concr. Res., Vol. 24 (1994) No. 7, pp. 1229-1236.

Cheewaket .T, Jaturapitakkul .C, Chalee .W, 'Long term performance of chloride binding capacity in fly ash concrete in a marine environment', Construction and Building Materials 24, (2010) 1352–1357

Chen, J.J., et al., 2004. Solubility and structure of calcium silicate hydrateMECHANISM OF PBIEDEL'S SALT FOBMATION

Chindaprasirt P, Rukzon S. Strength, porosity and corrosion resistance of ternary blend Portland cement, rice husk ash and fly ash mortar. Construct Build Mater 2008; 22:1601–6.

Concrete, hardened: accelerated chloride penetration: NT BUILD 443; 1995.

Cong, X. and Kirkpatrick, R.J., 1996. Si MAS NMR study of the structure of calcium silicate hydrate. Advanced Cement- Based Materials, 3, 144–156.

Connell M. The long term performance of high slag concrete. Concr (London) 1998;32:30–1.

Cook H, McCoy W. Influence of chloride in reinforced concrete. Am Soc Test Mater ASTM STP 1977;629:20–9.

Costa A, Appleton J. Chloride penetration into concrete in marine environment – Part I: Main parameters affecting chloride penetration. Matér Constr 1999; 32: 252–9.

Cti technical note C", 'chlorides in concrete', 2004

D.C. Grahame, Chem. Rev. 41 (1947) 441–501.

de Vera Almenar G. Ingreso de cloruros en hormigón. métodos de análisis, detección no destructiva y modelización del transporte tras un aporte inicial limitado. Ph.D. thesis, Universitat d'Alacant; 2000.

de Vera G, Climent M, Antón C, Hidalgo A, Andrade C. Determination of the selectivity coefficient of a chloride ion selective electrode in alkaline media simulating the cement paste pore solution. J Electroanal Chem 2010;639:43–9.

De Weerdt K., Kjellsen K.O., Sellevold E., Justnes H., 'Synergy between fly ash and limestone powder in ternary cements', Cem. Concr. Compos. 33 (2011) 30–38.

De Weerdt, K., Geiker, M. & Orsakova, D. (2014a), The impact of sulphate and magnesium on chloride binding in Portland cement paste. *Sub. to Cem Concr Res - Under review,* Under review.

Dehghanian .C, Arjmandi .M, 'INFLUENCE OF SLAG BLENDED CEMENT CONCRETE ON CHLORIDE DIFFUSION RATE', Cement and Concrete Research, Vol 27, No.6. 1997

Delagrave, A., Marchand, J., Ollivier, J.-P., Julien, S. and Hazrati, K.: "Chloride Binding Capacity of Various Hydrated Cement Paste Systems", Adv. Cem. Bas. Mat., Vol. 6 (1997) pp. 28-35.

Dent Glasser, L.S., et al., 1978. A multi-method study of C3S hydration. Cement and Concrete Research, 8, 733–740.

Deus JM, Díaz B, Freire L, Nóvoa XR. The electrochemical behaviour of steel rebars in concrete: an Electrochemical Impedance Spectroscopy study of the effect of temperature. Electrochim Acta 2014;131:106–15.

Dhir RK, El-Mohr MAK, Dyer TD. Chloride binding in GGBS concrete. Cem Concr Res 1996;26:1767–73.

Dhir RK, El-Mohr MAK, Dyer TD. Developing chloride resisting concrete using PFA. Cem Concr Res 1997;27:1633–9.

Dhir RK, Jones M.R. and McCarthy M.J, 'BINDER CONTENT INFLUENCES ON CHLORIDE INGRESS IN CONCRETE', *Cement and Concrete Research,* Vol 26, No.12. 1996

Dhir RK, Jones MR. Development of chloride-resisting concrete using fly ash. Fuel 1999;78:137–42.

Douglas G, Wendling L, Pleysier R, Trefry M. Hydrotalcite formation for contaminant removal from ranger mine process water. Mine Water Environ 2010;29:108–15.

Duffó G, Farina S, Giordano C. Characterization of solid embeddable reference electrodes for corrosion monitoring in reinforced concrete structures. Electrochim Acta 2009;54(3):1010–20.

Duffó G, Farina S, Giordano C. Characterization of solid embeddable reference electrodes for corrosion monitoring in reinforced concrete structures. Electrochim Acta 2009;54(3):1010–20.

Duffó G, Farina S. Development of an embeddable sensor to monitor the corrosion process of new and existing reinforced concrete structures. Constr Build Mater 2009; 23:2746–51.

Duffó G, Farina S. Development of an embeddable sensor to monitor the corrosion process of new and existing reinforced concrete structures. Constr Build Mater 2009;23:2746–51

Dzombak, D.A. and Morel, F.M.M., 'Surface complexation modeling – Hydrous ferric oxide' New York, John Wiley, (1990)

E.M. Theissing, P.v. Hest-Wardenier and G. de Wind, Cem. Concr. Res., (6), 683 (1978).

Ehtesham Hussain, S., Rasheeduzzafar and Al-Gathani, A.S. (1994): "Influence of Sulphates on Chloride Binding in Cements", Cem. Concr. Res., Vol 24 (1994), pp. 8-24.

Ehtesham Hussain, S., Rasheeduzzafar, Al-Musallam, A. and Al-Gahtani, A.S. (1995): "Factors Affecting Threshold Chloride for Reinforcement Corrosion in Concrete", Cem. Concr. Res., Vol. 25 (1995), No. 7, pp. 1543-1555.

Elsener B, Zimmermann L, Böhni H. Non destructive determination of the free chloride content in cement based materials. Mater Corros 2003; 54(6): 440–6.

Erdogdu S, Kondratova I, Bremner T. Determination of chloride diffusion coefficient of concrete using open-circuit potential measurements. Cem Concr Res 2004; 34:603–9.

Fajardo G, Valdez P, Pacheco J. Corrosion of steel rebar embedded in natural pozzolana based mortars exposed to chlorides. Construct Build Mater 2009;23:768–74.

Falciai R, Mignani A, Vannini A. Long period gratings as solution concentration sensors. Sen Actuat B: Chem 2001;74:74–7.

Fernández-Sánchez C, McNeil CJ, Rawson K. Electrochemical impedance spectroscopy studies of polymer degradation: application to biosensor development. TrAC Trends Anal Chem 2005; 24(1):37–48.

Florea M.V.A., Brouwers H.J.H., 'Chloride binding related to hydration products Part I: Ordinary Portland Cement', Cement and Concrete Research 42 (2012) 282–290

Fluge, F. (2003): Marine chlorides – A probabilistic approach to derive durability related provisions for NS-EN 206-1. The Norwegian Road Administration, Publication no. 19, Oslo, Norway, 2003, 22 pp.

Friedmann H, Amiri O, Aït-Mokhtar A, Dumargue P. A direct method for determining chloride diffusion coefficient by using migration test. Cem Concr Res 2004;34:1967–73

G. Sergi, S.W. Yu, C.L. Page, Diffusion of chloride and hydroxil ions in cementitius materials exposed to a saline environment, Magazine of Concrete Research 44 (158) (1992) 63–69.

Ganjian E, Pouya HS. The effect of Persian Gulf tidal zone exposure on durability of mixes containing silica fume and blast furnace slag. Construct Build Mater 2009; 23:644–52.

Glass G.K, Buenfeld N.R, 'The determination of chloride binding relationships', 1st RILEM workshop on Chloride Penetration into Concrete 15-18 october 1995, St Rémy lès Chevreuse, France

Glass GK, Buenfeld NR. 'The influence of chloride binding on the chloride induced corrosion risk in reinforced concrete'. Corros Sci 2000;42(2): 329–44.

Glass GK, Reddy B, Buenfeld NR. 'The participation of bound chloride in passive film breakdown on steel in concrete'. Corros Sci 2000;42(11):2013–21.

Glass, G., Hassanein, N. & Buenfeld, N. (1997), Neural network modelling of chloride binding. *Magazine of Concrete Research,* 49**,** 323-335.

Gowers K, Millard S. Measurement of concrete resistivity for assessment of corrosion severity of steel using Wenner technique. ACI Mater J 1999;96: 536–41.

GUTIERREZ, ALEXANDER, and JOHN HALLBERG. "Calibration of a 3D mesoscale FE model for chloride transport in concrete.", Master thesis, Chalmers university of technology, Goteborg, Sweden, 2014

H. Hirao, K. Yamada, H. Takahashi, H. Zibara, J. Adv. Concr. Technol. 3 (2005) 77–84.

H. Zibara, Binding of External chloride by cement pastes, PhD Thesis, University of Toronto, Department of Building Materials, 2001.

H.Hirao, K.Yamada, H.Takahashi, H.Zibara (2005), "Chloride binding of cement estimated by binding isotherms of hydrates", Journal of Advanced Concrete Technology, Vol.3, No.1, 77-84

Hansson CM, Frŏlund Th, Markussen JB. The effect of chloride cation type on the corposion of steel in concrete by chloride salts. Cem Concr Res 1985;15(1):65–73.

Haque, M.N. and Kayyali, O.A. (1995): "Free and Water Soluble Chloride in Concrete", Cem. Concr. Res., Vol. 25 (1995) No. 3, pp. 532-542.

Heath, T.G. and Tweed, C.J., 'Thermodynamic Modelling of the Sorption of Radioelements onto Cementitious Materials', Mat. Res. Soc. Symp. Proc. Vol.412, (1996), 58 – 65

Henocq P., Modeling ionic interactions on the surface of calcium silicate hydrates, PhD Thesis, Laval University, 2005.

Hewlett PC. Lea's chemistry of cement and concrete. 4th ed. Elsevier; 2004. 1057pp.

Hirao H., Yamada K., Takahashi H., Zibara H., 'Chloride binding of cement estimated by binding isotherms of hydrates', J. Adv. Concr. Technol. 3 (2005) 77–84.

Holden, W.R., Page, C.L., Short, N.R. (1983), Corrosion of Reinforcement in Concrete Construction, Ed. A.P. Crane, Ellis, Horwood, Chichester, 1983, pp. 143-150.

Hope .B, Page .J, Poland .J, ' The determination of the chloride content of concrete, Cement and concrete research Vol 15, 1985.

Hugenschmidt J, Loser R. Detection of chlorides and moisture in concrete structures with ground penetrating radar. Mater Struct 2008;41(4):785–92.

Hydrotalcite BejoyN. The clay that cures. Resonance 2001;6:57–61.

IN CEMENTS RICH IN TBI-CALCIUM ALUMINATE, 1499–1519.

Ingerslev LCF. Precast concrete for the Bahrain causeway. Concr Int 1989;11:15–20.

Ipavec .A,Vuk .T, Gabrovsek .R, Kaucic .V, 'Chloride binding into hydrated blended cements: The influence of limestone and alkalinity', Cement and Concrete Research 48 (2013) 74–85

Ipavec A., Gabrovsek R., Vuk T., Kaucic V., 'Carboaluminate phases formation during the hydration of calcite-containing Portland cement', J. Am. Ceram. Soc. 94 (2011) 1238–1242.

Jensen, H.-U. and Pratt, P.L. (1989): "The Binding of Chloride Ions by Pozzolanic Product in Fly Ash Cement Blends", Advances in Cement Research, Vol. 2 (1989) No. 7, pp. 121-129.

Jones, M.R, Macphee, D.E, Chudek J.A, Hunter .G, Lannegrand .R, Talero .R, Scrimgeour .S.N, 'Studies using Al MAS NMR of AF_m and AF_t phases and the formation of Friedel's salt', Cement and Concrete Research, Vol 33, 2003

Justnes, H. (1996), "A Review of Chloride Binding in Cementitious Systems, Cement and concrete", Trondheim, Norway

Kantro, D.L., Brunauer, S., and Weise, C.H., 1962. Development of surface in the hydration of calcium silicates. II. Extension of investigations to earlier and later stages of hydration. Journal of Physical Chemistry, 66, 1804–1809.

Kayali .O, Khan, M.S.H, Sharfuddin Ahmed .M, 'The role of hydrotalcite in chloride binding and corrosion protection in concretes with ground granulated blast furnace slag', Cement & Concrete Composites', 34 (2012) 936–945

Kayali O, Haque MN, Khatib JM. Sustain Emer Concr Mater Their Relevance Middle East Open Construct Build Technol J 2008;2:103–10.

Kayyali OA, Qasrawi MS. Chloride binding capacity in cement–fly-ash pastes. J Mater Civ Eng 1992;4:16–26.

Keddam M, Takenouti H, Nóvoa XR, Andrade C, Alonso C. Impedance measurements on cement paste. Cem Concr Res 1997; 27:1191–201

Kirkpatrick, R.J., et al., 1997. Raman spectroscopy of C-S-H, tobermorite, and jennite. Advanced Cement Based Materials, 5, 93–99.

Koleva DA, de Wit JHW, van Breugel K, Veleva LP, van Westing E, Copuroglu O, Fraaij ALA. Correlation of microstructure, electrical properties and electrochemical phenomena in reinforced mortar. breakdown to multi- phase interface structures. Part II: Pore network, electrical properties and electrochemical response. Mater Charact 2008;59:801–15.

Koleva DA, van Breugel K, de Wit JHW, van Westing E, Copuroglu O, Veleva L, et al. Correlation of microstructure, electrical properties and electrochemical phenomena in reinforced mortar. breakdown to multi-phase interface structures. Part I: Microstructural observations and electrical properties. Mater Charact 2008;59:290–300.

Kurczyk, H.G. and Schwiete, H.E., 1960. Concerning the hydration products of C3S and h-C2S. Proceedings of the 4th International Symposium on the Chemistry of Cement.

Lam C, Mandamparambil R, Sun T, Grattan K, Nanukuttan S, Taylor S, et al. Optical fiber refractive index sensor for chloride ion monitoring. Sens J, IEEE 2009;9:525–32.

Lambert, P., Page, C.L. and Short, N.R. (1984): "Diffusion of Chloride Ions in Hardened Cement Pastes Containing Pure Cement Minerals", Br. Ceram. Proc., Vol. 35 (1984) pp. 267-276.

Lambert, P., Page, C.L. and Short, N.R. (1985): "Pore Solution Chemistry of the Hydrated System Tricalcium Silicate/Sodium Chloride/Water", Cem. Concr. Res., Vol. 15 (1985) pp. 675-680.

Larsen, C. K. (1998), *Chloride binding in concrete: effect of surrounding environment and concrete composition,* PhD. Norwegian University of Technology and Science, Trondheim, Norway.

Li H, Li D-S, Song G-B. Recent applications of fiber optic sensors to health monitoring in civil engineering. Eng Struct 2004;26:1647–57.

Lin JK, Uan JY. Formation of Mg, Al-hydrotalcite conversion coating on Mg alloy in aqueous HCO_3^-/CO_3^{2-} and corresponding protection against corrosion by the coating. Corros Sci 2009;51:1181–8.

Loser .R, Lothenbach .B, Leemann .A,Tuchschmid .M, 'Chloride resistance of concrete and its binding capacity – Comparison between experimental results and thermodynamic modeling', Cement & Concrete Composites 32 (2010) 34–42

Lothenbach B., Winnefeld F., 'Thermodynamic modelling of the hydration of Portland cement', Cem. Concr. Res. 36 (2006) 209–226.

Loubser Du Plooy R. The development and combination of electromagnetic non-destructive evaluation techniques for the assessment of cover concrete condition prior to corrosion. Ph.D. thesis, Université de Nantes; 2013.

Lu .X, Li .C, Zhang .H, 'Relationship between the free and total chloride diffusivity in concrete', Cement and Concrete Research 32, 2002

Luo .R, Cai .Y, Wang .C, Huang .X, 'Study of chloride binding and diffusion in GGBS concrete', Cement and Concrete Research, Vol 33, 2003, 33:1–7.

.

Luping .T, Nilsson .L, 'Chloride binding capacity and binding isotherms of OPC pastes and mortars', Cement and Concrete Research, Vol 23, 1993

M.Sillanpaa, "The effect of cracking on chloride diffusion in concrete", Juune 2010

Mangat P.S, Limbachiya M.C, 'Effect of initial curing on chloride diffusion in concrete repair materials', Cement and Concrete Research 29 (1999) 1475–1485

Mangat, P.S. and Molley, B.T. (1995): "Chloride Binding in Concrete Containing PFA, GBS or Silica Fume under Sea Water Exposure", Magazine of Concrete Research, Vol. 47 (1995) No. 171, pp. 129-141.

Marchand, J., Samson, E., Maltais, Y., Lee, R.J., Sahu, S., 'Predicting the performance of concrete structures exposed to chemically aggressive environment - Field validation', *Mat. Struct.* **35** (2002) 623-631

Marinescu .M.V.A and Brouwers .H.J.H, 'Chloride binding in OPC hydration products'

Marinoni N, Birelli MP, Rostagno C, Pavese A. The effects of atmospheric multipollutants on modern concrete. Atmos Environ 2003; 37(33): 4701–12.

Markova, O.A. (1973): "Physiochemical Study of Calcium Hydroxide Chlorides", Zh. Fiz. Khim., Vol 47, No 4 (1973) p 1065 (på Russisk)

Massazza .F, Pozzolana and pozzolanic cements, Lea's Chemistry of Cement and Concrete, 4th ed., Arnold Publishers, London, 1998, p. 546.

Matschei T., B. Lothenbach, F.P. Glasser, 'The AFm phase in Portland cement', Cem. Concr. Res. 37 (2007) 118–130.

McCarter M, Chrisp TM, Starrs G, Adamson A, Owens E, Basheer P, et al. Developments in performance monitoring of concrete exposed to extreme environments. J Infrastruct Syst ASCE 2012;18:167–75.

McCarter WJ, Starrs G, Knadasami S, Jones R, Chrisp M. Electrode configurations for resistivity measurements on concrete. ACI Mater J 2009; 106: 258–64.

McCarter WJ, Vennesland O. Sensor systems for use in reinforced concrete structures. Constr Build Mater 2004; 18:351–8.

McPolin D, Basheer P, Long A, Grattan K, Sun T. Obtaining progressive chloride profiles in cementitious materials. Constr Build Mater 2005;19(9):666–73.

Meck, E., Sirivivatnanon, V., 'Field indicator of chloride penetration depth', *Cem. Conc. Res.* **33** (8) (2003) 1113-1117.

Megaw, H.D. and Kelsey, C.H., 1956. Crystal structure of tobermorite. Nature, 177, 390–391.

Midgley, H.G. and Illston, J.M. (1986): "Effect of Chloride Penetration on the Properties of Hardened Cement Pastes", Proc. 8th International Symposium on Chemistry of Cement, Rio de Janeiro, 1986, Part VII, pp. 101-103.

Miyata S. Physico-chemical properties of synthetic hydrotalcite in relation to composition. Clays Clay Miner 1980;28:50–6.

Mohammed T.U, Hamada H., 'Relationship between free chloride and total chloride contents in concrete', Cement and Concrete Research 33 (2003) 1487–1490

Mu, Song, Geert De Schutter, and B. G. Ma. "Study on chloride binding of self-compacting concrete with different crack lengths: non-steady state migration test." *International RILEM Conference on Advances in Construction Materials Through Science and Engineering*. Eds. Christopher Leung, and KT WAN. RILEM Publications SARL, 2011.

Muralidharan S, Vedalakshmi R, Saraswathi V, Joseph J, Palaniswamy N. Studies on the aspects of chloride ion determination in different types of concrete under macro-cell corrosion conditions. Build Environ 2005; 40(9): 1275–81.

Nagataki, S., Otsuki, N., Wee, T.H., Nakashita, K., 'Condensation of chloride ion in hardened cement matrix materials and on embedded steel bars', *ACI Mat. Journ.* **90** (3) (1993)323-332.

Nelder, J.A., Mead, R., *Computer Journal,* 7 (1965), pp. 308-313

Neville, A. (1995): "Chloride Attack of Reinforced Concrete: an overview", Materials and Structures, Vol. 28 (1995) pp. 63-70.

Newman .J, Seng Choo .B, 'Advanced Concrete Technology', Oxford, 2003

Nguyen, T.Q., Baroghel-Bouny, V., Dangla, P., 'Prediction of chloride ingress into saturated concrete on the basis of a multi-species model by numerical calculations', *Computers and Concrete*, Vol. 3, No. 6, p. 401-422, 2006.

Nilsson L.-O., Poulson E., Sandberg P., Sorensen H.E., Klinghoffer O., in: J.M. Fredriksen (Ed.), HETEK: Chloride Penetration into Concrete, Stateof- the-Art, Transport Processes, Corrosion Initiation, Test Methods and Prediction Models, Report, vol. 53, The Road Directorate, Denmark, 1996, 151 pp.

Nørlund Christensen, A., Fjellvåg, H. and Lehmann, M.S. (1986): "Time Resolved Powder Neutron Diffraction Investigation of Reactions of Solids with Water", Cement and Concrete Research, Vol. 16 (1986) pp. 871-874.

O. Stern, Z. Elektrochem. 30 (1924).

P. Hewlett, Lea's Chemistry of Cement and Concrete, Fourth Edition, 4th ed. Butterworth-Heinemann, 2004.

P.Nielsen .E, Herfort .D, Geiker .M, 'Binding of chloride and alkalis in Portland cement systems', Cement and Concrete Research, Vol 35, 2005

Page CL, Short NR, Holden WR. The influence of different cements on chlorideinduced corrosion of reinforcing steel. Cem Concr Res 1986;16:79–86.

Page CL, Vennesland O. Pore solution composition and chloride binding capacity of silica fume-cement pastes. Mater Struct 1983;16:19–25.

Page, C. L., Short, N. R. and Holden, W. R., The influence of different cements on chloride-induced corrosion of reinforcing steel. *Cement and Concrete Research, 1986, 16(l), 79-86.*

Page, C.L. and Vennesland, O. (1982): "Pore Solution Composition and Chloride Binding Capacity of Silica Fume Cement Pastes", SINTEF Report STF65 A82025, 1982-08-18, 18 pp.

Page, C.L. and Vennesland, Ø. (1983): "Pore Solution Composition and Chloride Binding Capacity of Silica Fume Cement Pastes", Matériaux et Constructions, Vol. 16, No. 91, pp. 19-25.

Pan .T, Xia .K, Wang .L, 'Chloride binding to calcium silicate hydrates (C-S-H) in cement paste: a molecular dynamics analysis', International Journal of Pavement Engineering, Vol. 11, No. 5, October 2010, 367–379

Patel SH. Processing Aids. In: Xanthos M, editor. Functional fillers for plastics. Wiley; 2005. p. 367–80 [chapter 20].

Plowman, C. and Cabrera, J.G. (1984): "Mechanism and Kinetics of Hydration of C3A and C4AF Extracted from Cement", Cement and Concrete Research, Vol 14 (1984) pp. 238-248.

Polder R. Test methods for on site measurement of resistivity of concrete – a RILEM TC-154 technical recommendation. Constr Build Mater 2001;15:125–31.

Pruckner F, Gjorv OE. Effect of CaCl2 and NaCl additions on concrete corrosivity. Cem Concr Res 2004;34(7):1209–17.

Qiang Yuan et al. (2009), 'Chloride binding of cement-based materials subjected to external chloride environment- Areviw', Construction and Building Materials 23, Issue 1, pp. 1-13

Ramachandran, V.S. (1971), Materials and Structures, Vol. 4, No. 19 (1971) pp. 3-12

Rasheeduzzafar, Ehtesham Hussain, S. and Al-Saadoun, S.S. (1991): "Effect of Cement Composition on Chloride Binding and Corrosion of Reinforcing Steel in Concrete", Cem. Concr. Res., Vol. 21 (1991) pp. 777-794.

Rasheeduzzafar, Ehtesham Hussain, S. and Al-Saadoun, S.S. (1992): "Effect of Tricalcium Aluminate Content of Cement on Chloride Binding and Corrosion of Reinforcing Steel in Concrete", ACI Materials Journal, January-February 1992, pp. 3-12

Rasheeduzzafar, M., Hussain, S. E. and Al-Saadoun, S. S., Effect of cement composition of chloride binding and corrosion of reinforcing steel in concrete. CementandConcrete *Research,* 1991,21(5), 777-794.

Reddy B, Glass GK, Lim PJ, et al. On the corrosion risk presented by chloride bound in concrete. Cem Concr Compos 2002;24(1):1–5.

Richardson, I.G. and Groves, G.W., 1992. Models for the composition and structure of calcium silicate hydrate (C-S-H) gel in hardened tricalcium silicate pastes. Cement and Concrete Research, 22, 1001–1010.

Richardson, I.G., 2000. The nature of the hydration products in hardened cement pastes. Cement and Concrete Composites, 22, 97–113.

RILEM TC 178-TMC. Round-Robin test on chloride analysis in concrete – part II: analysis of water soluble chloride content. Mater Struct 2001;34:589–98.

Robert A. Dielectric permittivity of concrete between 50 MHz and 1 GHz and {GPR} measurements for building materials evaluation. J Appl Geophys 1998;40:89–94.

Roberts M.H., Magazine of Concr. Res., 14, 143 (1962).

Ryou JS, Ann KY. Variation in the chloride threshold level for steel corrosion in concrete arising from different chloride sources. Mag Concr Res 2008;60(3):177–87.

Sakai, E., Imoto, H. and Daimon, M., 'Hydration and Strength Development of Blast-furnaceSlag Cement', Proceedings of the Japan Concrete Institute, Vol.26, No.1, (2004), 135 – 140 (in Japanese)

Sánchez I, Novoa XR, de Vera G, Climent MA. Microstructural modifications in portland cement concrete due to forced ionic migration tests. study by impedance spectroscopy. Cem Concr Res 2008;38:1015–25.

Sandberg, P. (1998): Chloride initiated reinforcement corrosion in marine concrete. Division of Building Materials, Lund Institute of Technology, Lund, Sweden, 1998, 115 pp.

Sbartaï Z, Laurens S, Balayssac J-P, Arliguie G, Ballivy G. Ability of the direct wave of radar ground-coupled antenna for {NDT} of concrete structures. {NDT}&E Int 2006;39(5):400–7.

Sbartaï Z, Laurens S, Viriyametanont K, Balayssac J, Arliguie G. Non- destructive evaluation of concrete physical condition using radar and artificial neural networks. Constr Build Mater 2009;23(2):837–45.

Shi .X, Xie .N, Fortune .K, Gong .L, 'Durability of steel reinforced concrete in chloride environments: An overview', Construction and Building Materials 30, (2012) 125–138

Shi C. Effect of mixing proportions of concrete on its electrical conductivity and the rapid chloride permeability test (ASTM C1202 or ASSHTO T277) results. Cem Concr Res 2004;34:537–45.

Shi M, Chen Z, Sun J. Determination of chloride diffusivity in concrete by AC impedance spectroscopy. Cem Concr Res 1999;29:1111–5.

Shu X, Gwandu BA, Liu Y, Zhang L, Bennion I. Sampled fiber bragg grating for simulataneous refractive-index and temperature measurement. Opt Lett 2001;26:774–6.

Smolczyk, H.G. (1969): "Chemical Reactions of Strong Chloride-Solutions with Concrete", Proc. 5th International Symposium on Chemistry of Cement, Tokyo, 1969, Supplementary paper III-31, pp. 274-280.

Soutsos M, Bungey J, Millard S, Shaw M, Patterson A. Dielectric properties of concrete and their influence on radar testing. NDT&E Int 2001; 34(6):419–25.

Standard test method for determing the penetration of chloride ion into concrete by ponding: ASTM C 1543-10A; 2010.

Standard test method for electrical indication of concrete's ability to resist chloride ion penetration: ASTM C 1202-10; 2010.

Sugiyama, D. and Fujita, T., 'A Thermodynamic Model of Dissolution and Precipitation of Calcium Silicate Hydrates', Cement and Concrete Research, Vol.36, Issue 2, Feb., (2006), 227 – 237

Sumranwanich T, Tangtermsirikul S. A model for predicting time-dependent chloride binding capacity of cement-fly ash cementitious system. Mater Struct 2004;37:387–96.

Suryavanshi AK, Narayan Swamy R. Stability of Friedel's salt in carbonated concrete structural elements. Cem Concr Res 1996;26(5):729–41.

Suryavanshi AK, Scantlebury JD, Lyon SB. Mechanism of Friedel's salt formation in cements rich in tri–calcium aluminate. Cem Concr Res 1996;26(5):717–27.

Suryavanshi, A.K., Scantlebury, J.D. and Lyon, S.B. (1995b): "Pore Size Distribution of OPC & SRPC Mortars in Presence of Chlorides", Cem. Concr. Res., Vol. 25 (1995) No. 5, pp. 980-988.

Suryavanshi, A.K., Scantlebury, J.D., Lyon, S.B. (1995a): "The Binding of Chloride Ions by Sulphate Resistant Cement", Cem. Concr. Res., Vol. 25 (1995) No. 3, pp. 581-592.

T.Q. Nguyen, V. Baroghel-Bouny, P. Dangla and P. Belin, 'IDENTIFICATION OF BINDING ISOTHERM AND PREDICTION OF CHLORIDE INGRESS INTO WATER SATURATED CONCRETE BY A NUMERICAL MULTI-SPECIES MODEL'

Talero R., Trusilewicz L., Delgado A., Pedrajas C., Lannegrand R., Rahhal V., Mejia R., Delvasto S., Ramirez F.A., 'Comparative and semi-quantitative XRD analysis of Friedel's salt originating from pozzolan and Portland cement', Construction and Building Materials 25 (2011) 2370–2380

Tang .L, Nilsson L.O, 'chloride binding isotherms –an approach by applying the modified bet equation', 1st RILEM workshop on Chloride Penetration into Concrete 15-18 october 1995, St Rémy lès Chevreuse, France

Tang J-L, Wang J-N. Measurement of chloride-ion concentration with long- period grating technology. Smart Mater Struct 2007; 16: 665–72.

Tang, L. and Nilsson, L.-O. (1993): "Chloride Binding Capacity and Binding Isotherms of OPC Pastes and Mortars", Cem. Concr. Res., Vol. 23 (1993) pp. 247-253.

Tang, L., Nilsson, L.O., 'Chloride binding capacity and binding isotherms of OPC pastes and mortars', *Cem. Conc. Res.* **23** (1993) 247-253.

Taylor HFW. Cement chemistry. London: Thomas Telford; 1997. 480 pp.

Taylor, H.F.W. and Howison, J.W., 1956. Relationships between calcium silicates and clay minerals. Clay Mineral Bulletin, 3, 98–111.

Taylor, H.F.W., 1986. Proposed structure for calcium silicate hydrate gel. Journal of the American Ceramics Society, 69, 464–467.

The European Union – Brite EuRam III (2000): DuraCrete – Final Technical Report – General Guidelines for Durability Design and Redesign, The European Union – Brite EuRam III, Lyngby, Denmark, 2000, 144 pp.

Theissing, E.M., Mebius-Van De Laar, T., De Wind, G. (1986): "The Combining of Sodium Chloride and Calcium Chloride by the Hardened Portland Cement Compounds C3S, C2S, C3A and C4AF", Proc. 8th International Symposium on Chemistry of Cement, Rio de Janeiro, 1986, pp. 823-828.

Torres-Luque, M., Bastidas-Arteaga, E., Schoefs, F., Sánchez-Silva, M., & Osma, J. F. (2014). Non-destructive methods for measuring chloride ingress into concrete: State-of-the-art and future challenges. *Construction and Building Materials*, *68*, 68-81.

Trætteberg, A. (1977): "The Mechanism of Chloride Penetration in Concrete", SINTEF Report STF65 A77070, 1977-12-30, 51 pp.

Tritthart, J. (1989a): "Chloride Binding in Cement. I. Investigations to Determine the Composition of Porewater in Hardened Cement", Cem. Concr. Res., Vol. 19 (1989) pp. 586-594.

Tritthart, J. (1989b): "Chloride Binding in Cement. II. The Influence of Hydroxide Concentration in the Pore Solution of Hardened Cement Paste on Chloride Binding", Cem. Concr. Res., Vol. 19 (1989) pp. 683-691.

U.A. Birnin-Yauri, F.P. Glasser, 'Friedel's salt, $Ca_2Al(OH)_6(Cl, OH)\cdot 2H_2O$: its solid solutions and their role in chloride binding', Cem. Concr. Res. 28 (1998) 1713–1723.

U.A. Birnin-Yauri, F.P. Glasser, Cem. Concr. Res. 28 (1998) 1713–1723.

V. Baroghel-Bouny, X. Wang, M. Thiery , M. Saillio, F. Barberon, 'Prediction of chloride binding isotherms of cementitious materials by analytical model or numerical inverse analysis', Cement and Concrete Research 42 (2012) 1207–1224

Valls S, Vazquez E. Accelerated carbonation of sewage sludge–cement–sand mortars and its environmental impacts. Cem Concr Res 2001;31(9):1271–6.

Van Gerven T, Cornelis G, Vandoren E, et al. Effects of progressive carbonation on heavy metal leaching from cement-bound waste. AIChE J 2006;52(2):826–37.

Geng J. The research on the deteriorated mechanisms of reinforced concrete in stray currents and chloride ion coexisted corrosion environment. PhD thesis. China: Wuhan University of Technology; 2008.

Vedalakshmi R, Devi R, Emmanuel B, Palaniswamy N. Determination of diffusion coefficient of chloride in concrete: an electrochemical impedance spectroscopic approach. Mater Struct 2008;41(7):1315–26.

Vedalakshmi R, Saraswathy V, Song H-W, Palaniswamy N. Determination of diffusion coefficient of chloride in concrete using Warburg diffusion coefficient. Corros Sci 2009;51: 1299–307.

Viallis-Terrisse, H., Nonat, A. and Petit, J-C, 'Zeta-Potential Study of Calcium Silicate Hydrates Interacting with Alkaline Cations', Journal of Colloid and Interface Science, Vol.244, (2001), 58 – 65

Wang J, Li D, Yu X, Jing X, Zhang M, Jiang Z. Hydrotalcite conversion coating on Mg alloy and its corrosion resistance. J Alloys Compd 2010;494:271–4.

Wang X., Thiéry M., and Baroghel-Bouny V., 'Determination of binding isotherms by inverse analysis and prediction of the influence of hydroxyl on chloride penetration', 3rd International RILEM PhD Student Workshop on Modelling the Durability of Reinforced Concrete – University of Minho, 22-24 October 2009, Guimarães, Portugal

Xu, **A.,** 'The structure and some physical properties of cement mortar with fly ash7, Licentiate thesis, Chalmers University of Technology (1990).

Xu, Y. (1997), The influence of sulphates on chloride binding and pore solution chemistry. *Cement and Concrete Research,* 27**,** 1841-1850.

Y. Elakneswaran, T. Nawa, K. Kurumisawa, Cem. Concr. Res. 39 (2009) 340–344.

Yoshida, N., Sakai, E., Mashimo, M. and Daimon, M., 'Fixation of Chloride Ion by the Various Type of Cement in the Marine Environment', Cement Science and Concrete Technology, No.56, (2002), 400 – 405 (in Japanese)

Yoshifumi Hosokawa, Kazuo Yamada, Björn F. Johannesson and Lars-Olof Nilsson, 'MODELS FOR CHLORIDE ION BINDINGS IN HARDENED CEMENT PASTE USING THERMODYNAMIC EQUILIBRIUM CALCULATIONS', 2nd International Symposium on Advances in Concrete through Science and Engineering 11-13 September 2006, Quebec City, Canada

Ytterdal, Silje Gystad. "The Effect of Fly Ash and GGBFS as Cement Replacement on Chloride Binding and Ingress in Mortar Samples.", Master thesis, Norwegian university of science and technology, Norway, (2014).

Yuan, Q., Shi, C., De Schutter, G., Audenaert, K. & Deng, D. (2009), Chloride binding of cement-based materials subjected to external chloride environment – A review. *Construction and Building Materials,* 23**,** 1-13.

Yuna Haebum, Pattona Mark E., James H. Garrett Jr.a,, Gary K. Fedder, Kevin M. Frederick, Jung-Jiin Hsu, Irving J. Lowe, Irving J. Oppenheim, Paul J. Sides, 'Detection of free chloride in concrete by NMR' Cement and Concrete Research 34 (2004) 379–390

Zhu .Q, Jiang .L, Chen .Y, Xu .J, Mo, L., 'Effect of chloride salt type on chloride binding behavior of concrete', Construction and Building Materials 37, (2012)

Zibara H., Hooton R.D., Thomas M.D.A., Stanish K., 'Influence of the C/S and C/A ratios of hydration products on the chloride ion binding capacity of lime-SF and lime-MK mixtures' , Cement and Concrete Research 38 (2008) 422–426

Zibara Hassan, (2001) "Binding of external chloride by cement pastes", PhD thesis, Department of Building Materials, University of Toronto, Canada

Zivica V, Bajza A. Acidic attack of cement based materials – a review: Part 1. Principle of acidic attack. Constr Build Mater 2001;15(8):331–40